National Library
of Canada

Canadian Theses Service

Ottawa, Canada
K1A 0N4

Bibliothèque nationale
du Canada

Services des thèses canadiennes

CANADIAN THESES

THÈSES CANADIENNES

NOTICE

The quality of this microfiche is heavily dependent upon the quality of the original thesis submitted for microfilming. Every effort has been made to ensure the highest quality of reproduction possible.

If pages are missing, contact the university which granted the degree.

Some pages may have indistinct print especially if the original pages were typed with a poor typewriter ribbon or if the university sent us an inferior photocopy.

Previously copyrighted materials (journal articles, published tests, etc.) are not filmed.

Reproduction in full or in part of this film is governed by the Canadian Copyright Act, R.S.C. 1970, c. C-30. Please read the authorization forms which accompany this thesis.

AVIS

La qualité de cette microfiche dépend grandement de la qualité de la thèse soumise au microfilmage. Nous avons tout fait pour assurer une qualité supérieure de reproduction.

S'il manque des pages, veuillez communiquer avec l'université qui a conféré le grade.

La qualité d'impression de certaines pages peut laisser à désirer, surtout si les pages originales ont été dactylographiées à l'aide d'un ruban usé ou si l'université nous a fait parvenir une photocopie de qualité inférieure.

Les documents qui font déjà l'objet d'un droit d'auteur (articles de revue, examens publiés, etc.) ne sont pas microfilmés.

La reproduction, même partielle, de ce microfilm est soumise à la Loi canadienne sur le droit d'auteur, SRC 1970, c. C-30. Veuillez prendre connaissance des formules d'autorisation qui accompagnent cette thèse.

THIS DISSERTATION
HAS BEEN MICROFILMED
EXACTLY AS RECEIVED

LA THÈSE A ÉTÉ
MICROFILMÉE TELLE QUE
NOUS L'AVONS REÇUE

NL 339 (r. 86/01)

Canada

299

National Library of Canada
Canadian Theses Division
Ottawa, Canada
K1A 0N4

Bibliothèque nationale du Canada
Division des thèses canadiennes

0-315-27030-6

PERMISSION TO MICROFILM — AUTORISATION DE MICROFILMER

- Please print or type — Écrire en lettres moulées ou dactylographier

Full Name of Author — Nom complet de l'auteur
DAVID RUSSELL KORPACH

Date of Birth — Date de naissance
AUGUST 31, 1958

Country of Birth — Lieu de naissance
CANADA

Permanent Address — Résidence fixe
13709 - 16th AVENUE
WHITE ROCK, BRITISH COLUMBIA
V4A 1P7

Title of Thesis — Titre de la thèse
STRESSES NEAR THE TUNNEL FACE

University — Université
UNIVERSITY OF ALBERTA

Degree for which thesis was presented — Grade pour lequel cette thèse fut présentée
MASTER OF SCIENCE

Year this degree conferred — Année d'obtention de ce grade
1983

Name of Supervisor — Nom du directeur de thèse
DR. N.R. MORGENSTERN

Permission is hereby granted to the NATIONAL LIBRARY OF CANADA to microfilm this thesis and to lend or sell copies of the film.

The author reserves other publication rights, and neither the thesis nor extensive extracts from it may be printed or otherwise reproduced without the author's written permission.

L'autorisation est, par la présente, accordée à la BIBLIOTHÈQUE NATIONALE DU CANADA de microfilmer cette thèse et de prêter ou de vendre des exemplaires du film.

L'auteur se réserve les autres droits de publication; ni la thèse ni de longs extraits de celle-ci ne doivent être imprimés ou autrement reproduits sans l'autorisation écrite de l'auteur.

Date
OCTOBER 14, 1983

Signature
David Korpach

NL-91 (4/77)

THE UNIVERSITY OF ALBERTA

STRESSES NEAR THE TUNNEL FACE

by

DAVID RUSSELL KORPACH

©

A THESIS
SUBMITTED TO THE FACULTY OF GRADUATE STUDIES AND RESEARCH
IN PARTIAL FULFILMENT OF THE REQUIREMENTS FOR THE DEGREE
OF MASTER OF SCIENCE

DEPARTMENT OF CIVIL ENGINEERING

EDMONTON, ALBERTA
FALL 1983

THE UNIVERSITY OF ALBERTA

RELEASE FORM

NAME OF AUTHOR DAVID RUSSELL KORPACH

TITLE OF THESIS STRESSES NEAR THE TUNNEL FACE

DEGREE FOR WHICH THESIS WAS PRESENTED MASTER OF SCIENCE

YEAR THIS DEGREE GRANTED FALL 1983

Permission is hereby granted to THE UNIVERSITY OF ALBERTA LIBRARY to reproduce single copies of this thesis and to lend or sell such copies for private, scholarly or scientific research purposes only.

The author reserves other publication rights, and neither the thesis nor extensive extracts from it may be printed or otherwise reproduced without the author's written permission.

(SIGNED) David Korpach

PERMANENT ADDRESS:

13709 16th Avenue
White Rock, British Columbia
V4A 1P7

DATED September 30 1983

THE UNIVERSITY OF ALBERTA

FACULTY OF GRADUATE STUDIES AND RESEARCH

The undersigned certify that they have read, and recommend to the Faculty of Graduate Studies and Research, for acceptance, a thesis entitled STRESSES NEAR THE TUNNEL FACE submitted by DAVID RUSSELL KORPACH in partial fulfilment of the requirements for the degree of MASTER OF SCIENCE.

Dr. N.R. Morgenstern ....
Supervisor

Dr. Z. Eisenstein ....

Dr. B. Stimpson ....B. Stimpson....................

DATED September 30 1983

TO DEBRA

ABSTRACT

The in situ stress is an important factor governing the ground behavior around an underground opening. It is generally not possible to deductively assess the virgin stress field in a rock mass due to the influence of genetic factors. In this study stress changes near the face of the tunnel were monitored and the results employed to back-calculate the in situ field stress and determine the mode of behavior around the opening.

Laboratory tests were performed on a large coal sample to gain confidence in the method of interpreting data from the Irad Gage stressmeters. Several tests were performed for this purpose and also to evaluate the accuracy of the instruments. Stress redistribution tests and one overcoring test were done.

An analytical study involved the determination of the optimum instrument locations around a circular opening excavated in a linear elastic material. Following evaluation of the field results these recommendations were extended to include openings where a softened zone adjacent to the tunnel wall exists.

The field instrumentation program was conducted at the Wolverine tunnel in northeastern British Columbia. Installations consisted of stress change gauges and extensometers. Finite element techniques were employed to analyze the results. The findings indicated that a zone of reduced stiffness around the opening had been induced by the

blasting and stress relief. The thickness of this zone was estimated from the stress change measurements and also from knowledge of the charge density which allowed for the determination of the maximum particle velocity. Agreement on the extent of the soft zone estimated by these two methods was very good.

ACKNOWLEDGEMENTS

I would like to extend a special thanks to Dr. P.K. Kaiser for his guidance and encouragement throughout this project. I would also like to thank Dr. N.R. Morgenstern for his contributions to this project, especially during the final preparation stages.

I am deeply indebted to AOSTRA and Hardy Associates (1978) Ltd. for providing personal funding during this research. Funding for the field instrumentation program was provided by the Central Research Fund, the University of Alberta, and I thank them for their participation. The cooperation from British Columbia Railways, Canadian Mine Services and Atkinson-Commonwealth during the field work was deeply appreciated. Many thanks to Mr. Clive Mackay who assisted with the field installations and offered many valuable suggestions on this and other aspects of the thesis.

A very sincere thanks goes out to Mr. G. Cyre and all his staff without whom the field and laboratory work would not have been possible.

I am very grateful for the support of all my fellow students who were always eager to help. A special thanks to Mr. Tom Casey for instructions on the use of his many helpful computer programs. Mr. Sean Maloney provided assistance during the laboratory program and offered helpful suggestions for the subsequent data interpretation. Thanks to Bob and Anna Powell who critically reviewed this thesis.

Many fruitful discussions were held with Messrs. Ivan Corbett and John Agar which provided valuable input to this project. Mr. Keith Kosar offered much helpful advice during the final preparation of this thesis.

Finally, a very heartfelt thank you to my parents for their patience and guidance over the years and for continually urging me onward during my studies.

Table of Contents

Chapter Page

1. INTRODUCTION 1

  1.1 Thesis Introduction 1

    1.1.1 Background Information 1

    1.1.2 Objective 2

    1.1.3 Scope of this Thesis 4

  1.2 Project Introduction 5

    1.2.1 Background Information 5

    1.2.2 The Convergence-Confinement Method (CCM) 7

      1.2.2.1 Introduction 7

      1.2.2.2 The Ground Convergence Curve (GCC) 7

      1.2.2.3 Determination of the Ground Convergence Curve 9

2. INTERPRETATION OF LABORATORY TEST DATA 13

  2.1 Introduction 13

    2.1.1 Objectives of Laboratory Test Program 13

    2.1.2 Background Information 13

  2.2 The Irad Gage Vibrating Wire Stressmeter 14

    2.2.1 Operation of the Stressmeter 14

    2.2.2 Optimum Gauge Locations 19

  2.3 Calibration of the Irad Gage Vibrating Wire Stressmeter 22

    2.3.1 Introduction 22

    2.3.2 Calibration Tests in Sample Without Opening 22

    2.3.3 Calibration Tests in Sample With Opening 28

      2.3.3.1 Gauge Locations 28

2.3.3.2 Loading History 29

2.3.3.3 Test Results 32

2.4 Re-evaluation of Field Data from Kipp Shaft 38

2.5 Rotation of Principal Stresses 41

2.5.1 Test Results 42

2.6 Stress Redistribution Tests 46

2.6.1 Background Information 46

2.6.2 Laboratory Testing Program 52

2.6.3 Test Results and Analysis 52

2.6.3.1 Without Opening- Before Loading History 52

2.6.3.2 Without Opening- After Loading History 54

2.6.3.3 With Opening- After loading History 56

2.6.4 Effects on the Ground Convergence Curve ...62

2.7 Overcoring Test 64

2.7.1 Introduction 64

2.7.2 Test Results 65

2.7.3 Analysis of the Results 68

2.8 Conclusions from Laboratory Testing 71

3. TUNNEL INSTRUMENTATION AND TEST RESULTS 73

3.1 Introduction 73

3.2 Geology 74

3.3 Proposed Instrumentation 78

3.3.1 Stressmeters 78

3.3.2 Extensometers 81

3.4 Installation Procedures 81

3.4.1 Stressmeters 81

3.4.2 Extensometers 83

3.5 Installation Difficulties 85

3.5.1 Stressmeters 85

3.5.2 Extensometers 87

3.6 Final Installations 87

3.7 Data Reduction 90

3.7.1 Stressmeters 90

3.7.2 Extensometers 91

4. ANALYSIS OF TUNNEL INSTRUMENTATION 95

4.1 Introduction 95

4.2 Analysis of Stressmeter Results 95

4.3 Estimation of the In Situ Stress Field by Finite Element Methods 98

4.3.1 Introduction 98

4.3.2 Two-Dimensional Plane Strain Analysis 101

4.3.2.1 Method of Analysis 101

4.3.2.2 Results from Analysis without Softened Zone 104

4.3.2.3 Results from Analysis with Softened Zone 104

4.4 AxiSymmetric Analysis 117

4.4.1 Method of Analysis 117

4.4.2 Discussion of Results 123

4.5 Verification of Soft Zone and Stressmeter Performance 128

4.6 Alternate Gauge Locations 132

4.7 Analysis of Extensometer Data 134

4.8 Calculation of the Ground Convergence Curve 139

4.9 Summary and Conclusions from the Field Monitoring Program 143

5. SUMMARY AND CONCLUSIONS 145

5.1 Introduction 145

5.2 Data Analysis Technique 145

5.3 Optimum Gauge Locations 146

5.4 Stress Change Measurements Near the Face 148

5.4.1 Findings from Laboratory Work 148

5.4.2 Findings from Field Program 149

5.5 Suggestions for Further Research 150

REFERENCES 152

APPENDIX A 159

APPENDIX B 163

APPENDIX C 177

APPENDIX D 189

List of Tables

Table Page

2.1 Stressmeter Locations Around Opening....................30

2.2 Results From Principal Stress Rotation Tests........43

4.1 Normalized Measured and Predicted Stress Changes...114

4.2 Measured and Predicted Stress Changes..............115

List of Figures

Figure Page

1.1 Site Location Plan 3

1.2 Characteristic Curves For a Uniformly Loaded Circular Tunnel 8

1.3 Radial Displacements Caused by the Advancing Tunnel Face 11

2.1 Plots of Principal Stress Ratio N versus Stress Change Ratio SCR measured by: two tangential gauges; one at $\theta=0°$ and one at $\theta=90°$ (after Kaiser *et al.* ,1983a). 21

2.2 Stressmeter Locations in Sample Without Opening 23

2.3 Loading History for Test MC7.09- Calibration Test Without Opening 25

2.4 Measured and predicted uniaxial rock stress change for Y Gauge: Prediction Method 1- Stress normal to gauge does not influence response; and Prediction Method 2- Stress normal to gauge does influence response. 26

2.5 Measured and predicted uniaxial rock stress change for 52° gauge: Prediction Method 1-Stress normal to gauge does not influence reading; and Prediction Method 2-Stress normal to gauge does influence reading. 27

2.6 Locations of Stressmeter Holes Around 152 mm Diameter Opening 31

2.7 Loading History for Test MC7.18- Calibration Test with Opening Present 33

2.8 Measured and Predicted Uniaxial Rock Stress Change- Gauge 10, Tangential Gauge in Hole A 34

2.9 Measured and Predicted Uniaxial Rock Stress Change- Gauge 12, Radial Gauge in Hole A 34

Figure Page

2.10 Example of Stress Distribution When a Yielded Zone Exists Adjacent to the Opening 36

2.11 Measured and Predicted Uniaxial Rock Stress Change- Gauge 3, Tangential Gauge in Hole F 37

2.12 Measured and Predicted Uniaxial Rock Stress Change- Gauge 4, Radial Gauge in Hole F 37

2.13 Measured and Predicted Uniaxial Rock Stress Change- Gauge 8, Tangential Gauge in Hole C 39

2.14 Measured and Predicted Uniaxial Rock Stress Change- Gauge 2, Radial Gauge in Hole C 39

2.15 Measured and Predicted Uniaxial Rock Stress Change- Gauge 5, Tangential Gauge in Hole E 40

2.16 Measured and Predicted Uniaxial Rock Stress Change- Gauge 6, Tangential Gauge in Hole B 40

2.17 Borehole Deformation Caused by Uniaxial Loading and Unloading With a Rigid Inclusion Present for: a) Loading normal to the gauge axis; and b) Loading parallel to the gauge axis. 45

2.18 Stress Distributions with Time Around an Unlined Circular Opening 48

2.19 Tangential Stress Distribution Around an Opening in Salt 50

2.20 Constant Stress Test- Without Opening in Sample Before Loading History (Gauge locations shown in Figure 2.2) 53

2.21 Constant Stress Test- Without Opening in Sample After Loading History (Gauge locations shown in Figure 2.2) 55

Figure Page

2.22 Stress Redistribution Test- Gauge 5 Tangential Gauge in Hole E (Gauge locations shown in Figure 2.6) 58

2.23 Stress Redistribution Test- Gauge 6 Tangential Gauge in Hole C (Gauge locations shown in Figure 2.6) 58

2.24 Stress Redistribution Test- Gauge 10 Tangential Gauge in Hole A (Gauge locations shown in Figure 2.6) 59

2.25 Stress Redistribution Test- Gauge 12 Radial Gauge in Hole A (Gauge locations shown in Figure 2.6) 59

2.26 Radial and Tangential Stress Distribution in Yielded Zone 61

2.27 Short and Long Term Characteristic Curves for a Circular Opening in a Uniform Stress Field 63

2.28 Rate of Advance During Overcoring 66

2.29 Rock Stress Change Measured During Overcoring 67

2.30 Finite Element Mesh Used for Analyzing Overcoring Results 69

3.1 Projected Geological Profile Along the Wolverine Tunnel 75

3.2 Example of Stresses in Horizontally Bedded Rock Mass 77

3.3 Proposed Stressmeter Locations for Wolverine Tunnel 79

3.4 Proposed Extensometer Locations 82

3.5 Extensometer Components 84

3.6 Stressmeter Installations at Wolverine Tunnel 88

3.7 Extensometer Installations at Wolverine Tunnel 89

Figure Page

3.8 Measured Uniaxial Stress Change with Tunnel Face Advance 92

3.9 Depth-Displacement Plot for North Wall Extensometers 94

3.10 Time-Displacement Plot for North Wall Extensometers 94

4.1 Finite Element Mesh for Two-Dimensional Plane Strain Analysis 99

4.2 View of Area Around Opening- Plane Strain Analysis 100

4.3 Stress Contours for N=1.0, σ_1=1.0, No Soft Zone. 102

4.4 Stress Contours for N=1.0, θ=0°, σ_1=1.0, Stiffness Reduction=5.0, Soft Zone: 2.0 m at Crown; 1.0 m at Springline 107

4.5 Horizontal Stress Contours for N=2.0, θ=55°, σ_1=0.5, Stiffness Reduction=10.0, Soft Zone: 2.0 m at Crown; 1.0 m at Springline 108

4.6 Vertical Stress Contours for N=2.0, θ=55°, σ_1=0.5, Stiffness Reduction=10.0, Soft Zone: 2.0 m at Crown; 1.0 m at Springline 109

4.7 Stress Contours for N=1.0, θ=55°, σ_1=1.0, Stiffness Reduction=2.0, Soft Zone: 2.0 m at Crown; 1.0 m at Springline 110

4.8 Stress Contours for N=1.0, θ=0°, σ_1=1.0, Stiffness Reduction=5.0, Soft Zone: 1.0 m at Crown; 0.5 m at Springline 111

4.9 Stress Contours for N=1.0, θ=55°, σ_1=1.0, Stiffness Reduction=10.0, Soft Zone: 2.0 m at Crown; 1.0 m at Springline 112

4.10 Finite Element Mesh Used for Axisymmetric Analysis 119

4.11 Influence of Advancing Face on Radial Displacements- Comparison of Finite Element Solutions 121

Figure Page

4.12 Radial Displacements Caused by Tunnel Excavation- Comparison of Finite Element and Closed Form Solutions 122

4.13 Comparison of Stresses from Finite Element and Closed Form Solutions 124

4.14 Influence of Advancing Face on Stresses- Elastic Case 126

4.15 Influence of Advancing Face on Stresses- 1.0 m Soft Zone 127

4.16 Typical Blast Pattern for Wolverine West Tunnel 130

4.17 Radial Displacements at Three Excavation Stages 135

4.18 Influence of Advancing Face on Displacements- Elastic Case 136

4.19 Influence of Advancing Face on Displacements- 1.0 m Soft Zone 137

4.20 Ground Convergence Curve for Wolverine Tunnel 141

B.1 Locations of Internal Displacement Measuring Instruments 165

B.2 MC7.18 Radial Strain at Sta. 81 166

B.3 MC7.18 Radial Strain at Sta. 81 166

B.4 MC7.18 Radial Strain at Sta. 106 167

B.5 MC7.18 Radial Strain at Sta. 106 167

B.6 MC7.18 Radial Strain at Sta. 56 168

B.7 MC7.18 Radial Strain at Sta. 131 168

B.8 MC7.18 Average Radial Strain 169

B.9 MC7.18 Radial Strain at Sta. 156 169

B.10 MC7.18 Longitudinal Strains 170

B.11 MC7.18 Lateral Strains 170

Figure Page

B.12 MC7.18 Tunnel Closure (152 mm Diameter) 171

B.13 MC7.18 Tunnel Closure (152 mm Diameter) 171

B.14 MC7.18 Average Block Strain 172

B.15 MC7.18 Average Tunnel Closure (152 mm Diameter) 172

B.16 MC7.18 Stress Level Maintenance 173

B.17 MC7.18 Stress Level Maintenance 173

B.18 Stress Redistribution Test- Gauge 2 Radial Gauge in Hole C 174

B.19 Stress Redistribution Test- Gauge 8 Tangential Gauge in Hole C 174

B.20 Stress Redistribution Test- Gauge 4 Radial Gauge in Hole F 175

B.21 Strain-Time Plots from Stress Redistribution Tests on Sample With Opening 176

C.1 Initial Biaxial Stress Condition 182

C.2 Notation for Biaxial Stresses Adjacent to Shaft in Isotropic Elastic Ground 183

C.3 Mohr Diagram Showing Stresses on an Arbitrary Plane 188

1. INTRODUCTION

1.1 Thesis Introduction

1.1.1 Background Information

In recent years there has been an increased awareness of the benefits incurred from monitoring underground excavations. It provides a method for validating empirical design, evaluating stability and determining the mode of ground behavior adjacent to the opening. Lane (1977) has shown that significant cost savings can be achieved by monitoring performance and subsequently adjusting the construction method and/or support design.

Lane (1977) discusses the usual objectives of tunnel instrumentation under six main categories:

a) *Warning*- for the recognition of potential instability (or other trouble) in time for corrective measures to be performed at a reasonable cost;

b) *Monitoring*- either for documenting performance for maintenance and future design work or for compliance with contract requirements;

c) *Resolve Uncertainties*- essentially for verifying the adequacy of the design and to assure safety without wasteful overdesign;

d) *Economize-* to identify the actual conditions to ensure economic remedies;

e) *Validate-* to identify behavior mechanisms and provide reliable data for improving concepts; and

f) *Pilot Test-* to test methods, equipment or design on a small scale for refining improvements at a larger scale.

The tunnel instrumentation program undertaken for this study attempts to identify the mode of ground behavior around an underground opening near the face. The field instrumentation was done at the Wolverine Tunnel located near Tumbler Ridge in northeastern British Columbia (see Figure 1.1).

1.1.2 Objective

The main purpose of this thesis is to measure the stress change near the tunnel face for back-calculating the in situ stress field. In conjunction with this, an appropriate analytical model describing the rock mass behavior will be determined. A vibrating wire stressmeter was chosen for the study because it is capable of measuring stress changes with time and the gauges were readily available. The implications of the results on the stability of the opening will be discussed herein. Extensometer measurements will be used to determine if the rock mass modulus, obtained from laboratory tests on small samples,

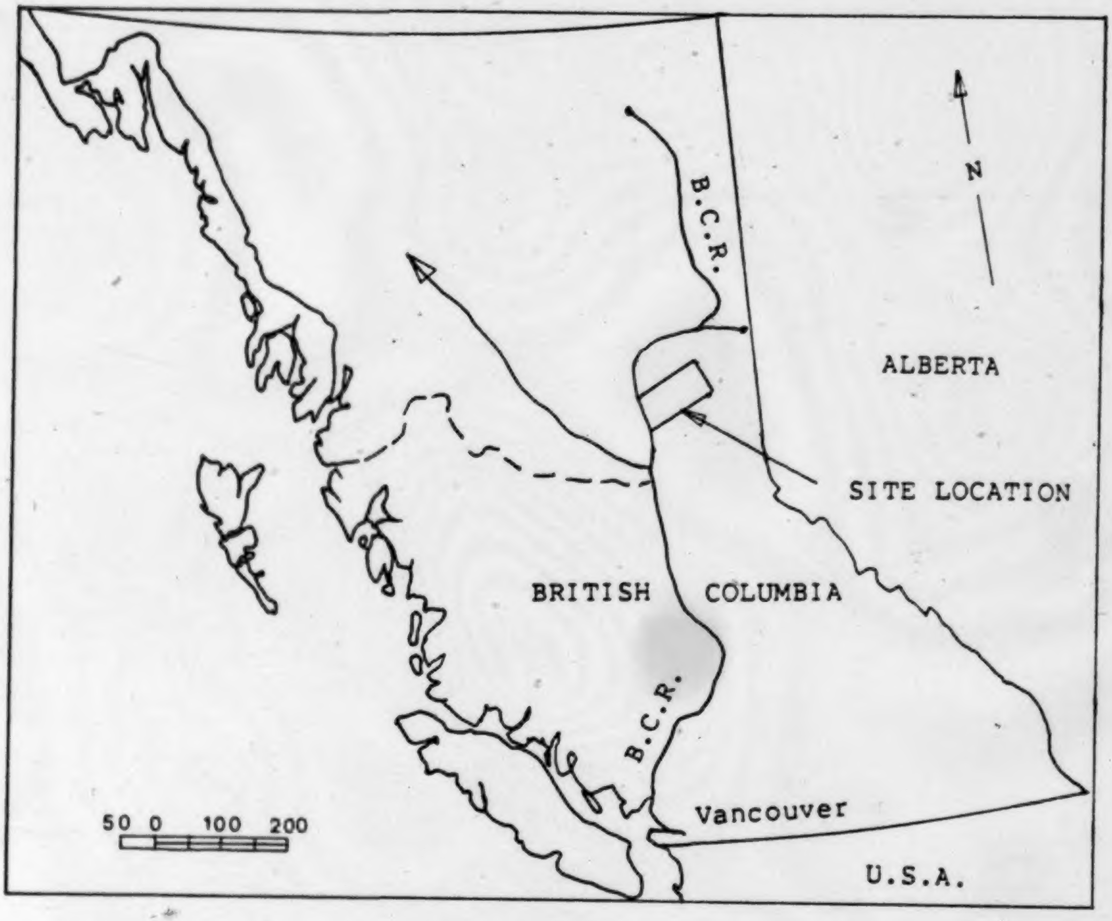

N
B.C.R.
ALBERTA
SITE LOCATION
BRITISH COLUMBIA
B.C.R.
Vancouver
U.S.A.
50 0 100 200

Figure 1.1 Site Location Plan

used for interpreting the stressmeter results was appropriate.

1.1.3 Scope of this Thesis

The second part of this chapter provides an introduction to the field project and the Convergence-Confinement Method (CCM), a method of evaluating the opening stability. Later chapters will show how certain conditions influence the shape and position of the ground convergence curve (GCC).

The laboratory test program included extensive calibration tests on the Irad Gage Vibrating Wire Stressmeter (used for measuring stress change), long term constant stress tests and one overcoring test to observe the stress change directly ahead of the tunnel face. Results from these tests are presented and discussed in Chapter 2. Some of the results have implications on the shape of the ground convergence curve and these will also be discussed in Chapter 2.

Chapter 3 presents the field results, provides a description of the test site and discusses the difficulties encountered during the instrument installation.

The field data has been analyzed using finite element techniques and the findings are reported in Chapter 4. Findings from the field measurements and finite element work are used to calculate the ground convergence curve.

Conclusions from the laboratory testing and field monitoring programs are presented in Chapter 5 followed by four Appendices. Appendix A contains a description of the test apparatus, outlines the laboratory procedures and provides the material properties of the coal used for the laboratory tests. Strain-time plots from the calibration tests have been included in Appendix B to aid with the interpretation of the stressmeter data. Derivation of the equations used for interpreting the stressmeter data are found in Appendix C. A copy of the paper by Kaiser *et al*. (1983a) containing some of the results from the Author's research work is included in Appendix D.

1.2 Project Introduction

1.2.1 Background Information

The in situ stress condition is one of the primary factors governing the mode of ground behavior around an underground opening. The failure mechanism depends on the relative magnitudes of the three principal stresses. Kaiser *et al*. (1983a) have stated that it is impossible to deductively predict the in situ stress field in a rock mass due to the influence of genetic factors. Thus, it is generally necessary to measure the in situ stress field by one of two basic groups of techniques; hydraulic fracturing or stress relief methods. This investigation is concerned not only with identifying the field stress, but also with measuring stress changes near the tunnel face.

The basic principles of the second technique were employed to measure the in situ stress field. Rather than overcoring a stiff inclusion, the stress change was recorded during "undercoring" or excavation of the opening between gauges measuring local changes in stress. A similar technique was employed by Mackay (1982). From these stress change measurements the in situ stress field can be determined, if the instruments record correctly the actual stress change during excavation and if an appropriate analytical rock mass response model can be found. Stress changes near the opening face were measured using the Irad Gage Vibrating Wire Stressmeter that was developed for the United States Bureau of Mines (U.S.B.M.) to provide a low cost system for monitoring long term stress changes in rock. Chapter 2 contains details on the operation of the gauge and the method of data interpretation.

In addition to providing a means for back-calculating the in situ stress field, stress change measurements can also be useful in determining the ground convergence curve (GCC). This is one of the two curves associated with the Convergence-Confinement Method (CCM), the other being the support reaction curve (SRC). The following section provides an introduction to this technique of evaluating stability.

1.2.2 The Convergence-Confinement Method (CCM)

1.2.2.1 Introduction

The Convergence-Confinement Method will be used throughout this thesis to illustrate the potential effects of certain findings, from both the laboratory work and the field monitoring program, on the stability of an underground opening. The method is applied by constructing two characteristic curves of radial stress versus radial displacement, one defining the ground behavior and the other for the support reaction. The state of equilibrium of the tunnel is defined by these two curves and the point of intersection, called the "Support Interaction Point", indicates the radial support pressure on the lining at equilibrium (see Figure 1.2). This study is concerned primarily with the determination of the ground convergence curve and the identification of some factors affecting the shape and position of this curve.

1.2.2.2 The Ground Convergence Curve (GCC)

Figure 1.2 presents the normalized ground convergence curve for a uniformly loaded circular opening. For this condition, the GCC originates at the same radial support pressure for all points around the opening. The GCC accounts for the three dimensional effects associated with the advancing face by considering either equivalent radial displacements or stress changes in a plane strain model. A circular opening excavated in a non-uniform stress field

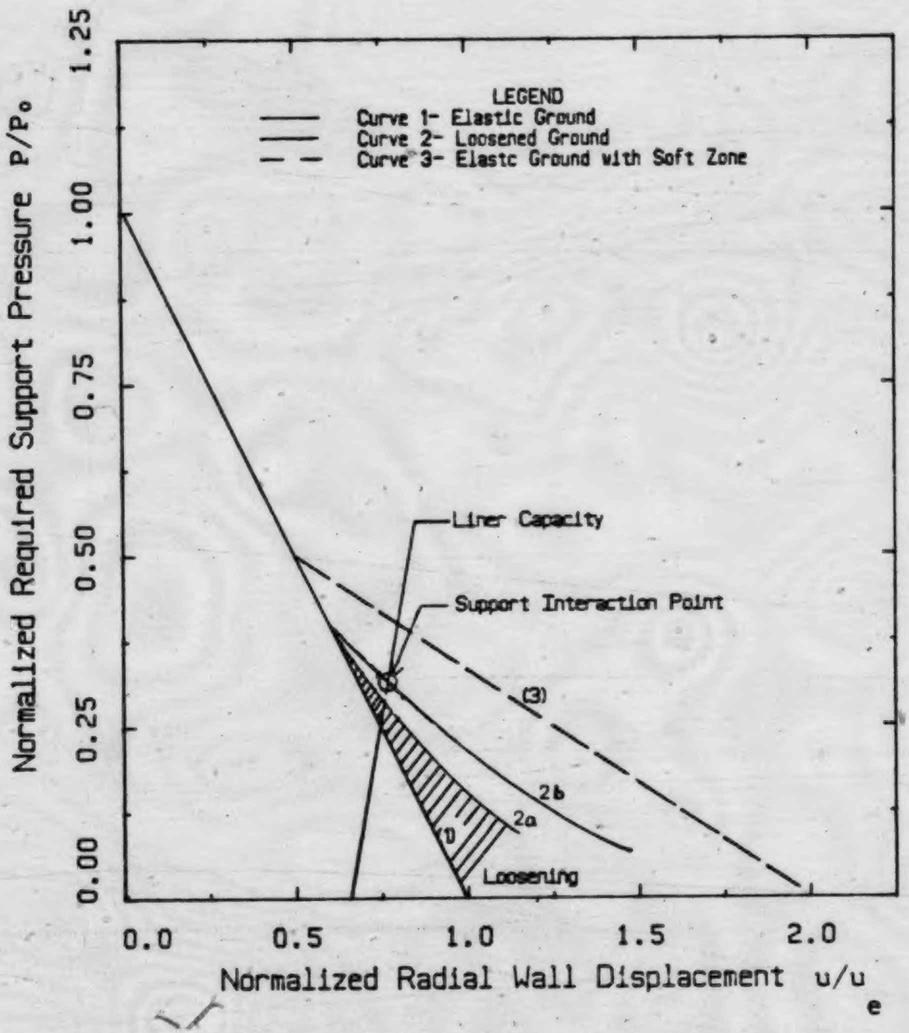

Figure 1.2 Characteristic Curves For a Uniformly Loaded Circular Tunnel

would have different GCC's for each point around the tunnel with the curves for points between the crown and springline lying between these two limiting curves.

For linear elastic ground behavior the GCC is linear with the slope of the curve being proportional to the shear modulus of the material (Curve 1, Figure 1.2). When yielding occurs the curve becomes non-linear due to plastic straining with the shape of the curve depending both on the extent of the yielding and the rock dilational characteristics (Curve 2a, Figure 1.2). Loosening, caused by dilation along the discontinuities due to gravitational forces, may also cause the GCC to become non-linear. This may cause the lower portion of the GCC to shift to the right (for the tunnel roof) as shown in Curve 2b, Figure 1.2. The GCC may become bilinear if softening of the rock adjacent to the opening occurs (Curve 3, Figure 1.2). Softening is the reduction of stiffness caused by removal of confinement or rock damage resulting from rock excavation techniques.

1.2.2.3 Determination of the Ground Convergence Curve

For the design of underground openings it is extremely important that both the shape and location of the ground convergence curve are correct because it is being used, along with the support reaction curve, to define the state of equilibrium of the tunnel. The most difficult quantity to predict is the displacement that occurs ahead of the face and before the support or extensometer installations. This is especially difficult in deep tunnels where radial displacement measurements ahead of the face are not possible.

It is necessary to predict the convergence curve with reasonable accuracy so the support requirements, type and time of installation can be determined. The curve can be predicted by one or both of two techniques; field measurements or numerical calculations. Egger (1980) summarizes the results from several field investigations where radial displacement measurements were taken ahead of the face. Curtis *et al.* (1976) present a case history where radial displacement measurements ahead of the face were taken. These results are plotted in Figure 1.3 where it can be seen that the percentage of displacement occurring at the face varies considerably from case to case. Thus, it is, in general, not possible to use the results from one site to confidently predict the ground behavior at another site.

Simplified theoretical methods have been developed for treating the three dimensional effects created by the advancing face. One technique is to use a two dimensional analysis and apply an internal pressure acting on the tunnel wall. Egger (1980) suggests that a state of spherical symmetry exists in the vicinity of the face and that this can be used effectively to simulate conditions at the face and predict the stresses and displacements here. However, theoretical predictions alone are often of limited value because field measurements are generally necessary to determine the mode of behavior around the opening and hence,

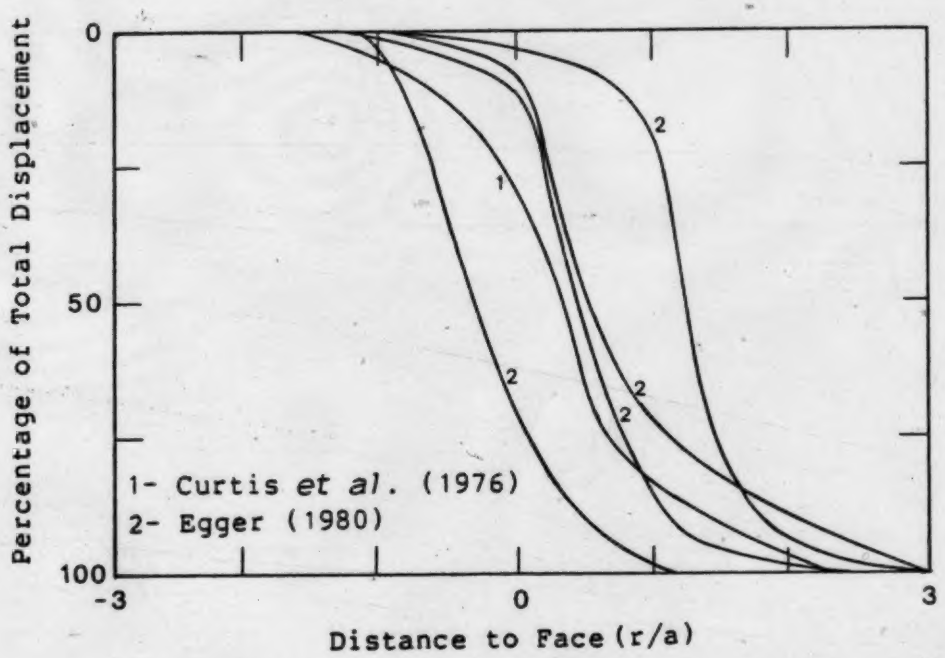

Figure 1.3 Radial Displacements Caused by the Advancing Tunnel Face

an appropriate rock mass response model.

Kaiser *et al.*(1983a) showed that without the use of stress change gauges installed ahead of the advancing face at the Kipp shaft the percentage of displacement recorded by the extensometers, based on theoretical predictions, would have led to a considerable underprediction of the rock mass modulus. This, in turn, would have produced an incorrect prediction of the rock mass response.

This study attempts to define the ground convergence curve by obtaining stress change measurements ahead of the face. In this manner, in combination with extensometer measurements after the face, the in situ stress can be estimated and the ground behavior predicted. A recent case history reported by Kaiser *et al.*(1982) has shown a similar procedure to be effective.

2. INTERPRETATION OF LABORATORY TEST DATA

2.1 Introduction

2.1.1 Objectives of Laboratory Test Program

The laboratory testing program was designed for the following purposes:

1) Re-evaluating the method of interpreting data from the Irad Gage Vibrating Wire Stressmeter by performing calibration tests;
2) Investigating the effects of rotation of the principal stresses on the gauge response;
3) Studying the long term stress redistribution adjacent to an opening for evaluating the long term stability;
4) Measuring the stress change immediately ahead of the advancing face to provide data for back-calculating boundary stresses; and
5) Re-evaluation and verification of the interpretation of field data collected by Mackay (1982).

2.1.2 Background Information

In order to accomplish these objectives an extensive laboratory program was designed and carried out over a five month period. The testing apparatus consisted of a large true triaxial machine designed and built in the Department of Civil Engineering at the University of Alberta. A brief description of the apparatus is given in Appendix A and a more detailed description is given by Kaiser (1979) and Kaiser and Morgenstern (1981). A regularly jointed coal sample with joint spacing of a few centimeters was used for the testing material because it represented a discontinuous rock mass and the strength of the coal was ideal for modelling a rock mass surrounding an opening. Eighteen tests were performed on the sample, some with an opening and some without. Only those tests where stress change measurements were taken are reported herein. The others are reported by Kaiser *et al.* (1983b). A description of the sample preparation and instrumentation along with a summary of the material properties is included in Appendix A.

2.2 The Irad Gage Vibrating Wire Stressmeter

2.2.1 Operation of the Stressmeter

All of the stress change measurements during both the laboratory testing and field monitoring program were made with the Irad Gage Vibrating Wire Stressmeter. Hawkes and Bailey(1973) provide a complete description of the gauge, its specifications, the installation techniques and the method of analysis. The gauge is available in two models, a hard rock gauge with a maximum contact angle between the gauge platens and borehole wall of 20° and a soft rock model with a maximum contact angle of 112°. The larger platens were used in the laboratory tests to reduce the possibility of local yielding. Essentially, the stressmeter consists of a hollow steel cylinder with a highly tensioned vibrating wire across the body in the direction that the measurement is taken. The gauge is activated diametrically by wedging the body against the walls of a 38.1 mm diameter borehole. A change in stress in the material surrounding the gauge creates a corresponding change in the wire tension which is recorded as a change in the frequency of vibration of the wire. This, in turn, is related to the change in wire stress and, finally, to the change in rock stress.

For a linear elastic material the relationship between the uniaxial rock stress change in the direction of the loading axis of the gauge and the wire tension [Hawkes and Bailey, 1973] is linear:

$$\Delta\sigma_R = \Delta\sigma_w / a \qquad \text{Eqn.2.1}$$

where a is the uniaxial gauge sensitivity factor and $\Delta\sigma_R$ and $\Delta\sigma_w$ are the changes in rock stress and wire stress, respectively. During the development of the gauge, Hawkes and Bailey (1973) experimentally determined relationships between the uniaxial gauge sensitivity factor and the Young's Modulus of the host material for both the hard rock and soft rock gauge models. For the soft rock gauge the uniaxial sensitivity factor a is:

$$a = 11.4 - 95.7 \times 10^{-9} E_R \text{ [kPa]} \qquad \text{Eqn.2.2}$$

and for the hard rock gauge:

$$\alpha = 9.4 - 72.5 \times 10^{-9} E_R \text{ [kPa]} \qquad \text{Eqn.2.3}$$

where E_R is the Young's modulus of the rock.

The basic assumption involved in the data interpretation is that the force across the stressmeter platens is proportional to the deformation (of the borehole) that would have occurred if the gauge had not been present [Hawkes and Bailey, 1973]. Merrill and Peterson (1969) provide a detailed derivation of the relationship between the radial displacement u of the borehole wall and the magnitude of the two principal stresses in the plane of the borehole in an elastic medium. For the plane stress condition it follows that:

$$u = D/E_R \left[(\sigma_1+\sigma_3) + 2\,(\sigma_1-\sigma_3)\cos 2\theta \right] \qquad \text{Eqn.2.4}$$

where: σ_1, σ_3 = principal stresses in the plane of the borehole or opening;

D = diameter of the opening; and

θ = angle measured from direction of σ_1 (clockwise).

Thus, it can be seen that, based on the previous assumption, the stress change recorded by a gauge is an "equivalent uniaxial stress" that is affected both by the stress in the direction of loading and by the stress normal to the loading axis. This equivalent uniaxial stress would cause deformations in the direction of the gauge that are equivalent to those that would be caused by the principal stresses in the gauge direction. The equivalent uniaxial stress recorded by the gauge can be expressed in terms of stress changes in the principal stress directions:

$$\Delta\sigma_G = 1/3\ (\Delta\sigma_1+\Delta\sigma_3) + 2/3\ (\Delta\sigma_1-\Delta\sigma_3)\cos 2\theta \qquad \text{Eqn. 2.5}$$

where: $\Delta\sigma_G$ = equivalent uniaxial stress recorded by the stress change gauge;

$\Delta\sigma_1$ = stress change in the major principal stress direction;

$\Delta\sigma_3$ = stress change in the minor principal stress direction; and

θ = angle measured from direction of σ_1 (clockwise) to the gauge location.

It can be shown (see Appendix C) that the pair of orthogonal stresses (i.e. radial and tangential) at 0° and 90° to the direction of the desired uniaxial stress change can be used in Eqn. 2.5 without introducing any error. Thus, Eqn. 2.5 can be rewritten for the specific case where radially and tangentially oriented gauges are used:

$$\Delta\sigma_G = 1/3\ (\Delta\sigma_\theta+\Delta\sigma_r) + 2/3\ (\Delta\sigma_\theta-\Delta\sigma_r)\cos 2\theta \qquad \text{Eqn. 2.6}$$

where: $\Delta\sigma_\theta$ = tangential stress change;

$\Delta\sigma_r$ = radial stress change; and

θ = angle measured from σ_θ (clockwise) to the gauge orientation.

Thus for a circular opening excavated in a linear elastic material, the uniaxial stress change recorded by radial and tangential gauges can be expressed in terms of the parameters S, θ, and N:

$$\Delta\sigma_{rG} = \Delta\sigma_r - 1/3\ \Delta\sigma_\theta \quad \text{or}$$

$$\Delta\sigma_{rG} = S[(-2\rho^2/3)(1+N) + (2\rho^4-2\rho^2)\cos2\theta(1-N)] \quad \text{Eqn. 2.7a}$$

and

$$\Delta\sigma_{\theta G} = \Delta\sigma_\theta - 1/3\ \Delta\sigma_r \quad \text{or}$$

$$\Delta\sigma_{\theta G} = S[(2\rho^2/3)(1+N) + (2\rho^2/3 - 2\rho^4)\cos2\theta(1-N)] \quad \text{Eqn.2.7b}$$

where: $\Delta\sigma_{rG}$ = uniaxial stress change recorded by a radial gauge;

$\Delta\sigma_{\theta G}$ = uniaxial stress change recorded by a tangential gauge;

S = the major principal stress;

N = principal stress ratio; and

ρ = a/r (a=radius of opening; r=distance to point of stress determination).

A detailed derivation of Eqn. 2.7 can be found in Appendix C.

For the most general case, at least three measurements are required to define the stress field. However, it is important to have a high degree of redundancy to obtain a good average reading for consistent data interpretation. This is necessary because local stiffness variations and the discontinuous nature of the rock mass may cause stress redistribution leading to local stress variations.

2.2.2 Optimum Gauge Locations

For a field monitoring program it is important to establish the optimum gauge locations to obtain the most accurate results and the highest degree of redundancy for the minimum cost. The following considers a circular opening excavated in a linear elastic material where the orientation of the principal stress is known or can be assumed with sufficient accuracy.

The optimum locations can best be evaluated by varying individual parameters and comparing the different combinations of these parameters. From Eqns. 2.7 it can be seen that, for a known orientation θ, the principal stress S can be expressed in terms of N, the gauge position ρ, and a stress change recorded by a gauge. For any two gauge measurements, either radial or tangential at $\theta = 0°$ or $90°$, two equations for S can be determined and these can be equated to obtain N in terms of the stress change ratio SCR and ρ. The stress change ratio is a ratio of any two selected stress change measurements recorded by the gauges. Kaiser *et al.*(1983a) present the complete derivation of the equation for two tangential gauges at 90° to each other (see Appendix D).

Double logarithmic plots of principal stress ratio N versus stress change ratio SCR have been generated for various gauge locations (θ =0° or 90°), orientations (radial or tangential), and positions (ρ). A sample plot is shown in Figure 2.1 for two tangential gauges: one at θ=0° and one at θ=90° for varying distances from the tunnel wall. A more complete set of these plots is contained in the paper found in Appendix D.

Some of the important conclusions found by Kaiser *et al.* (1983a) are summarized below. For intermediate N values the best combination consists of two tangential or two radial gauges at 90° to each other at ρ_1= ρ_2= 0.816. However, this arrangement is not acceptable for extreme N values in excess of 8. It may be prudent to install some gauges at smaller ρ-values because the error introduced by inaccurate ρ determination is not as significant when the distance from the opening increases. One tangential and one radial gauge on the same side at ρ=0.65 can be used effectively to determine N-values between 0.4 and 3.0. If θ is assumed to be 0° or 90° and deviations of ±15° from the principal stress axis occur significant errors will not be introduced for N values between 0.3 and 3.0. This finding

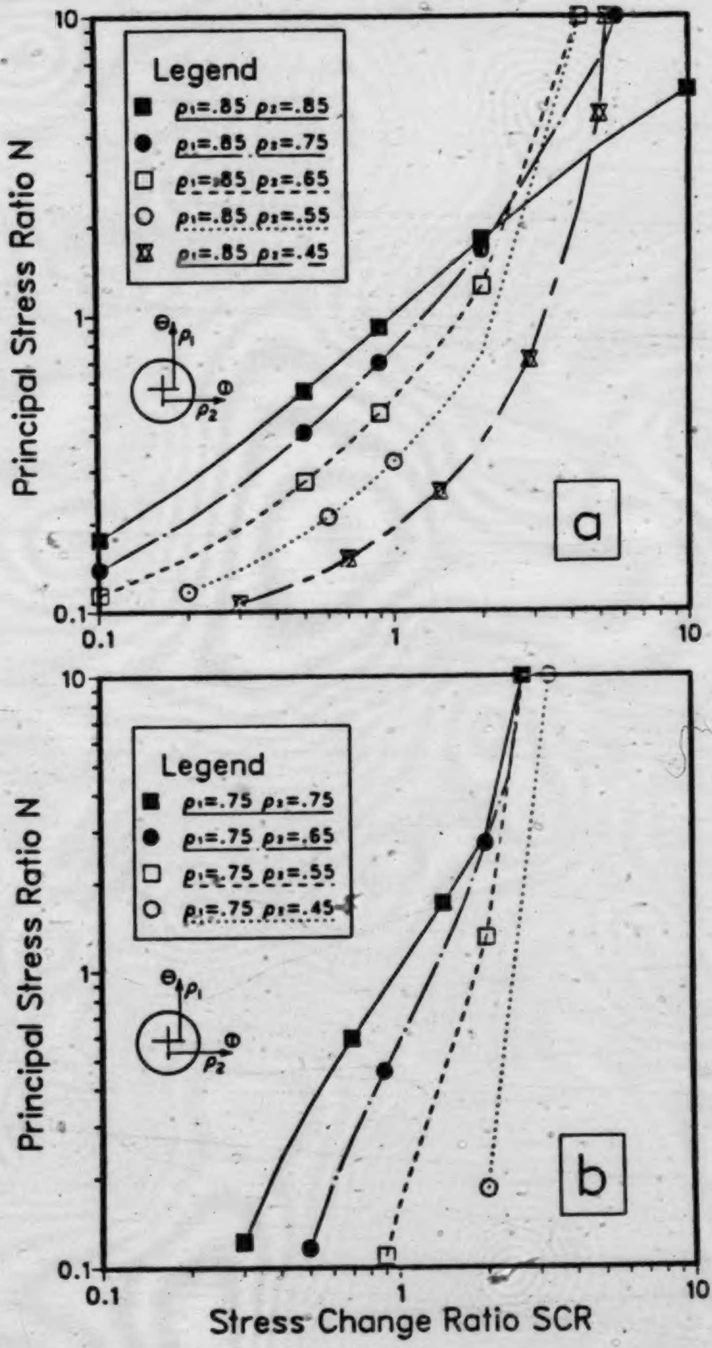

Figure 2.1 Plots of Principal Stress Ratio N versus Stress Change Ratio SCR measured by: two tangential gauges; one at $\theta=0°$ and one at $\theta=90°$ (after Kaiser *et al.* ,1983a).

has significance for application to cases where the principal stress directions are not known. Gauges can be placed at 30° intervals over a consecutive 150° range to provide at least two sets of gauges in the principal stress directions (within ±15°). This is beneficial because gauges placed along the principal stress axes provide a more accurate N determination as was shown by Mackay (1982). Appendix D provides a more detailed discussion of these results.

2.3 Calibration of the Irad Gage Vibrating Wire Stressmeter

2.3.1 Introduction

Two sets of calibration tests were performed; one with no opening in the sample and the other with a 152mm diameter opening in the center of the sample. In conjunction with these tests the effects of rotating the principal stresses on the gauge response were studied and constant stress tests were conducted to observe stress redistribution with time. Only the calibration tests will be discussed here and the other results will be presented in Sections 2.5 and 2.6.

2.3.2 Calibration Tests in Sample Without Opening

A description of the testing apparatus and the properties of the coal are given in Appendix A. Two stressmeters were installed in a 38.1mm diameter hole at the location shown in Figure 2.2. The lower gauge was placed

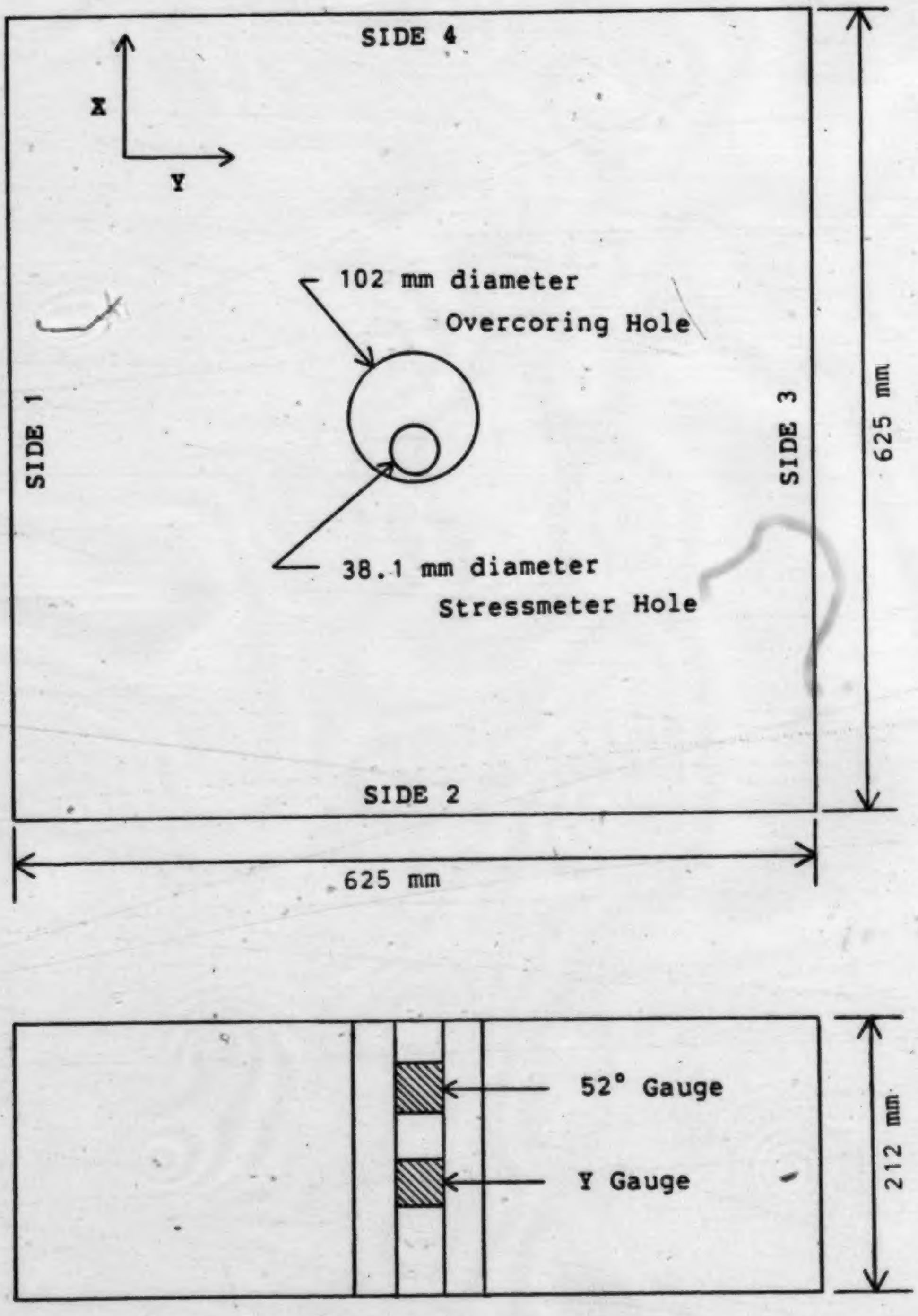
SIDE 4
X
Y
102 mm diameter Overcoring Hole
SIDE 1
SIDE 3
625 mm
38.1 mm diameter Stressmeter Hole
SIDE 2
625 mm
52° Gauge
Y Gauge
212 mm

Figure 2.2 Stressmeter Locations in Sample Without Opening

with the loading direction parallel to the Y axis and the upper gauge was set at 52° to the Y axis, approximately perpendicular to the jointing. After maintaining a constant stress condition for about 12 hours the sample was subjected to a repeated loading history shown in Figure 2.3.

Results from the calibration tests are presented in graphical form in Figures 2.4 and 2.5 for the Y direction gauge (Y gauge) and the gauge at 52° to the Y axis (52° gauge), respectively. Each plot portrays three curves: (a)Prediction Method 1- the expected stress change was calculated assuming that the gauge response is insensitive to the stress normal to the loading axis; (b)Prediction Method 2- the expected stress change was determined by considering the stress normal to the loading axis as suggested by Hawkes and Bailey (1973) and as outlined in the previous section; and (c) Measured- the stress change recorded by the gauge based on a Young's modulus of E_R = 1500 MPa and α=11.23 (calculated from Eqn. 2.2).

Close examination of the plots shows that up to a time of about 75 minutes there is excellent agreement between the measured values and those from Prediction Method 2. The stress change from Prediction Method 1 is consistently greater than that measured. A significant difference between the predicted and measured curves arises when the sample has been unloaded back to the initial stress level. Jaworski *et al.*(1982) found that the value of α changes after the first loading cycle and remains relatively constant for future

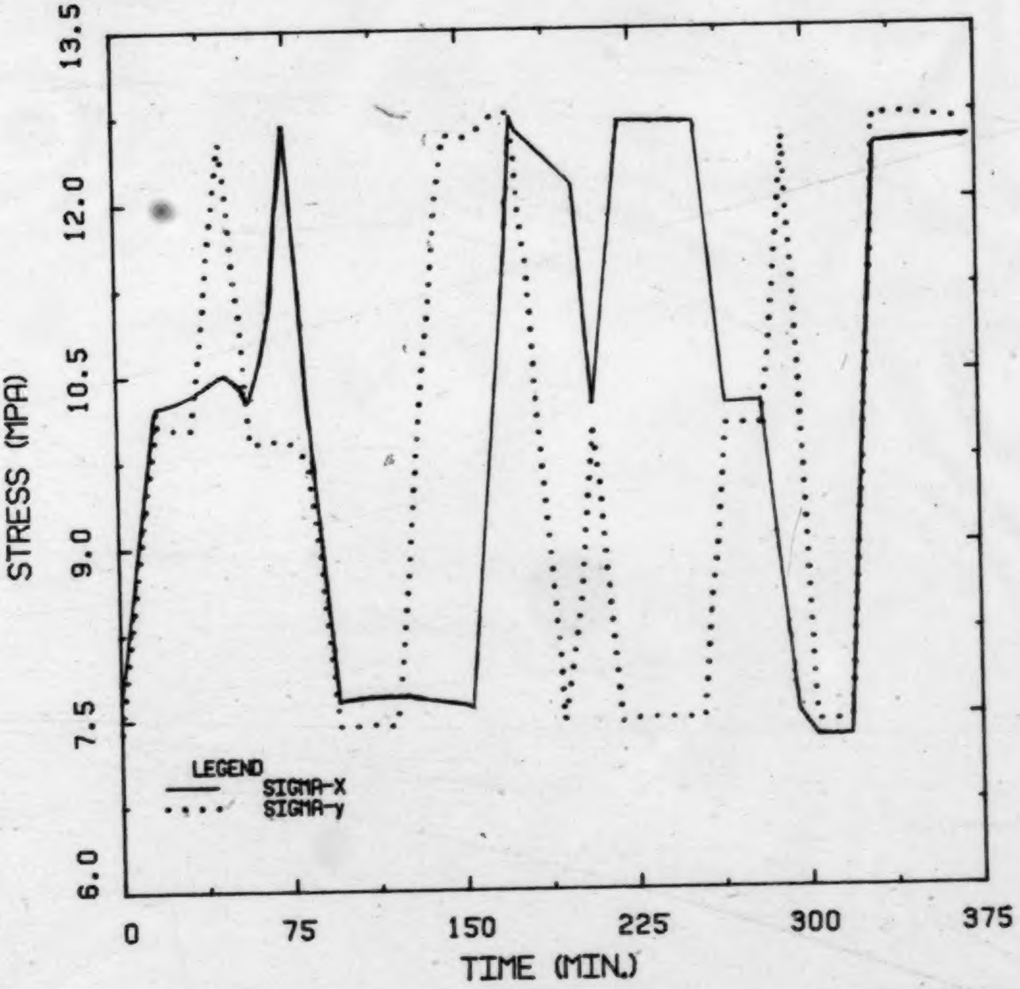

Figure 2.3 Loading History for Test MC7.09- Calibration Test Without Opening

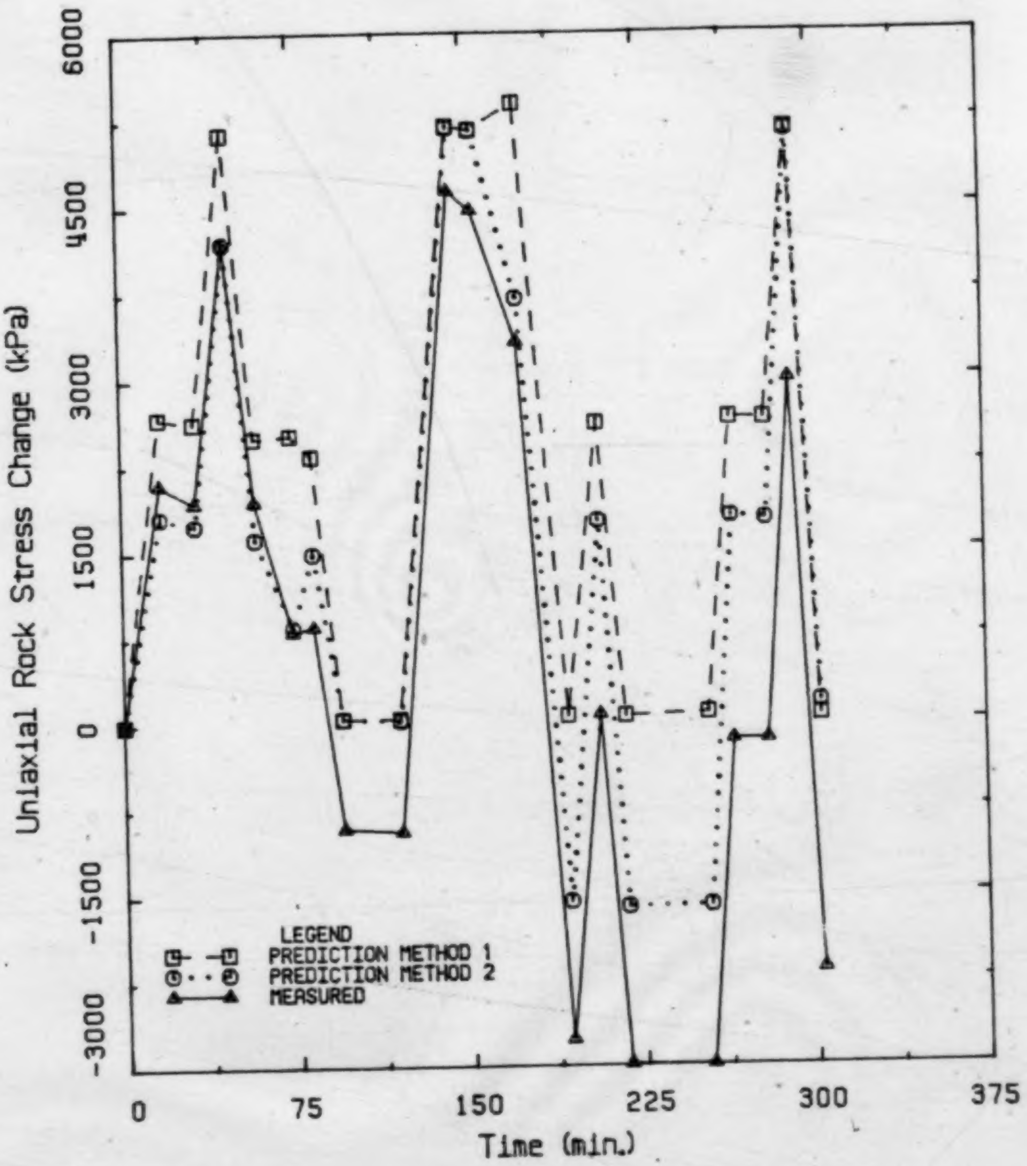

Figure 2.4 Measured and predicted uniaxial rock stress change for Y Gauge: Prediction Method 1- Stress normal to gauge does not influence response; and Prediction Method 2- Stress normal to gauge does influence response.

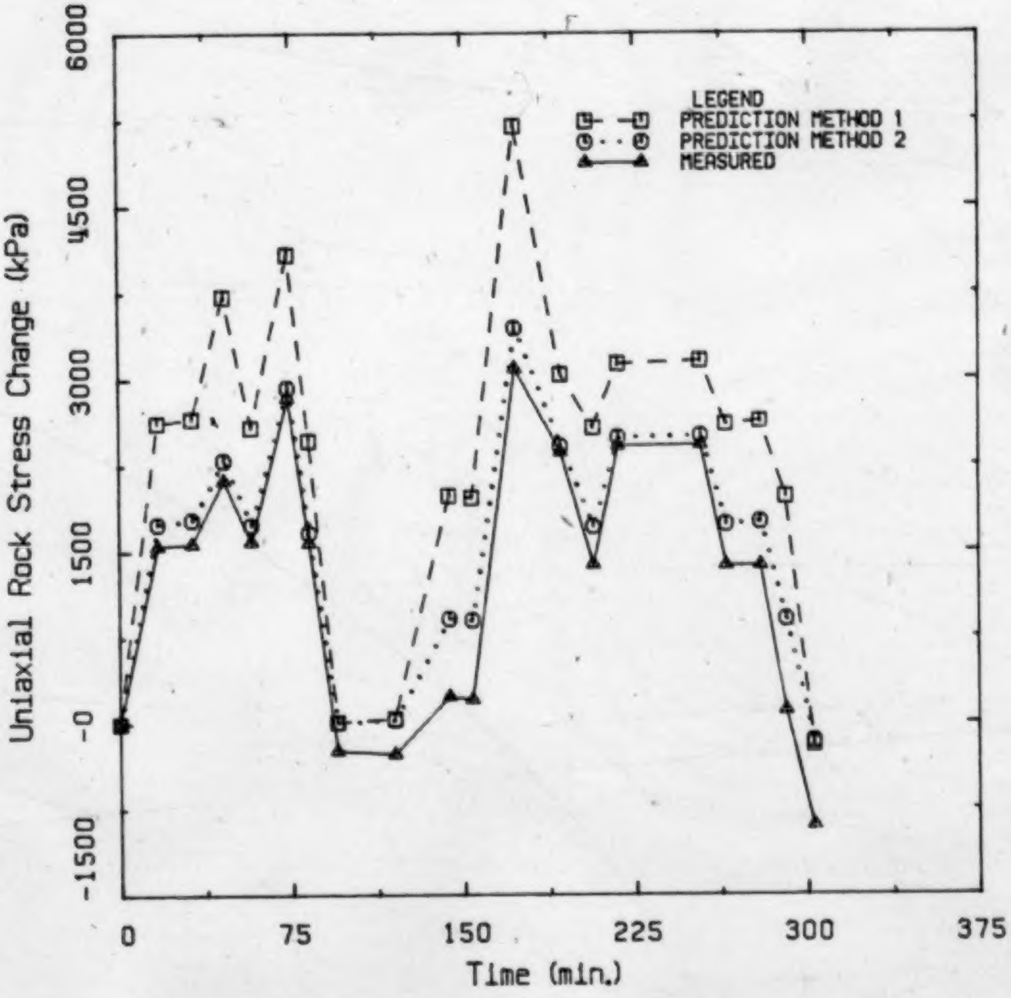

Figure 2.5 Measured and predicted uniaxial rock stress change for 52° gauge: Prediction Method 1-Stress normal to gauge does not influence reading; and Prediction Method 2-Stress normal to gauge does influence reading.

loading cycles. They also found that local yielding at the contacts may occur at high stress levels. It is possible that some local yielding has taken place at the contacts as the sample was loaded. The effect is not as great for the 52° gauge because the maximum stress experienced in this direction is considerably less than that in the Y direction. If at a time of 75 minutes the measured values are adjusted to correspond to those from Prediction Method 2, the agreement between these two curves over the remainder of the loading history would be quite good.

In conclusion, it has been verified that the stress normal to the gauge must be taken into consideration for correct interpretation of the gauge results. Similar findings have been made by Jaworski *et al.*(1982), Fossum *et al.* (1976) and Babcock (1981). It has also been shown that a uniaxial gauge sensitivity factor of $\alpha = 11.23$ obtained from the relationship suggested by the manufacturer is acceptable. In the field, gauges are not subjected to repeated loading and the important results are those from the first loading. These were predicted with high accuracy.

2.3.3 Calibration Tests in Sample With Opening

2.3.3.1 Gauge Locations

The locations of the gauges around the 152mm diameter opening were restricted by several factors. First, extensometers were located along lines passing through the center of the opening in the X and Y directions as well as diagonally. Second, it was necessary to leave adequate clear spacing between the stressmeter holes and the opening to prevent the stressmeter holes from collapsing into the opening. The gauge diameter was 38.1 mm and the distance from the gauge to the opening was taken from the centre of the stressmeter hole. This diameter is approximately 25% of the opening diameter and therefore, has a significant effect on the ρ value. These limitations made it impossible to place the gauges in the optimum locations discussed previously in Section 2.2.2.

Six stressmeter holes were cored through the entire thickness of the sample at the locations shown in Figure 2.6 using a 38.1 mm diameter core barrel. Great care was taken during drilling to ensure smooth borehole walls for the installations. Table 2.1 contains a description of the borehole locations, the condition of the boreholes following drilling and the installations at each location. Ten Irad Gage stressmeters (soft rock models) were installed in these six holes. Gauge 11 in Hole B never worked following installation and only occasional readings could be obtained from gauge 1 in Hole D.

2.3.3.2 Loading History

All of the stress change gauges were installed under conditions of no load and were only preloaded until they were activated in the holes. The sample was subsequently loaded to 5 MPa under plane strain conditions and held there for 24 hours to allow the gauges to seat in the holes. A

Table 2.1 Stressmeter Locations Around Opening

Hole # & Gage #	Location c.c.w. from σ_y	Position (ρ-Value)	Orientation	Comments
A- #10	8°	0.57	Tangential	Small chips out of hole at 70 & 95 mm from top.
A- #12	8°	0.57	Radial	
B- #6	30°	0.39	Tangential	Good condition at location of gauge 6
B- #11	30°	0.39	Radial	
C- #8	81°	0.36	Tangential	Good Hole.
C- #2	81°	0.36	Radial	
D- #1	38°	0.45	Tangential	Good Hole.
E- #5	39°	0.41	Tangential	Badly broken; only good for one gauge at bottom.
F- #3	82.5°	0.55	Tangential	Very good hole.
F- #4	82.5°	0.55	Radial	

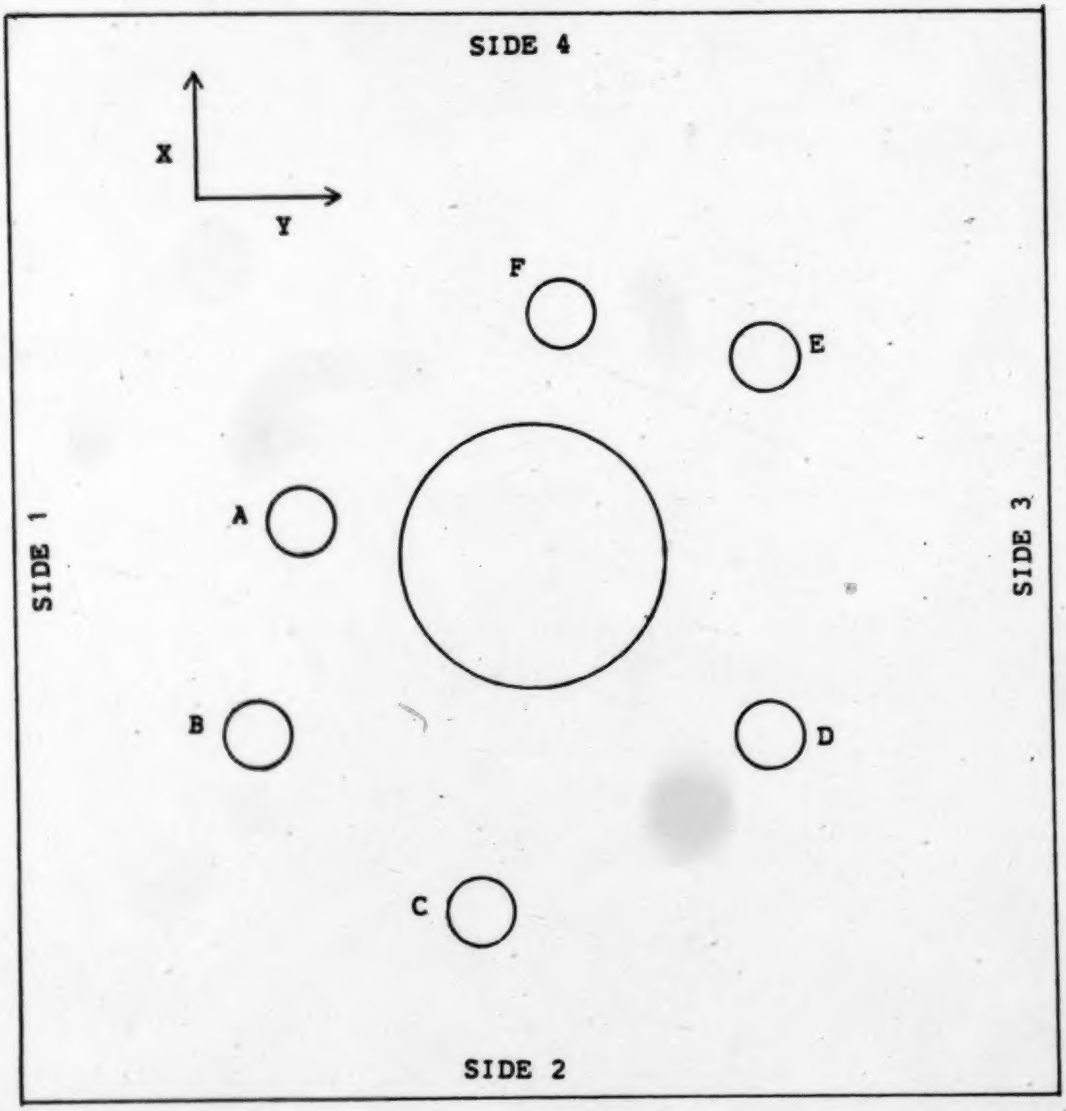
SIDE 4
X
Y
F
E
A
SIDE 1
SIDE 3
B
D
C
SIDE 2

Figure 2.6 Locations of Stressmeter Holes Around 152 mm Diameter Opening

loading history similar to that used previously was applied to the sample (see Figure 2.7).

2.3.3.3 Test Results

Results from the gauges at each stressmeter hole will be discussed in this section. Figures 2.8 to 2.16 show plots of the predicted and measured stress change with time for each of the eight gauges that provided continuous readings. To help interpret the results, strain-time plots from each of the extensometers have been included in Appendix B, Figures B.2 to B.17.

Results from gauges 10 (tangential) and 12 (radial) located in Hole A, 8° counterclockwise from the Y direction at ρ=0.57, are shown in Figures 2.8 and 2.9, respectively. Both figures show good agreement between the measured and predicted values up to a time of about 140 minutes at which point the measured stress changes begin to differ considerably from those predicted by elastic theory. The tangential gauge measures stress changes much larger than those predicted while the radial gauge measured values lower than predicted. Discrepancies between the measured and predicted values from the radial gauge are not as great as those of the tangential gauge because the maximum stress level experienced by the radial gauge was lower. Figure B.2, Appendix B, shows that the strains from the outer row of extensometers at ρ=0.61, 81 mm below the top of the sample. At the same time that the measured values began to differ from those predicted, excessive straining occured on Side 1

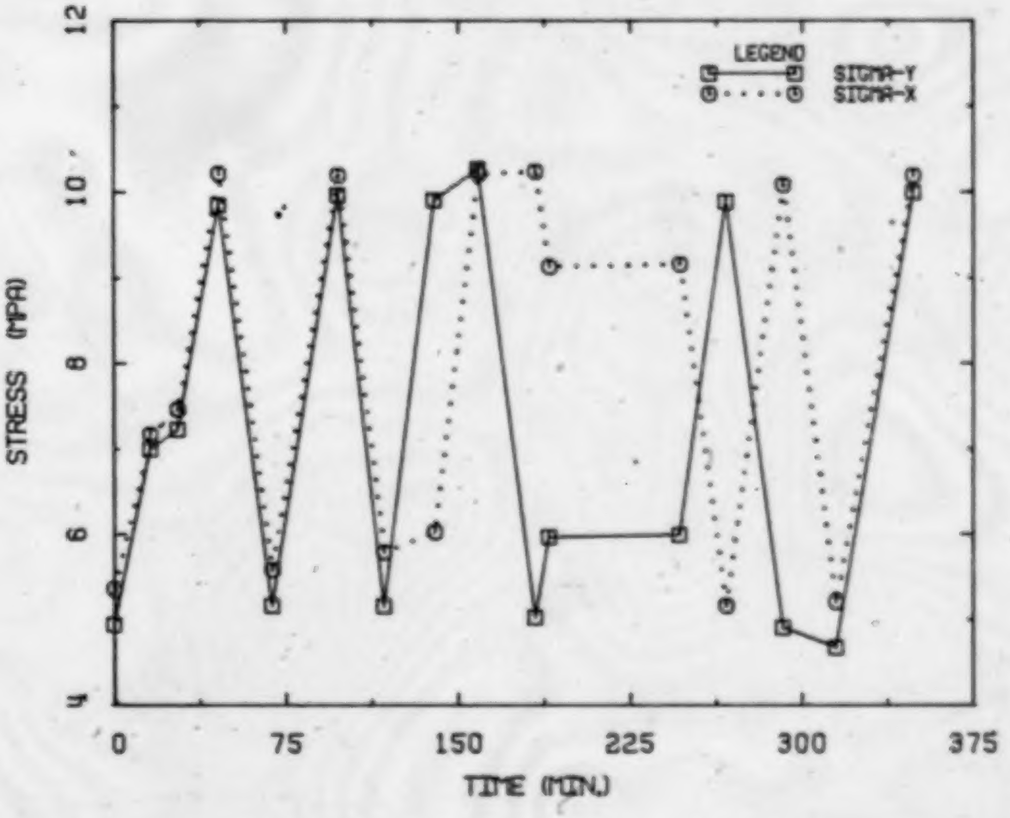

Figure 2.7 Loading History for Test MC7.18- Calibration Test with Opening Present

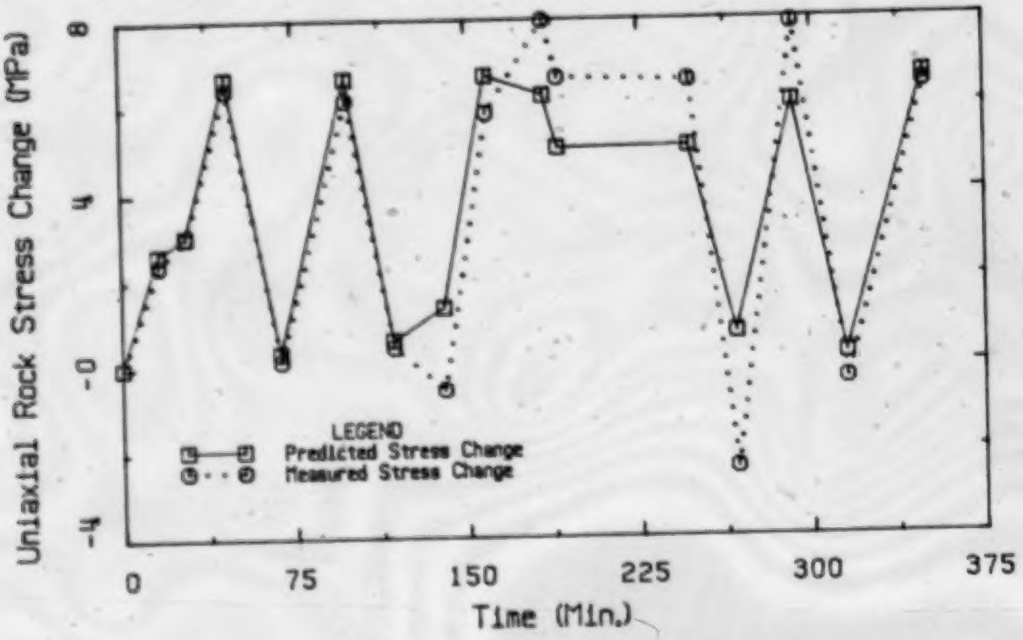

Figure 2.8 Measured and Predicted Uniaxial Rock Stress Change- Gauge 10, Tangential Gauge in Hole A

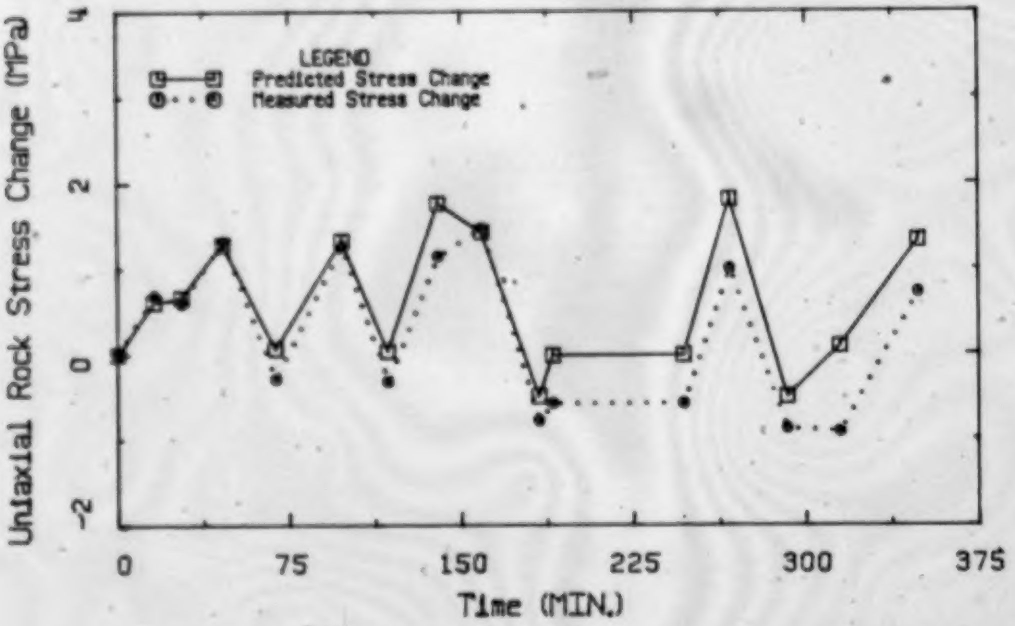

Figure 2.9 Measured and Predicted Uniaxial Rock Stress Change- Gauge 12, Radial Gauge in Hole A

directly beside the gauges and on Side 3, opposite the gauges.

Pariseau and Eitani (1977) found that the gauge sensitivity factor α is only about 4% less for elastic-plastic behavior as compared to that for perfectly elastic behavior. Thus, it appears that the actual tangential stress change occuring at this location is much greater than that predicted by elastic theory. McCreath (1981) has shown that large tangential stress concentrations can occur near the limit of the plastic zone in a yielded material (see Figure 2.10). The stress change measurements and results from the strain-time plots suggest that these gauges are located near the extent of the yielded zone.

The remaining six gauges were located in areas that appeared to behave elastically. The period of the wire vibration, or the gauge reading, has a range of 1500 to 4000 units (specified by the manufacturer) which actually represents a period change from $1500x10^{-7}$ to $4000x10^{-7}$ seconds. Results from gauge 3 (Figure 2.11), the tangential gauge in Hole F, are viewed with much skepticism because the upper limit of this range was exceeded on the first loading. Hawkes and Bailey (1973) stated that exceeding this limit may cause buckling of the high tension wire which would produce incorrect results. It was found by Cook and Ames (1979) that when this range was exceeded an artificial change in reading occurred due to excitation of the wire.

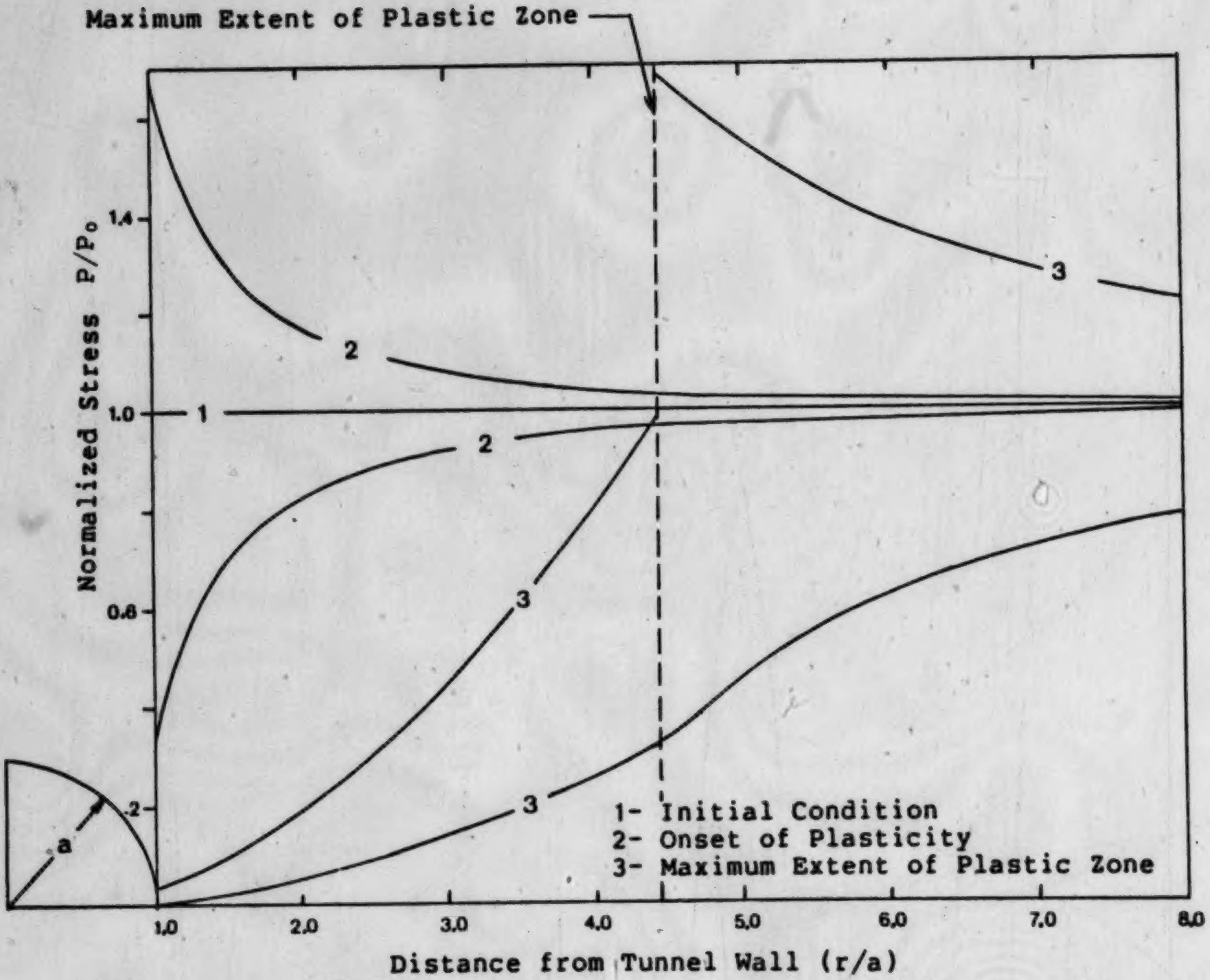

Figure 2.10 Example of Stress Distribution When a Yielded Zone Exists Adjacent to the Opening

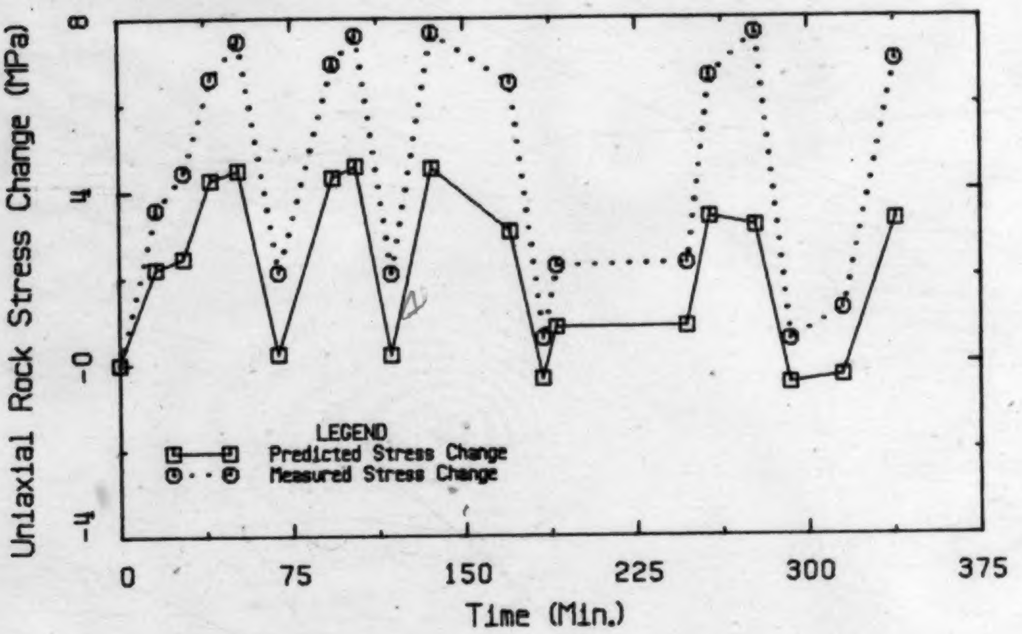

Figure 2.11 Measured and Predicted Uniaxial Rock Stress Change- Gauge 3, Tangential Gauge in Hole F

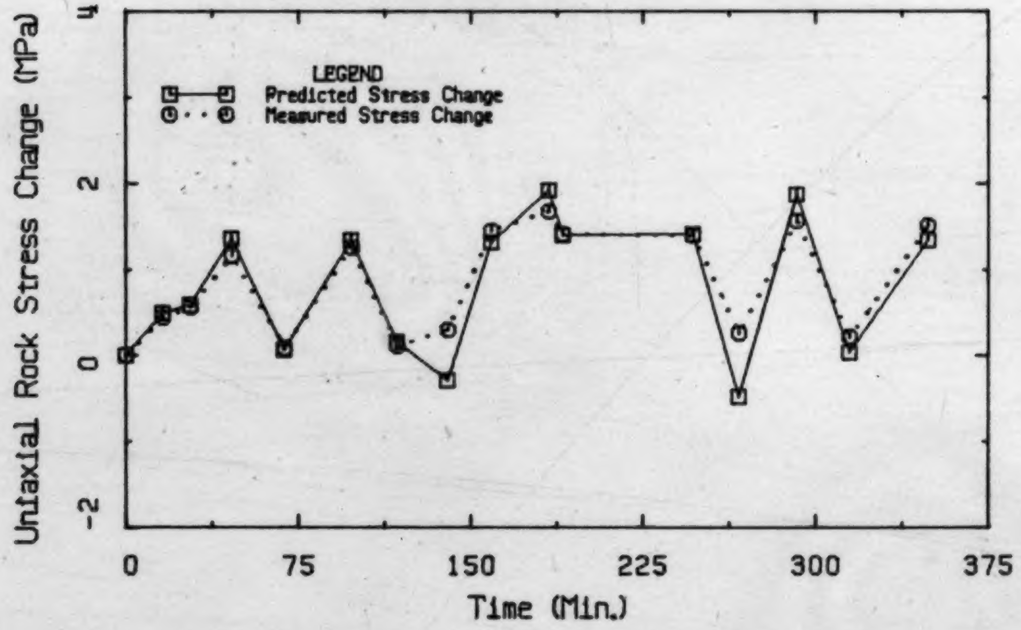

Figure 2.12 Measured and Predicted Uniaxial Rock Stress Change- Gauge 4, Radial Gauge in Hole F

Figures 2.12 to 2.16 show the results for the five other gauges. The agreement between the measured and predicted values for all of these gauges is very good for the first one or two loading cycles. Later in the loading history the magnitude of the measured values varies from the predicted stress change, but the trends are followed closely, i.e., if an increase is predicted the gauge measured an increase. Jaworski *et al.* (1982) have shown that the uniaxial gauge sensitivity factor a may change with repeated loading due to local yielding at the contacts. Findings from the calibration tests concur with this observation.

2.4 Re-evaluation of Field Data from Kipp Shaft

In 1980 a field monitoring program was conducted during the sinking of a vertical shaft at Kipp near Lethbridge in southern Alberta. A description of the project along with details of the instrument installations and a summary of the previous findings is given by Kaiser *et al.* (1983a).

Stress change measurements at this site were used to predict the in situ stress field by Kaiser *et al.* (1982) and Mackay (1982). In both cases the measurements were interpreted assuming that the stress change recorded by the gauge was independent of the stress normal to the gauge, i.e., a radially oriented gauge measured only the radial stress change. Kaiser *et al.* (1983a) re-evaluated these results accounting for the influence of the stress in the

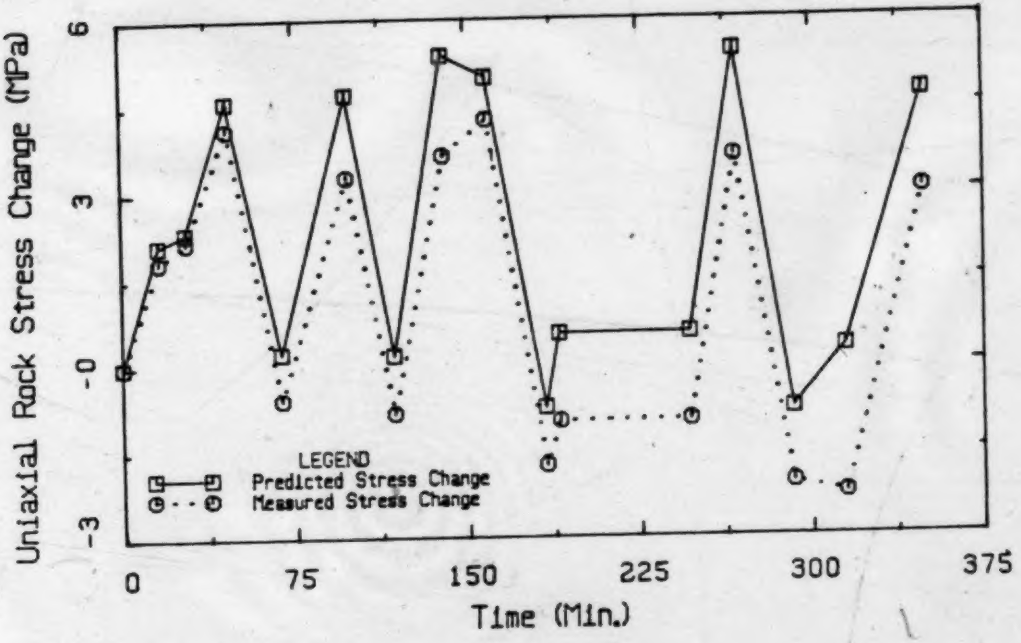

Figure 2.13 Measured and Predicted Uniaxial Rock Stress Change- Gauge 8, Tangential Gauge in Hole C

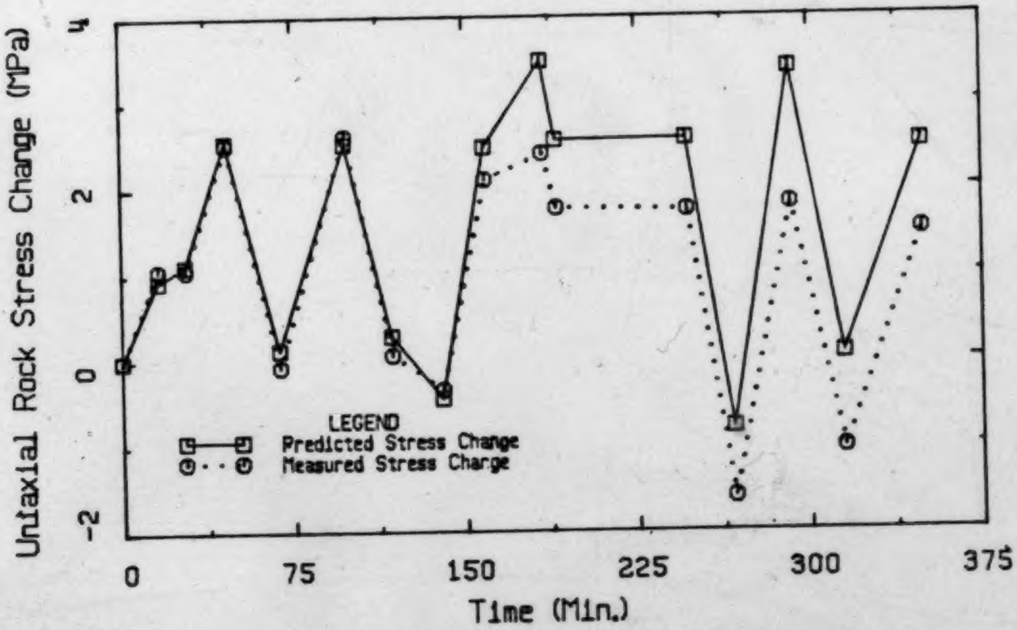

Figure 2.14 Measured and Predicted Uniaxial Rock Stress Change- Gauge 2, Radial Gauge in Hole C

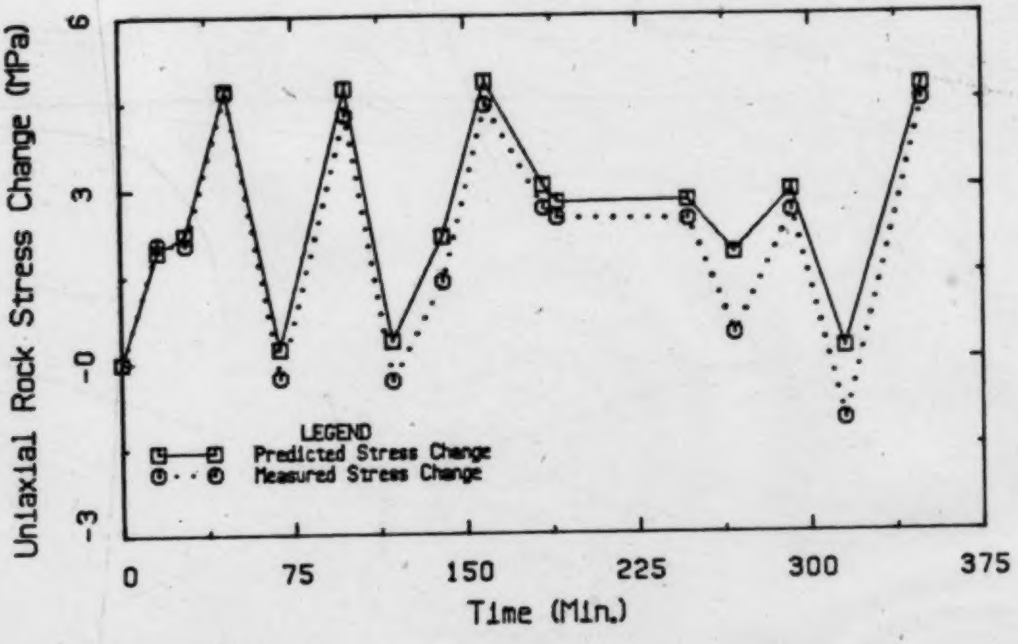

Figure 2.15 Measured and Predicted Uniaxial Rock Stress Change- Gauge 5, Tangential Gauge in Hole E

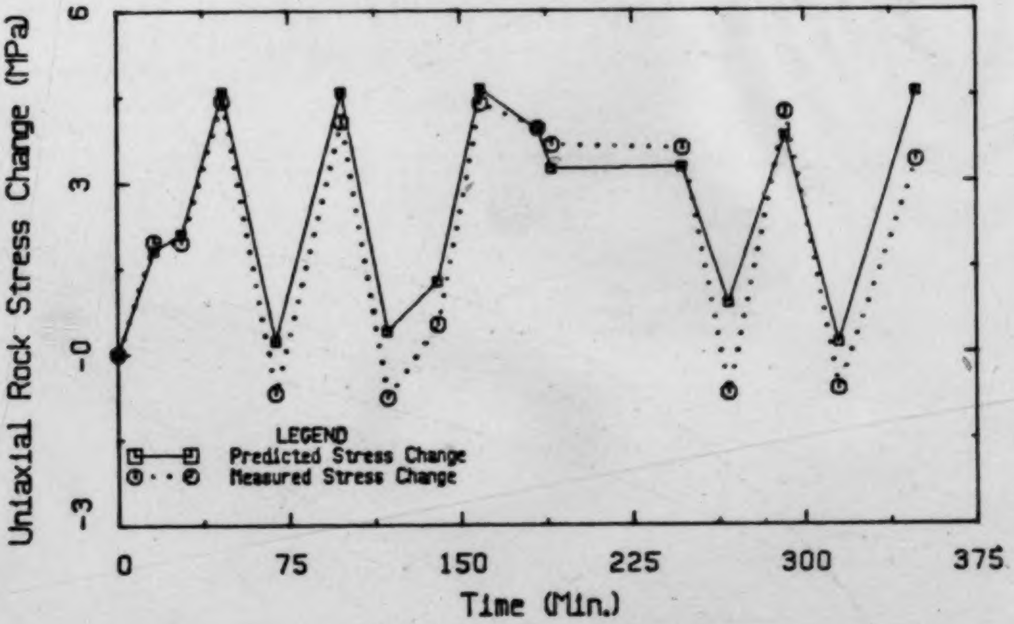

Figure 2.16 Measured and Predicted Uniaxial Rock Stress Change- Gauge 6, Tangential Gauge in Hole B

direction normal to the loading axis of the gauge and present a detailed discussion of the results.

The findings from the three analyses have been reviewed and several observations pertaining to the data interpretation and selection of gauge locations can be made:

- an incorrect orientation of the major principal stress may be calculated when radial gauge results are not considered;
- neglecting the influence of the stress normal to the gauge does not appear to affect the determined orientation of the principal stress θ, but does affect the estimated magnitude of the principal stress; and
- gauges should be placed in the direction of the principal stress for the most accurate determination of the stress ratio N.

2.5 Rotation of Principal Stresses

Monitoring stress changes in situ may be complicated by a change in both the direction and the magnitude of the principal stress which may be caused by the excavation of an opening. It is important to determine the effect of rotation of the principal stresses on the gauge response to ensure correct data interpretation. Pariseau (1978) states that the data reduction formulae generally used for calculating in situ stresses from borehole deformation data are not applicable when there is a change in the direction of the principal stress. However, he shows by example that if the stress change in a given direction is used in the calculation rather than the change in the major (or minor) principal stress, the result is correct. Thus, when interpreting gauge results the stress change in a given direction must be considered rather than a change in magnitude of the principal stresses.

Several tests involving rotation of principal stresses were included in the loading histories and the gauge response was observed. The expected stress change was calculated as before and this was compared with the measured results.

2.5.1 Test Results

Results from the stress rotation tests are shown in Table 2.2 which provides the incremental measured and predicted stress changes during the principal stress rotation cycle. The discussion will concentrate on the results from the first test , Test MC7.09a, because the results from the following tests show similar trends, but with more discrepancy between the measured and predicted results. One of the main reasons for these increased differences is that repeated loading tends to create yielding at the contacts and also the shape of the borehole becomes less circular with the increasing number of non-uniform loads applied to the sample.

Table 2.2 Results From Principal Stress Rotation Tests

			Y-GAUGE ($\Delta\sigma$)		52°-GAUGE ($\Delta\sigma$)	
TIME (min.)	σ_x	σ_y	PREDICTED (MPa)	MEASURED (MPa)	PREDICTED (MPa)	MEASURED (MPa)
TEST MC7.09a						
32	10.33	10.03				
46	10.51	12.45	2.45	2.25	0.52	0.55
58	10.29	9.89	-2.57	-2.24	-0.56	-0.53
74	12.70	9.92	-0.78	-1.14	1.19	1.26
83	10.20	9.73	-0.65	0.05	-1.26	-1.27
TEST MC7.09b						
120	7.70	7.44				
154	7.67	12.56	5.13	5.41	0.87	0.47
173	12.73	12.78	-1.46	-1.15	2.54	2.89
193	12.51	7.46	-5.26	-6.08	-1.03	-0.73
207	10.21	10.00	3.32	2.83	-0.70	-0.98
TEST MC7.09c						
207	10.21	10.00				
254	12.69	7.48	-3.36	-3.07	0.79	1.04
280	10.28	10.04	3.36	2.85	-0.75	-1.05
291	7.69	12.55	3.38	3.13	-0.85	-1.26
303	7.32	7.45	-4.97	-5.15	-1.06	-1.01

Test MC7.09a also shows excellent agreement between the measured and predicted results for the 52° gauge. The results from the Y gauge show good agreement between the measured and predicted values when loading is in the direction of the gauge. Test MC7.09a illustrates that as the stress normal to the gauge loading axis becomes sufficiently larger than the stress parallel to it (at a time of 74 minutes), the agreement between the measured and predicted values is not so good.

When loading is at 90° to the gauge the borehole tends to become elliptical (with the major axis in the direction of the gauge) and the contact angle is reduced. Pariseau and Eitani (1977) show that as the contact angle changes a also changes. When the sample is unloaded back to a uniform stress condition not all of the strain is recovered and the hole does not return to its original circular shape, but remains oval shaped as shown in Figure 2.17a.

When the sample is loaded in the direction of the gauge the contact angle would increase, if there is not already full contact, and the borehole would become elliptical again, but with the major axis at 90° to the gauge. However, the high stiffness of the gauge resists deformation and the hole takes the shape shown in Figure 2.17b. This phenomenon is not as prominent when the gauge is set at an angle to the principal stress direction. Jaworski *et al*. (1982) reported that at 45° to uniaxial loading only a small increase in contact angle would be expected. Thus, the borehole would

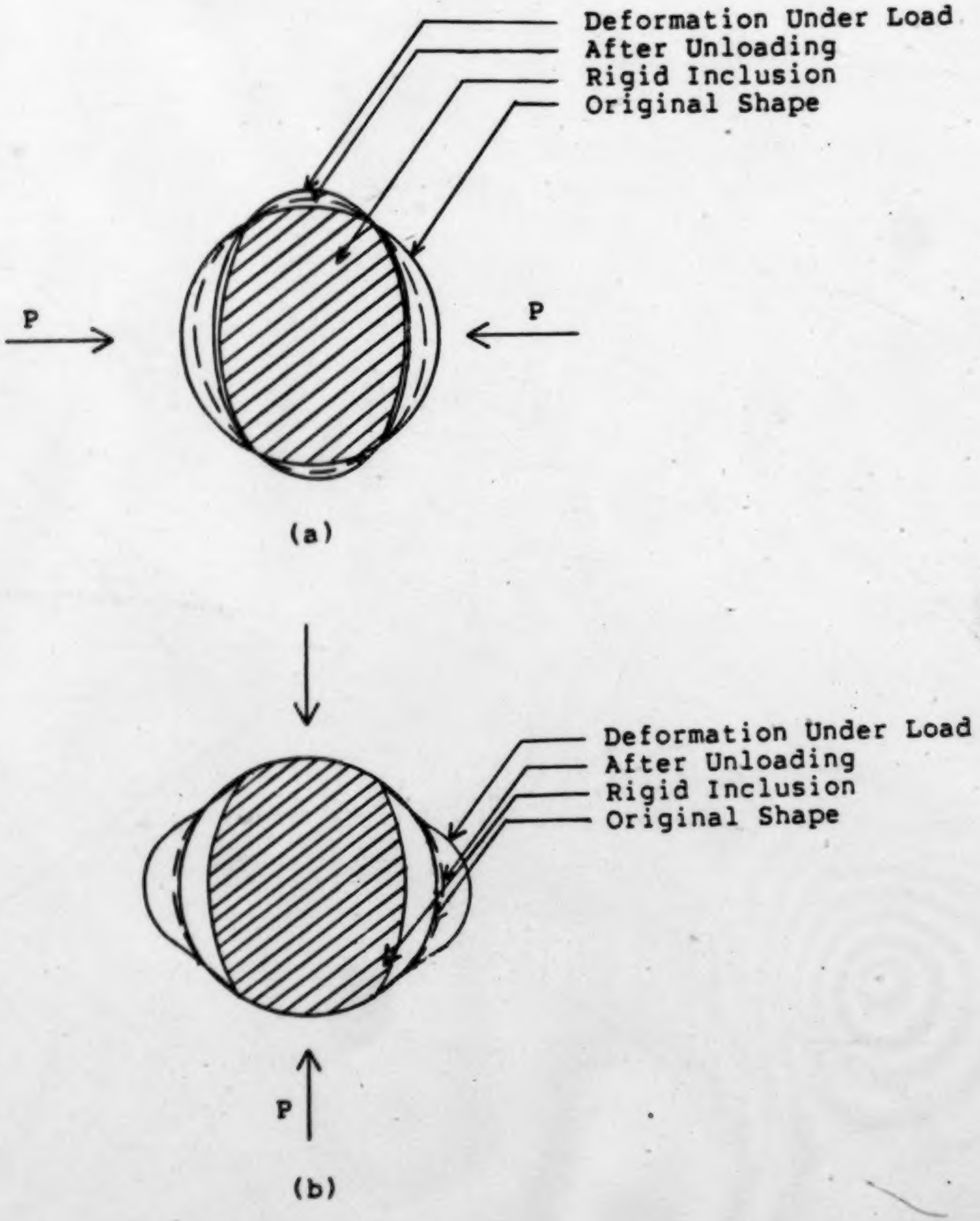
Deformation Under Load
After Unloading
Rigid Inclusion
Original Shape
P
P
(a)
Deformation Under Load
After Unloading
Rigid Inclusion
Original Shape
P
(b)

Figure 2.17 Borehole Deformation Caused by Uniaxial Loading and Unloading With a Rigid Inclusion Present for: a) Loading normal to the gauge axis; and b) Loading parallel to the gauge axis.

tend to remain more circular rather than take on an elliptical shape. Similar arguments apply for the 52° gauge. For this reason the results from the 52° gauge are expected to be more consistent than those from the Y gauge.

In conclusion, it follows that for stress determination around an opening tangential gauges would provide more reliable results than radial gauges when soft rock models are used. This is because there is generally a radial stress decrease and a tangential stress increase adjacent to an opening. However, for the hard rock gauge this condition would not be as significant because the initial contact angle between the gauge and the borehole is much smaller. The laboratory results have shown that the method of interpreting the gauge response can be applied to cases where there is rotation of principal stresses, but if repeated loading occurs errors in the measured stress change may arise.

2.6 Stress Redistribution Tests

2.6.1 Background Information

Stress redistribution is one factor that is associated with the time dependent behavior of an opening. It is usually caused by creep and yield processes. Kaiser and Morgenstern (1981) identify several major deformation processes which may lead to stress redistribution:

a) stress redistribution due to time dependent rock mass deformation properties;

b) stress redistribution due to non-homogeneous creep properties such as local soft spots or stiffness variations;

c) stress redistribution due to local yielding;

d) stress redistribution due to global yielding; and

e) stress redistribution during failure propagation due to time dependent "post-peak" strength loss.

Although the stresses usually are not an observable quantity it is important to recognize the transfer mechanism associated with the time dependent deformation because it may have an effect on the overall equilibrium of the opening. Very few field measurements are available (in the literature) pertaining to the stress redistribution around an opening. Da Fontoura (1980) summarized analytical work by Aiyer (1969) who investigated the stress redistribution around a cylindrical opening in a visco-elastic isotropic medium under uniform stress. He found that initially stress redistribution occurs such that there is a decrease in tangential stress near the opening wall and an increase in zones further from the wall (see Figure 2.18). This figure shows that the stress transfer process occurs at a decreasing rate and the majority of the stress change occurs within the first day of creep. For a given set of material properties, Nair *et al*. (1968) and da Fontoura (1980) also

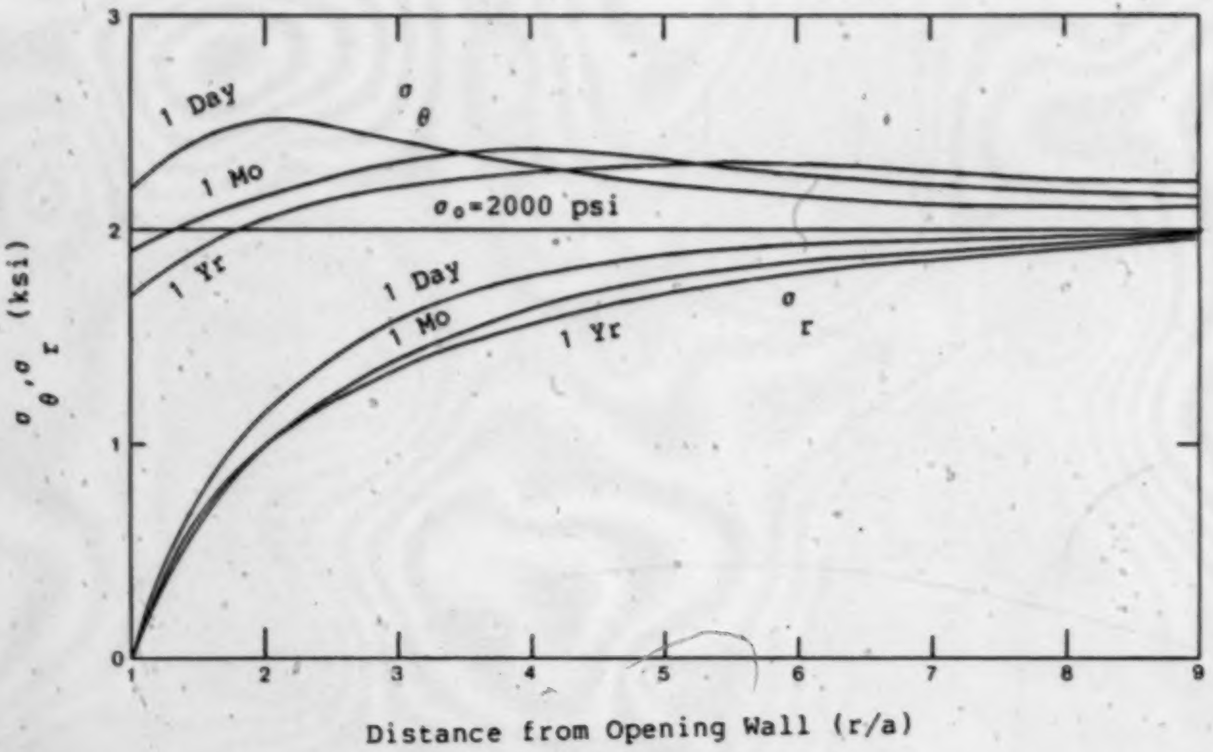

Figure 2.18 Stress Distributions with Time Around an Unlined Circular Opening

observed that most of the stress redistribution occurred within the first 24 hours. Radial stress change also occurs, but it is of a much smaller magnitude than the tangential stress change. Tangential stress change measurements around a 2.0 m diameter circular opening in a deep salt mine in Yugoslavia [Osmanagic and Jasarevic, 1976] show a reduction in the tangential stress near the wall (Figure 2.19) which agrees with findings by Aiyer (1969).

An empirical creep relationship to describe the time dependent deformations around an opening and a differential equation describing the time dependent stress redistribution for a two dimensional axisymmetric plane strain boundary value problem were presented by da Fontoura (1980). To check the accuracy and validity of his procedure da Fontoura used the results from laboratory tests reported by Guenot (1979). These tests were performed on coal, using the same laboratory equipment employed during the present investigation. A linear elastic material model was used by da Fontoura (1980) to describe the initial material behavior. A Young's modulus of 1000 MPa and a Poisson's ratio of 0.3 were chosen. The sample had a 120 mm diameter opening in the center and was subjected to a stress level of 4.8 MPa with a stress ratio of approximately 1.0. Results from da Fontoura's (1980) simulation showed that the radial and tangential stress distributions were relatively constant with time.

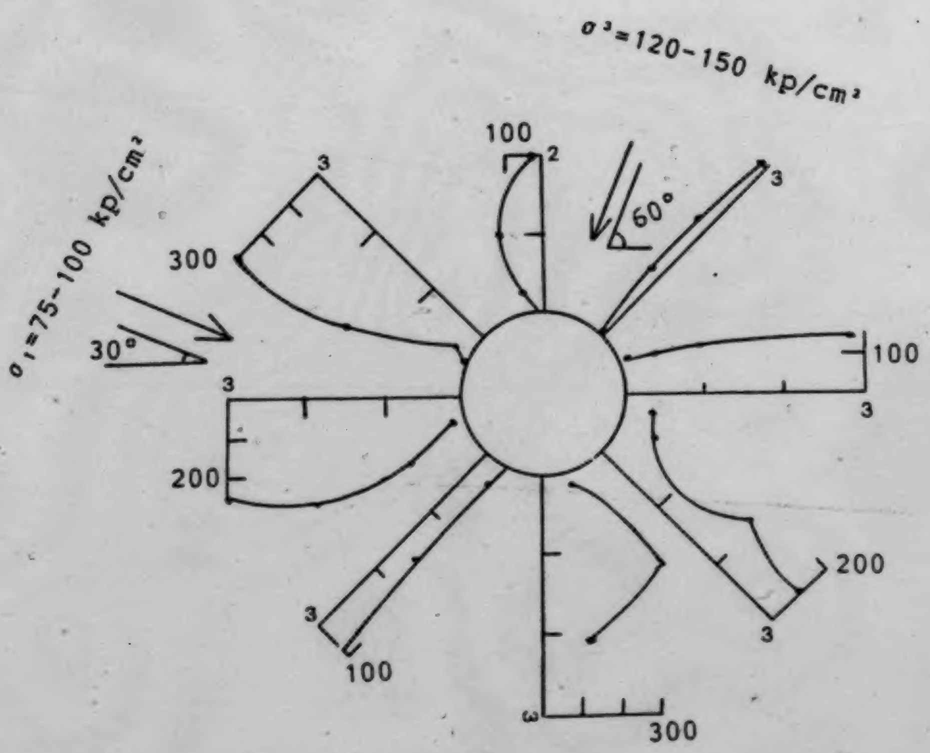

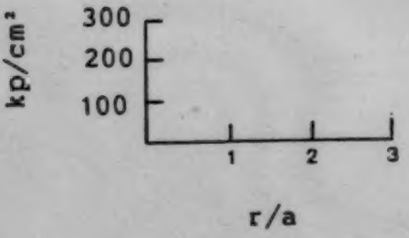

Scale

Figure 2.19 Tangential Stress Distribution Around an Opening in Salt

Further simulations by da Fontoura (1980) indicated that varying the creep parameters may have a significant effect on the amount of tangential stress redistribution near the opening, but the amount of radial stress redistribution always remained small. Larger changes in stress level were associated with larger creep movements. It was also shown that increasing the deformation modulus led to greater tangential stress redistribution. For an initially 'elastic' stress distribution the change in stress level reaches values of less than 25% at points as close as one radius to the opening wall. Based on this, da Fontoura (1980) states that if appreciable creep strains are not caused, the area of stress redistribution would be more or less concentrated around the opening. An important conclusion from da Fontoura's (1980) work was that the stress redistribution process is highly dependent on the creep properties of the medium.

Lacerda and Houston (1973) did work on the relaxation behavior of clay and found a linear stress drop with the log of time with the slope of all curves being similar. They also found a delay in the stress relaxation response with the logarithm of the time delay being proportional to the time spent reaching the initial stress. From a review of these and other reported findings da Fontoura (1980) suggested that the relaxation behavior could be described by the following equation:

$$\sigma = \sigma_o - (s)\log(t/t_o) \qquad \text{Eqn.2.8}$$

where σ = the current stress;

σ_o = stress associated with t_o;

t = total time elapsed; and

t_o = time delay.

2.6.2 Laboratory Testing Program

Three tests were performed to measure stress redistribution and relaxation in the coal. The first test was conducted immediately following the installation of the two gauges (see Figure 2.2 for gauge locations) to measure the stress relaxation that occurred in a 12 hour period. A second test was done with the gauges at the same locations following the application of the loading history. Finally, three constant stress tests were conducted with the gauges placed around the 152 mm diameter opening at the locations shown in Figure 2.6. For all the tests a constant uniform boundary stress was applied for the duration of the test and displacements were allowed to occur without restraint.

2.6.3 Test Results and Analysis

2.6.3.1 Without Opening- Before Loading History

Figure 2.20 shows a plot of the uniaxial stress change measured by the gauges with the logarithm of time for the constant stress test performed on the sample with no opening under a uniform stress of 7.5 MPa. This test studies the

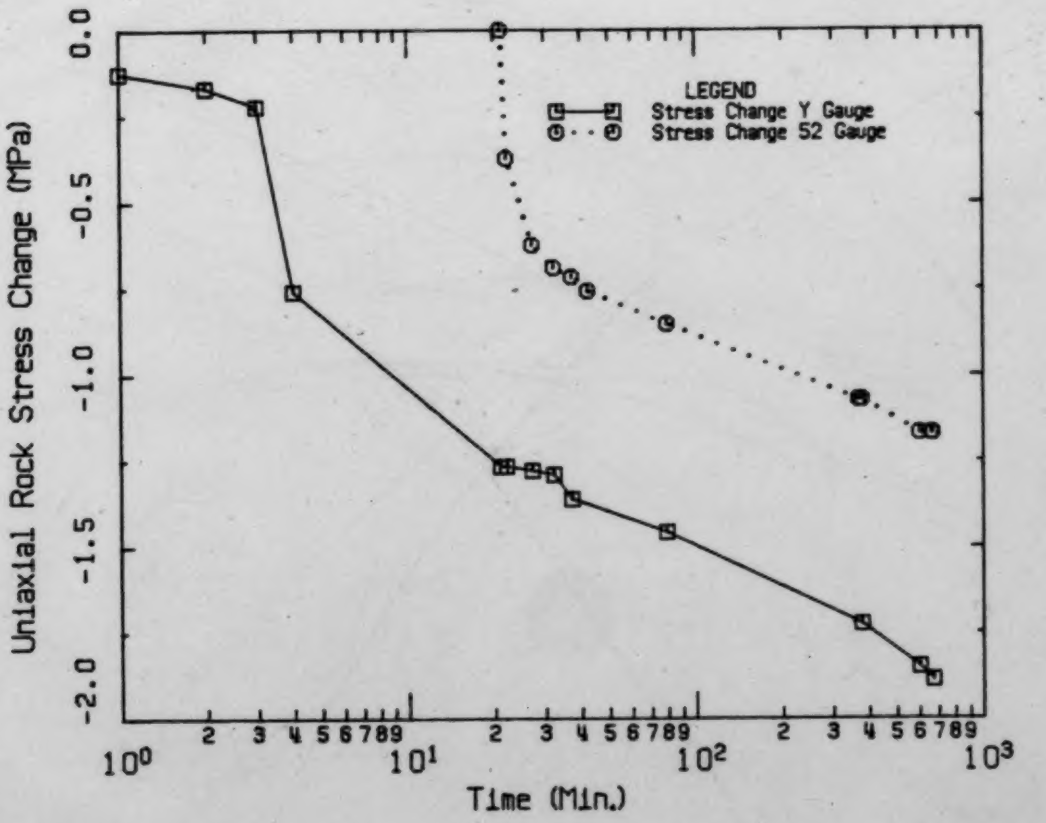

Figure 2.20 Constant Stress Test- Without Opening in Sample Before Loading History (Gauge locations shown in Figure 2.2)

stress relaxation behavior of the coal. It is not a true relaxation test because displacements are not restrained. The large initial stress drops that are recorded by both gauges correspond to the setting of the gauge and the subsequent release of the setting tool. Following this, the curves become approximately linear with the logarithm of time (at a time of 40 minutes) with the curves from both gauges being closely parallel. This agrees with the findings by Lacerda and Houston (1973). The curves can be described by the relationship given by da Fontoura (1980) in Eqn. 2.8.

Only one stress level was tested here and it is not known if "s" is a function of the stress level for this material. A slope of s = 0.357 can be calculated for the uniaxial stress relaxation in the coal at this stress level. Previous tests performed on the intact sample were at relatively low stress levels and there were no indications of yielding at this time.

2.6.3.2 Without Opening- After Loading History

Results, recorded by the same gauges, from the constant stress tests carried out after the loading history are shown in Figure 2.21. The sample was again under uniform load, but a stress level of 12.5 MPa was used for this test. A small time delay, varying from 3 to 20 minutes, was observed before the curves became linear which agrees with observations made by Lacerda and Houston (1973). During the loading history the maximum stress level achieved was 12.5 MPa and it is possible that local crushing of the asperities

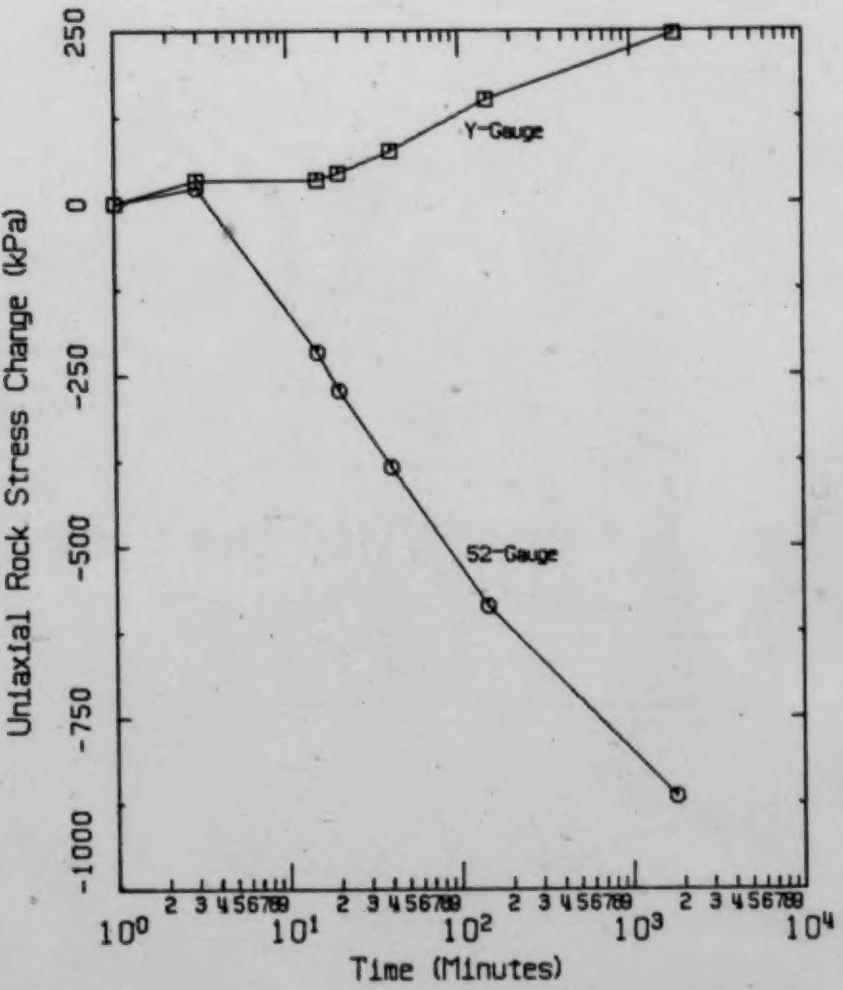

Figure 2.21 Constant Stress Test- Without Opening in Sample After Loading History (Gauge locations shown in Figure 2.2)

may have taken place at the contacts between the gauge platens and the borehole wall. It has been shown earlier that the uniaxial stress at 52° to the Y axis does not reach the same high stress levels experienced by the Y gauge which would suggest that crushing of the asperities would be greater in the Y direction. If only relaxation occurs the results from this test should match those from the previous test if "s" is independent of stress level.

Inspection of Figure 2.21 shows that the stress change recorded by the 52° gauge closely corresponds to that measured in the previous test . Here the slope of the line is s = 0.343 compared with s=0.357 previously. This suggests that "s" is independent of the stress level which concurs with Lacerda and Houston (1973) who found that all curves were closely parallel. Results from the Y gauge do not at all match the previous ones. The gauge records an increase in the stress (s = -.12) which would indicate that some stress redistribution is occurring. At present this is believed to be due to both local yielding at the contacts and the changing shape of the borehole with the application of loads normal to the gauge axis, as was discussed in Section 2.5 and illustrated in Figure 2.17.

2.6.3.3 With Opening- After loading History

Three constant stress tests were done following the repeated loading at stress levels of 10.92, 11.30 and 11.95 MPa and ranging in duration from 27 to 69 hours. It has been noted previously that, following the loading history, all of the gauges, with the exception of numbers 10 and 12 placed in stressmeter hole A, were in locations where behavior corresponded to that predicted by a linear elastic model.

Plots showing the uniaxial stress change with time for three of the gauges in the elastic areas have been included in Appendix B, Figures B.18 to B.20. In each of these locations the total amount of stress redistribution that occurred was less than 1% of the boundary stress. These three gauges are all close to or more than one radius away from the opening and no appreciable creep deformations were occurring at the locations. An insignificant amount of stress redistribution occurred which is in agreement with predictions by da Fontoura (1980).

The other two gauges in the elastic area, numbers 5 and 6, are located in separate holes that both lie close to the diagonal running perpendicular to the jointing. Since both gauges were set tangentially they have their loading axis approximately parallel to the jointing. Results from these two gauges are shown in Figures 2.22 and 2.23. The increase in stress recorded by these gauges may be due to slip along the discontinuities. However, the amount of stress redistribution occurring is only about 2% of the boundary stress and more data is required to confirm this hypothesis.

Gauges 10 and 12 were located within a zone that showed signs of yielding during the loading history. Figures 2.24 and 2.25 show the results for gauges 10 and 12, respectively. The tangential gauge results from the test at

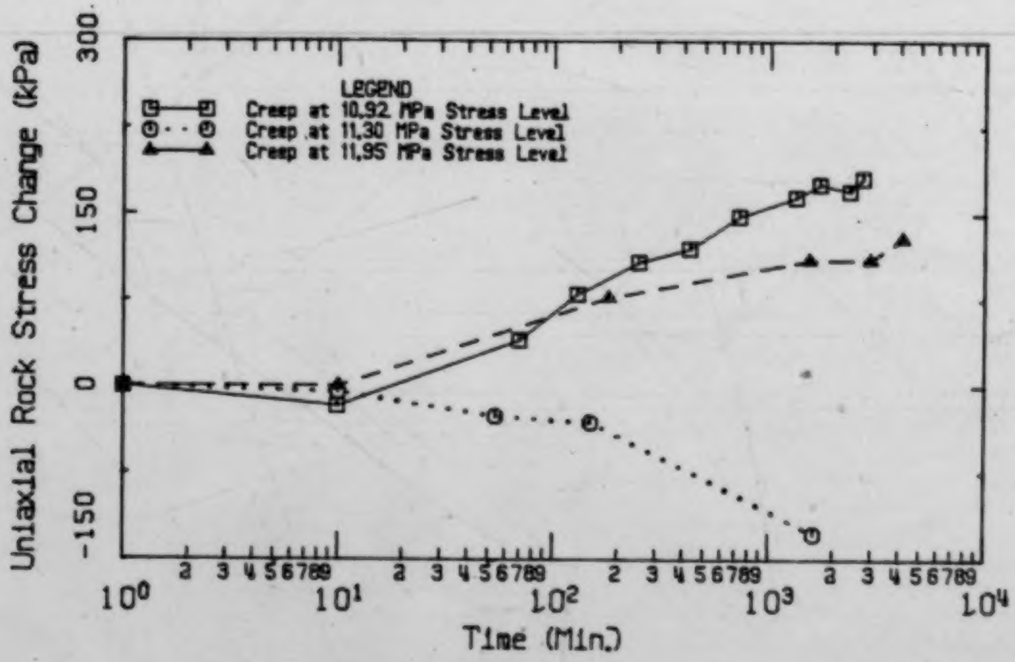

Figure 2.22 Stress Redistribution Test- Gauge 5 Tangential Gauge in Hole E (Gauge locations shown in Figure 2.6)

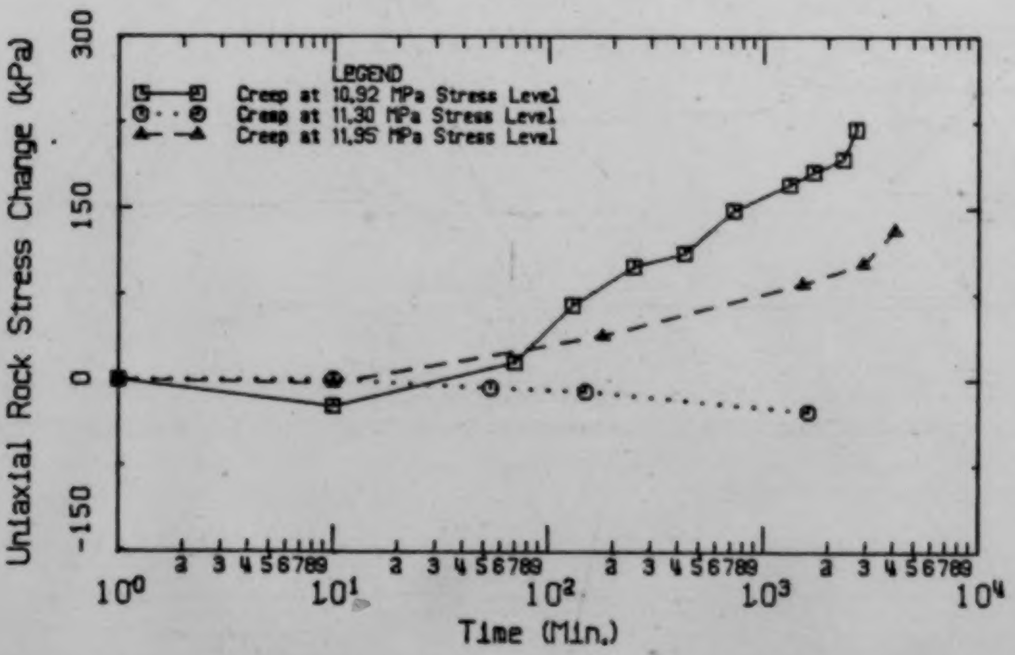

Figure 2.23 Stress Redistribution Test- Gauge 6 Tangential Gauge in Hole C (Gauge locations shown in Figure 2.6)

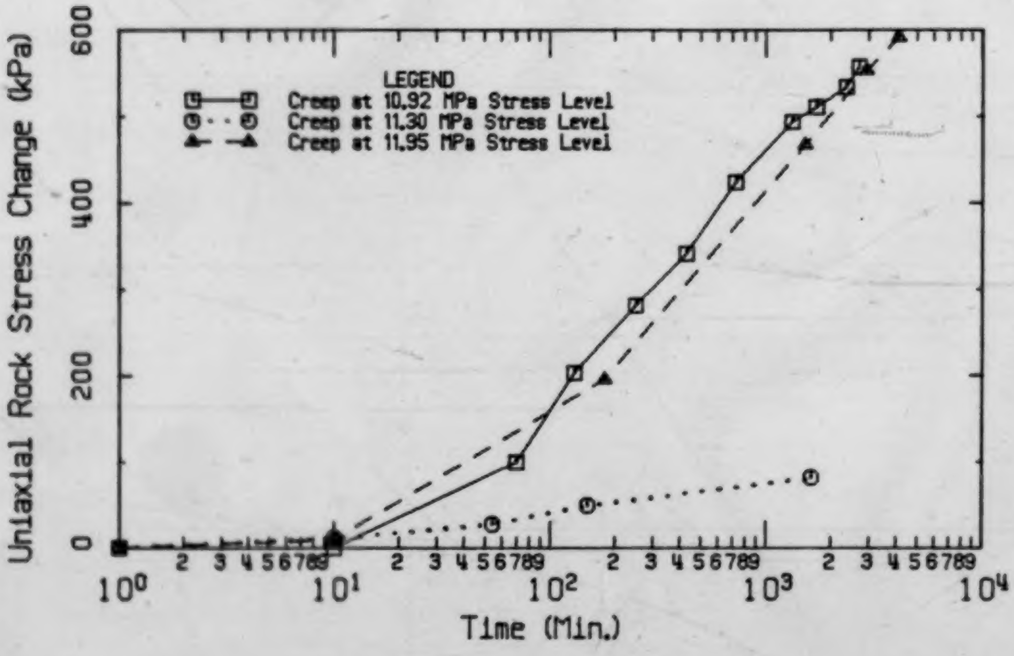

Figure 2.24 Stress Redistribution Test- Gauge 10 Tangential Gauge in Hole A (Gauge locations shown in Figure 2.6)

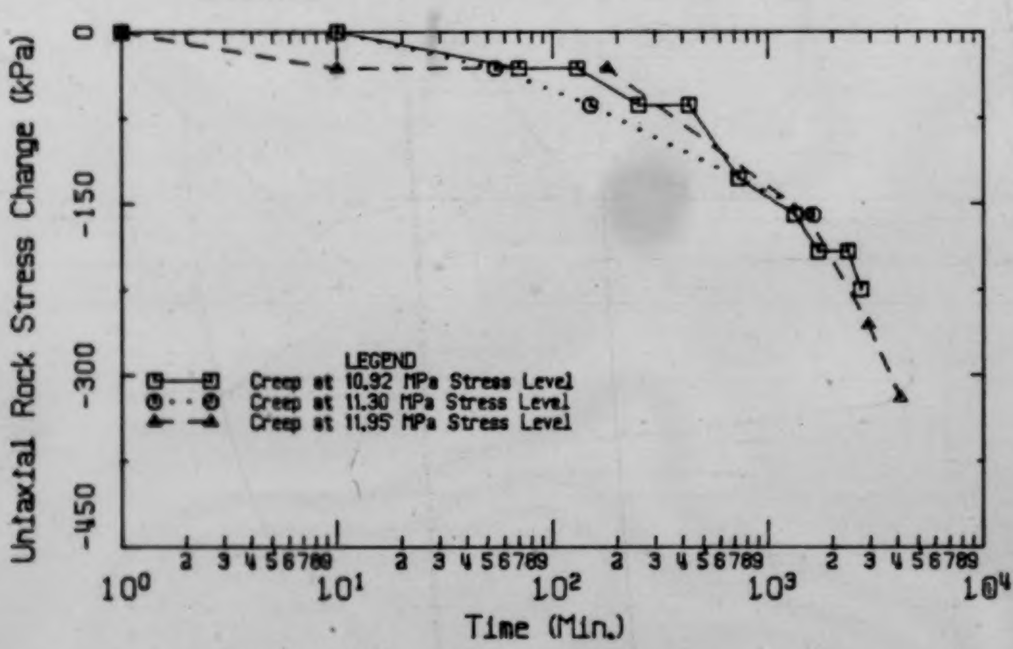

Figure 2.25 Stress Redistribution Test- Gauge 12 Radial Gauge in Hole A (Gauge locations shown in Figure 2.6)

11.30 MPa show a relatively small amount of stress increase with time. The load increment applied to reach this stress level was only 0.38 MPa, 3.5% of the boundary stress. It is possible that the sample did not respond to this small increase as a change in stress conditions. If this is the case, the measurements from the gauge at 11.30 MPa should provide an extension of the curve from the previous stress level. When these measurements are included with those from the previous test the results follow the trend of the existing curve at 10.92 MPa stress level. This hypothesis is supported by the strain measurements that show much smaller strains occurring at the 11.30 MPa stress level (see Appendix B, Figure B.21).

The tangential gauge (number 10) shows a stress increase that is closely linear with the log of time and the radial gauge shows a similar decrease. Extensometer measurements indicate that this area has been yielded for the entire depth of the sample and therefore, it may be valid to assume that the gauges are responding as if they were coplanar, i.e., that the stress change in the radial and tangential directions is the same for the entire depth of the borehole. If this is true, the gauge readings can be separated into actual radial and tangential stress changes. This has been done for the results from the tests at 10.92 and 11.95 MPa and the new curves are shown in Figure 2.26.

The results show that the radial stress fluctuates above and below the zero stress change level and eventually

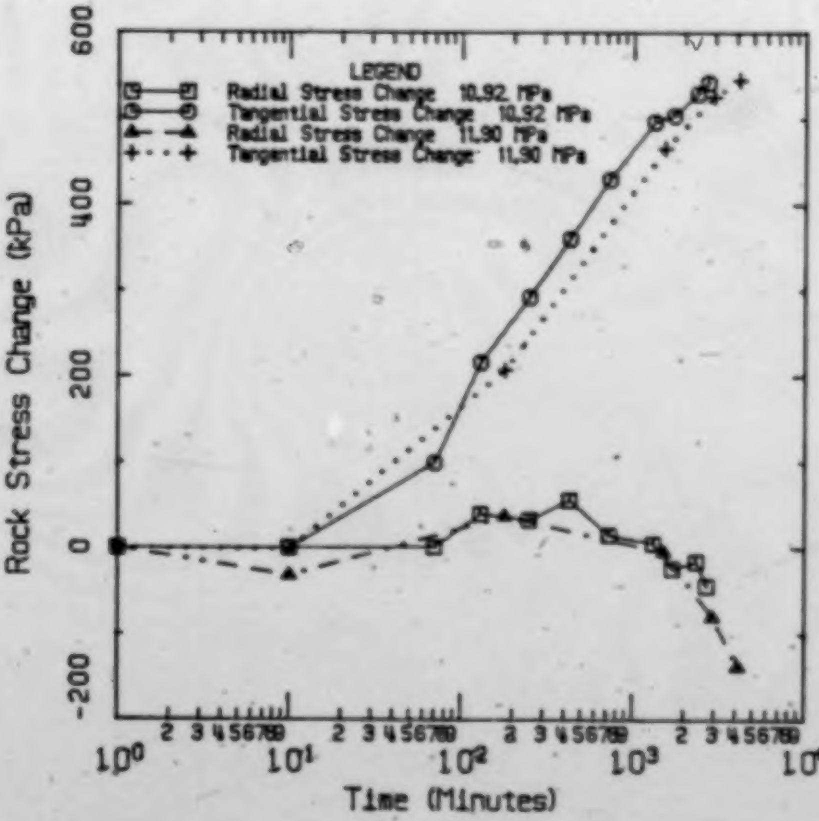

Figure 2.26 Radial and Tangential Stress Distribution in Yielded Zone

there is a small decrease. Within a yielded zone near the opening wall the radial stress is small and therefore, would not be expected to exhibit much stress change with time (for an unlined opening). Stress in the tangential direction shows an increase that, after an initial time delay, is approximately linear with the log of time. The curves at both stress levels have similar slopes. These results confirm expectations that the tangential stress increases with time in a yielded zone adjacent to an unsupported opening.

2.6.4 Effects on the Ground Convergence Curve

Rock mass properties may change with time due to creep effects [Ladanyi, 1974] and this can be reflected by stress redistribution. As noted in Section 2.6.3.3 this may have serious implications on the stability of an opening. Figure 2.27 shows characteristic curves for the case of a circular opening excavated in a uniform stress field for both the short and long term. Ground convergence curves are shown for the linear elastic case (Curve 1) and for yielding ground (Curve 2) for the short term. Within the yielded zone the lab tests indicate that a tangential stress increase and a radial stress decrease occur. This redistribution is more significant than that in areas that behave elastically. A reduction in the radial stress contributes to a loss in the load carrying ability of the ring of rock in the immediate vicinity of the opening. With time the ground convergence

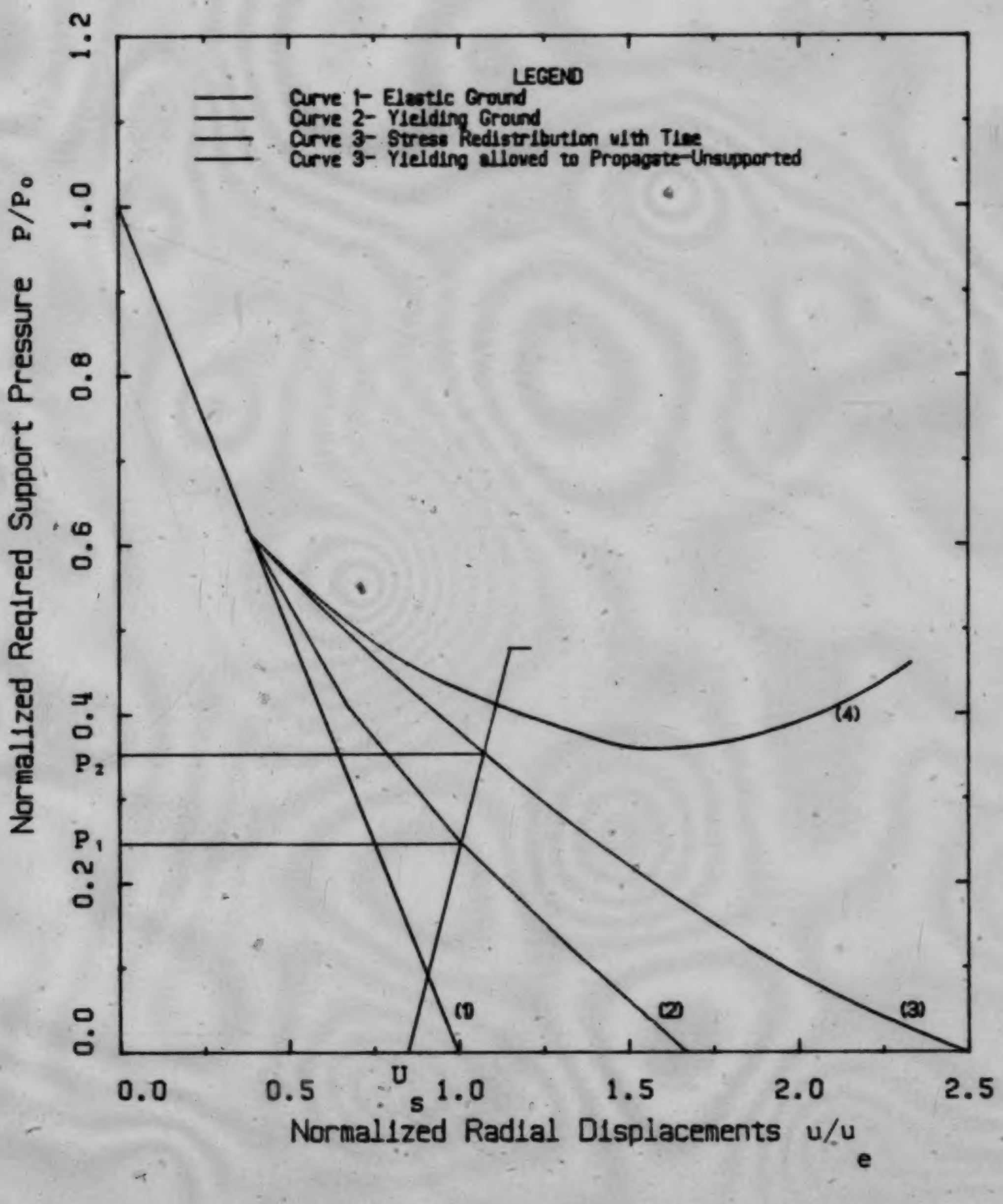

Figure 2.27 Short and Long Term Characteristic Curves for a Circular Opening in a Uniform Stress Field

curve shifts to the right (Curve 3). If the opening was approaching an unstable condition and no support was applied yielding may propagate and the opening may become unstable (Curve 4).

The presence of a liner restricts the amount of time dependent radial displacement that can occur at the tunnel wall and thus, the radial stress near the wall is prohibited from decreasing. This is reflected in an increase in the equilibrium support pressure. For example, a support may be installed at U_s (see Figure 2.27) and a support load of P_1 is anticipated, but as time passes there are time dependent deformations and the pressure on the lining builds up to P_2. It is important to account for time effects when dimensioning linings to ensure that adequate support capacity is provided.

2.7 Overcoring Test

2.7.1 Introduction

The overcoring test was performed following the calibration test with the two gauges located near the center of the sample. Figure 2.2 shows the location of a 102 mm diameter stress release channel that was drilled over the 38.1 mm diameter stressmeter hole. The stress relief channel was drilled with the sample at a uniform stress of 12.5 MPa. In considering the results, it is important to recall that the stress change recorded by the gauges is affected by changes in both principal stresses. Since the sample is loaded uniformly, it is reasonable to assume that the stress change in the X and Y directions will be equivalent. The following sections present an analysis of the test results.

2.7.2 Test Results

The stress relief channel was drilled at a constant rate (see Figure 2.28) until it had passed beyond the bottom of the lower gauge. At this time difficulties were encountered and there was a delay prior to completing the overcoring hole. However, the results were not affected because all of the stress change had occurred prior to this delay.

Figure 2.29 shows the changes in stress in the X and Y directions, calculated from the gauge readings, plotted against time. The times when the core barrel reached the top and bottom of each gauge is indicated. The 52° gauge is located close to the top of the sample and the measurements observed prior to the stress relief channel reaching the top of the gauge may be affected by the proximity of the boundary. At the time when the stress relief channel reached the top of the lower gauge a stress increase of 2.45 MPa, approximately 19.6% of the field stress, was recorded. This value was calculated based on a uniaxial gauge sensitivity factor of $\alpha=11.23$.

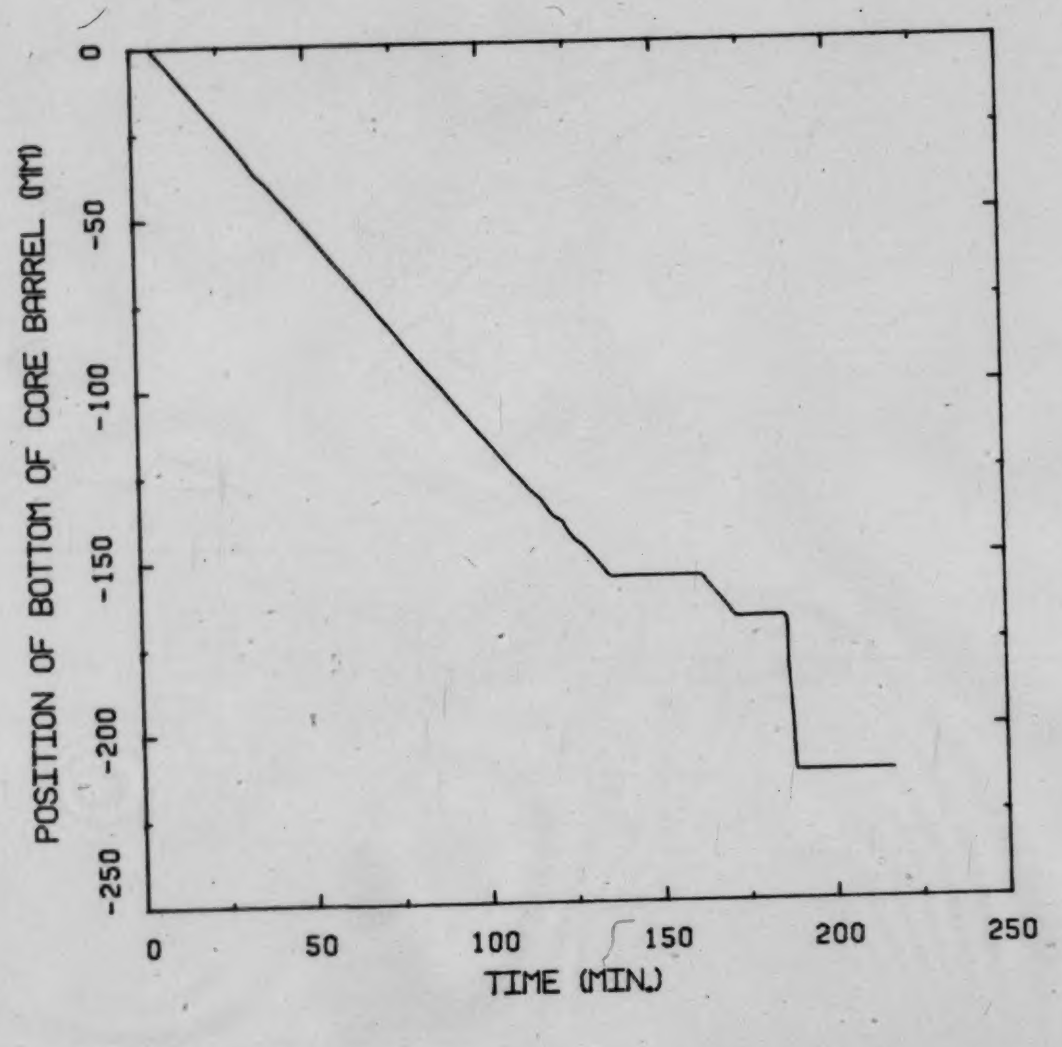

Figure 2.28 Rate of Advance During Overcoring

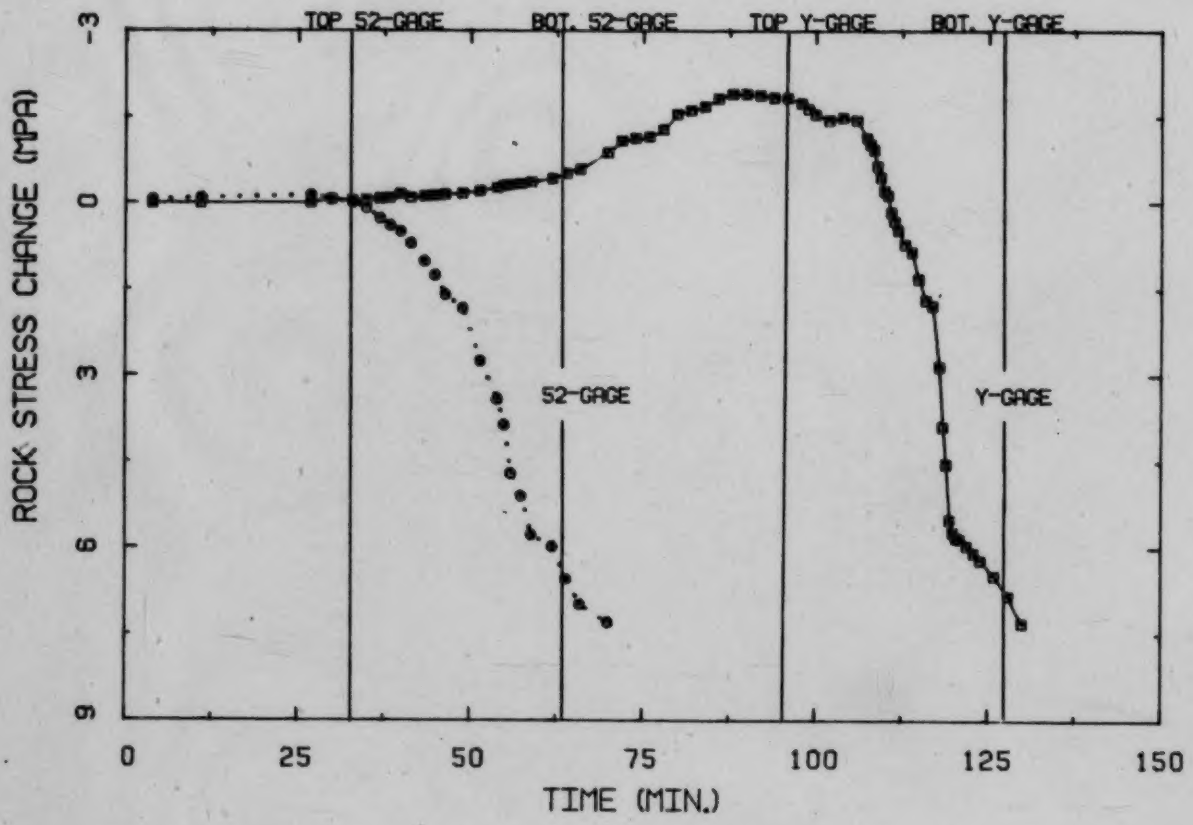

Figure 2.29 Rock Stress Change Measured During Overcoring

2.7.3 Analysis of the Results

In order to analyze the results, the stress change at the end of a flat borehole was considered. Only results from the Y gauge will be assumed valid because of potential boundary effects on the other gauge. Several simplifications have been made to allow for the use of an axisymmetric finite element analysis. First, it was assumed that the gauge was located directly in the center of the stress relief channel. Second, the mesh employed for the analysis was similar to the one used for the analysis of the field data, but with a few minor modifications (see Figure 2.30). This mesh does not match the exact test conditions because the boundary where excavation begins is much further away from the gauge than in reality. However, the lower gauge is 3 borehole diameters from the top of the sample and this inconsistency should not have a significant effect on the results. All of the elements were removed from the stressmeter hole except those at the gauge locations which were assigned a stiffness of 39.3 MPa, equal to that of the gauge [Hawkes and Bailey, 1973]. The longitudinal load was set to 0.2 times the load perpendicular to the tunnel axis to model the laboratory conditions. The stress relief channel was excavated incrementally to the top of the Y gauge by reducing the stiffness of the elements in the opening to a very low value. In Chapter 4 it will be shown that this method of incremental excavation predicts stresses and displacements that are in good agreement with those from

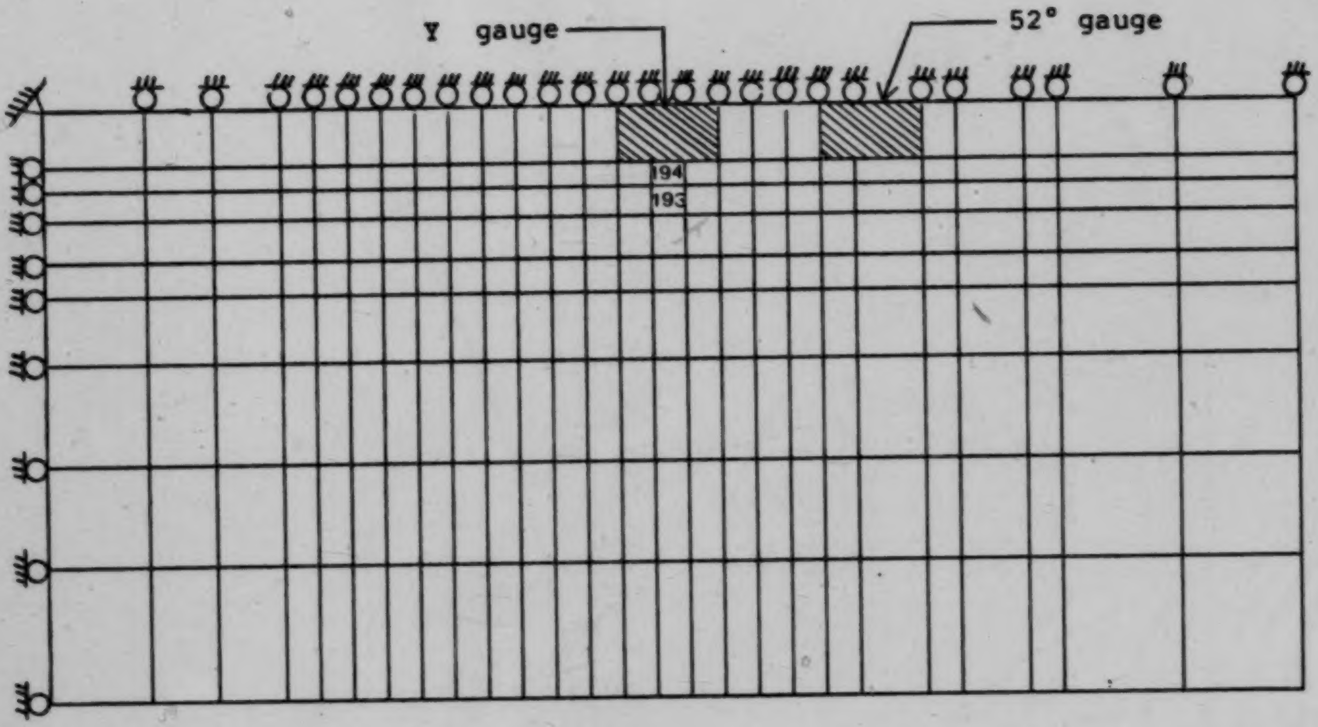
Y gauge
52° gauge
194
193

Figure 2.30 Finite Element Mesh Used for Analyzing Overcoring Results

closed form solutions and other analyses.

The result of interest is the amount of stress increase that occurs in the elements ahead of the face when the overcoring channel is at the top of the gauge. To determine the theoretical stress change at the gauge location the two elements directly below and in the centre of the gauge were considered, elements 193 and 194 (see Figure 2.30 for locations). These showed an average stress concentration equal to 18.7% of the initial boundary stress. Recalling that the stress change measured at this point was 2.45 MPa the boundary stress can be back-calculated to be 13.1 MPa, assumming a uniform stress condition exists. This is in good agreement with the actual boundary stress of 12.5 MPa. However, the measured value of 2.45 MPa was determined based on a uniaxial gauge sensitivity factor of α=11.23. The value of α during the final loading for the Y gauge was found to be 12.56. If this new α value is used the measured stress change would be 2.19 MPa or 17.6% of the boundary stress and the back-calculated initial stress would be 11.80 MPa, still within 6% of the actual value. Either one of these α values would produce a back-calculated boundary stress that closely corresponds to the known value.

This analysis is not completely correct because the stressmeter was not located in the centre of the stress relief channel. Also, with only one gauge, it was necessary to know that a uniform stress field existed in order to employ this analysis to back-calculate the boundary stress.

More results are required to determine the applicability of this instrument for use in back-calculating the in situ stress field by this method. The results from this study are encouraging, but are too few to draw definite conclusions. If the gauges are preloaded to a high enough value, i.e. to a stress greater than the field stress, they may not become loose in the hole if adequate cover is provided. For this case the total stress changes recorded by the gauges could also be used to calculate the field stress. Thus, a second method of estimating the stress field could be employed as a check.

2.8 Conclusions from Laboratory Testing

This chapter has presented a re-evaluation of the method of interpreting the data from the vibrating wire stressmeter. The technique of data interpretation has been verified through calibration tests on a large coal sample. After gaining confidence in the method of analyzing the gauge results several stress redistribution tests were performed in the lab and the results from the Kipp shaft were re-evaluated.

It was found that if the gauges were not subjected to repeated loading they would predict the actual stress change with high accuracy. However, with continued cyclic loading the borehole becomes deformed and the reliability of the measurements is decreased. At this time the measurements still follow the predicted trends closely, recording a decrease when there was a predicted decrease. Similar observations were made pertaining to the effects of rotation of principal stresses on the gauge response. Early in the loading history results are in good agreement with those predicted, but after several loading cycles there is a noticable difference between the predicted and measured values.

Results from stress redistribution tests suggest that the shape of the borehole changed with successive loadings and that this has a greater effect on the results of a gauge in the direction of the principal stress. They also showed, as expected, a tangential stress build up with time in yielded areas adjacent to the opening. This has important implications on the stability of an opening. If this condition is not arrested yielding may propagate and, under certain conditions, lead to an unstable opening. It was shown that time effects must be considered when dimensioning linings because load build up with time may occur.

A re-evaluation of the results from the Kipp shaft indicated that neglecting the stress normal to the gauge axis during data interpretation introduces an error in the estimated magnitude of the principal stress.

Results from the overcoring test suggest that this technique may be used to back-calculate the in situ stress, but more work is necessary to verify the applicability of this technique in the field.

3. TUNNEL INSTRUMENTATION AND TEST RESULTS

3.1 Introduction

The Wolverine Tunnel was mined for British Columbia Railways (BCR) as a part of the Tumbler Ridge Branch Line. The new branch line was constructed to transport coal from the coalfields of northeast British Columbia to the BCR mainline at Anzac. The tunnel was driven simultaneously from an east and west heading using a full-face drill and blast technique of excavation with an advance of between 3.5 and 4.5 m per round or approximately 13 m per day. The rounds were drilled by a rail mounted jumbo with two hydraulic drills mounted on each of three levels.

Mining of the west heading of the Wolverine tunnel was completed in late April, 1983 approximately one month prior to completion of the Wolverine east contract. This difference in completion time provided an excellent opportunity to install instruments ahead of the west face for the purpose of monitoring stress changes and movements as the east face advanced towards the instrumented section.

The remaining sections of this chapter discuss the field instrumentation program with special emphasis on the problems encountered during installation. A brief description of the geology is given and results from the field measurements are presented herein.

3.2 Geology

The Wolverine tunnel passes through the Hart Range of the Rocky Mountains which consist predominantly of sedimentary rocks laid down in the Permo-Carboniferous Triassic Period. It is bounded on the west by the Sukunka Valley and on the east by the headwaters of the Wolverine River. Two west dipping thrust faults with shearing localized in the siltstone units intersect the tunnel between km 71+940 and 72+040. Mackay *et al.* (1983) found that this structure was a steeply inclined isoclinal syncline fold through excellent quality rock. Figure 3.1 shows the projected geological profile along the Wolverine tunnel as determined from surface field mapping and diamond drilling information [Klohn Leonoff, April 1981]. Mackay *et al.* (1983) observed only minor deviations from this profile during construction.

The instruments were installed over a 12 m section from km 73+300 to 73+312, approximately 2545 m from the west portal (see Figure 3.1). The overburden at this location is about 650 m. At the instrumented section the rock consisted of a bioclastic limestone with the bedding dipping at 40° west and striking approximately perpendicular to the tunnel axis. Two joint sets were also identified at this section, one dipping at 75-80° E and the other dipping at 75-80° S. These joint sets were striking at approximately 30° and 45° to the tunnel axis, respectively. The spacing of the joints for all three sets of discontinuities was about 300 mm with

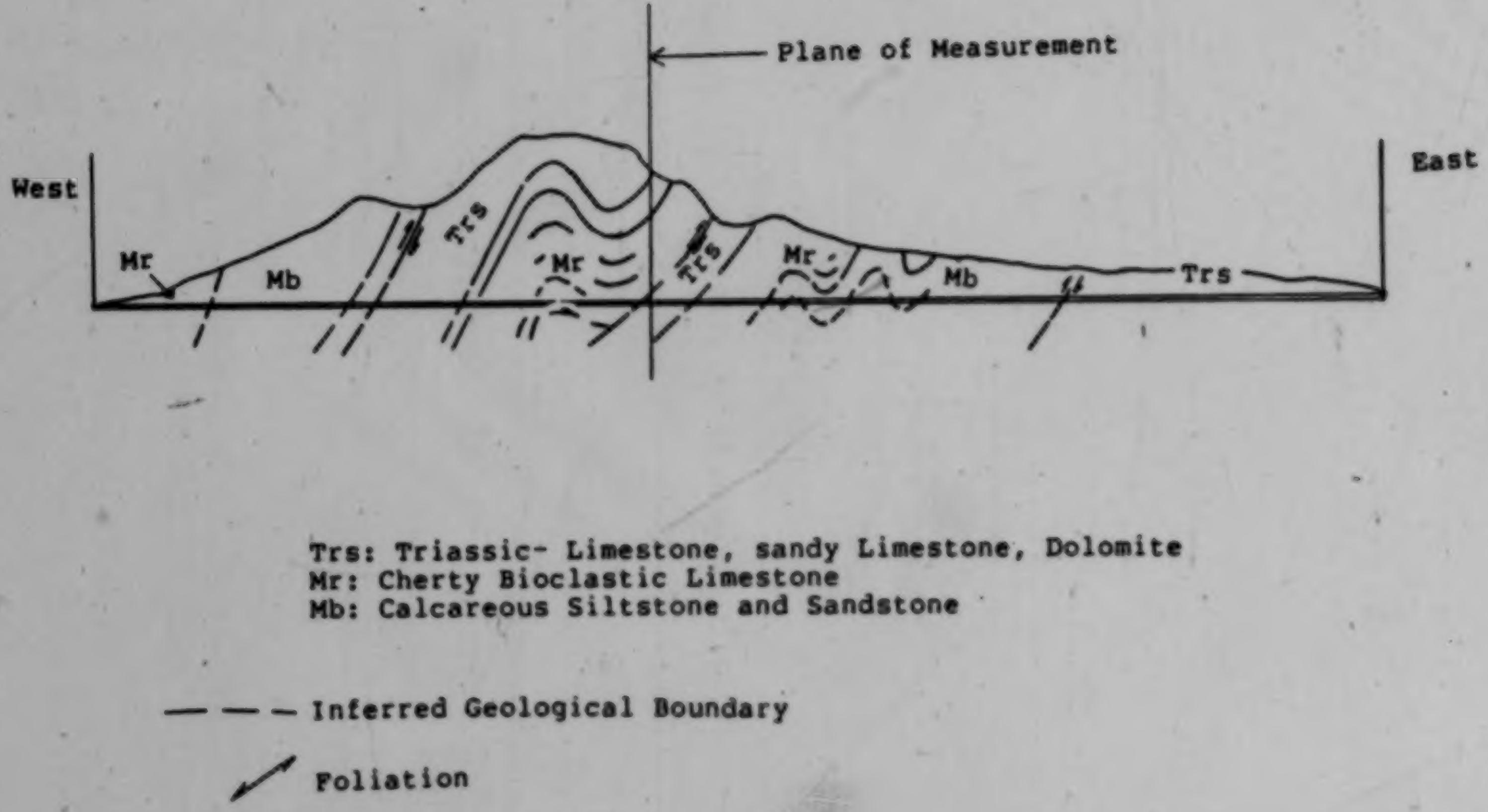
Plane of Measurement
West
East
Mr
Mb
Trs
Mr
Trs
Mr
Mb
Trs

Trs: Triassic- Limestone, sandy Limestone, Dolomite
Mr: Cherty Bioclastic Limestone
Mb: Calcareous Siltstone and Sandstone

— — — Inferred Geological Boundary

Foliation

Figure 3.1 Projected Geological Profile Along the Wolverine Tunnel

the joint surfaces being slightly rough, but tight and unaltered. The joint set dipping steeply to the south was only continuous over lengths of 1 to 3 m at the test section. An estimate of the RQD at this section produced a value of 80%. The uniaxial compressive strength of the bioclastic limestone is in the order of 75 to 100 MPa.

Occasional roof popping near the test section suggested that horizontal stresses were comparable or slightly higher than the vertical stress. For a horseshoe shaped opening high horizontal stress concentrations are anticipated near the crown. If the horizontal stress was much greater than the vertical stress the popping would have been much more violent. For the condition of small horizontal stresses the popping would not have been expected. Thus, it is believed that the stress ratio should be near unity or slightly greater; probably in the range between 0.8 and 3.0.

The tunnel is deep and it is anticipated that comparable stress levels exist. Also, the rock at this location is of good quality and it is unlikely that a large broken or softened zone would be created by the excavation. Thus, any effects of gravity would be negligible compared to the stresses induced by the excavation with the exception of a limited zone of damaged rock near the tunnel wall.

Figure 3.2 presents the results from a photoelastic stress analysis [from Descoeudres, 1978] performed on a square opening with low friction on the horizontal bedding and roof bolting. Large fluctuations in the horizontal

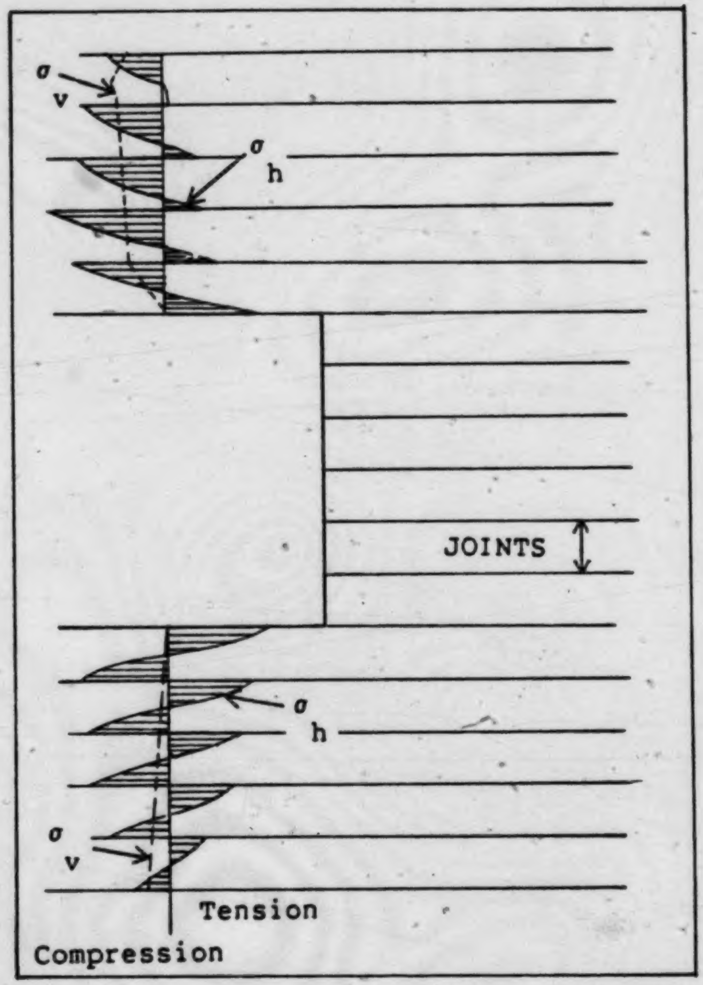
σ
v
σ
h
JOINTS
σ
h
σ
v
Tension
Compression

Figure 3.2 Example of Stresses in Horizontally Bedded Rock Mass

stress at the crown and floor occur upon stress release due to flexure of the beds. Stresses in the vertical direction and those along the sidewalls of the opening are not affected significantly. However, if bedding was vertical and striking parallel to the tunnel axis, Figure 3.2 would essentially be rotated 90° and there would be large fluctuations in the vertical stress along the sidewalls, but the stresses at the crown and floor would not be greatly affected. The beds at the instrumented location are dipping at 40° and striking perpendicular to the tunnel axis. Both joint sets were steeply dipping, but neither of them were striking closely parallel to the tunnel axis. Thus it is believed that flexure of the beds would not have a large effect on the stresses around the opening for these conditions.

3.3 Proposed Instrumentation

3.3.1 Stressmeters

A detailed analytical study was performed to determine the optimum gauge locations around a circular opening excavated in a linear elastic material where the principal stress direction is known within ±15°. The findings from this study have been presented by Kaiser *et al.* (1983a) and are summarized in Section 2.2. The upper section of the horseshoe tunnel shown in Figure 3.3 represents a semi-circle with a radius of 2.7 m. It was decided that for

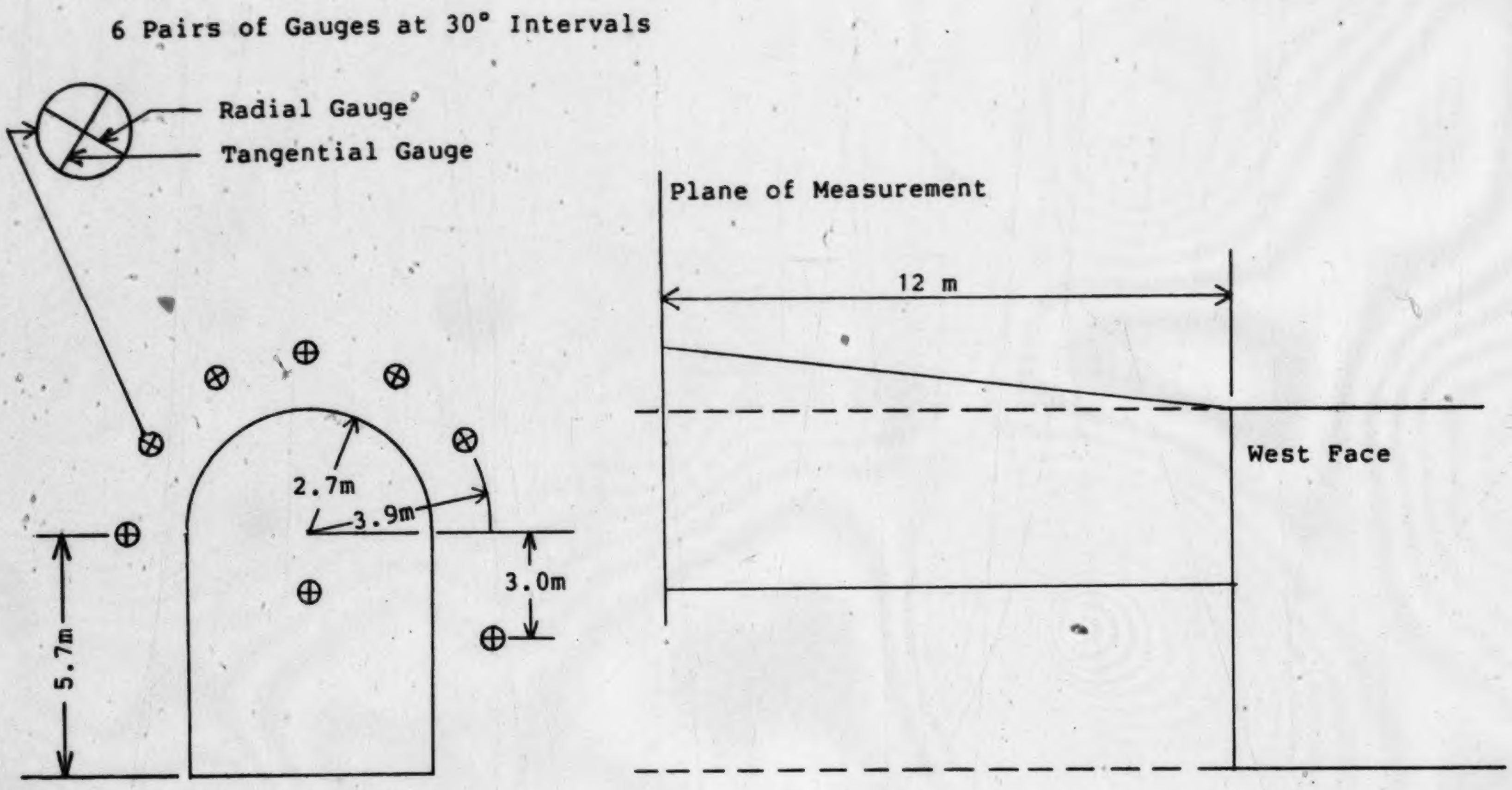
6 Pairs of Gauges at 30° Intervals
Radial Gauge
Tangential Gauge
2.7m
3.9m
3.0m
5.7m
Plane of Measurement
12 m
West Face

Figure 3.3 Proposed Stressmeter Locations for Wolverine Tunnel

an initial analysis the tunnel could be treated as an equivalent circular opening. Thus, most of the gauges were proposed for installation at or above the springline. In order to gain a complete picture of the stress field one pair of gauges was designated for installation at 3 m below the springline.

Laboratory overcoring results indicated a stress concentration ahead of the face and it was of interest to place a set of two gauges directly ahead of the face to determine if this technique of back-calculating the stresses could be applied in the field.

Gauges in the crown area were set at 30° intervals to cover all possible directions of the principal stresses as discussed in Section 2.2. The gauges were to be set at 1.2 m from the tunnel wall to allow for a small damaged zone adjacent to the wall. This distance corresponds to $\rho=0.69$ when no broken zone is considered and the radius "a" is taken as the radius of the semi-circular crown, 2.7 m. If a 0.5m softened zone is assumed and the distance to the gauges is measured from the boundary of the broken zone then $\rho=0.82$ and for a 1.0 m soft zone $\rho=0.95$. These thicknesses are based on previous results reported by Mackay (1982) and Nishida *et al.* (1982). Hocking (1976) suggested that at 3.7 radii ahead of the face the influence of the opening on the in situ stress field is small. Based on this the gauges were to be installed at 12 m ahead of the face. The proposed locations of the stressmeters are shown in Figure 3.3.

3.3.2 Extensometers

It was proposed to install four sets of single point extensometers, one set with four points and the others with three points. The three point sets were to be placed at the springlines and in the crown as close to the face as possible. The anchors for the three points were to be at 1.5, 3.0, and 6.0 m and those for the four point set at 6.0, 9.0, 12.0, and 15.0 m. This latter set was to go directly ahead of the face in the centre of the tunnel. The extensometer measurements were to be used in conjunction with the stress change measurements to back-calculate the rock mass modulus. The proposed locations of the extensometers are shown in Figure 3.4 .

3.4 Installation Procedures

3.4.1 Stressmeters

The stressmeter holes were drilled from a rail-mounted jumbo with three decks each having two hydraulic drills. The holes were drilled from the two upper decks. All holes were aligned using a Brunton compass and drilled to within 0.5 m of the desired final depth with a 45 mm diameter bit. The holes were completed with a long shank cross bit that had been built up with four weld beads along the shank, as recommended by the gauge manufacturer. This was necessary to provide the correct hole diameter for the stressmeters. Prior to setting the gauges the holes were checked with a

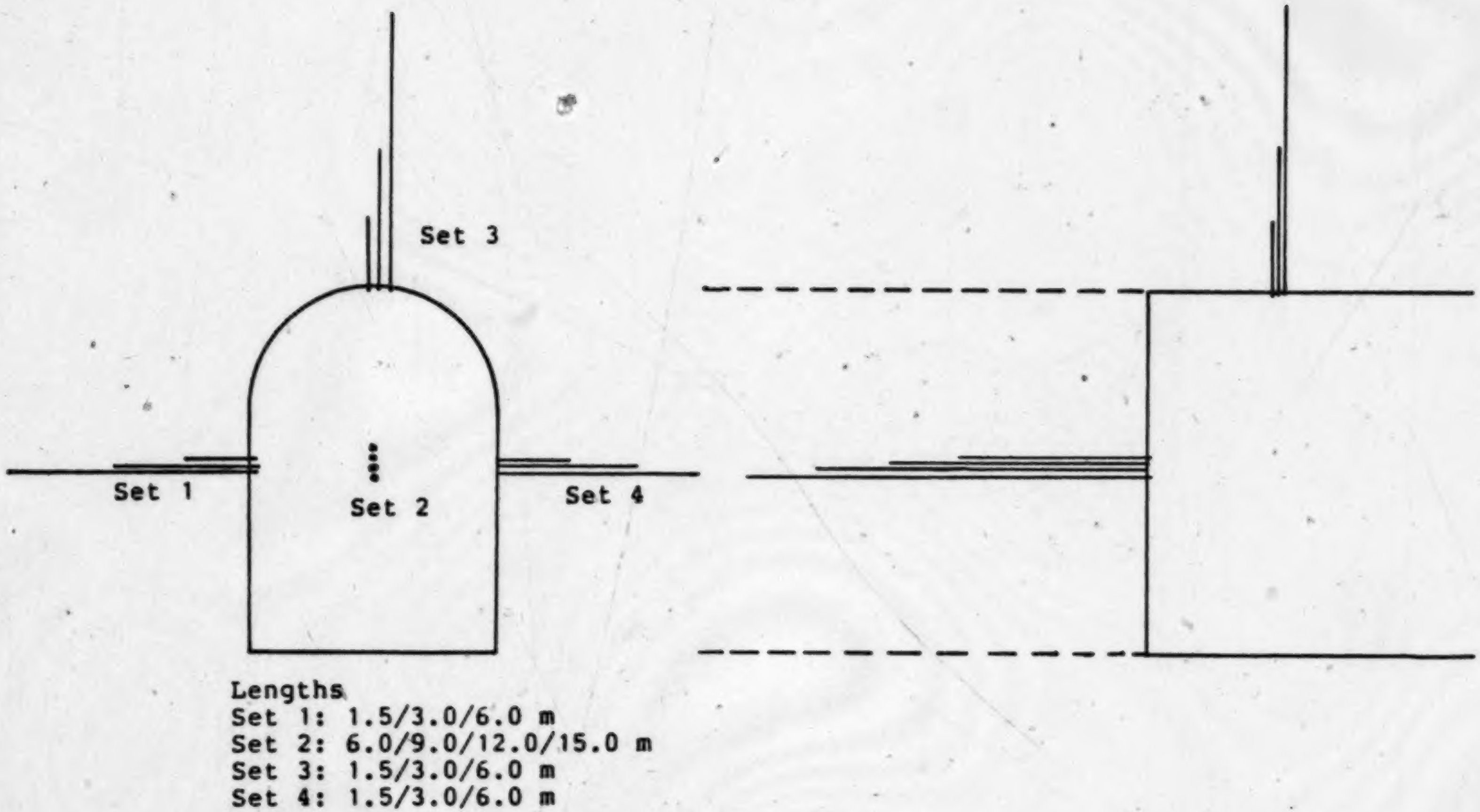
Set 3
Set 1
Set 2
Set 4
Lengths
Set 1: 1.5/3.0/6.0 m
Set 2: 6.0/9.0/12.0/15.0 m
Set 3: 1.5/3.0/6.0 m
Set 4: 1.5/3.0/6.0 m

Figure 3.4 Proposed Extensometer Locations

"Go/No-Go" gauge to determine if the final hole diameter was acceptable for the gauge tolerance. Following this the location of each hole was determined using a magnetic single shot survey instrument. This instrument measures both declination from magnetic north and inclination from the vertical. Knowing the bearing of the tunnel axis (with respect to magnetic north), the angles measured by the instrument can be used to calculate the location of the end of the borehole. Two shots were taken in each stressmeter hole, one at 3 m into the hole and the other at 7 m. Using this technique it was possible to locate the final positions of the stressmeter holes accurately.

The stress gauges used for the investigation were the hard rock type vibrating wire stressmeters supplied by Irad Gage. They were installed with a hydraulic setting tool following procedures outlined by Hawkes and Bailey (1973) and the Irad Gage Stressmeter Users Manual (1977).

3.4.2 Extensometers

Single point extensometers consisting of a 25 mm diameter Williams mechanical rock bolt , two pieces of black steel pipe and a threaded coupler (see Figure 3.5) were used for measuring displacements. The larger steel pipe slides over the 38 mm diameter steel pipe and is forced over the expanded end of the smaller pipe by screwing the threaded coupler onto the end of this smaller pipe. In this manner the 51 mm pipe is wedged against the borehole wall providing

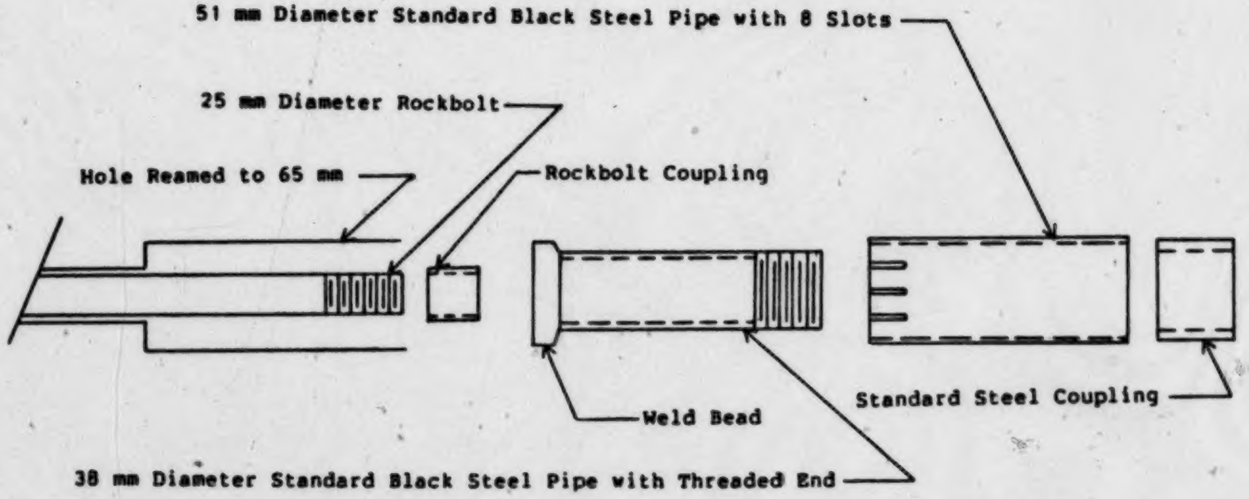
51 mm Diameter Standard Black Steel Pipe with 8 Slots
25 mm Diameter Rockbolt
Hole Reamed to 65 mm
Rockbolt Coupling
Weld Bead
Standard Steel Coupling
38 mm Diameter Standard Black Steel Pipe with Threaded End

Figure 3.5 Extensometer Components

an anchor point at about 460 mm from the wall. Holes for the extensometers were drilled with a 45 mm bit and subsequently reamed out to 65 mm diameter to a depth of 460 mm to accommodate the extensometer heads. All readings were taken with a depth micrometer.

3.5 Installation Difficulties

3.5.1 Stressmeters

A total of sixteen stressmeters were proposed for installation at the test section. However, due to difficulties encountered during installation and time limitations only seven of these were functional following installation.

Access to the face from the jumbo was only available for two 8 hour shifts. Thus, all of the instruments had to be installed during this time period. To ensure that all the holes could be drilled, the distance the holes extended ahead of the face was decreased from 12 to 9 m. As well, rock bolts and mesh were being placed near the face which created crowded working conditions, especially on the top level of the jumbo. Far better success with the installations was experienced on the middle deck than on the top deck. This is also attributed to cleaner working conditions and a cleaner setting tool since instruments from this deck were installed first.

Another problem was that the drill wandered over the length of the holes and it was impossible to predetermine the final position of the holes. One of the stressmeter holes in the crown had to be abandoned because the drill rods began wedging in the hole.

The stressmeter wedges are designed such that at a hydraulic jack pressure of about 2500 psi the platen/wedge shear pin will break and the gauge will be released from the tool. However, at pressures in excess of 3000 psi these "eyes" were not shearing out and the gauges had to be released using an alternate procedure recommended by the manufacturer. When this procedure is employed the sharp ends of the setting tool may cut the gauge wires. Lead wires from four gauges that had been installed were broken off during the setting of a second gauge in the same hole.

It would be prudent to test some of these wedges prior to use in the field to determine if the shear pins break out properly in order to save time and costs. If this is done great care must be taken during repair in order to attain the original strength. One possible alternative is to obtain extra wedges and choose a random sample which, hopefully, will be representative of the entire batch of wedges.

One positive aspect of the stressmeter installation program was that all of the holes met the stringent diameter tolerance requirements of the gauges. It can be concluded that the drilling procedure adopted and the bit used were adequate.

3.5.2 Extensometers

Fewer problems were encountered with the extensometer installations. The number of extensometers installed had to be reduced because of time limitations. Those installed in the sidewalls and the crown could not be placed as close to the face as was planned because when the jumbo drill arms were rotated they could only get within 3 m of the face. Two of the extensometers in the crown malfunctioned because the heads were improperly anchored.

3.6 Final Installations

Figures 3.6 and 3.7 show the final installations at the test section. A total of seven stressmeters and seven extensometers were installed for the instrumentation program. Above the springline radially oriented gauges refer to those set with their loading axis in the direction of a line pointing towards the centre of the semi-circular arc that represents the crown and tangential gauges are perpendicular to these. At locations below the springline, gauges with their loading axis in a radial direction are perpendicular to the line representing the tunnel perimeter. Tangential gauges have their loading axis parallel to this line. The instruments were monitored for several days immediately following installation until the stressmeters were seated in the holes. Monitoring was resumed when the east heading was 48 m from the plane of the stressmeters. Access to the extensometers in the crown was not possible

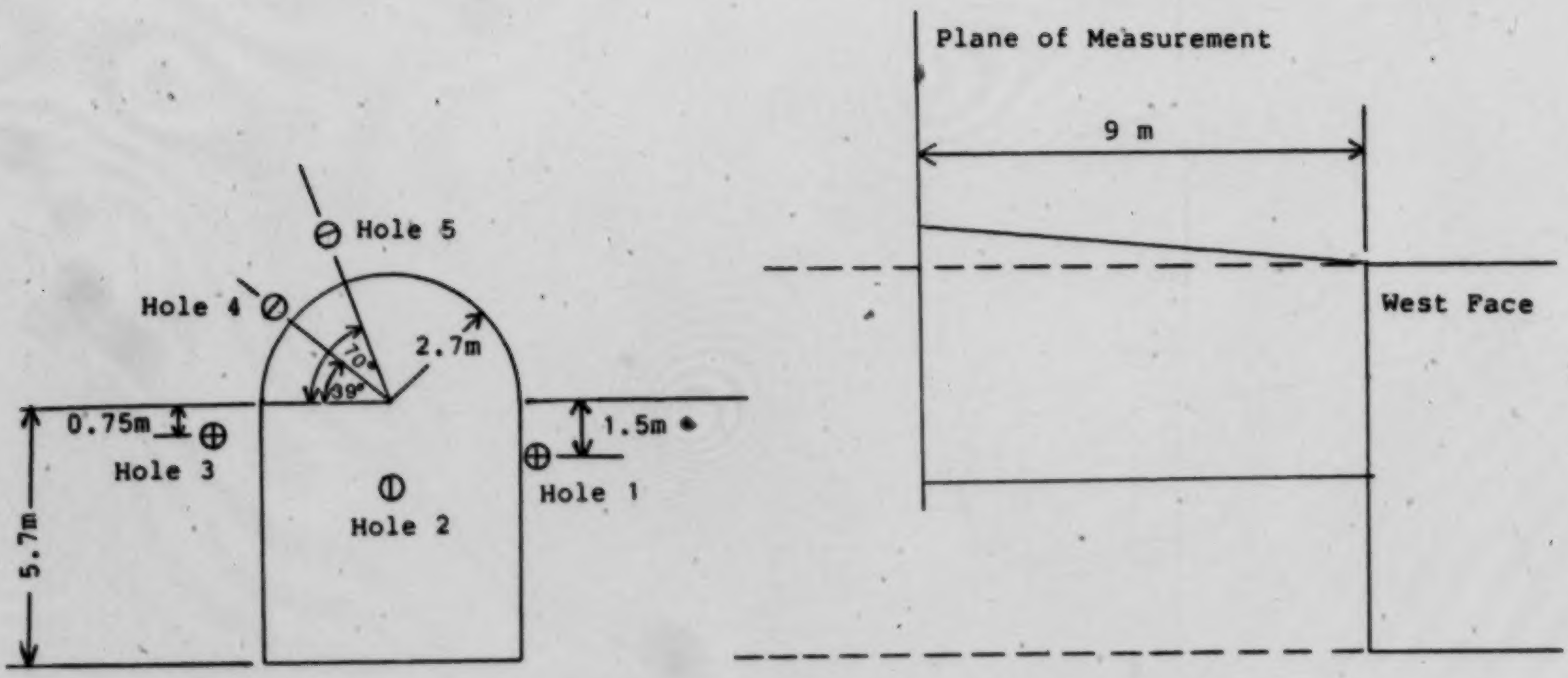
Hole 5
Hole 4
70°
39°
2.7m
0.75m
Hole 3
1.5m
Hole 1
Hole 2
5.7m
Plane of Measurement
9 m
West Face

Hole 1 $\rho = 0.90$
Hole 3 $\rho = 0.75$
Hole 4 $\rho = 0.89$
Hole 5 $\rho = 0.73$

$\rho = a/r$ (a=2.7 m)

Figure 3.6 Stressmeter Installations at Wolverine Tunnel

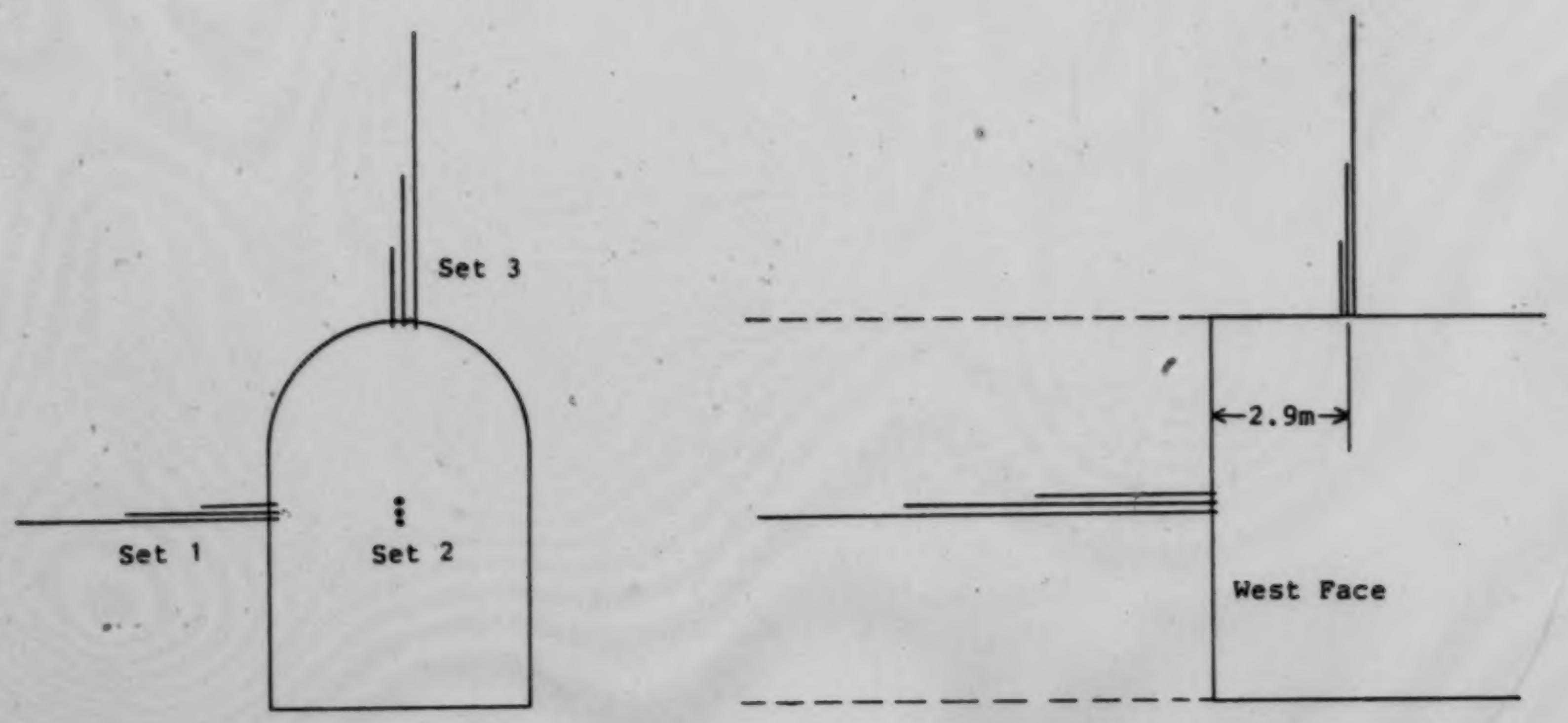
Set 3
Set 1
Set 2
←2.9m→
West Face

Lengths
Set 1: 1.5/3.0/6.0 m
Set 2: 3.0/6.0/9.0 m
Set 3: 1.5/3.0/6.0 m

Extensometer Spacing within each Set= 30 cm

Figure 3.7 Extensometer Installations at Wolverine Tunnel

because inflowing water created silting problems and the jumbo could not readily be moved back to the face area. Also, during shotcreting these extensometers had been partially covered.

Following the round prior to break-through the west face was badly broken and several large pieces of rock had fallen from the face. A final reading on the one remaining extensometer in the face was not possible. The wire from the radial gauge in stressmeter hole S1 was sheared off during the second last round when the face was 0.2 m beyond the plane of measurement. All remaining wires were pushed into the holes as far as possible and a string that had been tied to the wires was left dangling from the hole. A small piece of PVC tubing was secured into each of the holes to protect the wires. After the final blast none of the wires could be found intact, but some pieces of wire were found up to 20 m from the break-through point.

3.7 Data Reduction

3.7.1 Stressmeters

Along the length of the tunnel several different rock units were encountered. These vary considerably in age and origin and thus, it is likely that the virgin stress in each of these units is not consistent. Also, the depth of overburden varies significantly over the length of the tunnel which further complicates the stress condition.

Therefore, the stresses that have been recorded and the stress field that will be back-calculated from these results is highly localized.

The method of analyzing the data from the stressmeters has been discussed in Chapter 2. A modulus of deformation for the rock mass of 75000 MPa was chosen based on laboratory tests reported by Klohn Leonoff Ltd. (1981). Substituting this modulus value into Eqn. 2.3 results in a uniaxial gauge sensitivity factor of a=3.96.

The gauges were installed to monitor the stress change near the opening face as the tunnel advanced towards the instruments for the purpose of back-calculating the in situ stress field. Figure 3.8 shows a plot of the measured stress change with distance from the face. The tangential gauge in hole S4 fell below its base level and it is not known what the total stress change at this point would have been. It will be shown later that the actual magnitude of the stress change is not as important as the fact that the gauge recorded a substantial stress decrease. The gauge in hole S2 located directly ahead of the face did not record any stress change. The last possible reading from this gauge was taken when the advancing face was 4.0 m from the gauge.

3.7.2 Extensometers

The extensometer at 6.0 m ahead of the face was the only one in its group to measure any longitudinal displacement. A movement of 0.43 mm into the east face (the

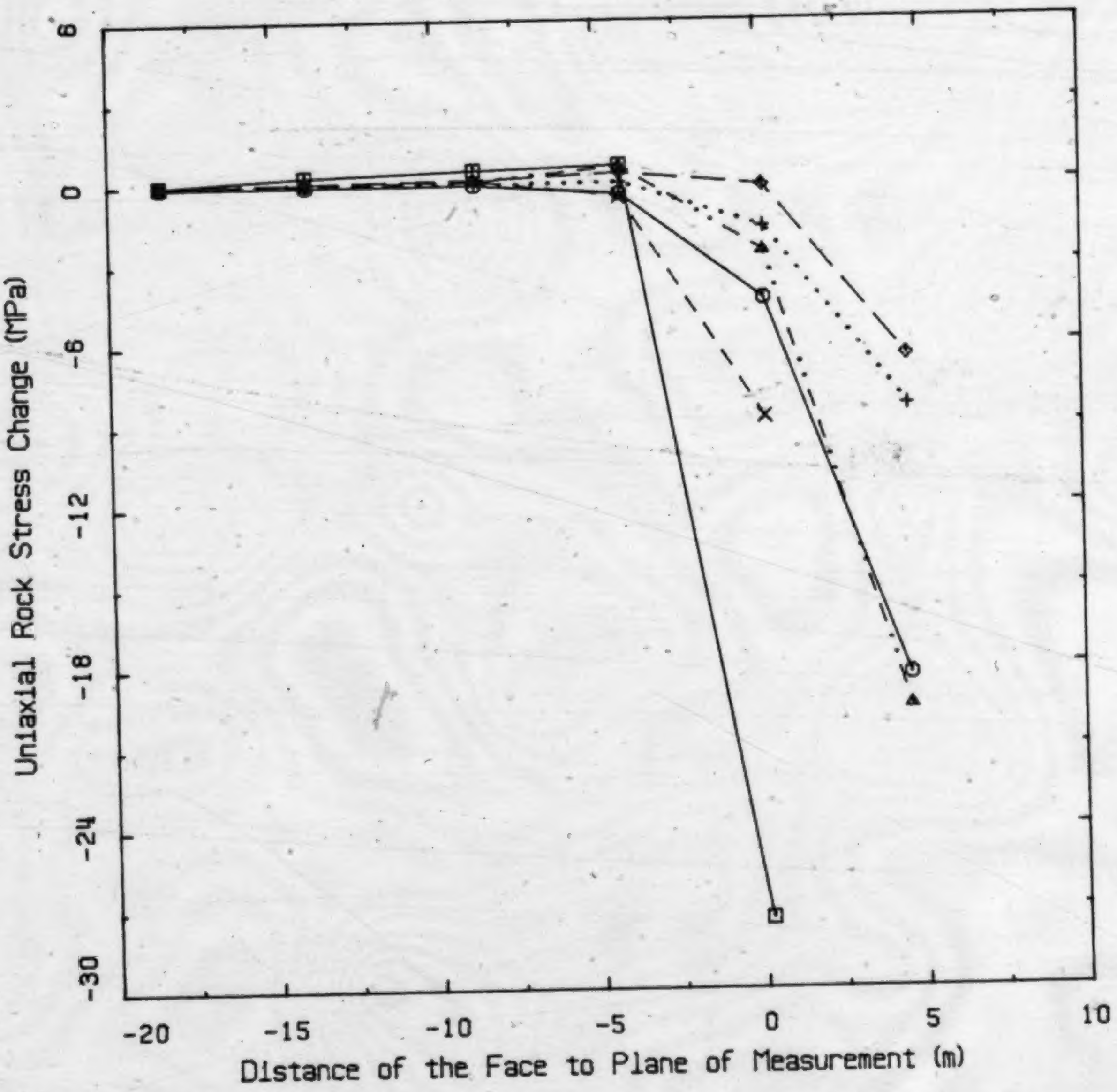

Figure 3.8 Measured Uniaxial Stress Change with Tunnel Face Advance

actively advancing face) was recorded when this face was 2.8 m from the anchor. The extensometers in the sidewall did not show any movement until after break-through. The data is presented as recommended by Cording *et al.* (1975) showing both depth-displacement and time-displacement diagrams (Figures 3.9 and 3.10).

The time-displacement plot gives the displacement distribution at various times after break-through. An increase in distance between the reference head and the anchor head is shown as positive. The depth-displacement plot shows the displacement distribution at the north wall 2.9 m back from the break-through point after the final blast. The inward displacement of the tunnel wall was taken as the displacement between the reference head and the 6.0 m anchor. Similarily, both intermediate displacements were subtracted from the assumed tunnel wall displacement to produce a displacement distribution relative to the deepest anchor.

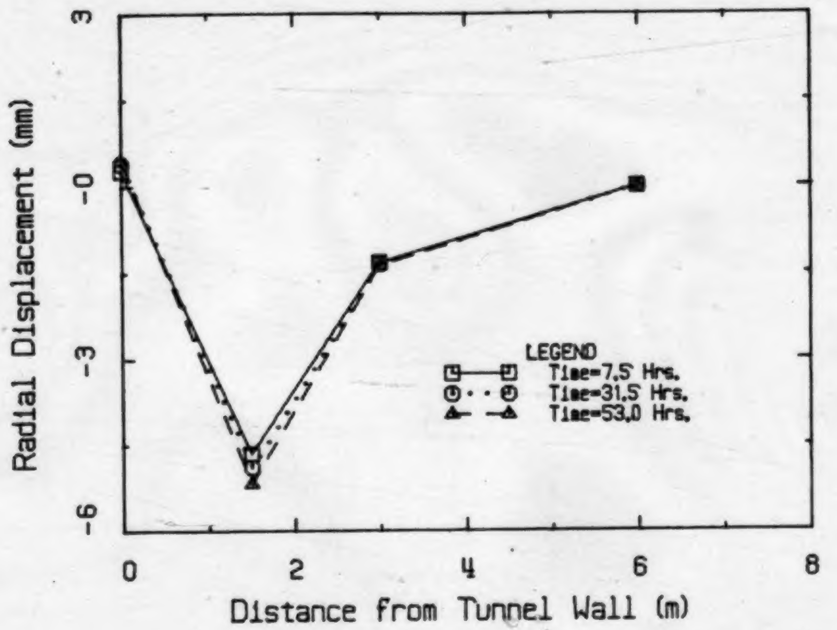

Figure 3.9 Depth-Displacement Plot for North Wall Extensometers

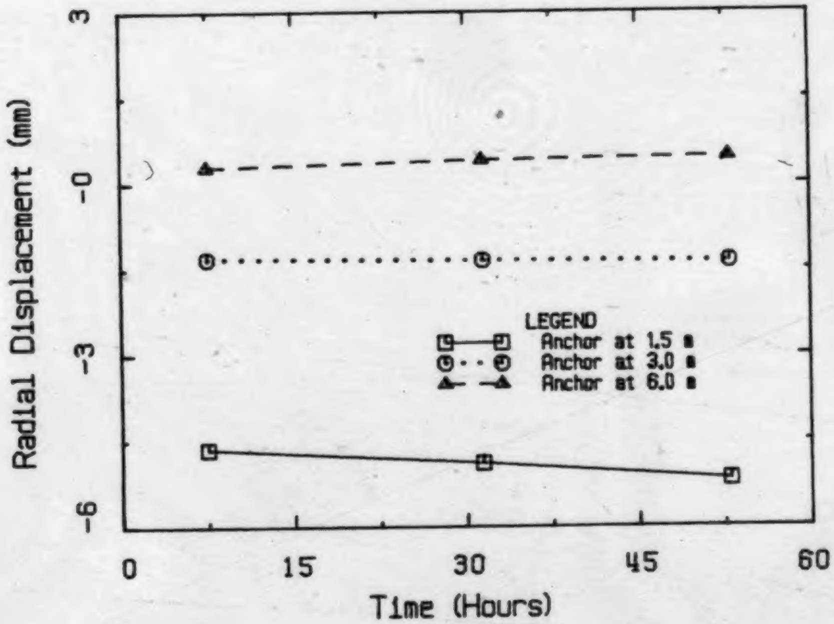

Figure 3.10 Time-Displacement Plot for North Wall Extensometers

4. ANALYSIS OF TUNNEL INSTRUMENTATION

4.1 Introduction

This chapter presents the analysis of the data obtained from the stressmeters and extensometers. The shape of the opening and the nature of the results from the stressmeters necessitated the use of finite element techniques to interpret the data. Practical implications will be discussed and it will be shown how the results can be used to determine the ground convergence curve.

4.2 Analysis of Stressmeter Results

Inspection of Figure 3.8 reveals that all gauges, except for the one directly ahead of the face, show a significant stress decrease after the face passes beyond the plane of measurement. The in situ stress field will be determined based on the assumption that the gauges have recorded all of the stress change prior to being destroyed. After the stress field has been estimated an axisymmetric finite element analysis will be performed to check the validity of this assumption.

Results from the axisymmetric analysis (Figure 4.15) will show that for the simplified shape, some stress change should have occurred at 4.0 m from the gauge directly ahead of the face. The amount of this directional stress change is approximately 15%. The tangential and radial stress increases are equal and when these are combined to obtain an "equivalent uniaxial stress" (discussed in Section 2.2) the stress change measured by the gauge would be less than 10% of the field stress. Both the opening shape and diameter have a significant effect on the calculated amount of stress change at this point and the value obtained from this analysis may not be indicative of the actual stress change at this point. The distance ahead of the face that the blast damage extends would also influence the amount of stress change that occurred. Another factor that cannot be overlooked is that the gauge may have malfunctioned. When readings were taken the readout value fluctuated several units and an accurate reading was not possible. None of the other gauges exhibited this behavior.

There was no previous information about the stress field in the immediate area of the tunnel. Thus, it was necessary to at least try to define a possible range for each of the variables, N (principal stress ratio), θ (orientation of the principal stress), and σ_1 (the major principal stress), to provide a starting point for the finite element analysis. Various simplifications were made to the problem to allow the use of closed form and other available solutions for making an initial prediction of the stress field.

First an equivalent circular opening in a linear elastic medium was assumed. However, it soon became evident that, regardless of the direction or magnitude of the principal stress, there was no combination of parameters that would produce a decrease in stress, as measured, at all gauge locations.

Hoek and Brown (1980) provide plots of principal stresses around a horseshoe opening for the case where the principal stresses are vertical and horizontal. Again, the opening is in a linear elastic material. As before, no value of N could be found such that a stress decrease was predicted at all gauge locations. In their book Hoek and Brown (1980) also provide plots of principal stress contours around an elliptical opening for the principal stress acting at 45° to the major axis of the opening. The major and minor axis of this ellipse correspond closely to the tunnel dimensions. When the opening was treated as an ellipse no combination of parameters would predict a stress decrease at all the desired locations.

From these initial analyses it was concluded that finite element techniques would be required to define the stress condition at this site because either a softened zone or a yielded area around the opening existed. Kaiser (1981) has shown that the design of tunnels in yielding ground can be reduced to the evaluation of an opening with a softened zone if the correct parameters can be determined. For this analysis a reduction in stiffness adjacent to the opening will be considered.

4.3 Estimation of the In Situ Stress Field by Finite Element Methods

4.3.1 Introduction

The finite element program ADINA (Automatic Dynamic Incremental Nonlinear Analysis) was employed to calculate the stress field for various combinations of parameters. The complete analysis consisted of two steps: 1) using a two dimensional plane strain analysis with the actual opening shape and size to match the measured results; and 2) subsequently employing a simplified axisymmetric analysis to determine approximately how much of the expected stress change was recorded by the gauges before they were destroyed. Figures 4.1 and 4.2 show the complete finite element mesh and an enlarged view of the area around the opening.

The mesh chosen for the plane strain analysis had to fulfill several requirements. First, thin elements were necessary near the opening wall because some of the gauges were within 0.25 m of the wall. Second, the mesh must allow for application of the principal stress in various directions. Following a review of the loading capabilities of the program it was decided that a rotating outer layer of elements was the simplest solution. It was not of importance to accurately obtain the stress concentration factors near the corners at the bottom of the opening so the elements here were made slightly larger. Similarily, the tangential

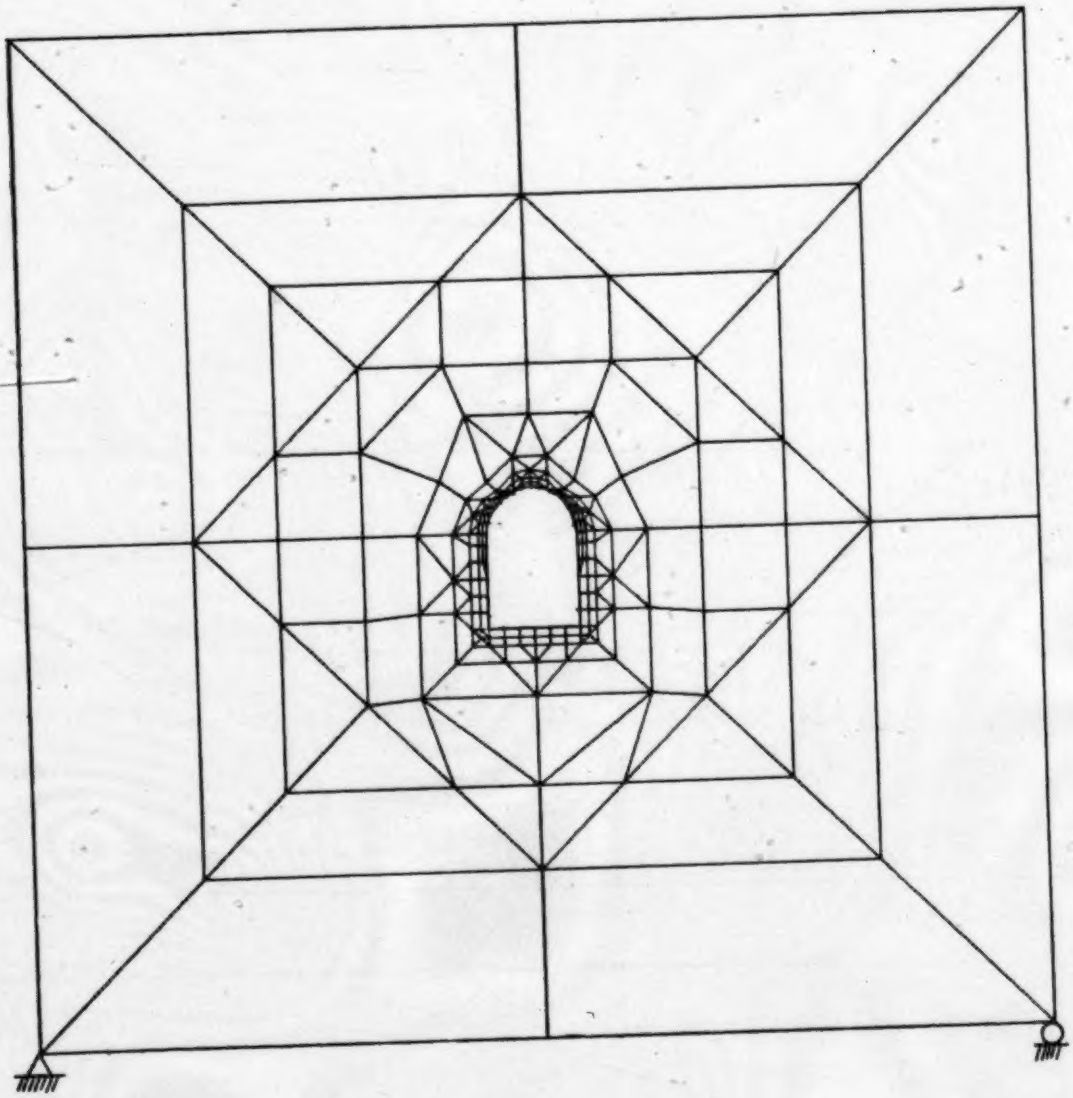

Figure 4.1 Finite Element Mesh for Two-Dimensional Plane Strain Analysis

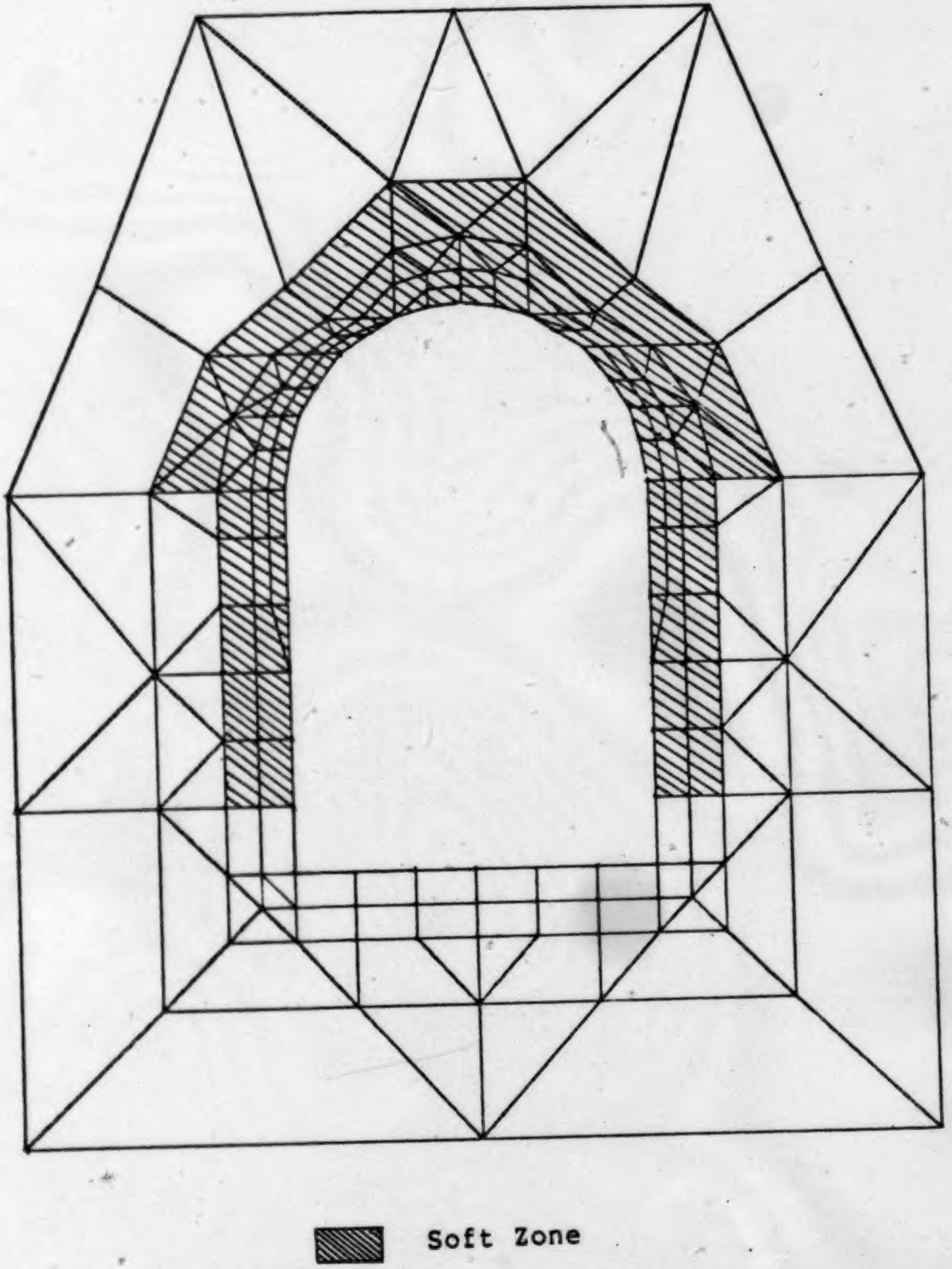

Figure 4.2 View of Area Around Opening- Plane Strain Analysis

stress concentrations at the opening wall were not of importance and thus, only stresses at the element centres were calculated.

Near the instrumented section shotcrete had been applied to within about 3 m of the west face and rock bolts were installed at the crown. On the east side (advancing face side) bolting and meshing were following 1 or 2 rounds behind the excavation, but shotcreting was well back of the face. For the analysis it was decided to neglect any support because the shotcrete was placed more for safety reasons than for actual support and most of the stress release and displacements had probably already occurred at the time of application.

4.3.2 Two-Dimensional Plane Strain Analysis

4.3.2.1 Method of Analysis

The mesh used in the two dimensional plane strain analysis is shown in Figure 4.1 with the elements that represented the opening omitted. The displacement boundary conditions are also shown on the mesh. A trial case was run to become familiar with the program and check the adequacy of the mesh. A uniform load was applied to the mesh, on all four boundaries, with an opening which was excavated by reducing the stiffness of the elements within the opening to a very low value. The results showed that stresses in all elements within the opening were zero and the surrounding stresses were compared to those from Hoek and Brown (1980).

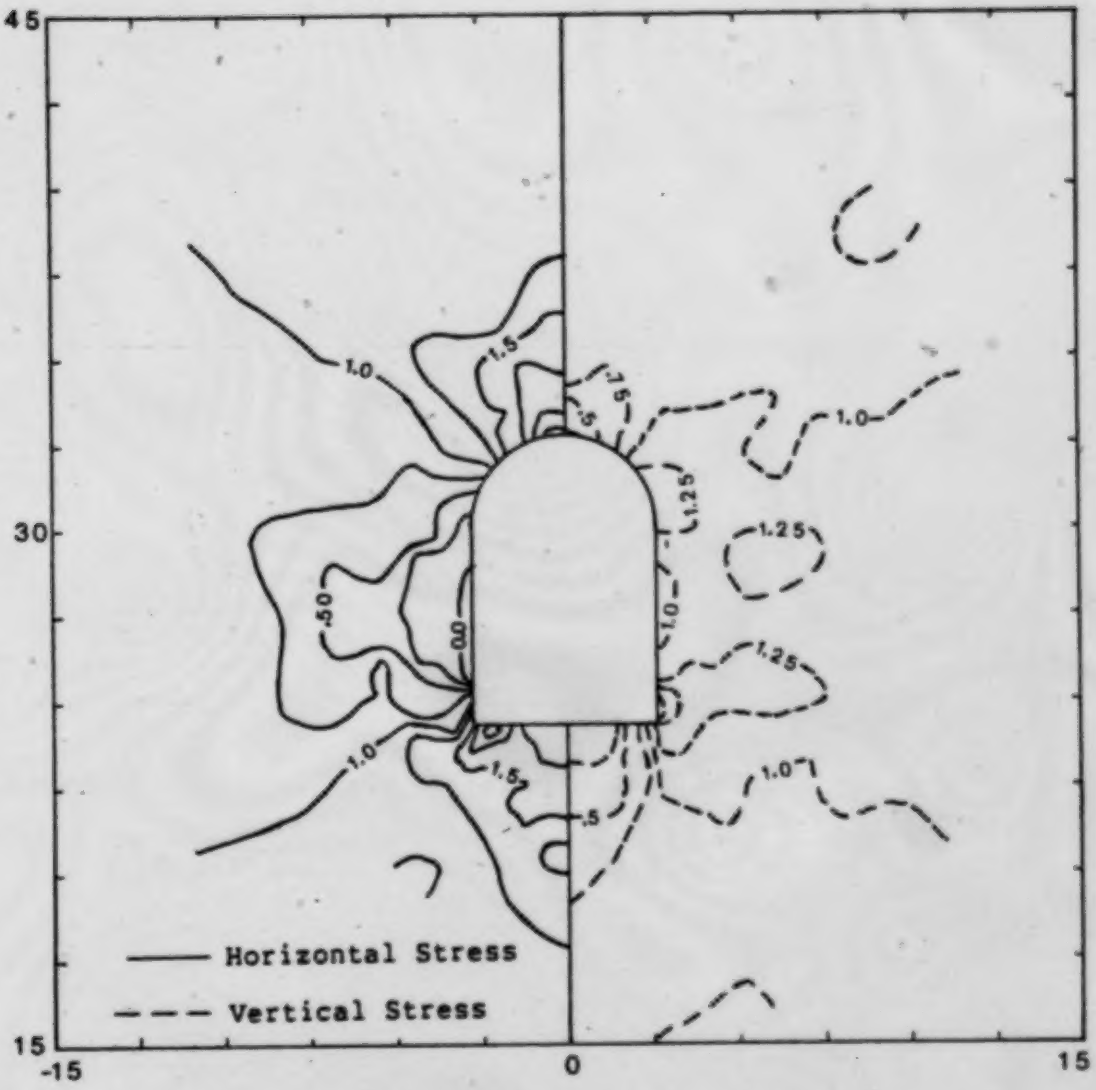

Figure 4.3 Stress Contours for N=1.0, σ_1=1.0, No Soft Zone.

Figure 4.3 shows the elastic stress distribution around the opening for a uniform stress condition (compression is positive). The contours plotted are for σ_y and σ_x, the vertical and horizontal stresses. It was chosen to plot these stresses rather than the principal stresses because four of the six gauges were oriented in either the X or Y directions. The stress concentrations near the corners and at the opening wall are not as high as those predicted by Hoek and Brown (1980) because the stresses were calculated at the element centres. Aside from these discrepancies the two sets of results are in good agreement.

Initially, a linear elastic model with no softened zone around the opening was considered. The major principal stress direction was rotated counterclockwise from vertical to horizontal with applications included at 45° and 55° from vertical. Following this, a linear elastic model with a softened zone around the tunnel was examined. Nishida *et al.* (1982) measured thicknesses of softened zones and velocities around openings for different excavation methods. For the drill and blast method of excavation they found that the thickness of the softened zone ranged from 0.5 to 1.3 m (around a horseshoe opening with an average radius of 2.6 m) which corresponds to a ρ of about 0.74. The wave velocity, which is closely proportional to the stiffness, in the softened zone was found to be approximately 0.22 times the velocity in areas further from the opening.

4.3.2.2 Results from Analysis without Softened Zone

Figure 4.3 shows the results from the trial case with N=1.0 and the principal stress vertical. Results for other N values, with σ_1 vertical and horizontal were investigated using the figures from Hoek and Brown (1980) and the findings were discussed earlier. The principal stress orientation was rotated to 45° from the vertical and again emloying various N values did not produce any set of parameters that indicated a stress decrease at all the gauge locations. The outer boundary was further rotated to test stress conditions at θ=55° counterclockwise from the vertical. Again, regardless of the N value some of the tangential stress changes at the gauge locations would show an increase. It was concluded that the stress conditions measured in the field could not be matched assuming perfectly elastic behavior.

4.3.2.3 Results from Analysis with Softened Zone

With a softened zone around the opening only two directions for the principal stresses were used to estimate the field stress. For each of these directions several sets of parameters describing the stress field were tested. It is important to recognize that the measurements recorded may not be exactly correct. However, the lab tests have shown that the gauges do record correctly whether there is an increase or a decrease in stress. They also indicated that if repeated loading does not occur the results are quite reliable. These findings provide confidence that indeed there was a significant stress decrease at all the gauge locations.

Evidence from field observations and the instruments suggest that a stress ratio close to unity exists at the test location. As mentioned earlier there was some roof popping near the instrumented section (see Section 3.2). The overburden at the instrument locations was about 650 m which should correspond to a vertical stress of about 17 MPa assuming that this stress is equal to the overburden pressure. Most of the radial stress would have been released at the locations of the two radial gauges near the springline because they are close to the tunnel wall and are probably within the softened zone. If the gauge results are broken down into actual radial and tangential components, the average radial stress release at these locations would be about 30 MPa. This would suggest a stress ratio of approximately 1.8.

Stress ratios of between 0.25 and 4.0 were employed during the analysis and trials were performed using various thicknesses of soft zones with different stiffness reductions. It was found that a stress ratio of approximately 1.0 provided the best fit to the measured values and thus the emphasis was placed on investigating different parameters with this stress ratio. For each assumed stress condition the calculated stress changes at the gauge locations were observed and compared to the measured values. Different thicknesses of soft zones were used for the crown and springline because it was felt that the roof popping may have induced a larger soft zone in the crown.

Plots showing vertical and horizontal stress contours for 5 different sets of parameters are shown in Figures 4.4 to 4.9:

- Figure 4.4

  $N=1.0$, $\theta=0°$, $\sigma_1=1.0$, $E_R/E_S = 5$

  Soft zone: 2.0 m at crown; 1.0 m at springline;

- Figures 4.5 and 4.6

  $N=2.0$, $\theta=55°$, $\sigma_1=0.5$, $E_R/E_S = 10$

  Soft zone: 2.0 m at crown; 1.0 m at springline;

- Figure 4.7

  $N=1.0$, $\theta=55°$, $\sigma_1=1.0$, $E_R/E_S = 2$ (same as $\theta=0°$)

  Soft zone: 2.0 m at crown; 1.0 m at springline;

- Figure 4.8

  $N=1.0$, $\theta=0°$, $\sigma_1=1.0$, $E_R/E_S = 5$

  Soft zone: 1.0 m at crown; 0.5 m at springline;

- Figure 4.9

  $N=1.0$, $\theta=55°$, $\sigma_1=1.0$, $E_R/E_S = 10$ (same as $\theta=0°$)

  Soft zone: 2.0 m at crown; 1.0 m at springline;

where E_R, E_S = modulus of the undamaged and softened rock, respectively.

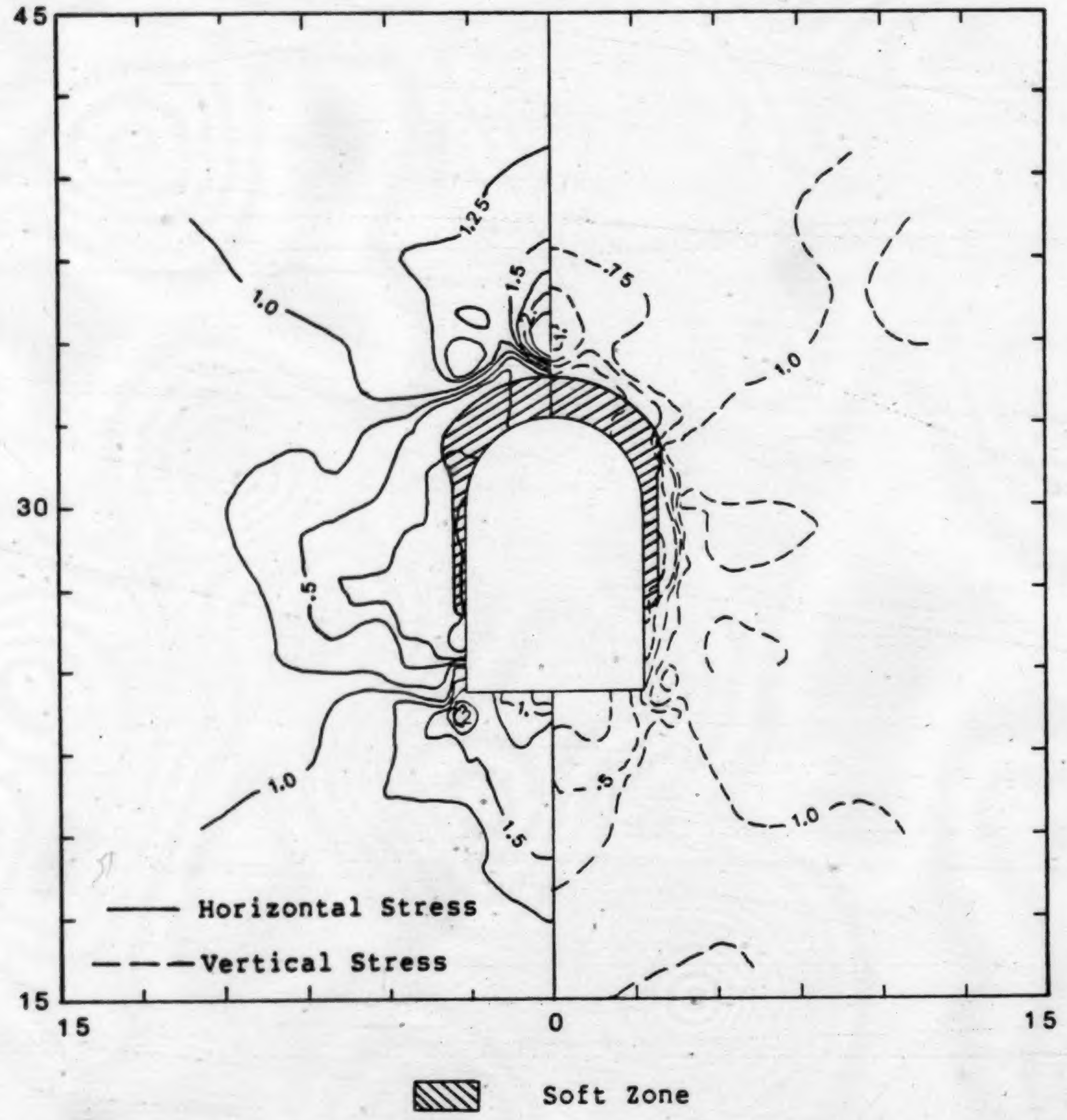

Figure 4.4 Stress Contours for N=1.0, $\theta=0°$, $\sigma_1=1.0$, Stiffness Reduction=5.0, Soft Zone: 2.0 m at Crown; 1.0 m at Springline

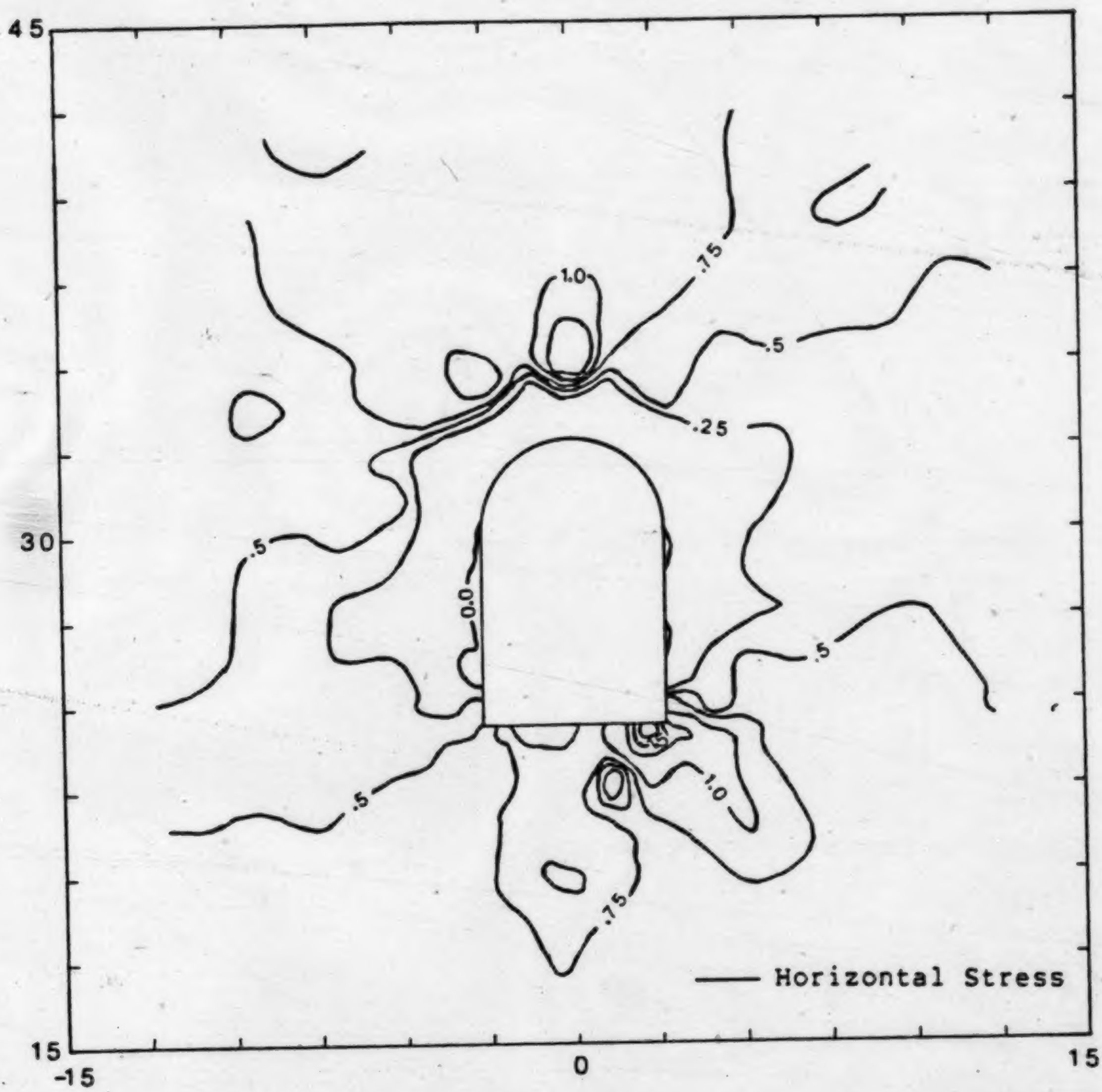

Figure 4.5 Horizontal Stress Contours for N=2.0, θ=55°, σ_1=0.5, Stiffness Reduction=10.0, Soft Zone: 2.0 m at Crown; 1.0 m at Springline

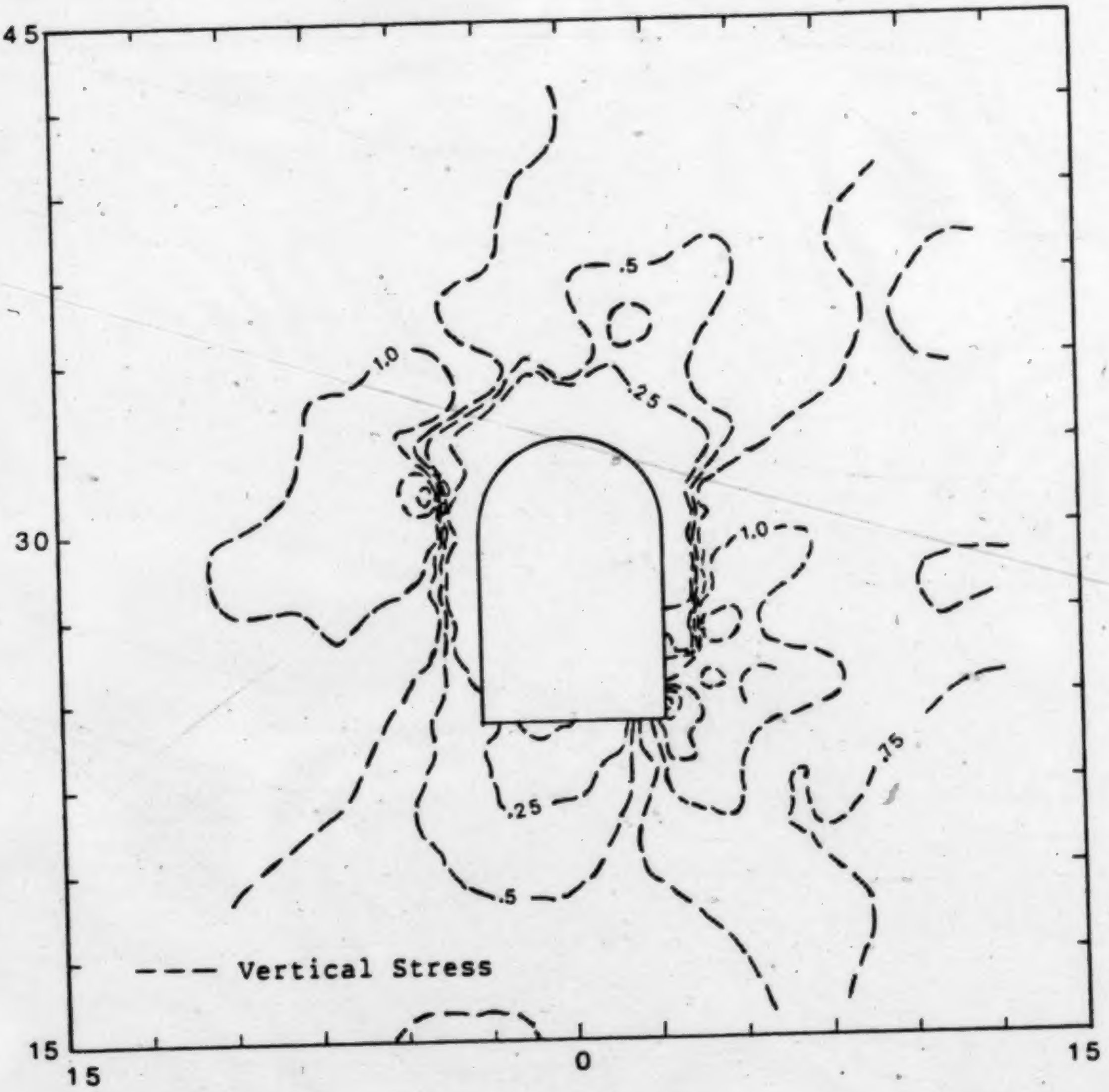

Figure 4.6 Vertical Stress Contours for N=2.0, θ=55°, σ_1=0.5, Stiffness Reduction=10.0, Soft Zone: 2.0 m at Crown; 1.0 m at Springline

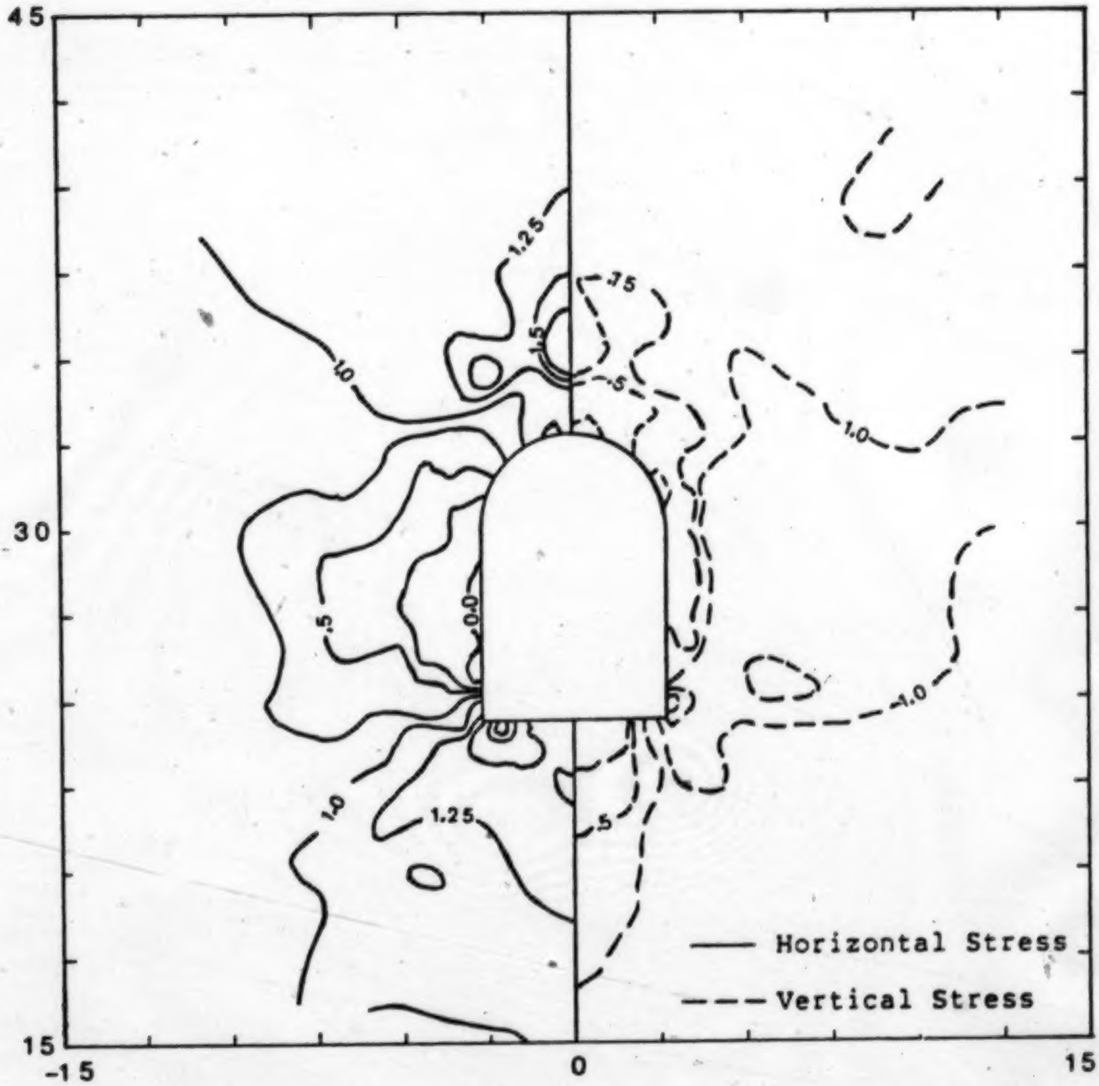

Figure 4.7 Stress Contours for N=1.0, θ=55°, σ_1=1.0, Stiffness Reduction=2.0, Soft Zone: 2.0 m at Crown; 1.0 m at Springline

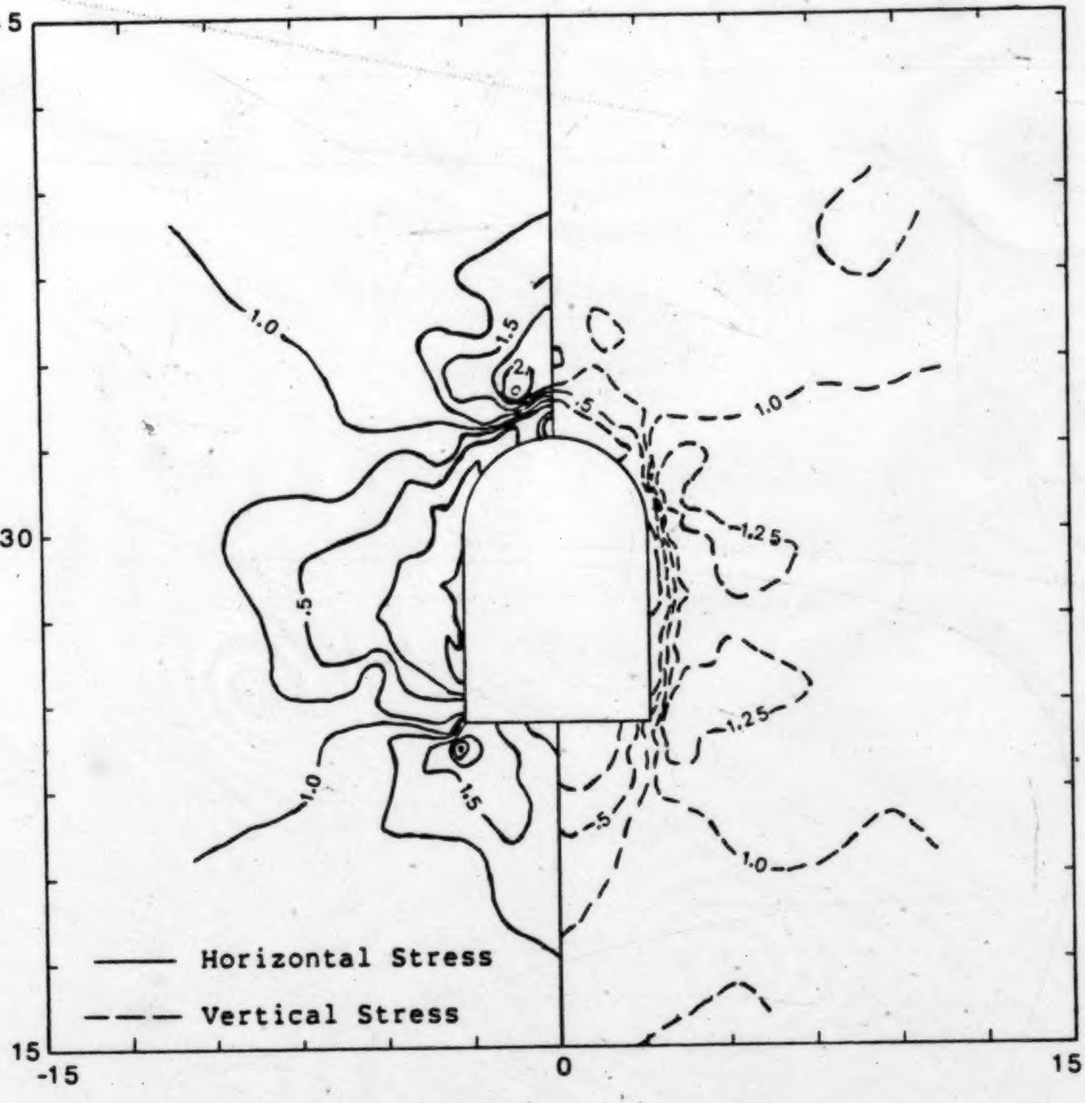

Figure 4.8 Stress Contours for N=1.0, $\theta=0°$, $\sigma_1=1.0$, Stiffness Reduction=5.0, Soft Zone: 1.0 m at Crown; 0.5 m at Springline

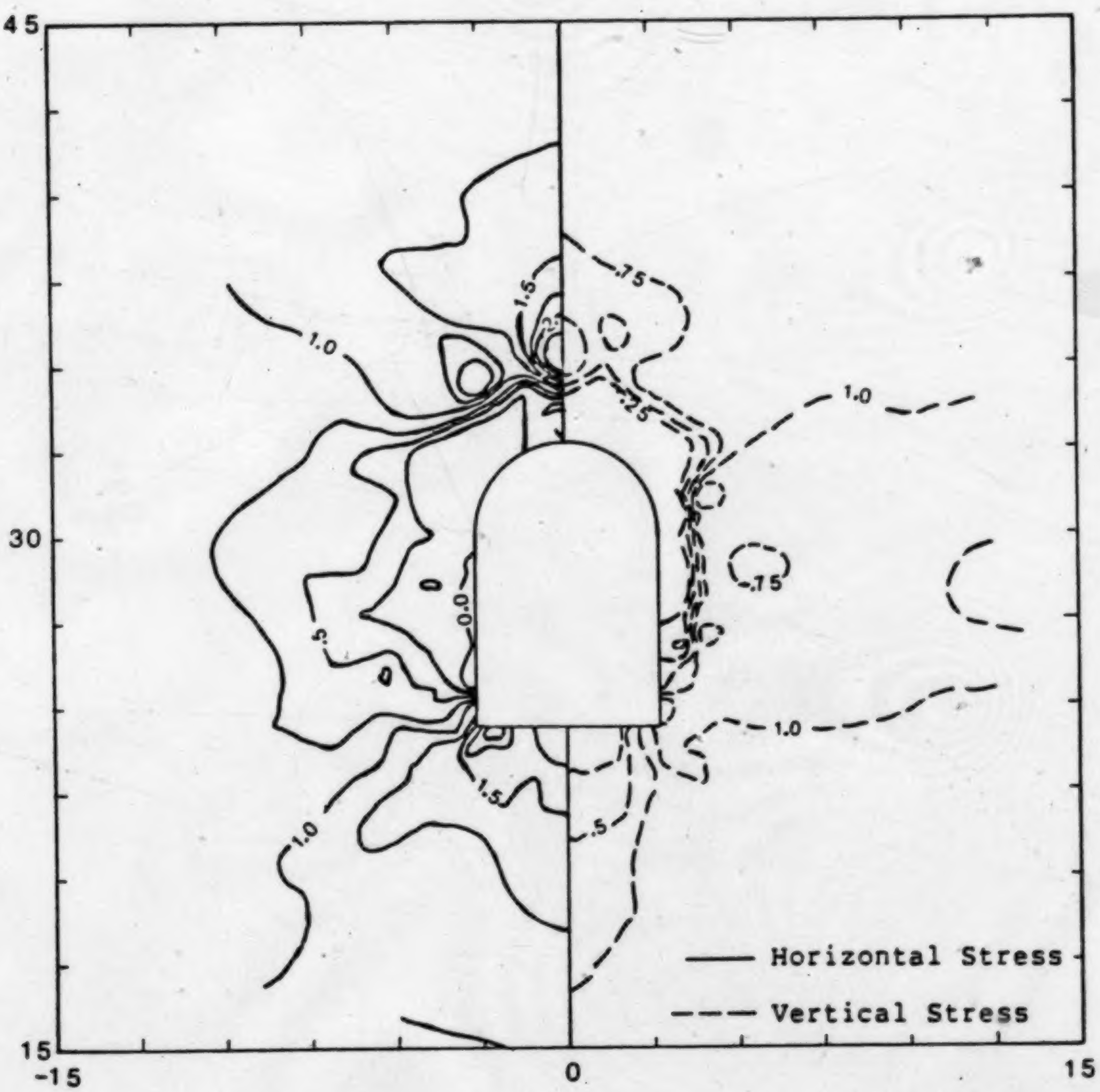

Figure 4.9 Stress Contours for N=1.0, θ=55°, σ_1=1.0, Stiffness Reduction=10.0, Soft Zone: 2.0 m at Crown; 1.0 m at Springline

Table 4.1 presents the calculated and measured uniaxial stress changes at the gauge locations. The results are presented as ratios with the stress change at the radial gauge in hole S1 being taken as 1.0. Table 4.2 shows the actual measured final stress change and the calculated stress change at the gauge locations. All the finite element analysis were performed with σ_1 = 1.0 MPa and the principles of superposition were employed to determine the stresses for various values of σ_1.

A comparison of Figures 4.4 and 4.8 shows that for a stiffness reduction of 5 times stress concentrations occur immediately outside the softened zone. The boundary (extent) of the soft zone used in finite element analysis is shown in Figure 4.4. Thus, as the soft zone increases in thickness the distance from the opening wall to the point where the stress concentration occurs also increases. Therefore, the gauges must all lie within the softened area (for this set of parameters) because all instruments recorded a stress decrease.

When the stiffness reduction is very small, e.g. a stiffness of 0.5 times the original value, there is only a small amount of stress redistribution in the horizontal direction. However, in the vertical direction there is a reduction in the stress near the sidewall and an increase further from the wall as the stiffness is reduced (see Figures 4.3 and 4.7). Table 4.1 shows that this stress condition (Figure 4.7) does not match the measured results

Table 4.1 Normalized Measured and Predicted Stress Changes

LOCATION	MEASURED	CALCULATED				
		CASE 1	CASE 2	CASE 3	CASE 4	CASE 5
1-Radial	1.00	1.00	1.00	1.00	1.00	1.00
1-Tang.	0.67	0.61	0.75	0.11	0.64	1.27
3-Radial	0.71	1.03	1.00	1.00	1.41	1.00
3-Tang.	0.30	0.51	0.77	0.11	-0.59	1.27
4-Tang.	0.32	0.32	0.49	-0.81	0.73	0.66
5-Tang.	0.24	0.52	0.77	0.25	0.53	1.17

Case 1: $N=1.0$, $\sigma_1=1.0$, $\theta=0°$, $E_R/E_S=5.0$,
Soft Zone: 2.0 m at Crown; 1.0 m at Springline.

Case 2: $N=1.0$, $\sigma_1=1.0$, $\theta=55°$, $E_R/E_S=10.0$,
Soft Zone: 2.0 m at Crown; 1.0 m at Springline.

Case 3: $N=1.0$, $\sigma_1=1.0$, $\theta=55°$, $E_R/E_S=2.0$,
Soft Zone: 2.0 m at Crown; 1.0 m at Springline.

Case 4: $N=1.0$, $\sigma_1=1.0$, $\theta=0°$, $E_R/E_S=5.0$,
Soft Zone: 1.0 m at Crown; 0.5 m at Springline.

Case 5: $N=2.0$, $\sigma_1=0.5$, $\theta=55°$, $E_R/E_S=10.0$,
Soft Zone: 2.0 m at Crown; 1.0 m at Springline.

Table 4.2 Measured and Predicted Stress Changes

HOLE #	ORIENTATION	MEASURED STRESS CHANGE (MPa)	PREDICTED STRESS CHANGE	
			CASE 1	CASE 2
1	Radial	-27.40	-22.50	-21.30
	Tangential	-18.35	-12.90	-15.90
3	Radial	-19.53	-23.10	-21.30
	Tangential	-8.33	-10.50	-16.50
4	Tangential	-8.75	-7.20	-10.50
5	Tangential	-6.50	-11.70	-16.50

Case 1: N=1.0, σ_1=30.0, $E_R/E_S=5.0$,
Soft Zone: 2.0 m at Crown; 1.0 m at Springline.

Case 2: N=1.0, σ_1=30.0, θ=55°, $E_R/E_S=10.0$,
Soft Zone: 2.0 m at Crown; 1.0 m at Springline.

(Case 3).

For the loading condition shown in Figures 4.5 and 4.6 it can be seen that both the horizontal and vertical stresses are close to zero adjacent to the opening, except near the floor of the opening. This loading produces much higher tangential stress decreases than predicted.

Figures 4.4, 4.7 and 4.9 can be compared to investigate the effects of the amount of stiffness reduction on the stresses around the opening. The area around the bottom of the opening has not been softened so all of the cases exhibit similar stresses here. Looking at the horizontal stress it can be seen that as the stiffness reduction is increased from $E_R/E_S=2$ to 5 there is a much larger stress concentration outside the soft zone in the crown. The stress condition is not significantly altered as the stiffness is further reduced to $E_R/E_S=10$. When $E_R/E_S=2.0$ the vertical stress within the soft zone along the sidewalls is more than 50% of the field stress. Upon increasing this to a value of 5 the vertical stress at this location is reduced to about 25% of the field stress and then increases sharply outside the softened zone. The vertical stress at the springline is reduced to less than 25% of the field stress when E_R/E_S is increased to 10. This further decrease in stiffness causes the calculated tangential stress decreases at the gauge locations to exceed those measured (see Table 4.1, Case 2). A stiffness reduction of $E_R/E_S=5$ produces the best agreement between the measured and calculated results.

With a large softened zone present and no measurements outside this zone, it is not possible to estimate the stress field accurately at this site. The orientation of the major principal stress cannot be determined exactly. However, there is strong evidence in support of a stress ratio near unity which is also supported by the finite element results. If the stress ratio is unity or very close to it, then the direction of the principal stress is not important. Findings from the finite element work suggest that E_R / E_S is in the order of 5. Employing all of these values it is possible to estimate the magnitude of the principal stress. Considering all the factors discussed above, the in situ stress field at this location is estimated to be:

σ_1 = 30 ± 8 MPa
θ = 0°
N = 1.4 ± 0.6
E_R/E_S = 5
Soft Zone: 2.0 m at crown & 1.0 m at springline.

4.4 AxiSymmetric Analysis

4.4.1 Method of Analysis

An axisymmetric finite element analysis was performed to determine at what location all the stress change at the plane of measurement had occurred. An equivalent circular opening with a diameter of 7.0 m was assumed. Two cases were tested: 1) assuming perfectly elastic behavior; and 2) assuming a 1.0 m softened zone both ahead of the face and along the sidewalls with a stiffness reduction of 5 times.

ADINA has the ability to kill elements or have elements born at a given time. This is excellent for the case where no softening occurs. However, when the stiffness of several elements must be reduced with each excavation step problems arise. Thus, a different procedure was adopted. For both cases the program was rerun for each excavation step and the elements in the opening were assigned a low stiffness and the softened elements were given the desired reduced stiffness. This is not exactly correct because the displacements caused by an excavation step should be applied at the nodes before excavating the next step. The proximity of the boundary may also have an adverse effect on the results.

A further problem with determining the boundary conditions was encountered. Hutchinson (1982) found that a boundary condition with rollers along the tunnel axis and at the boundary opposite to where excavation starts did not restrict longitudinal displacements at the boundary where excavation commences. A pin was placed at the corner between the two surfaces with rollers and load was applied to the free boundaries.

The case under study is somewhat different in that excavation must take place from both boundaries. The mesh and boundary conditions chosen are shown in Figure 4.10.

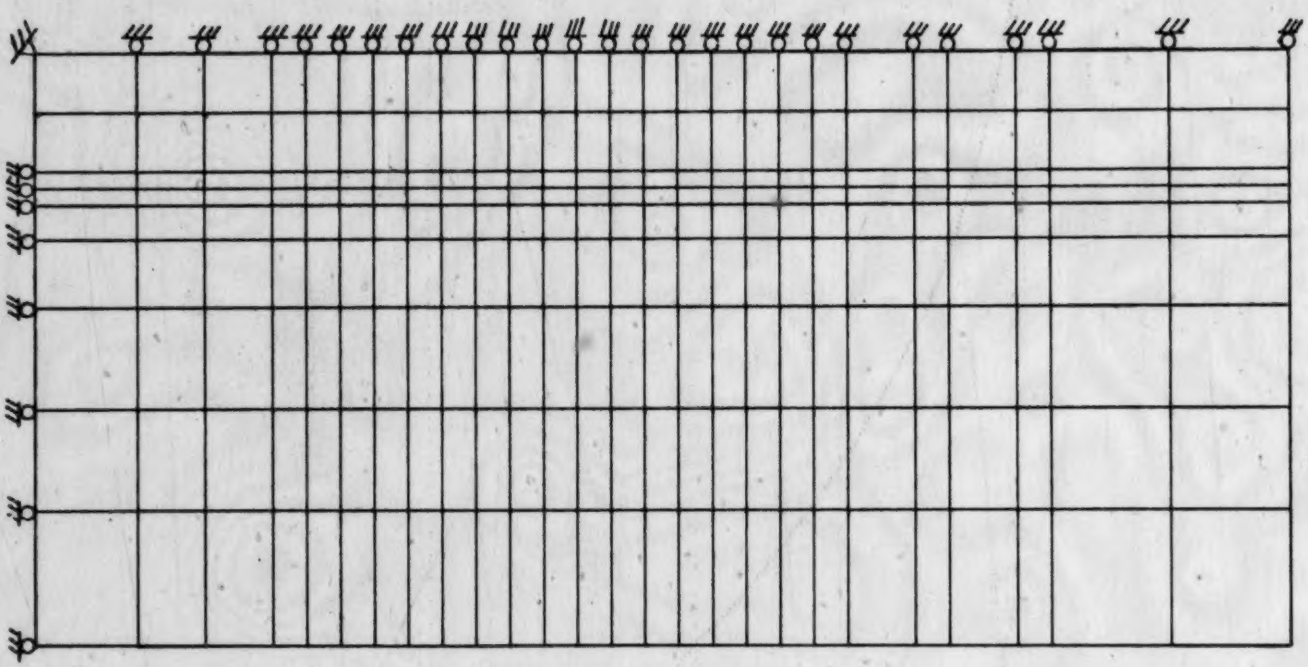

Figure 4.10 Finite Element Mesh Used for Axisymmetric Analysis

There are two rows of elements to be excavated from the tunnel. Several trial runs were made and it was found that the roller at the node that lies within the area to be excavated should be removed as excavation commences from that boundary and should not be replaced. Also, the two elements at the free boundary that lie within the tunnel should not be loaded after excavation commences from this boundary.

In order to determine the magnitude of the error introduced by these inconsistencies the results from the perfectly elastic case are compared with closed form solutions and other published results. Hanafy and Emery (1980) published results showing the influence of the advancing face on the radial displacements at a given location. Figure 4.11 shows the results of their findings along with the results from the present analysis. The radial displacement is plotted as a percentage of the total movement because the two analyses employed different elastic parameters. The agreement between the two analyses is very good.

Figure 4.12 shows a comparison between the final radial displacements caused by excavation, calculated from the axisymmetric analysis, and those predicted from a closed form solution for linear elastic plane strain behavior. The displacements predicted by the finite element analysis are slightly larger than those predicted by the closed form solution. This difference increases with distance from the

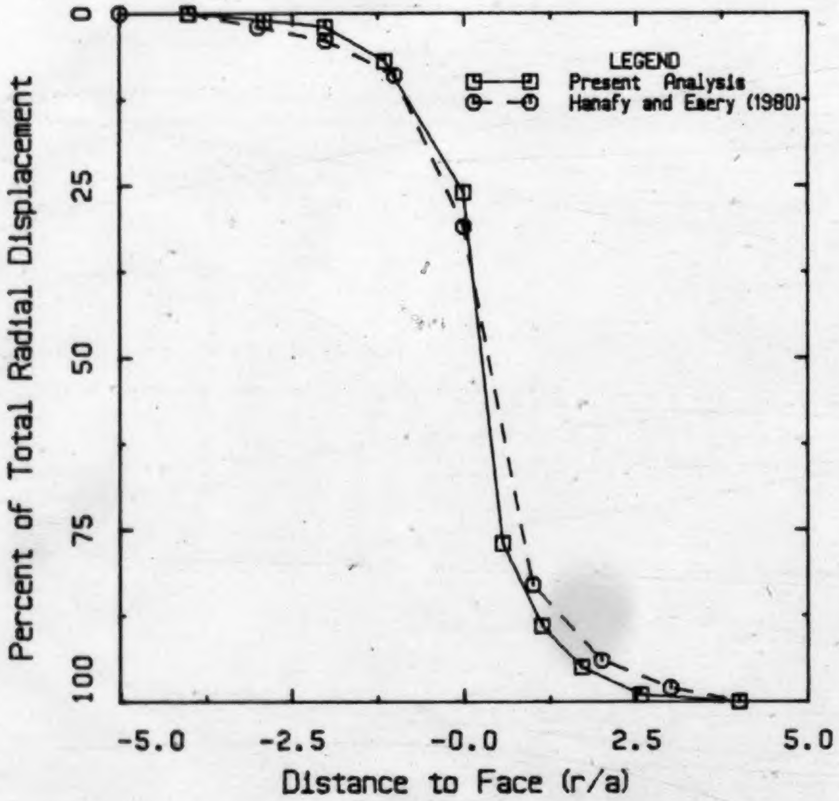

Figure 4.11 Influence of Advancing Face on Radial Displacements- Comparison of Finite Element Solutions

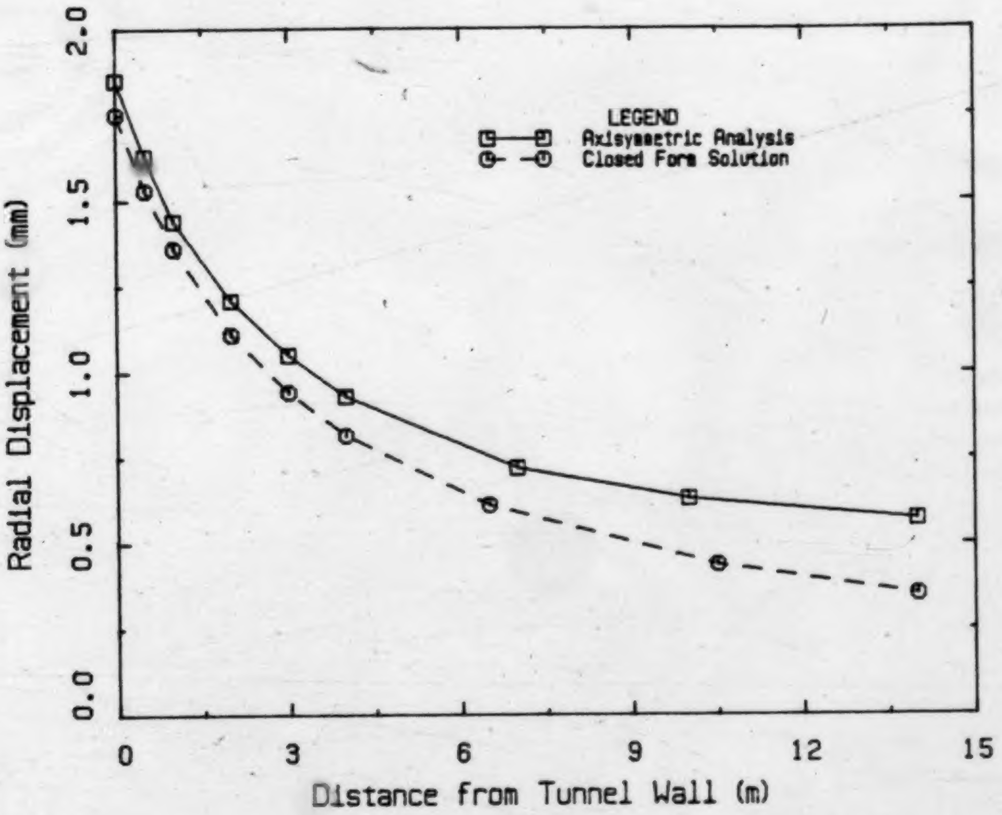

Figure 4.12 Radial Displacements Caused by Tunnel Excavation- Comparison of Finite Element and Closed Form Solutions

opening wall because the proximity of the boundary begins to affect the results. These two comparisons show that the excavation technique employed has a minimal effect on the displacements and that these results are acceptable for the present analysis.

With regard to stresses, Kulhawy (1977) states that the number of excavation steps should not affect the stresses in a homogeneous isotropic body. A comparison of the calculated final radial and tangential stresses and those predicted from Kirsch's equations [Timoshenko and Goodier, 1970] is shown in Figure 4.13. This figure shows good agreement between the calculated and predicted stresses which is in accordance with observations made by Kulhawy (1977). These results indicate that the excavation technique employed will provide adequate accuracy for this study.

4.4.2 Discussion of Results

The main purpose of the axisymmetric analysis was to predict how much of the total expected stress change had occurred at the gauge locations before the gauges were destroyed. For both cases, perfectly elastic and with a softened zone near the wall, distance to face-stress plots are shown for three elements. One element is adjacent to the opening wall with its centre at 0.25 m from the wall, a second is directly below this at 1.5 m from the wall (outside the softened zone); and the third element is above the previous two near the centre of the opening. These

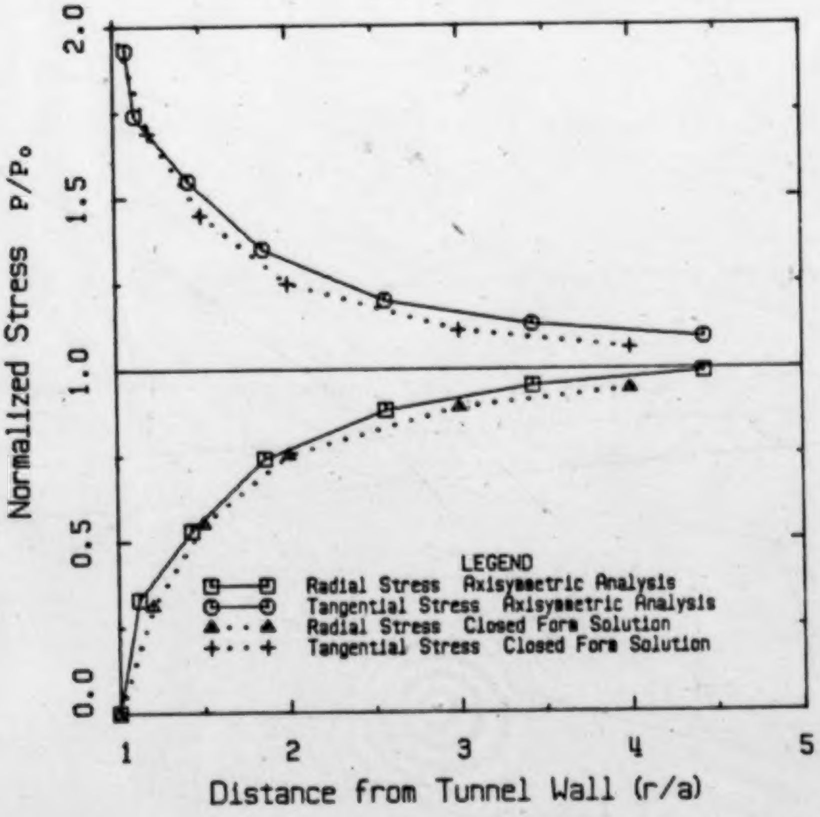

Figure 4.13 Comparison of Stresses from Finite Element and Closed Form Solutions

element locations are shown in Figures 4.14 and 4.15.

Figure 4.14 shows the calculated stress distribution at the plane of measurement for the three elements as the face advances towards them for the perfectly elastic case. It can be seen that very little stress change takes place more than 2a (where a is the radius of the opening) before or after the face passes the measuring plane. The results clearly show that this could not be the stress condition at the field site because the tangential stress shows a large increase as the opening passes the plane of measurement.

Results from the case when a 1.0 m soft zone is placed around the opening are shown in Figure 4.15. For this condition all of the tangential stress change in the element adjacent to the wall (in the soft zone) has occurred when the face reaches the measuring plane. At this same point over 80% of the radial stress has been released. The results indicate that very little stress change had taken place at the gauge locations before their installation. These results also suggest that all of the expected stress change had already occurred prior to the gauges being destroyed, for all but one of the stressmeters. This was the radial gauge at hole S1 where approximately 90% of the expected stress change had occurred. It can be concluded that the initial assumption, i.e., that the gauges recorded all the stress change, is acceptable and the estimated stress field parameters do not have to be adjusted.

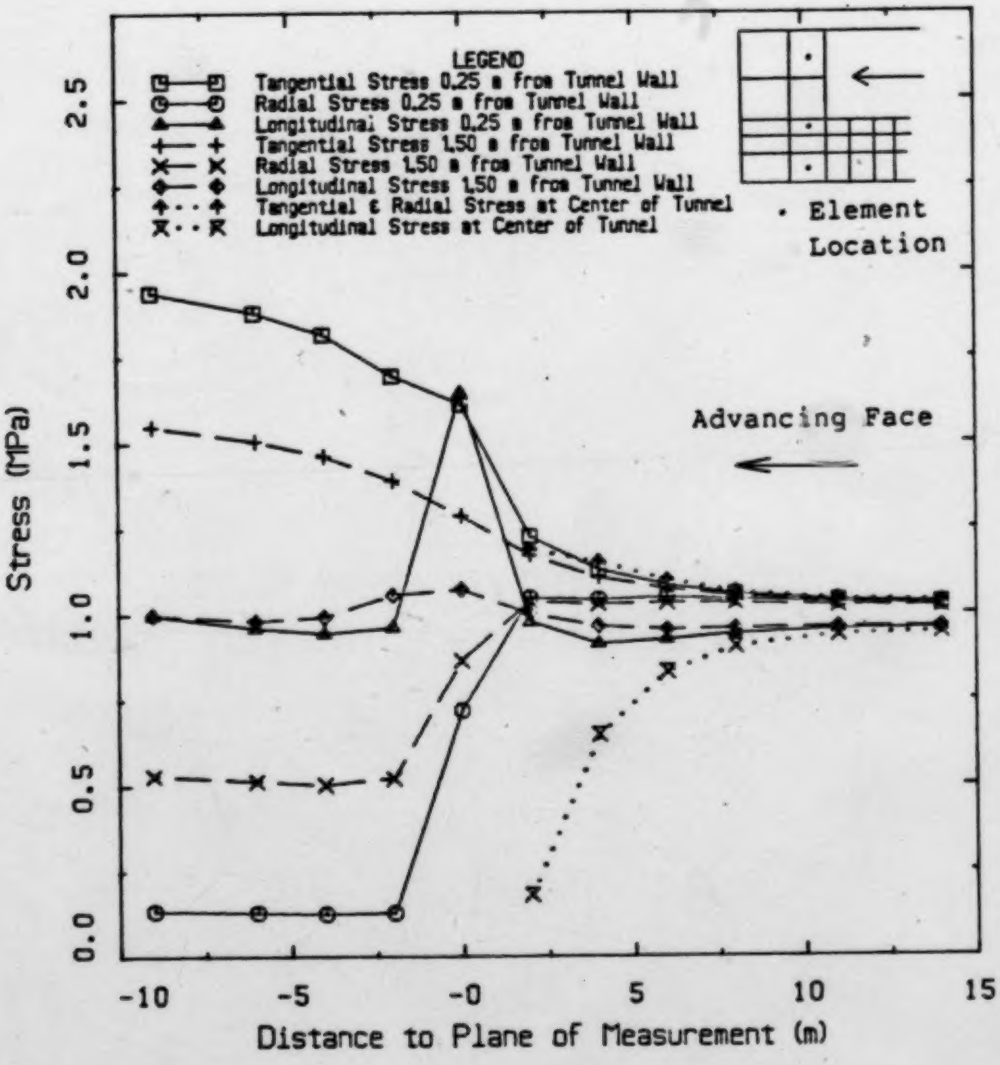

Figure 4.14 Influence of Advancing Face on Stresses- Elastic Case

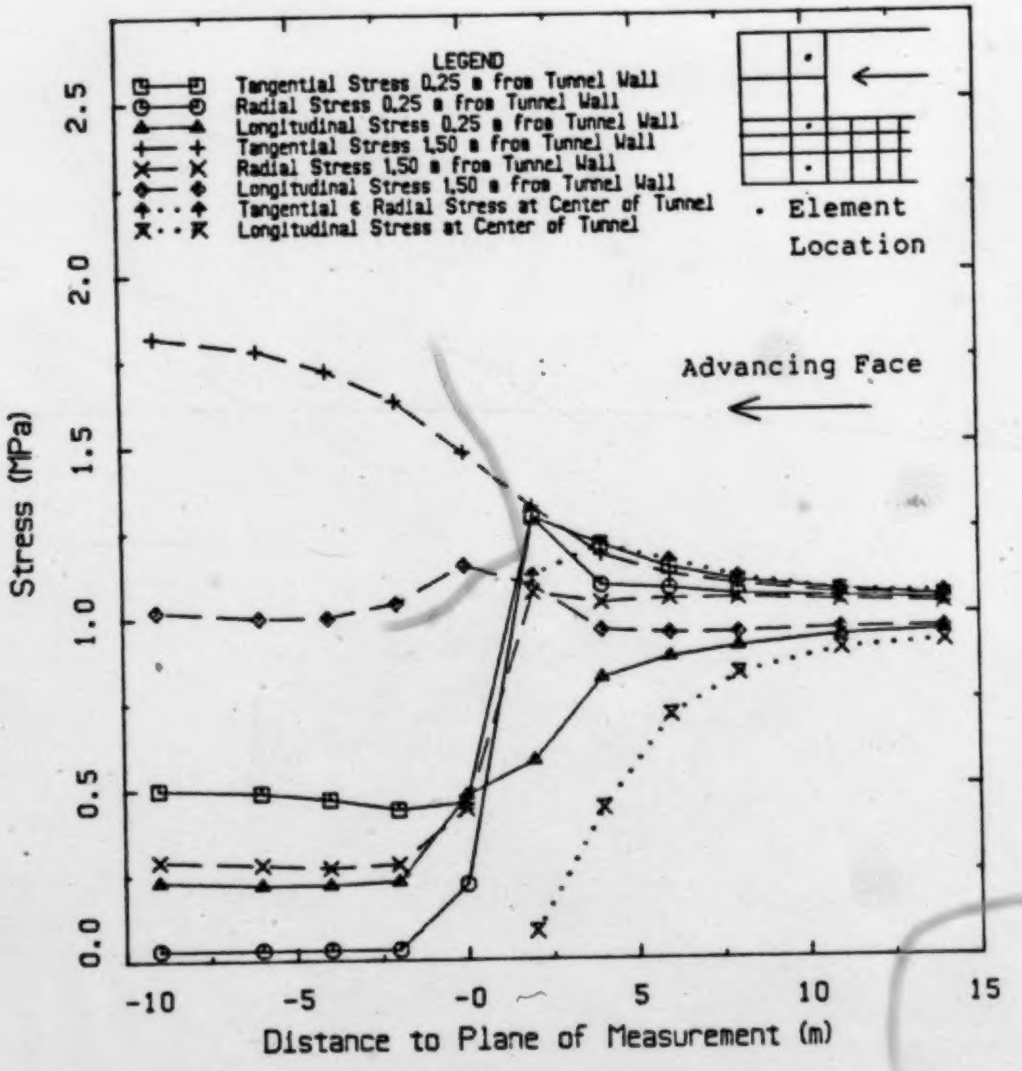

Figure 4.15 Influence of Advancing Face on Stresses- 1.0 m Soft Zone

4.5 Verification of Soft Zone and Stressmeter Performance

There are methods available for estimating the extent of the damaged zone created by blasting based on the charge density and the rock mass properties. Three of these available methods will be used to produce estimates of the thickness of the softened zone for comparison with that determined from the stress change measurements.

Brawner (1981) provides suggested extents of zones of loosening for the conventional drill and blast drive technique applicable for rock masses that are traversed by three or more joint sets. This method considers the joint spacing, the rock texture, the unconfined compressive strength of the rock and the natural moisture content of the material. Using Brawner's chart a soft zone thickness of 0.5b (where b=the width of the opening) would be predicted, For the Wolverine tunnel this would correspond to a soft zone thickness of 2.7 m. This value is somewhat larger than that determined from the stress change measurements; 1.0 m at the springline and 2.0 m at the crown. However, there are two factors that indicate the value predicted from Brawner's method is conservative (on the high side). Firstly, although there are three joint sets at the instrumented section, one of these is discontinuous. Secondly, the strength of the limestone is considerably greater than the value used for the prediction. Thus, it is believed that this estimate is high and therefore, this predicted depth to which blast damage extends closely matches the extent of the soft zone determined from the field measurements.

Studies of vibrations and their impact on structures have suggested that the peak particle velocity provides a good index for assessing potential blast damage [Stimpson, 1982]. This approach has been extended to rock excavations using the induced normal stress which is proportional to the maximum particle velocity.

$$\sigma_i = \gamma c V_{max} \qquad \text{Eqn. 4.1}$$

where σ_i = induced normal stress;
γ = rock mass density;
c = P-wave velocity; and
V_{max} = maximum particle velocity.

Holmberg and Persson (1980) show results of some Swedish research on damage thresholds. These plots allow for the estimation of peak vibration velocities at various distances from the point of detonation for different linear charge densities. Figure 4.16 depicts the typical blasthole layout used for the Wolverine west tunnel. From this information, a very conservative estimate (on the high side) of the linear charge density of 2.0 to 2.5 kg/m was calculated. Using a charge density of 2.5 kg/m velocities high enough to cause rock damage occur up to approximately 1.7 m from the tunnel wall (based on this charge density at the holes nearest the perimeter blastholes).

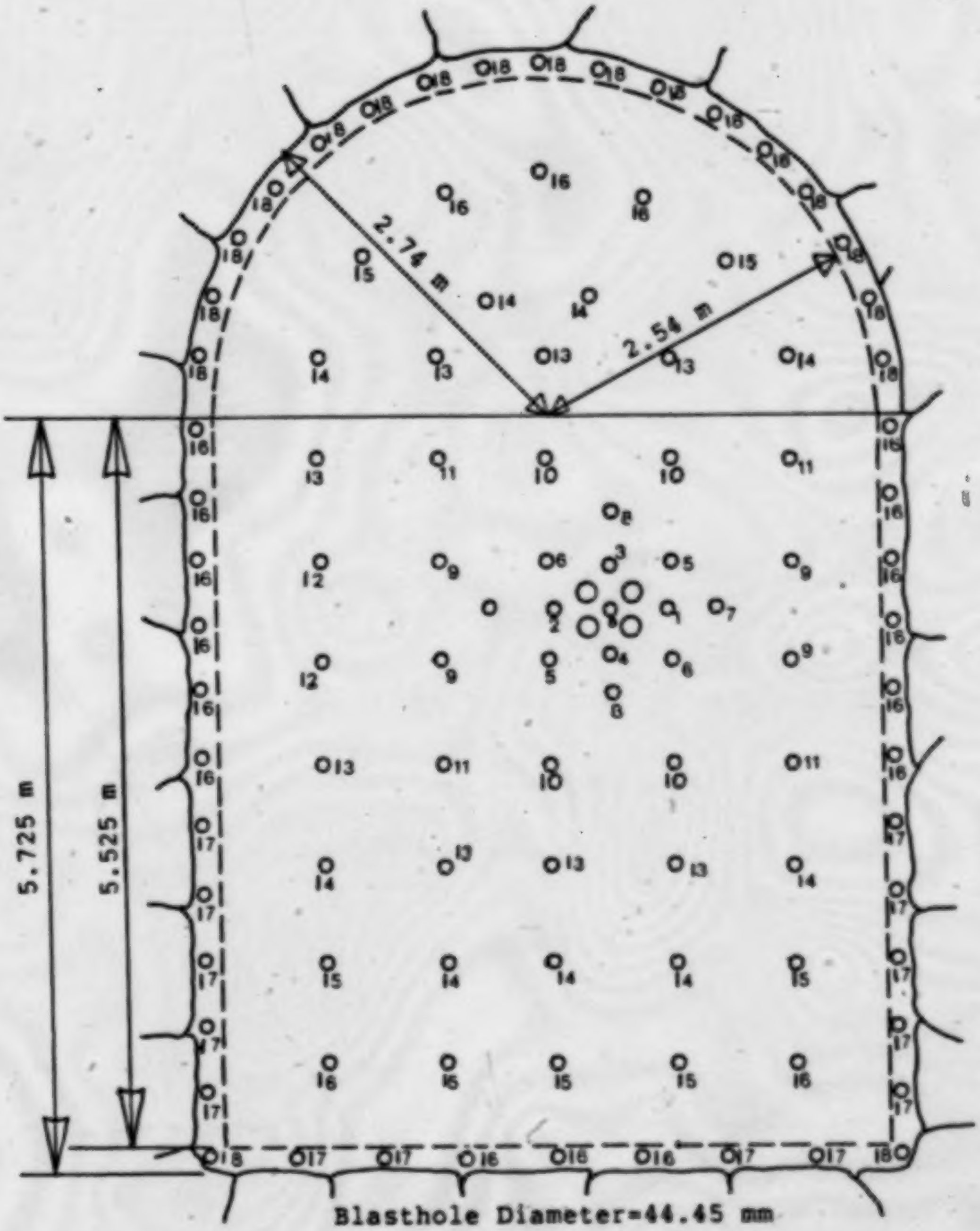
2.74 m
2.54 m
5.725 m
5.525 m

Blasthole Diameter=44.45 mm

Depth=3.65 m

Total Powder=430.8 kg

Powder Load=2.85 kg/m³

Figure 4.16 Typical Blast Pattern for Wolverine West Tunnel

Alternately, the induced stress at various locations from the tunnel wall can be calculated. At the tunnel wall the peak particle velocity caused by the blast from the holes immediately inside the perimeter holes was determined to be 2.3 m/sec. The rock density is about 2400 kg/m^3 and the P-wave velocity is about 3660 m/sec. Substituting these values into Eqn. 4.1 yields an induced stress of 20 MPa at the tunnel wall. If this number is doubled to allow for concentration effects and is then added to the field stress, the total stress would be in the order of 70 MPa which is approaching the uniaxial compressive strength of the rock. This suggests that the extent of damage outside the tunnel perimeter caused from the firing of these holes would be minimal.

Smooth blasting was used and the perimeter holes were closely spaced. Therefore, it is believed that the particle velocities and induced stresses from the detonation of these holes would be considerably less than those sited previously. Thus, the softened zone would not be expected to be increased significantly from the perimeter blast.

With the exception of the gauge in hole S4 all of the stressmeters were preloaded to an extremely high value. The previous findings suggest that the blast would not have loosened the gauges from their boreholes, i.e. induced stresses at the stressmeter hole locations do not exceed the unconfined compressive strength of the rock and spalling of the borehole walls would not be anticipated. Further evidence supporting this statement comes from the gauge readings themselves. Measurements were taken immediately following the blast (within about 1 hour) and again several hours later prior to the upcoming blast. During this time no stress change was recorded by the gauges. If the stressmeter holes had been damaged by the blast and the gauges were loosened, a decrease in reading with time would have been expected. Thus, it is unlikely that this was the case. Furthermore, the results from the gauges correspond to the expected stress at the test location (based on field observations).

In summary, it has been shown that the blast damaged zone estimated from these techniques may be in the order of 1.0 to 2.0 m. This value is in good agreement with that determined from the stress change measurements which provides confidence that this soft zone thickness is reasonable. Also, it can be concluded that the gauges did not become loose in the boreholes and therefore, the readings were not adversely affected by the blasting.

4.6 Alternate Gauge Locations

All of the gauges at the site were located within the softened zone. As shown previously it is difficult to accurately predict the in situ stress field from results of gauges at these locations. Based on the findings from this instrumentation program, it appears prudent to install some gauges outside the soft zone. The finite element results indicate that these gauges would be very useful in defining both the extent of the softened zone and the in situ stress field. Immediately outside the softened zone tangential stress concentrations occur because stress is redistributed to the stiffer elements. The radial stress is not as greatly affected by the softening process since it is generally reduced to a low value near the opening wall.

Results similar to those found at this site were observed by Lukajic (1983) at another site. He found that all of the tangential gauges, both at the crown and springline of a horseshoe shaped opening, recorded a stress decrease. One of these gauges in the crown was about 3.6 m away from the opening (ρ=0.56). A high horizontal stress condition was known to exist at this site and the tangential stress in the crown should have increased significantly.

These two case histories suggest that a softened zone may extend to at least ρ=0.50 or 1.0 times the radius from the opening wall. When the drill and blast method of excavation is used it appears that some gauges should be placed at least one radius from the opening wall to ensure installation in undamaged ground. It is important to have gauges both inside and outside the softened zone to properly define the stress field.

4.7 Analysis of Extensometer Data

The results from the extensometer measurements have been presented in Figures 3.9 and 3.10. The displacements were observed in order to back-calculate or more appropriately verify the value chosen for the rock mass modulus E_R. The stress field has been estimated and the assumptions checked by an axisymmetric analysis which also provided displacements for comparison with those measured.

There are many uncertainties associated with the magnitude of the calculated displacements. Although the stress ratio may vary over a much larger range, the principal stress is known within about 25%. Second, the actual opening is being represented by an equivalent circular opening. The rock mass modulus was estimated from laboratory tests on small samples and may not be a representative value.

Figure 4.17 shows the radial displacements calculated from the axisymmetric analysis for three excavation stages under a uniform stress of 30.0 MPa and with a 1.0 m softened zone: 1) before any excavation had taken place; 2) just prior to installation of the extensometers; and 3) after the excavation had been completed. The radial and longitudinal displacements that occur at a point as the tunnel face approaches are presented in Figures 4.18 and 4.19 for the elastic case and the case of a 1.0 m softened zone around the tunnel. The longitudinal movement recorded by the extensometer 6.0 m ahead of the face was 0.43 mm towards the

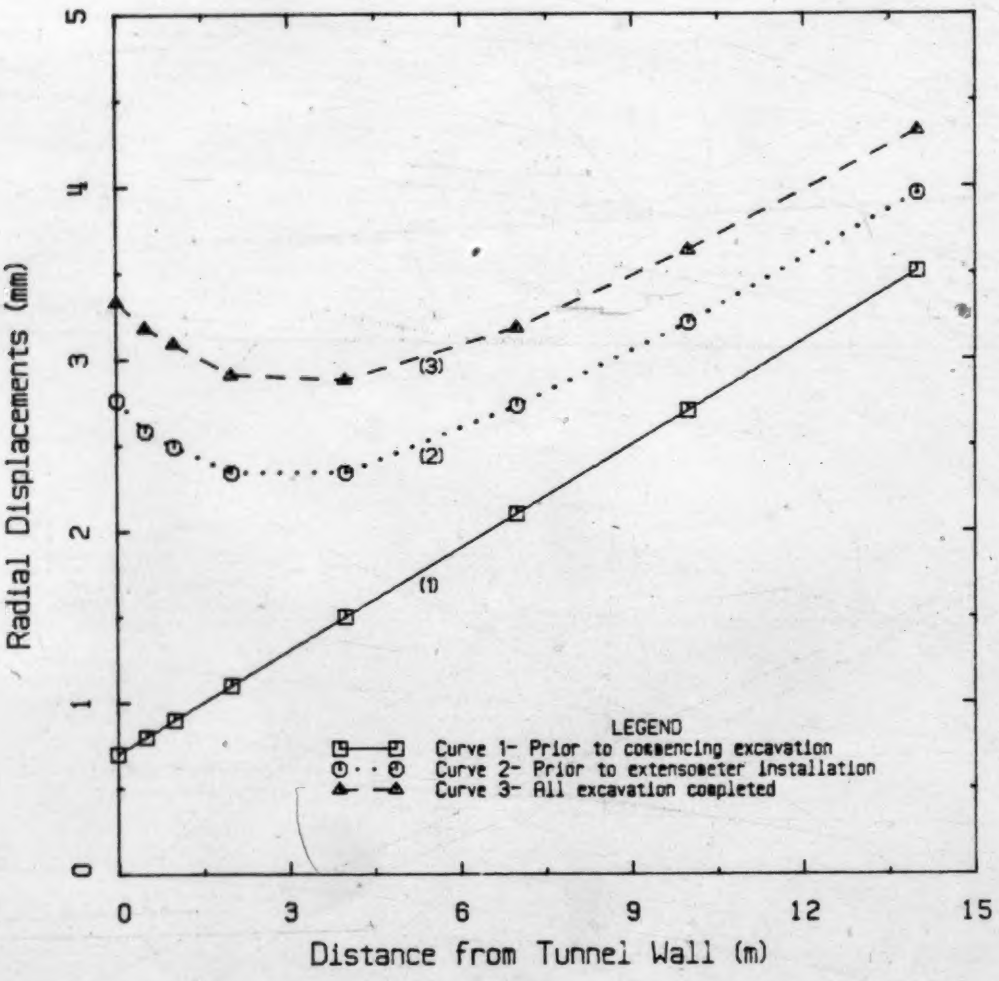

Figure 4.17 Radial Displacements at Three Excavation Stages

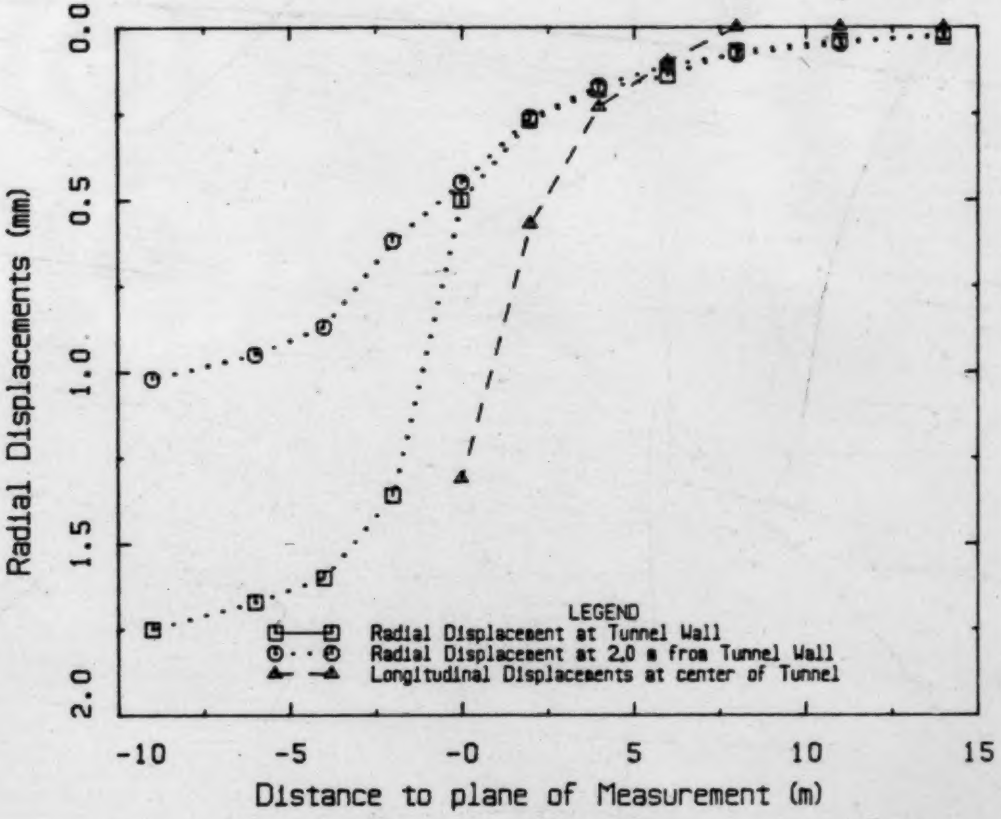

Figure 4.18 Influence of Advancing Face on Displacements-Elastic Case

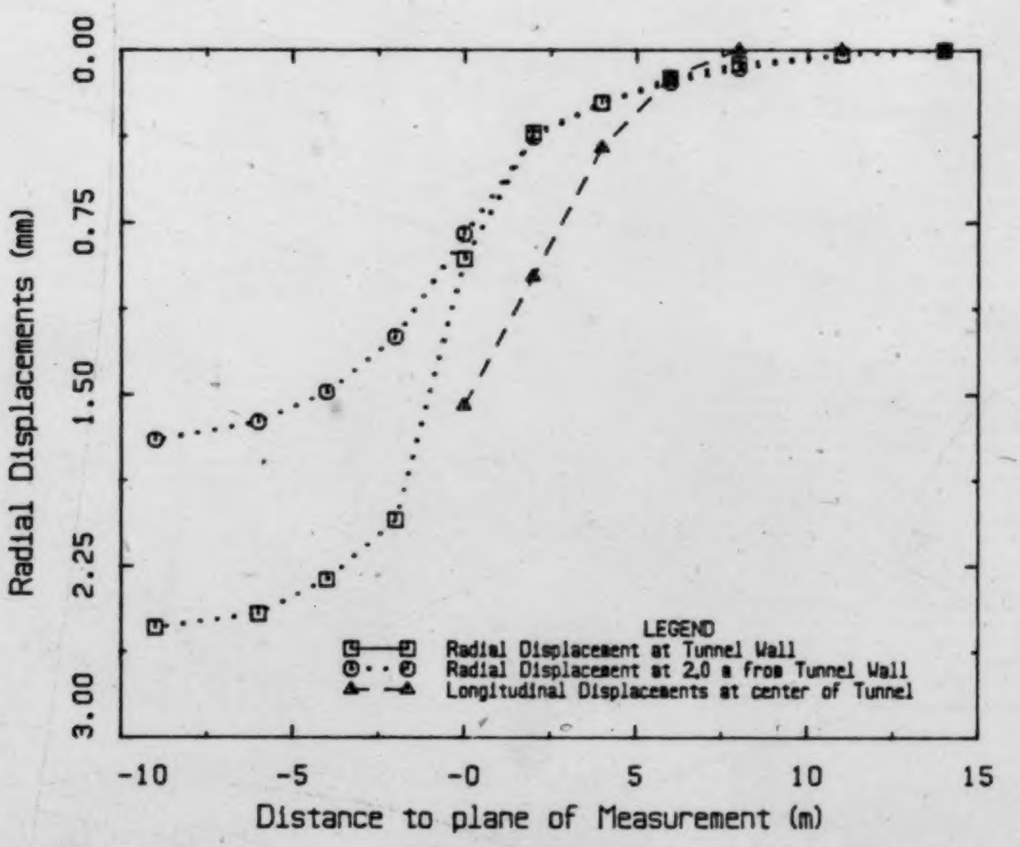

Figure 4.19 Influence of Advancing Face on Displacements- 1.0 m Soft Zone

east face when it was 2.8 m from the anchor. The recorded total radial displacement at the wall was 0.46 mm. Calculated displacements for the longitudinal and radial directions corresponding to these points are 0.69 mm and 0.57 mm, respectively (see Figures 4.17 and 4.19). Assuming that all factors except for the rock mass modulus do not have a significant effect on the displacements a new rock mass modulus of 85000 MPa could be calculated. This is in good agreement with the assumed value, but the assumptions involved with this calculation are very restrictive. The extensometer measurements do, however, provide further evidence that the estimated stress field parameters are a reasonable approximation of the in situ stress conditions.

The extensometers at 1.5 and 3.0 m from the sidewall measured a significant amount of compression. Readings prior to break-through suggested that these extensometers were functioning properly and there was no evidence of damage to them after the final blast. The inner extensometer measured a compression in excess of 5 mm. The calculated elastic radial displacement that would be caused by excavating an equivalent circular opening (7.0 m diameter) is 1.75 mm. Mackay (1982) also found a small zone of compression adjacent to the opening wall, but not nearly as large in magnitude as that found here. Presently, there is no reasonable explanation available for these results, but it is believed to be associated with a "consolidation" following the softening process.

4.8 Calculation of the Ground Convergence Curve

This section is concerned with the development of the ground convergence curve. As before it will be assumed that the shotcrete at the crown is for safety only and is providing a negligible amount of support. The following paragraphs will discuss how the ground convergence curve can be calculated. The field measurements have been used to predict the ground behavior around the opening and the in situ stress condition. The parameters necessary to calculate the ground convergence curve are:

a) opening shape;
b) in situ stress, both σ_1 and N ;
c) initial rock mass stiffness and Poisson's ratio;
d) stiffness reduction within the softened zone;
e) extent of the softened zone;
f) required support pressure at the point where the GCC becomes non-linear,
g) total radial displacement at the wall; and
h) the stress change or radial wall displacement that occurred at the face.

Most of the essential parameters for determining the GCC were obtained from the field measurements. The horseshoe tunnel will be treated as a circular opening with an equivalent diameter of 7.0 m. This diameter is not critical because the results are plotted on a normalized curve (see

Figure 4.20). A Young's modulus of 75000 MPa has been obtained from lab tests on small samples and was shown to be an appropriate value from the field measurements. The in situ stress field has been estimated from the field measurements; N = 1.0 and σ_1 = 30 MPa. Poisson's ratio has been taken as 0.25 for the analysis. The rock mass behavior around the opening has been predicted from the stressmeter measurements. It has been shown that a softened zone of about 1.0 m thickness with a stiffness of 15000 MPa adequately describes the ground conditions around the opening.

The total radial displacement, 2.55 mm or u/u_e=1.46, was obtained from the axisymmetric finite element analysis. Mackay (1982) found that the tangential stress change vs distance from the advancing face curve had the same shape as the corresponding curve for radial wall displacement in elastic ground. He used the tangential stress change measurements to predict the amount of stress change that had occurred at the face. However, when a softened zone exists, these curves do not have similar shapes and an alternate method of determining the stress change at the face must be employed. A closed form solution summarized by Hutchinson (1982) was used to calculate the required support pressure at the point where the GCC becomes bilinear. Initially the calculated curve corresponds to the elastic curve because some displacement occurs before the rock becomes softened. A value of σ/σ_1=0.39 was calculated by this method. From the

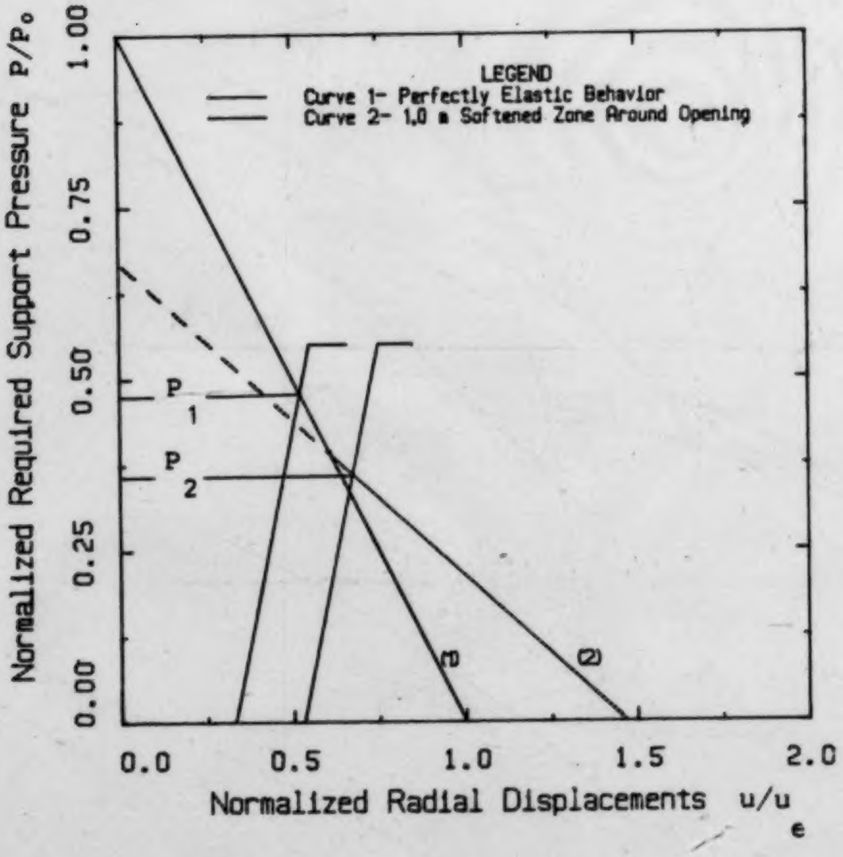

Figure 4.20 Ground Convergence Curve for Wolverine Tunnel

axisymmetric finite element analysis it was found that the radial displacement at the face was $u/u_e = 0.53$.

There are many simplifications that have been made and the curve that is shown may not represent the actual conditions at this tunnel accurately. However, the curve is valid for the conditions stated and thus, it can be used for illustrative purposes to show how softening around the opening may be beneficial by reducing the amount of required support pressure.

Employing these parameters the GCC can be constructed. Figure 4.20 shows a normalized plot of required support pressure versus radial displacement for the case under consideration and for linear elastic behavior (with the same parameters). Several observations can be made from these two curves. First, the total displacement that occurs with a soft zone present is larger than that for the perfectly elastic case. Also, more displacement has taken place at the face if a soft zone exists. This has important implications on the required support pressure. Consider a hypothetical situation where the support is installed at the face. If elastic ground conditions exist a support pressure of P_1 would be required. For the same installation location, but with a softened zone present the support requirements would be reduced by about 20% to P_2 because more displacement has occurred at the face. Thus, softening can be beneficial as long as the gravitational component due to strength loss does not dominate and the stability of the opening is not jeopardized. A more detailed discussion of the effects of softening around an opening is given by Kaiser (1981).

4.9 Summary and Conclusions from the Field Monitoring Program

Results from the extensometers and stressmeters have been analyzed in this chapter. Finite element techniques were employed to calculate stresses around the opening for different loading conditions. These were compared to the measured results to provide an estimation of the in situ stress field at the monitored site. From these results, a ground convergence curve for a simplified opening shape was calculated.

It has been shown that a reasonable model describing the rock mass behavior around the opening can be obtained from measuring the stress change near the face. This may not describe the actual ground behavior accurately because the area adjacent to the opening may be yielded, but these parameters still can be employed to model the behavior. Similar conclusions were stated by Kaiser (1981). However, it was not possible to predict the in situ stress field accurately because all of the gauges were within the soft zone. With gauges installed both inside and outside the softened zone a better estimation of the in situ stress could be made. It has been suggested that additional gauges be placed a minimum of one opening radius from the wall to provide installations in undamaged ground.

For the simplified case of a circular opening, the parameters determined from the field and the computer study were employed to construct the GCC. This exercise confirmed previous findings (Kaiser, 1981) that suggest a softened zone around an opening may be beneficial. The findings also support statements by Kaiser and Hutchinson (1982) who suggested that even a small stiffness reduction may cause stress redistribution. Stress contours shown in Figures 4.3 to 4.9 illustrate that there is a stress transfer to areas further from the tunnel when a softened zone exists. Thus, stresses near the opening wall where potential yielding areas exist are reduced which creates a more stable condition.

5. SUMMARY AND CONCLUSIONS

5.1 Introduction

This thesis has examined the stress change near the face of an underground opening. It consisted essentially of three independent studies: 1) determination of the optimum gauge locations to obtain the highest degree of redundancy from the least number of instruments; 2) verification of the method of data interpretation for results from the stressmeters; and 3) application of these previous findings in a field monitoring program.

The following sections of this chapter present the conclusions of this study and the implications on the opening stability are discussed. Suggestions for further research are also included.

5.2 Data Analysis Technique

Laboratory calibration tests were performed using coal as the host material to study the gauge response in a controlled biaxial stress field. From these results it can be concluded that the method of analysis presented by Hawkes and Bailey (1973) is correct for the first loading or unloading cycle. However, when repeated loading occurs, the measured values deviate from those predicted because the changing shape of the borehole and yielding at the contacts may create a change in contact angle. These deviations may or may not be significant depending on the material properties and the stress levels experienced. If loading is in the direction of the gauge axis, the contact angle would not be as greatly affected, assuming that initial contact was high.

The results clearly indicate that the stress normal to the gauge loading axis must be taken into account for proper interpretation of the measurements. The re-evaluation of a case history by Kaiser *et al.* (1983a) found that neglecting this normal stress resulted in an under-estimation of the magnitude of the principal stress.

Rotation of the principal stresses does not have a significant influence on the gauge response. Any discrepencies that do occur are related to the repeated loading that had taken place prior to the rotation of stresses.

Two important conclusions from this portion of the laboratory work are:

1) for the first loading cycle the gauges record the actual stress change with high accuracy; and
2) the gauges record correctly whether there is a stress increase or decrease.

5.3 Optimum Gauge Locations

A re-evaluation of the technique of data analysis indicated that, for a restrictive set of conditions, the optimum gauge locations could be predicted. This was done for a circular opening in a linear elastic material for the case when the direction of the principal stress was known. It was found that two radial or tangential gauges at 90° to each other at $\rho_1=\rho_2=0.816$ would be a good combination to cover a wide range of stress ratios. This analysis was done prior to the field work which showed that there are additional considerations that cannot be ignored.

Results from the field investigation showed that a softened zone exists around an opening excavated by the drill and blast technique. Although no detailed analysis has been performed, it is believed that gauges should be placed both inside and outside the softened zone for proper in situ stress determination. It was suggested that some gauges be placed at least one radius away from the opening wall ($\rho=0.5$) to ensure some measurements are taken in undamaged material.

Gravity and stress release causing flexure in layered rock masses may also influence the gauge readings. The attitudes of the discontinuities must be considered when determining stressmeter locations. For some conditions, gauges at or below the springline may be best, whereas for others the stresses around the opening may be least affected at the crown. For deep tunnels, such as the one monitored in this study, gravity is believed to have an insignificant effect on the gauge response. The attitudes of the discontinuities at this tunnel are such that flexure of the beds due to removal of confinement would not greatly affect the stresses around the opening.

5.4 Stress Change Measurements Near the Face

Stress change measurements near the face of an opening were taken both in the laboratory under controlled stress conditions and in the field. The laboratory work consisted of stress measurements during overcoring and stress redistribution tests. In the field stress measurements were taken outside the perimeter of the advancing face and directly ahead of the face.

5.4.1 Findings from Laboratory Work

As the face advances there is a stress concentration directly ahead of the tunnel face. This concentration was measured and compared to the results from a simplified axisymmetric finite element analysis. The two values were in very good agreement which suggests that this technique may have potential use for back-calculating the in situ stress. Using this technique is complicated by the fact that the gauge response is affected by changes in both principal stresses in a biaxial stress field.

Stress redistribution tests confirmed the expectation that there is a tangential stress build up with time in yielded areas adjacent to an opening. This has significant implications on the stability of an opening. If these areas are left unsupported yielding may propagate and increase the size of the broken zone which may, under certain conditions, lead to instability. Also, it is important to recognize this when determining support requirements. It was illustrated with ground convergence curves that increasing loads on the liner may be expected with time with the increase being greater when a yielded zone exists.

5.4.2 Findings from Field Program

During the instrument installations a very poor success rate was achieved. This was due in part to a limited time available for the installations, but more importantly, due to the failure of the shear pins to break and release the gauges from the tool. When the eyes would not shear out an alternate recommended procedure had to be employed to release the gauges. The sharp ends of the setting tool may cut the lead wires of other gauges installed in the same hole when this procedure is used. Extra wedges should be obtained from the manufacturer and tested in the laboratory prior to commencing with the field installations to help save time and reduce costs.

Only one gauge ahead of the face was functional after installation. This gauge was installed to measure the stress concentration ahead of the face as was done in the lab. The final reading from this gauge was obtained when the face was 4 m from the gauge. In the next blast the gauge was destroyed. It can be conluded that the success of instruments at this location is highly dependent on the blasting sequence. If a reading had been obtained closer to the face the gauge may have provided some valuable information for verifying the stress field.

It has been shown that from stress change measurements at only a few locations, a model that approximately describes the rock mass behavior can be determined. As well, the in situ stress can be back-calculated, but measurements at more locations are necessary to define the stress field more accurately.

With reference to the ground convergence curve it has been shown that softening around an opening may be beneficial, if the gravitational component does not dominate the stability of the opening. This occurs because when a softened zone is present, more displacement occurs at the face (and all points after the face) than predicted by elastic theory. Thus, the installation of the support would occur after greater displacement had taken place and the load on the liner would be reduced.

5.5 Suggestions for Further Research

In order to properly locate instruments around an opening the expected rock mass response must be considered. Further research is required to develop a better knowledge of the thickness of soft zones that may be induced either by removal of confinement or blast damage. In conjunction with this, the amount of the stiffness reduction is important in order to properly evaluate the opening stability. This reduction factor, as well as the soft zone thickness, varies depending on the method of excavation.

Stress redistribution around an opening has been a topic of much discussion, but very few field or laboratory results are available on the subject. This study has only briefly touched on the the pheneomenon and there is still much work to be done to determine the importance of the stress redistribution caused by each of the major deformation processes outlined in Chapter 2.

REFERENCES

Aiyer, A. K., 1969. An analytical study of the time-dependent behavior of underground openings. Ph. D. Thesis, Department of Civil Engineering, University of Illinois, Urbana, Illinois, 246 pp.,

Babcock, C.O., 1981. Design concepts for a unidirectional response drill hole stress or strain measuring gage. Proceedings of the 22nd U.S. Symposium on Rock Mechanics, pp 397-402.,

Bathe, K.J., 1978. ADINA, A finite element program for automatic dynamic incremental nonlinear analysis. Massachusetts Institute of Technology, Report 82448-1.,

Brawner, C.O., 1981. Geological and geotechnical criteria for assessing the stability of inclines, headings and tunnels. From "Rock Stability in Underground Openings", Edited by C.O. Brawner, 1981.,

Cook, C.W. and E.S. Ames, 1979. Borehole inclusion stressmeter measurements in salt. 20th U.S. Symposium on Rock Mechanics, Austin, Texas, pp. 481-489.,

Cording, E.J., J.A. Hendron, H.H. Macpherson, W.H. Hansmire, R.A. Jones, J.W. Mahr and T.D. O'Rourke, 1975. Methods for geotechnical observations and instrumentation in tunnelling. Volumes 1 and 2, Report Prepared for the U.S. National Science Foundation, Washington, D.C. NTIS No. PB252585-PB252586.,

Curtis, D.J., L.M. Lake, W.T. Lawton and D.E. Crook, 1976. In-situ ground and lining studies for the Channel Tunnel

Project. Proceedings of Symposium "Tunnelling '76", London, 1976, pp. 231-242.,

da Fontoura, S.A.B., 1980. Time-dependent response of rock masses during tunnelling. Ph. D. Thesis, Department of Civil Engineering, University of Alberta, 341 pp.,

Descoeudres, F., 1978. Analysis and design of near-surface openings in stratified rock. Prepared for Special Summer Program "Current Developments in Rock Engineering", M.I.T. 1978, 28 pp.,

Egger, P., 1980. Deformation at the face of the heading and determination of the cohesion of the rock mass. Underground Space, Vol. 4, No. 5, pp 313-318.,

Fossum, A.F., J.E. Russell and F.D. Hansen, 1976. Analysis of vibrating wire stress gage in soft rock. Society for Experimental Stress Analysis, Spring Meeting, Silver Springs, May, 1976., pp. 261-264.,

Guenot, A., 1979. Investigation of tunnel stability by model tests. M. Sc. Thesis, Department of Civil Engineering, University of Alberta, 217 pp.,

Hanafy, E.A. and J.J. Emery, 1980. Advancing face simulation of tunnel excavation and lining placement. 22nd Canadian Rock Mechanics Symposium, Vol. 22, CIM, pp. 119-125.,

Hawkes, I. and W.V. Bailey, 1973. Low cost cylindrical stress gauge. Report prepared for U.S. Bureau of Mines, NTIS No. PB243347, 142 pp.,

Heuer, R.E. and A.J. Hendron, 1971. Geomechanical model study of the behavior of underground openings in rock subjected to static loads. U.S. Corps of Engineers Report N-69-1, Report 2, Contract No. DACA39-67-c-0009, 222 pp.,

Hocking, G., 1976. Three-dimensional elastic stress distribution around the flat end of a cylindrical cavity. International Journal of Rock Mechanics and Mining Sciences & Geomechanics Abstracts, Vol. 13, pp 331-337.,

Hoek, E. and E.T. Brown, 1980. Underground excavations in rock. Institution of Mining and Metallurgy, London, 527 pp.,

Holmberg, R. and P. Persson, 1980. Design of tunnel perimeter blasthole patterns to prevent rock damage. Institution of Mining and Metallurgy, London, Transactions Section A, Vol. 89, pp. 37-40.,

Hutchinson, D.E., 1982. Effects of construction procedures on tunnel and shaft performance. M. Sc. Thesis, Department of Civil Engineering, University of Alberta, 267 pp.,

Irad Gage Inc., 1977. Vibrating wire stressmeter instruction manual. 33 pp.,

Jaworski, G.W., B.C. Dorwart, W.F. White and W.R. Beloff, 1982. Behavior of a rigid inclusion stressmeter in an anisotropic stress field. 23rd U.S. Symposium on Rock Mechanics, pp. 211-218.,

Kaiser, P.K., 1981. A new concept to evaluate tunnel performance- Influence of excavation procedure. 22nd

U.S. Rock Mechanics Symposium, Boston, 1981, pp. 264-271., Kaiser, P.K., 1979. Time dependent

Kaiser, P.K., 1979. Time dependent behavior of tunnels in jointed rock masses. Ph. D. Thesis, Department of Civil Engineering, University of Alberta, 395 pp.,

Kaiser, P.K., and D.E. Hutchinson, 1982. Effects of construction procedure on tunnel performance. 4th International Conference on Numerical Methods in Geomechanics, Vol. 2, pp. 561-570.,

Kaiser, P.K., D. Korpach and C. Mackay, 1983a. In situ stress and deformation property determination during excavation of underground openings. Submitted for publication to the Canadian Geotechnical Journal, July 1983, 55 pp.,

Kaiser, P.K., C. Mackay and N.R. Morgenstern, 1982. Performance of a shaft in weak rock (Bearpaw Shale). ISRM Symposium on Caverns and Pressure Shafts, Aachen, Vol. 2, pp. 613-622.,

Kaiser, P.K., S. Maloney and N.R. Morgenstern, 1983b. Support design for underground cavities in weak rock. Part III. Energy Resources Research Fund Contract No. U-80-3, 157 pp.,

Kaiser, P.K. and N.R. Morgenstern, 1978. Time-dependent deformations of rock near failure. Proceedings of the 4th International Congress on Rock Mechanics, Montreux, Switzerland, Vol. 1, pp. 195-202.,

Kaiser, P.K. and N.R. Morgenstern, 1981. Time-dependent deformations of small tunnels- Part I- Experimental Facilities; Part II- Typical test data. International Journal of Rock Mechanics and Mining Sciences & Geomechanics Abstracts, Vol. 18, No. 2, pp. 129-152.,

Klohn Leonoff Ltd., 1981. Geological investigations and engineering- Tumbler Ridge Branch Line Tunnels. Prepared for British Columbia Railways, Vol. 1, April 1981, 116 pp.,

Kulhawy, F.H., 1977. Numerical methods in geotechnical engineering. Chapter 16, Embankments and Excavations, Editors C.S. Desai and J.J. Christian, McGraw Hill, pp 528-555.,

Lacerda, W.A. and W.N. Houston, 1973. Stress relaxation in soils. Proceedings of the 8th International Conference on Soil Mechanincs and Foundation Engineering, Moscow, pp. 221-227.,

Ladanyi, B., 1974. Use of long-term strength concept in the determination of ground pressure on tunnel linings. Proceedings of the 3rd International Congress on Rock Mechanincs, Denver, Colorado, Vol. 2B, pp. 1150-1156.,

Lane, K.S., 1977. Instrumented tunnel tests: a key to progress and cost saving. Underground Space, Vol. 1 pp. 247-259.,

Lukajic, B., 1983. Personal Communications. Ontario Hydro.

Mackay, C.H.R., 1982. Performance of a shaft in weak rock. M. Sc. Thesis, Department of Civil Engineering, University of Alberta, 257 pp., Mackay, C., P.K. Kaiser and N.R. Morgenstern, 1983. Evaluation of rock classification for tunnelling. Report I. Prepared for British Columbia Railways-Tumbler Ridge Branch Lines, September, 1983, (in preparation).,

McCreath, D.R., 1980. Analysis of formation pressures on tunnel and shaft linings. M. Eng. Report, Department of Civil Engineering, University of Alberta, 100 pp.,

Merrill, R.H. and J.R. Peterson, 1969. Deformation of a borehole in rock. U.S. Bureau of Mines, RI5881, 32 pp.,

Morgenstern, N.R. and D.K.J. Noonan, 1974. Fractured coal subjected to direct shear. Proceedings of the 3rd International Congress on Rock Mechanics, Denver, Colorado, Vol. 2a, pp. 282-287.,

Nair, K., R.S. Sandhu and E.L. Wilson, 1968. Time-dependent analysis of underground cavities under an arbitrary initial stress field. 10th U.S. Symposium on Rock Mechanics, Texas, Chapter 27, pp. 699-730.,

Nishida, T., Y. Matsumura, Y. Miyanaga and M. Hori, 1982. Rock mechanical viewpoint on excavation of pressure tunnel by tunnel boring machine. ISRM Symposium on Caverns and Pressure Shafts, Aachen, pp. 815-826.,

Osmanagic, M. and I. Jasarevic, 1976. Stresses and strains around underground openings in rock with viscous-elastic-plastic properties. Proceedings of the International Symposium on Investigation of Stresses in Rock, Sydney, Australia, pp. 107-114.,

Pariseau, W.G., 1978. A note on monitoring stress changes in situ. International Journal of Rock Mechanics and Mining Sciences & Geomechanics Abstracts, Vol. 15, No. 4, pp. 161-166.,

Pariseau, W.G. and I.M. Eitani, 1977. Post-elastic vibrating wire stress measurements in coal. International Symposium on Field Measurements in Rock Mechanics, Zurich, Vol. 1, pp. 255-273.,

Stimpson, B., 1982. Tunnel drilling and blasting. Review paper presented at Short Course on Design and Construction of Tunnels and Shafts for Engineers in Urban Development, Transportation and Resource Development, 1982, Edmonton, Alberta, 33 pp.,

Timoshenko, S.P. and J.N. Goodier, 1970. Theory of Elasticity. 3rd Edition, McGraw Hill, New York, 567 pp.

APPENDIX A

Sample Description and Testing Apparatus

Sample Description and Properties

The coal sample used for the laboratory testing was cut from a large block of coal in the manner described by Kaiser (1979). Joint spacing varied between 5 and 25 mm with the major joint set striking at approximately 40° to the major principal stress direction (Y direction). This joint set was discontinuous.

The final dimensions of the sample were 625x625x212 mm. All sides of the sample were hand sanded to ensure the surfaces were planar. The sample was coated with plaster of paris, separated from the coal surface by wax paper, to help ensure a more uniform load distribution. Holes for the extensometers were drilled and the instruments installed keeping accurate records of the exact locations. Sheets of teflon were placed on all surfaces of the sample isolating it from the loading head to minimize friction. Locations of the extensometers measuring average radial strain are given in Appendix B, Figure B.1 along with strain-time plots from test MC7.18. Details of the stressmeter locations have been given in Chapter 2.

Several tests were done on the intact sample to determine representative rock mass properties. This investigation is concerned primarily with the time independent properties that are required to interpret the stressmeter results. Kaiser *et al.* (1983b) report both the time dependent and the time independent properties of the sample. They found that the first loading produced appreciable strains due to crack closure and compression of the plaster of paris and thus, the stress-strain curves were non-linear. Subsequent loadings produced a more repeatable stress-strain response.

It was found by Kaiser *et al.* (1983b) that no significant anisotropy existed in the plane of bedding which was perpendicular to the proposed tunnel axis. In order to completely describe the behavior of a linear elastic, transverse isotropic material a total of five parameters are needed; two Young's moduli and three Poisson's ratios. Methods of determining these parameters have been discussed by Kaiser *et al.* (1983b) . For the purposes of this investigation only the Young's modulus and the Poisson's ratio in the plane of isotropy are of interest. These values were found to be 1.47 ± 0.32 GPa and 0.225 ± 0.064, respectively.

A more complete set of the properties of this material have been presented by Morgenstern and Noonan (1974), Kaiser and Morgenstern (1978, 1981), Kaiser *et al.* (1983b) and da Fontoura (1980) who also provides a summary of some of the previous results.

Model Testing Equipment

The testing apparatus was designed by Kaiser (1979) based on work by Heuer and Hendron (1971). Kaiser and Morgenstern (1981) summarize the important considerations in the design of the test system. The equipment essentially consists of a reaction frame with lateral and longitudinal restraint, a hydraulic pressure loading system including twelve rams, a safety system, and a data acquisition system.

The sample is placed in the apparatus such that the tunnel axis is vertical so that gravity does not have to be included and so the tunnel can be excavated under load. A large concrete block covered with a steel plate comprises the lower reaction frame while four rams are used to provide the upper longitudinal reaction. Applied loads are monitored by load cells, one for each ram, and the longitudinal displacements are measured by LVDT's (linear variable differential transformers) and dial gauges. The dial gauges provide instant data to aid in maintaining plane strain conditions during loading.

Load in the horizontal direction was applied by eight rams (two on each face) and was transferred to the sample through load cells and a set of triangles. The triangles have been shown to provide a satisfactory stress distribution [Heuer and Hendron, 1971]. The lateral reaction was provided by a cantilever with moveable steel tie rods. This inhibited bending stresses and allowed for easy sample installation.

Details of the hydraulic loading system are given by Kaiser (1979) and are summarized by Kaiser and Morgenstern (1981). The hydraulic loading system was designed to supply and maintain constant oil pressure to each ram and to lock in this pressure. As well, each ram can be pressured individually by a hand pump. Safety switches were placed at each ram to turn off the air pressure if excessive movement or rotation took place.

With the exception of readings from the stressmeters, all of the data was recorded automatically by a Fluke 2240B Datalogger. The data can be recorded either on paper or magnetic tape (or both). From the magnetic tape the data can be transferred directly to the computer where programs have been developed to generate the desired plots. Thus, data from each test can be analyzed prior to applying a new load.

APPENDIX B

This Appendix contains strain-time plots from test MC7.18 that are used to aid in interpreting the stress change measurements from this test. Also included are three strain-time plots that are referred to in Chapter 2, one from each of three constant stress tests that were done. Results for three of the gauges from the constant stress tests done when the opening was present are included.

Figure B.1 shows the sample and locations of the internal instrumentation used for measuring displacements. The instruments are located by reference to a cylindrical co-ordinate system with the polar axis corresponding to that of the principal stress direction. Station 0 is taken as the top of the sample. All Station numbers refer to the vertical distance from the top of the sample to the point of measurement in mm. The lateral boundary displacements were measured midway along the sides at Station 131 for Sides 1 and 4, at Station 181 for Side 2 and at Station 136 for Side 3. Longitudinal boundary displacements were recorded at each corner of the sample on top of the loading head.

Relative radial displacements were measured at the locations outlined below with r being the distance from the centre of the sample to the midpoint of the instrument gauge length:

Station 56: r = 104.1 ± 1.2 mm at orientations of $\theta = 45°$, 90°, 225° and 270°;

Station 81: r = 128.6 ± 3.0 mm at 45° intervals from $\theta = 0°$ to 315° inclusive;

Station 106: r = 104.2 ± 1.6 mm at 45° intervals from $\theta = 0°$ to 315° inclusive;

Station 131: r = 128.0 mm at an orientation of $\theta = 90°$; and

Station 156: r = 103.7 ± 1.9 mm at orientations of $\theta = 45°$, 90° and 225°.

Longitudinal displacements were recorded at the four corners of the sample on top of the loading head. Tunnel convergence measurements were taken parallel and perpendicular to the major principal stress at Stations 139 and 62, respectively, parallel to the major joint set at Station 113 and perpendicular to the major joint set at Station 88.

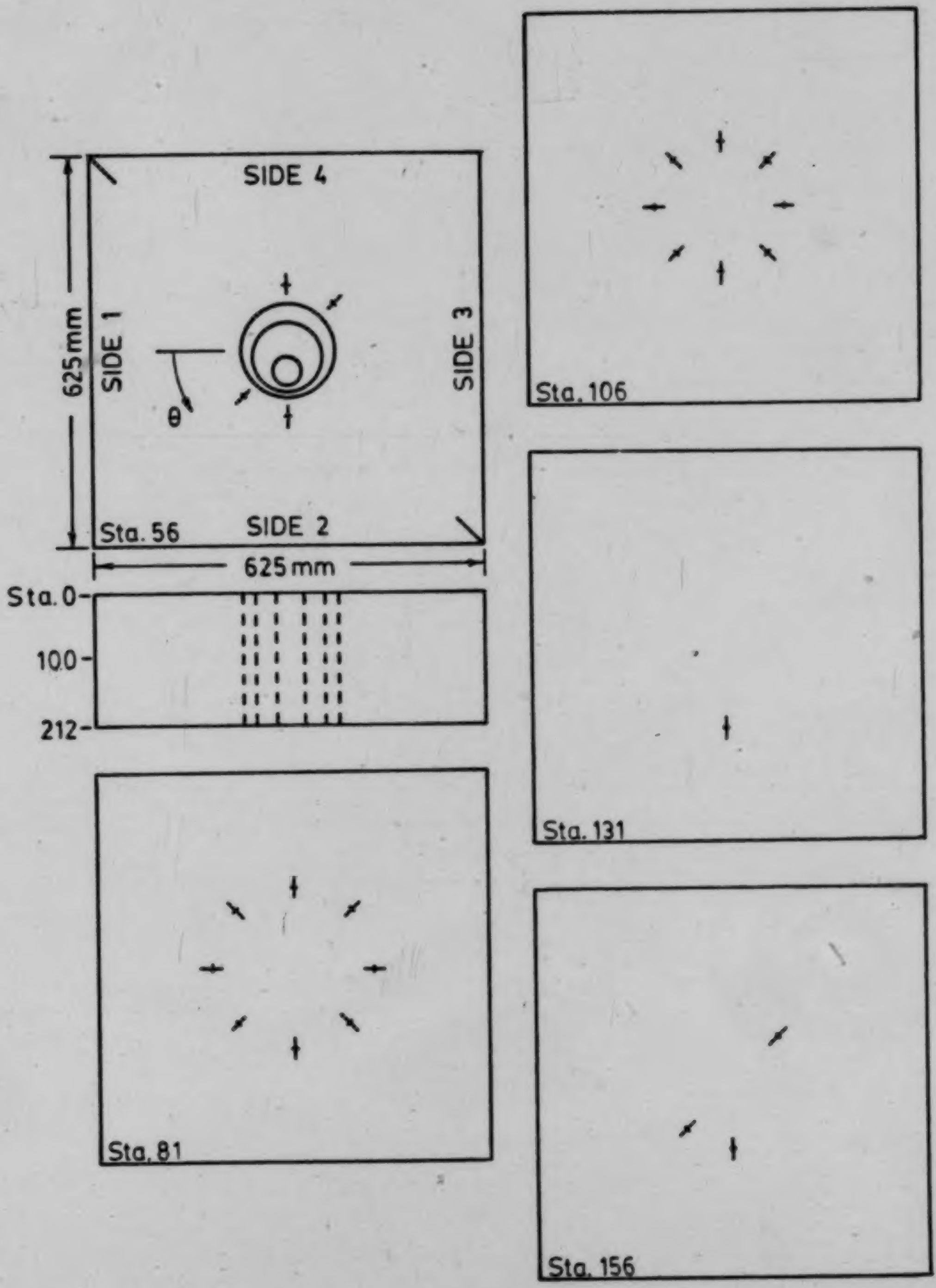
SIDE 4
625mm
SIDE 1
θ
SIDE 3
Sta. 56
SIDE 2
625mm
Sta. 0
100
212
Sta. 106
Sta. 131
Sta. 81
Sta. 156

Figure B.1 Locations of Internal Displacement Measuring Instruments

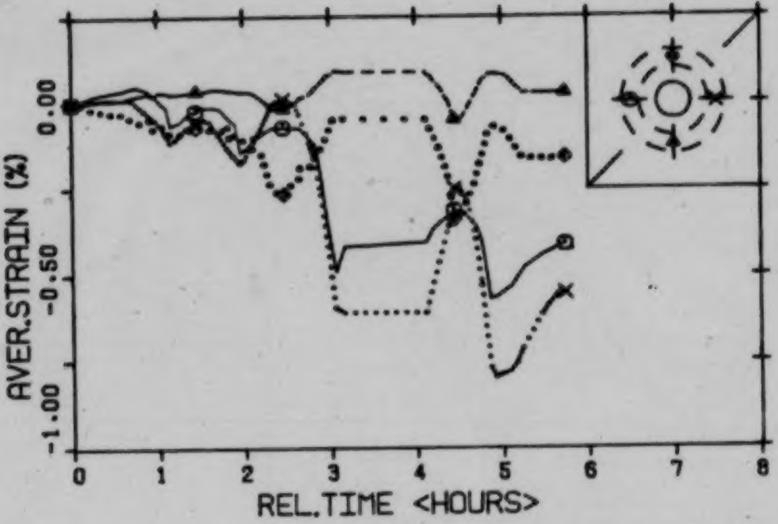

Figure B.2 MC7.18 Radial Strain at Sta. 81

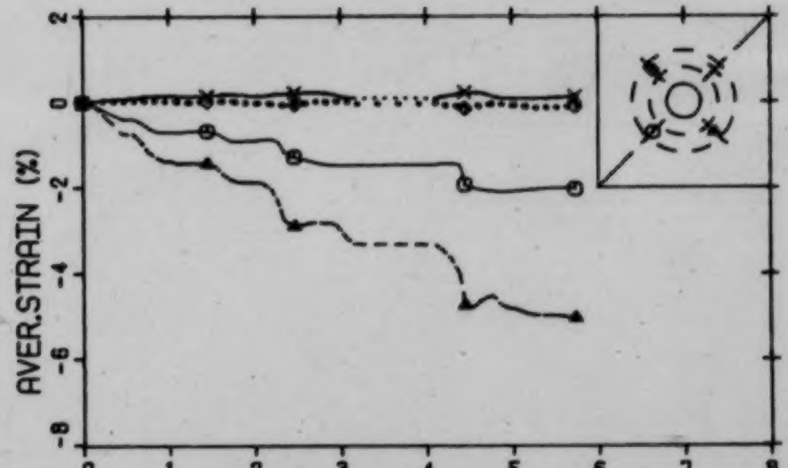

Figure B.3 MC7.18 Radial Strain at Sta. 81

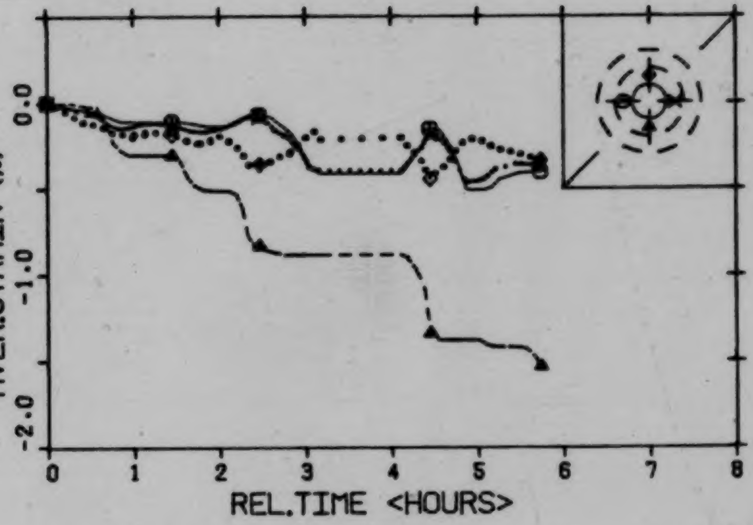

Figure B.4 MC7.18 Radial Strain at Sta. 106

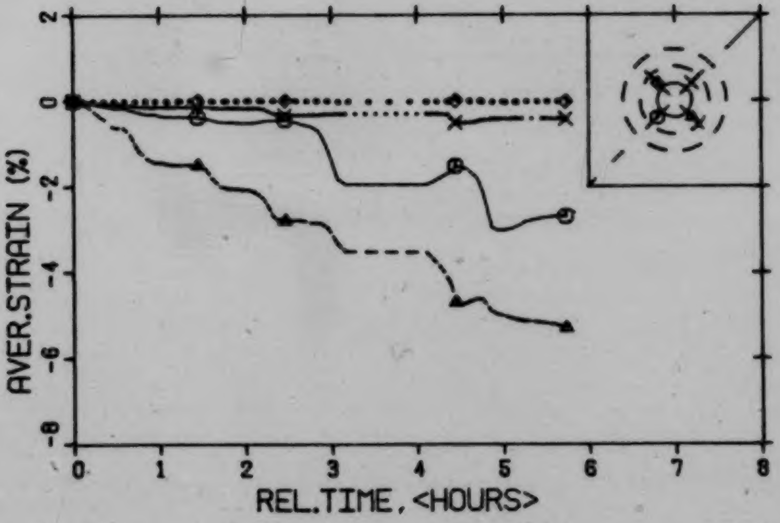

Figure B.5 MC7.18 Radial Strain at Sta. 106

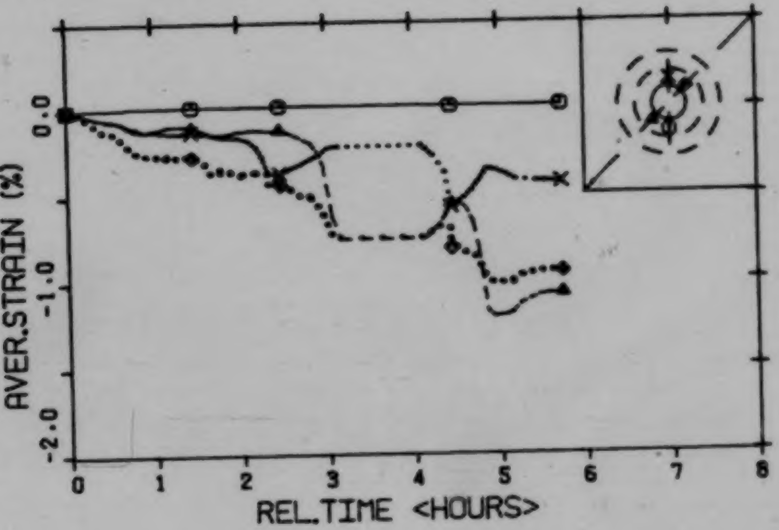

Figure B.6 MC7.18 Radial Strain at Sta. 56

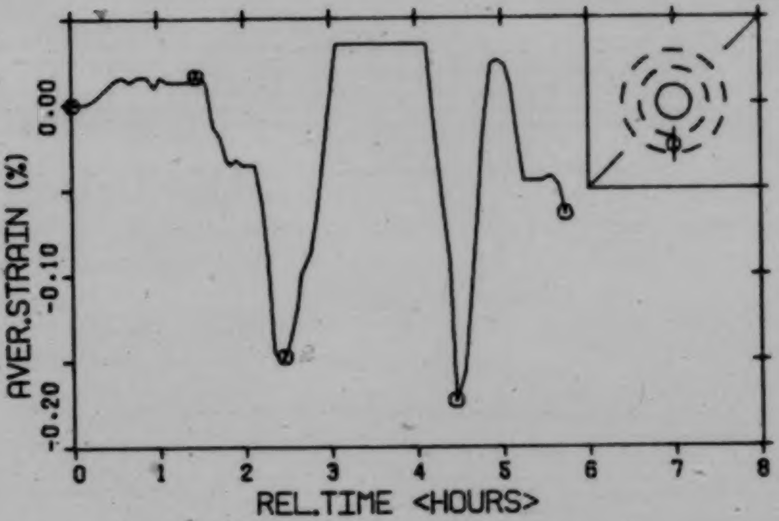

Figure B.7 MC7.18 Radial Strain at Sta. 131

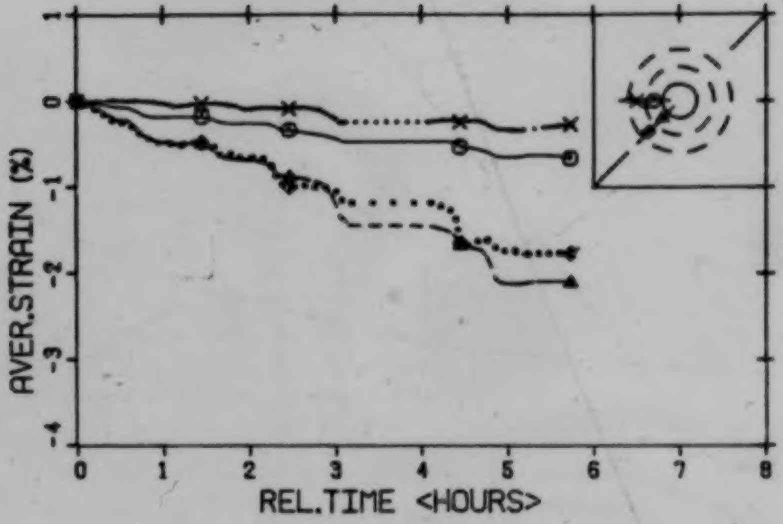

Figure B.8 MC7.18 Average Radial Strain

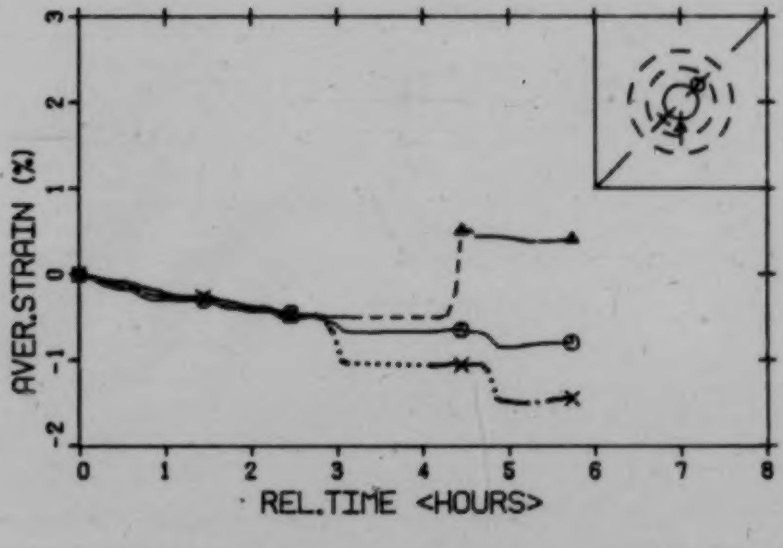

Figure B.9 MC7.18 Radial Strain at Sta. 156

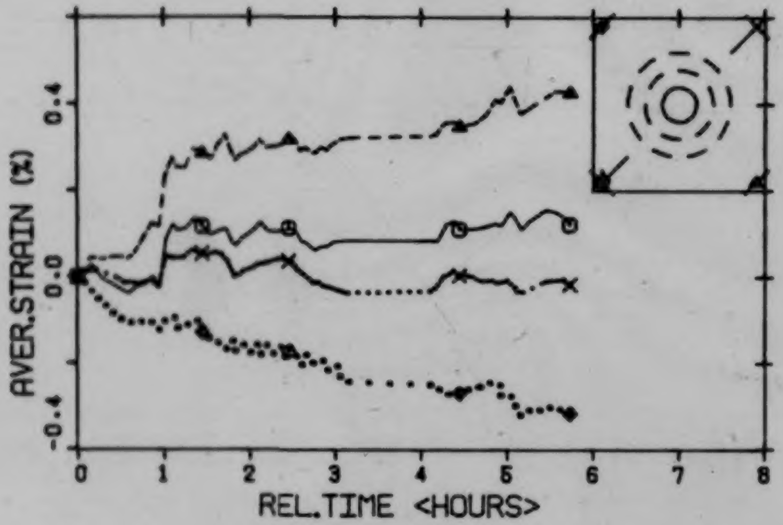

Figure B.10 MC7.18 Longitudinal Strains

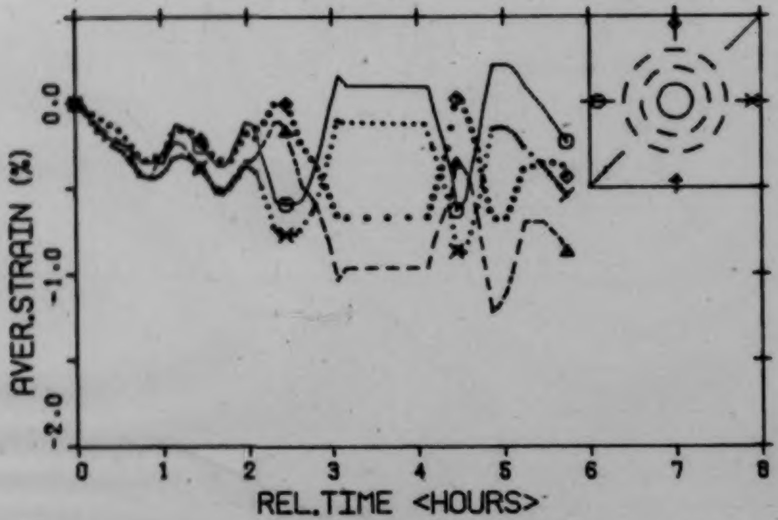

Figure B.11 MC7.18 Lateral Strains

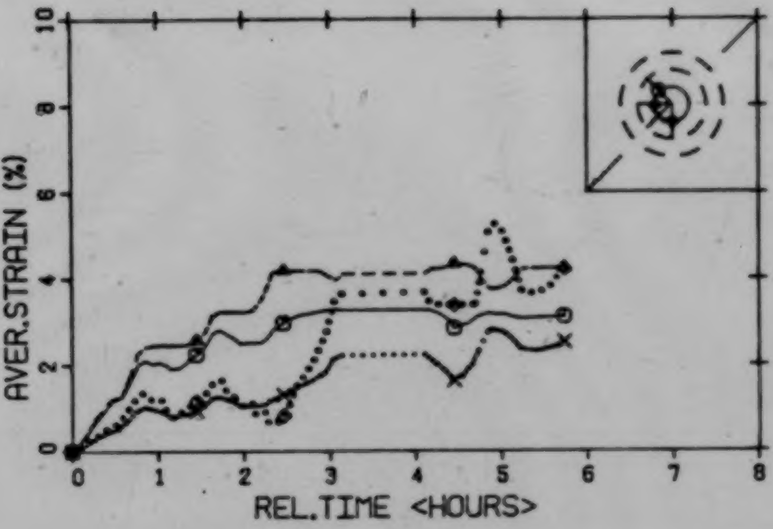

Figure B.12 MC7.18 Tunnel Closure (152 mm Diameter)

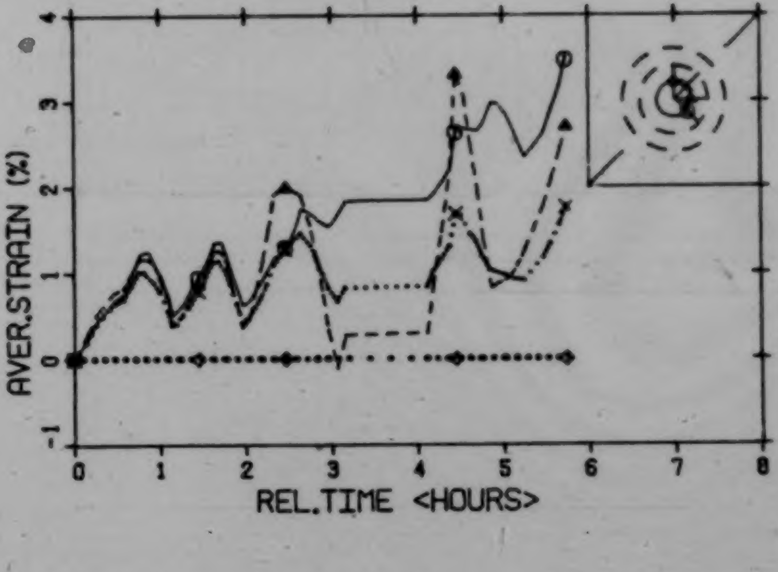

Figure B.13 MC7.18 Tunnel Closure (152 mm Diameter)

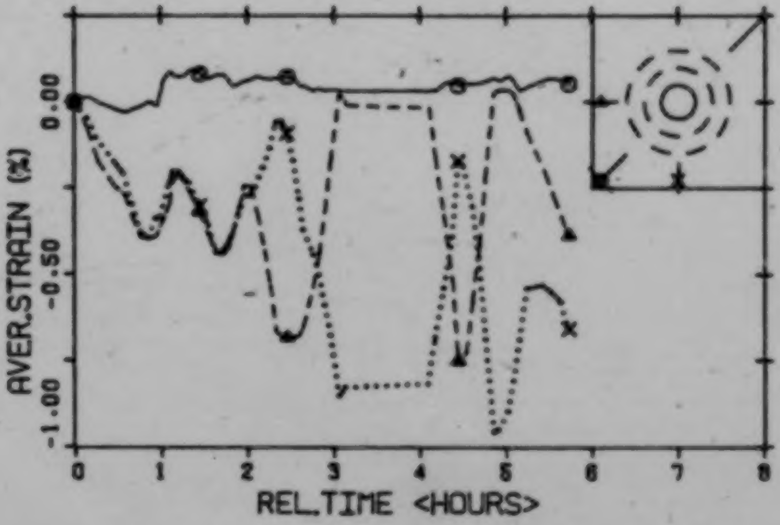

Figure B.14 MC7.18 Average Block Strain

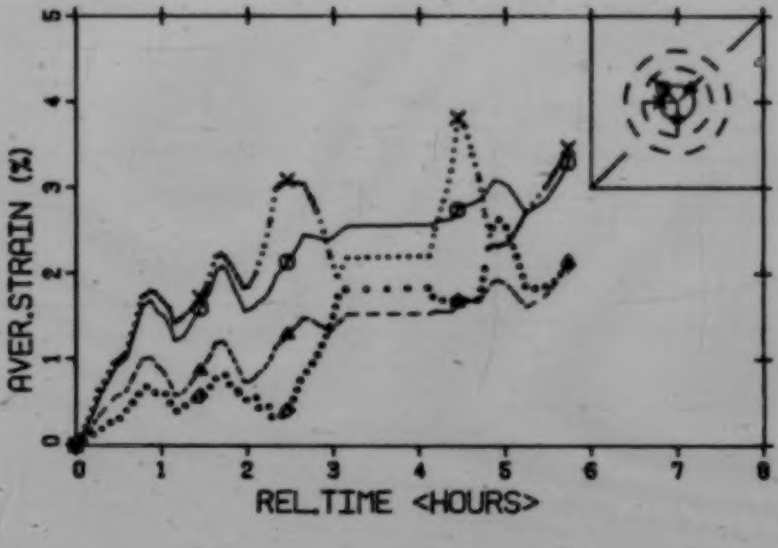

Figure B.15 MC7.18 Average Tunnel Closure (152 mm Diameter)

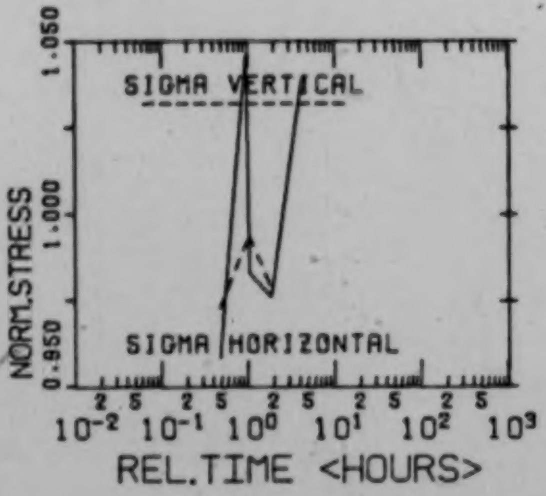

Figure B.16 MC7.18 Stress Level Maintenance

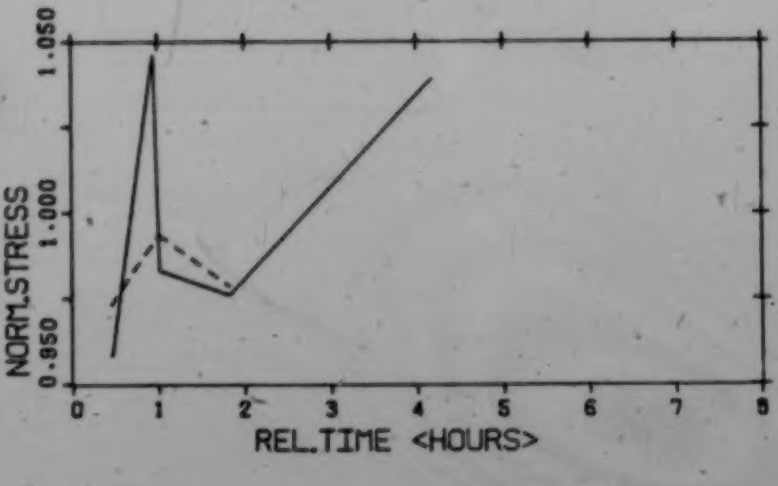

Figure B.17 MC7.18 Stress Level Maintenance

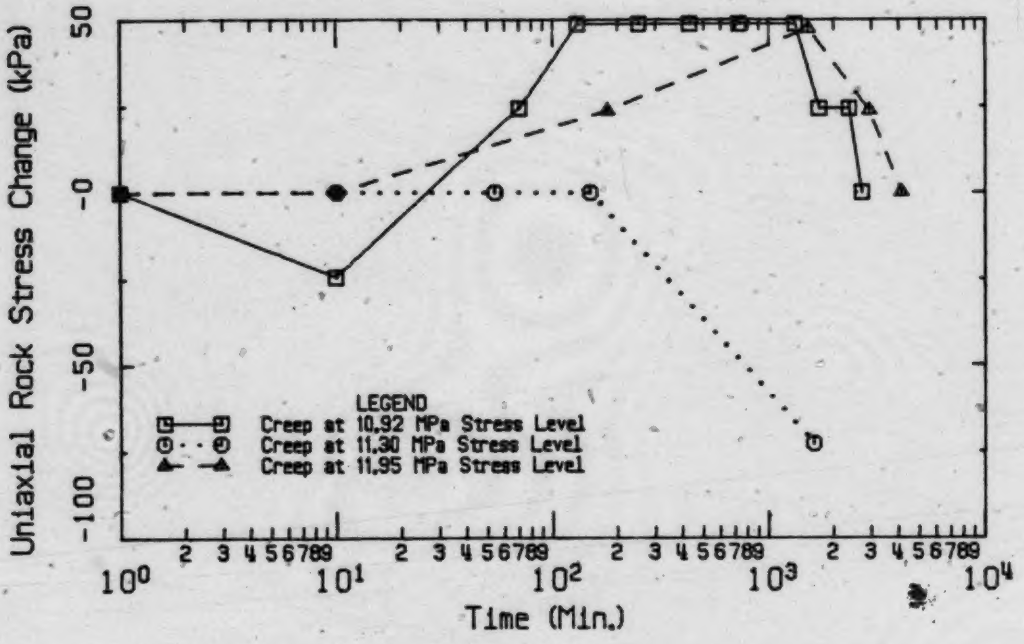

Figure B.18 Stress Redistribution Test- Gauge 2 Radial Gauge in Hole C

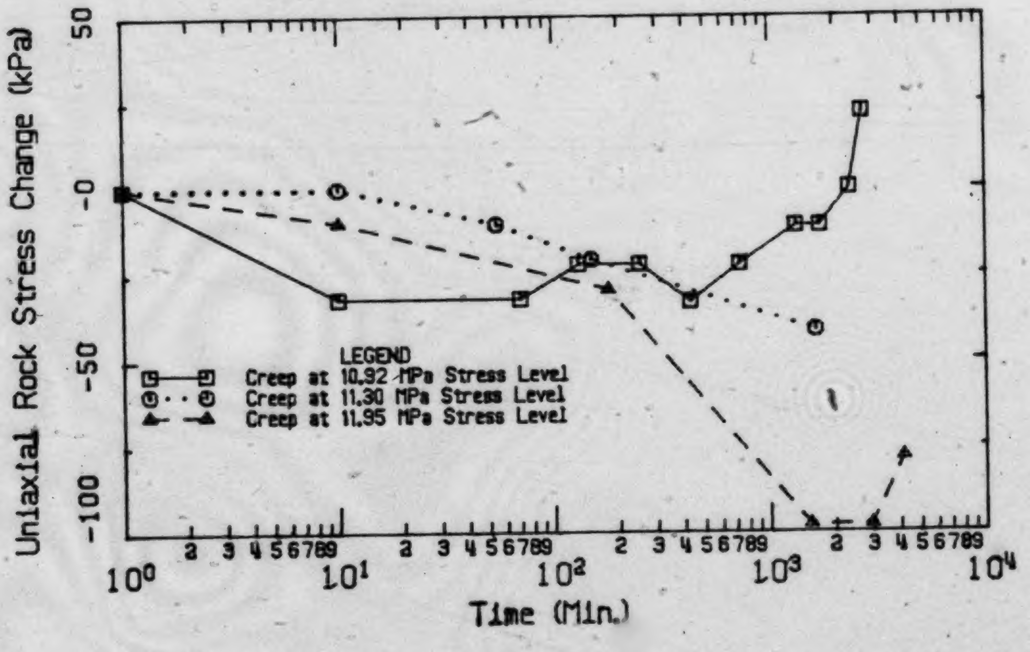

Figure B.19 Stress Redistribution Test- Gauge 8 Tangential Gauge in Hole C

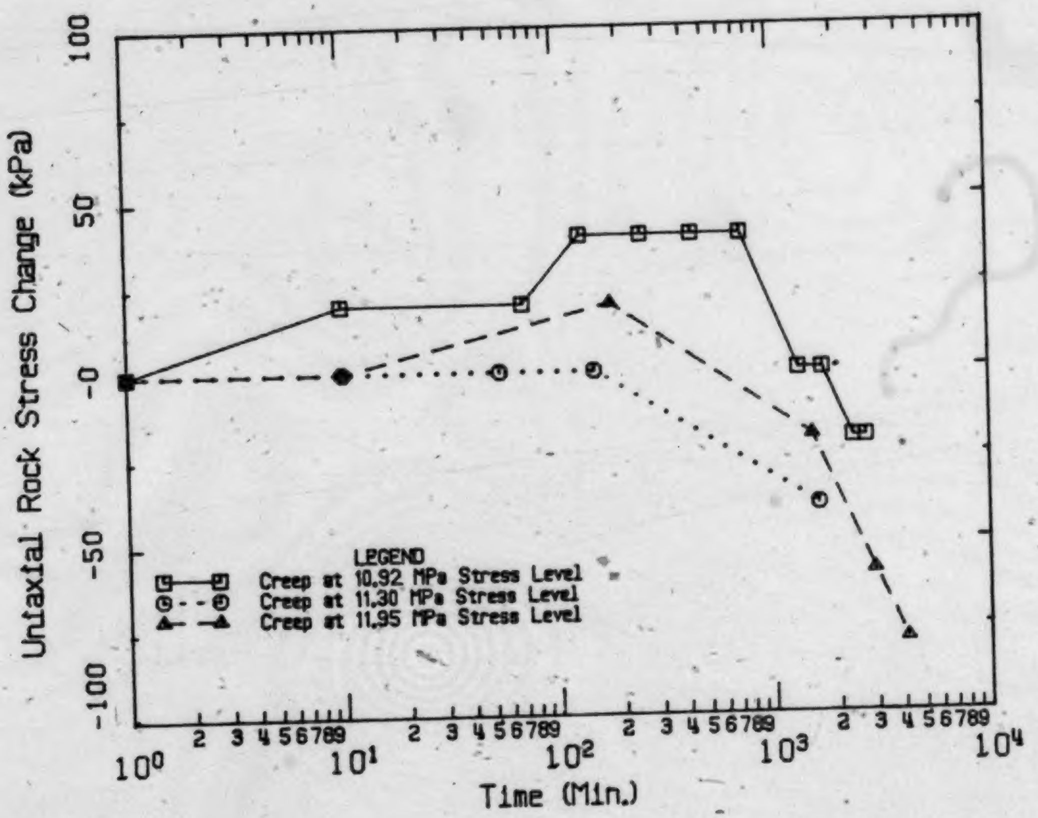

Figure B.20 Stress Redistribution Test- Gauge 4 Radial Gauge in Hole F

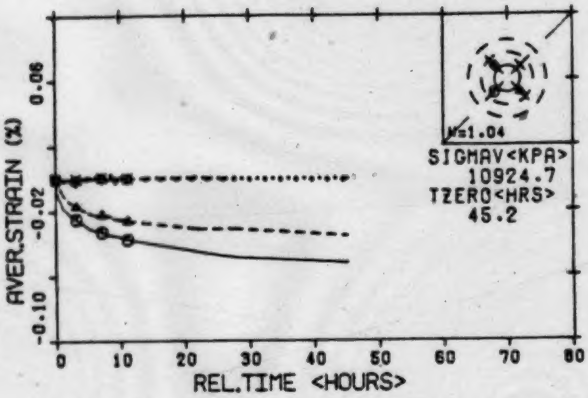

MC-7.18C RADIAL STRAIN AT STA. 106

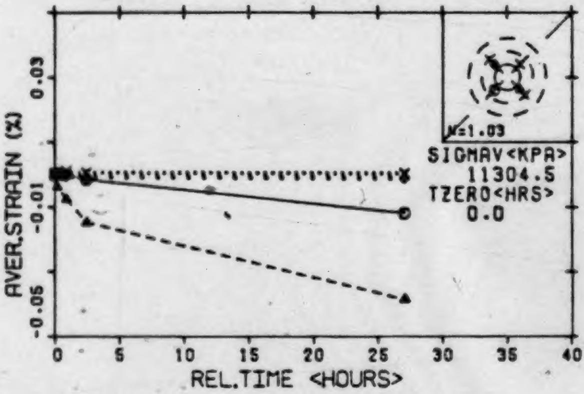

MC-7.18C RADIAL STRAIN AT STA. 106

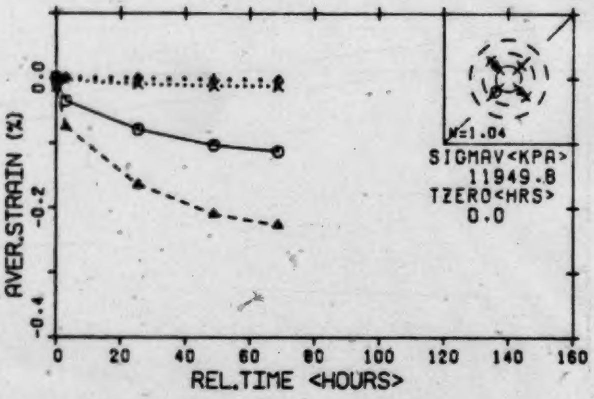

MC-7.18C RADIAL STRAIN AT STA. 106

Figure B.21 Strain-Time Plots from Stress Redistribution Tests on Sample With Opening

APPENDIX C

Analysis of Stress Change Measurements

This Appendix deals with the interpretation of the results from the vibrating wire stressmeter installed either in a borehole or adjacent to an opening. The coal used in the model tests is assumed to behave in a linear elastic and isotropic manner [Kaiser *et al.*, 1983b]. The modulus of deformation, E_R, is directional, but this does not significantly affect the gauge response because the modulus is relatively small. All tests were conducted under plane strain conditions. Pariseau (1978) found that the plane stress and plane strain cases are within 6% for a Poisson's ratio of 0.25. Thus, the plane stress analysis will be used for interpreting the results.

Hawkes and Bailey (1973) describe the development of the gauge and present a method of analysis based on the assumption of plane strain conditions. They also assumed that the force measured across the stressmeter platens is proportional to the deformation that would have occurred in the gauge direction if the gauge had not been present. Merrill and Peterson (1969) show that the radial displacement of a borehole is dependent on the magnitude of both the principal stresses. For the plane stress condition:

$$U=D/E_R\;[(\sigma_1+\sigma_3)+2(\sigma_1-\sigma_3)\cos(2\theta)] \qquad \text{Eqn. C.1}$$

where: σ_1, σ_3 = major and minor principal stresses in the plane of the borehole;

D = diameter of the borehole;

E_R = modulus of deformation of the rock; and

θ = angle measured (clockwise) from the direction of σ_1.

An "equivalent uniaxial stress", σ_u, can be defined and expressed in terms of the principal stresses. σ_u would cause a displacement in the direction of the gauge equivalent to those caused in the same direction by the principal stresses. The radial displacement in the direction of loading, U_u, can be expressed as:

$$U_u = 3\sigma_u D/E_R \qquad \text{Eqn. C.2}$$

Setting $U_u = U$ and substituting Eqn C.1 into C.2 yields:

$$\sigma_u = [1/3(\sigma_1+\sigma_3)+2/3(\sigma_1-\sigma_3)\cos(2\theta)] \qquad \text{Eqn. C.3}$$

Based on the assumption of Hawkes and Bailey (1973) the actual deformation at the gauge location must also be proportional to the force measured. Hence,

$$U_a = 3\sigma_u D/E_G \qquad \text{Eqn. C.4}$$

where: U_a = radial displacement of the borehole in the direction of uniaxial loading with the gauge present; and

E_G = the gauge stiffness.

Combining Eqn. C.2 and C.4 gives:

$$U_u/U_a = E_G/E_R \qquad \text{Eqn. C.5}$$

Pariseau (1978) presents a method of interpreting stress change measurements obtained from both hard and soft rock gauges based on expected displacements. Hard gauges, such as the vibrating wire stressmeter, act as rigid inclusions in the borehole because the gauge stiffness is much greater than the stiffness of the surrounding medium. He has suggested a relationship for the expected displacements that occur in a borehole containing a rigid inclusion:

$$U_u/U_a = (1 + f_2/f_3) \qquad \text{Eqn. C.6}$$

where: f_2 = a constant related to the rock properties, borehole diameter and contact area (a flexibility); and

f_3 = a constant related to the properties of the gauge (a flexibility).

Within the elastic range of deformation a very rough approximation of the flexibility ratios was given as:

$$f_2/f_3 = E_G/E_R \qquad \text{Eqn. C.7}$$

For E_G much greater than E_R, as is the case for the laboratory tests and also in general for soft rock, Eqns. C.5 and C.6 are essentially equivalent. For the Irad Gage hard rock stressmeter Pariseau's "flexibilities" may give a significantly different result from Hawkes and Bailey (1973) when E_G/E_R approaches unity. However, an indepth study of the factors in the analysis presented by Pariseau (1978) would be required to determine if indeed there was a large difference and, more importantly, if this method is more correct. Such a review is beyond the scope of this thesis and the method of analysis outlined by Hawkes and Bailey (1973) will be employed for interpreting measurements from both the soft rock and the hard rock gauges. This data analysis technique was shown to produce results that are in good agreement with those predicted during laboratory calibration tests.

Stress Change Adjacent to a Circular Opening

This section deals with the interpretation of vibrating wire stress change measurements taken adjacent to a circular opening excavated in an isotropic and linearly elastic material. Figure C.1 shows a general initial biaxial stress condition in terms of a global X-Y coordinate system. The stress changes in the X and Y directions are:

$$\Delta\sigma_x = \sigma_{x(final)} - \sigma^{\circ}_{x(initial)}$$

$$\Delta\sigma_y = \sigma_{y(final)} - \sigma^{\circ}_{y(initial)} \qquad \text{Eqn. C.8}$$

Prior to excavation, the initial stress condition may be expressed as:

$$\sigma^{\circ}_x = 1/2[(P+N\ P)+(P-N\ P)\cos 2\theta]$$

$$\sigma^{\circ}_y = 1/2[(P+N\ P)-(P-N\ P)\cos 2\theta] \qquad \text{Eqn. C.9}$$

Following excavation of the opening, the final stresses at a given location are found from Kirsch's Equations [Timoshenko and Goodier, 1970]. Using the notation in Figure C.2:

$$\sigma_r = P/2\ [(1+N)(1-\rho^2)+(1-N)(1+3\rho^4-4\rho^2)\cos 2\theta]$$

$$\sigma_\theta = P/2\ [(1+N)(1+\rho^2)-(1-N)(1+3\rho^4)\cos 2\theta] \qquad \text{Eqn. C.10}$$

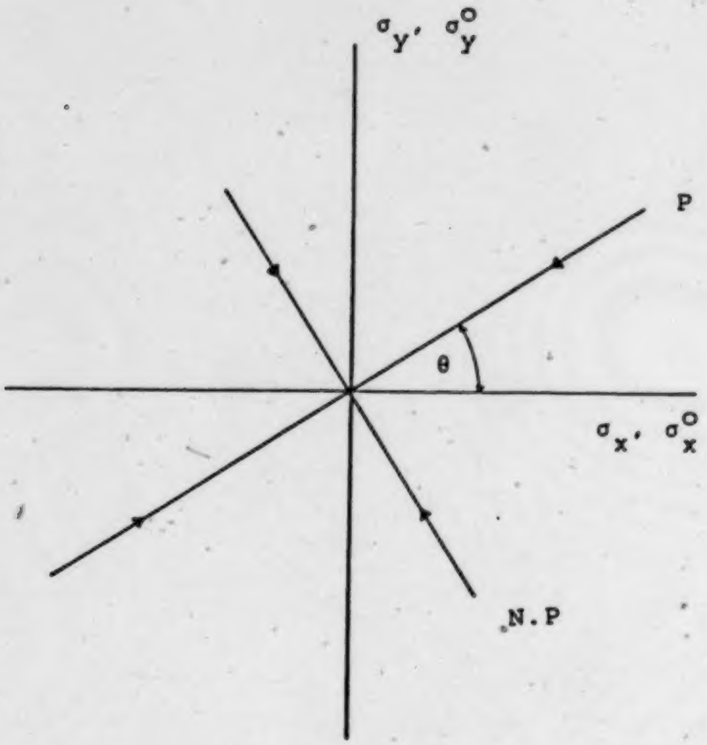
σ_y, σ_y^o
P
θ
σ_x, σ_x^o
N.P

σ_x^o, σ_y^o = Initial Stresses

σ_x, σ_y = Final Stresses

σ_1^o = P = Major Principal Stress

σ_3^o = N.P. = Minor Principal Stresses

Figure C.1 Initial Biaxial Stress Condition

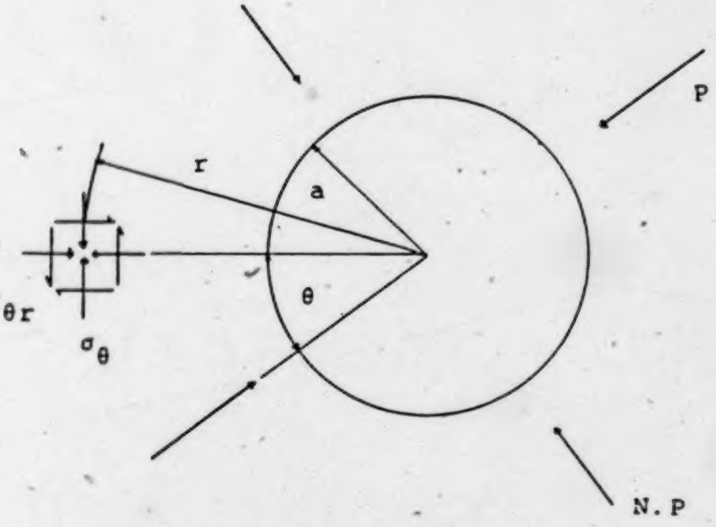

P
r
a
σ_r
$\tau_{\theta r}$
σ_θ
θ
N.P

Figure C.2 Notation for Biaxial Stresses Adjacent to Shaft in Isotropic Elastic Ground

where ρ = a/r (r= radial distance to gauge from opening centre).

The coordinate system can be arranged such that:

$$\sigma^{\circ}_{r} = \sigma^{\circ}_{x}$$

$$\sigma^{\circ}_{\theta} = \sigma^{\circ}_{y} \qquad \text{Eqn. C.11}$$

The changes in tangential and radial stress are found by combining Eqns. C.8, C.9, and C.10 and simplifying:

$$\Delta\sigma_{r} = P/2[(1+N)(-\rho^{2})+(1-N)(3\rho^{4}-4\rho^{2})\cos2\theta]$$

$$\Delta\sigma_{\theta} = P/2[(1+N)(\rho^{2})-(1-N)(3\rho^{4})\cos2\theta] \qquad \text{Eqn. C.12}$$

Eqn. C.12 represents the real stress changes that would occur after the excavation of the opening. However, it has been shown that the stress change measured by the Irad stressmeter is dependent on changes in both the principal stresses. Later in this Appendix it will be shown that σ_1 and σ_3 in Eqn. C.3 can be replaced by a specific pair of orthogonal stresses, one of which coincides with the gauge direction. Thus, for gauges placed either radially or tangentially, P and N.P. (or σ_1 and σ_3) can be replaced by σ_r and σ_θ. A stress change recorded by the gauge can be expressed as:

$$\Delta\sigma_{\theta G} = 1/3(\Delta\sigma_{\theta} + \Delta\sigma_{r}) + 2/3(\Delta\sigma_{\theta} - \Delta\sigma_{r})\cos 2a$$

$$\Delta\sigma_{rG} = 1/3(\Delta\sigma_{\theta} + \Delta\sigma_{r}) + 2/3(\Delta\sigma_{\theta} - \Delta\sigma_{r})\cos 2a \qquad \text{Eqn. C.13}$$

where: $\Delta\sigma_{\theta G}$, $\Delta\sigma_{rG}$ = stress change measured by tangential and radial gauges, respectively; and

a = angle measured from the tangential direction (clockwise).

This is further reduced to:

$$\Delta\sigma_{\theta G} = \Delta\sigma_{\theta} - 1/3\Delta\sigma_{r}$$

$$\Delta\sigma_{rG} = \Delta\sigma_{r} - 1/3\Delta\sigma_{\theta} \qquad \text{Eqn. C.14}$$

Subsituting Eqn. C.12 into C.14 and simplifying gives:

$$\Delta\sigma_{rG} = P\,[(-2\rho^2/3)(1+N) + (2\rho^4 - 2\rho^2)\cos 2\theta(1-N)]$$

$$\Delta\sigma_{\theta G} = P\,[(2\rho^2/3)(1+N) + (2\rho^2/3 - 2\rho^4)\cos 2\theta(1-N)] \qquad \text{Eqn. C.15}$$

The preceding analysis is applicable for gauges installed in a prestressed material. The laboratory testing involved gauges installed under zero stress. For this condition the change in radial and tangential stress are equal to the stresses following excavation of the opening

(Eqn. C.10). Substituting Eqn. C.10 into Eqn. C.14 gives the gauge results:

$$\Delta\sigma_{\theta G} = P[(1+N)(1/3+2/3\rho^2)+(1-N)(-2/3-2\rho^4+2\rho^2/3)\cos 2\theta]$$

$$\Delta\sigma_{r} = P[(1+N)(1/3-2/3\rho^2)+(1-N)(2/3+2\rho^4-2\rho^2/3)\cos 2\theta] \quad \text{Eqn.C.16}$$

or

$$\Delta\sigma_{\theta G} = P[(C+CN)+(-B+BN)\cos 2\theta]$$

$$\Delta\sigma_{rG} = P[(A+AN)+(B-BN)\cos 2\theta] \quad \text{Eqn. C.17}$$

where: $A = 1/3+2\rho^2/3$

$B = 2/3+2\rho^4-2\rho^2/3$

$C = 1/3+2\rho^2/3.$

This section provides a derivation to show that for the special case of $\theta = 0°$ or $90°$:

$$1/3(P+N\,P)+2/3(P-N\,P)\cos 2\theta =$$

$$1/3(\sigma_x+\sigma_y)+2/3(\sigma_x-\sigma_y)\cos 2\alpha \qquad \text{Eqn C.18}$$

Figure C.3 shows a Mohr circle for a general stress condition with arbitrary principal stresses. Employing the principles of the Mohr circle, P and N.P. can be expressed, as follows, in terms of σ_x, σ_y, θ and α with respect to any plane A-A;

$$P=(\sigma_x+\sigma_y)/2 + (\sigma_x-\sigma_y)/\,[2\cos(2\theta-2\alpha)]$$

$$N\,P = (\sigma_x+\sigma_y)/2 - (\sigma_x-\sigma_y)/\,[2\cos(2\theta-2\alpha)] \qquad \text{Eqn C.19}$$

When Eqns. C.19 are substituted into the left hand side of Eqn. C.18 it can be seen that the two sides of Eqn. 18 are equal provided $\theta = 0°$ or $90°$.

The preceding steps can be applied both before and after excavation. Therefore, replacing the principal stresses in Eqn. C.3 with a pair of orthogonal stresses, one of which is parallel to the direction of the measured uniaxial stress, does not influence the final result.

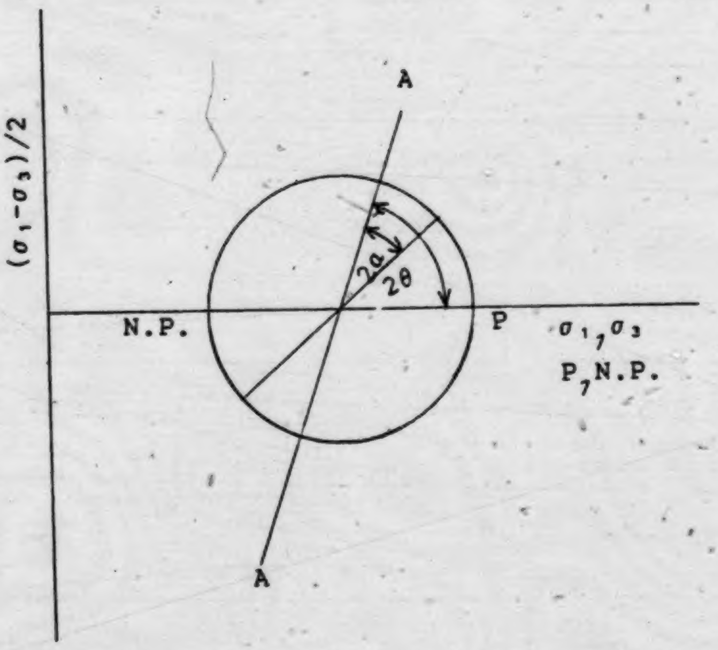
A
$(\sigma_1-\sigma_3)/2$
2α
2θ
N.P.
P
σ_1, σ_3
P, N.P.
A

α= angle from σ_x direction to Plane A-A

θ= angle from σ_1 direction to Plane A-A

P= major principal stress (=σ_1)

N.P.= minor principal stress (=σ_3)

σ_x, σ_y = normal stresses on a given plane

Figure C.3 Mohr Diagram Showing Stresses on an Arbitrary Plane

APPENDIX D

This Appendix contains a paper co-authored by the Author of this thesis. It contains a description of the operation of the Irad Gage Vibrating Wire Stressmeter. Also included in the paper is some analytical work done by the Author to determine the optimum gauge locations around a circular opening in a linear elastic material. A description of the instrumentation program at the Kipp shaft and a summary of the previous results are presented. The results are re-evaluated using the method of data interpretation outlined in Appendix C.

IN SITU STRESS AND DEFORMATION PROPERTY DETERMINATION DURING EXCAVATION OF UNDERGROUND OPENINGS

by

P.K. Kaiser*
D. Korpach**
and
C. Mackay***

submitted for publication to the
'Canadian Geotechnical Journal'

July, 1983

*Associate Professor
**Graduate Student
***Former Graduate Student

Department of Civil Engineering
University of Alberta
Edmonton, T6G 2G7

Abstract

An innovative approach for the determination of the in situ stresses in clay shale was adopted during the construction of a shaft. The stress changes that resulted during face advance were recorded by stiff inclusions measuring uniaxial stress changes. From these stress change measurements it was possible to calculate the in situ stress field and, together with extensometer measurements, to determine the in situ deformation modulus of the rock mass. The test procedure and the data interpretation are discussed together with an evaluation of the optimum instrument locations. Some longterm measurements are also presented.

Keywords

In situ stress, stressmeter, rock mass deformation properties, monitoring, instrumentation, shaft, underground openings.

1. Introduction

Owners, contractors and engineers are becoming increasingly aware of the benefit incurred from monitoring of underground excavations. Monitoring can provide a means of validating empirical design criteria and evaluating safety and performance of the rock support system. Lane (1977) has shown that full-scale test sections on some projects have resulted in significant cost savings. In these cases the performance was evaluated by comparison with predictions made for the support design and the construction method was then adjusted to reduce tunnelling costs.

The design of a liner for an underground opening requires knowledge of the in situ stress field, the ground water conditions, the deformation and strength behaviour of the rock mass and the properties of the support system. This paper deals with two of these aspects: the determination of the in situ stress field and the rock mass deformation properties.

It is impossible a priori to assess conclusively the in situ state of stress in rocks because of many effects of genetic factors that influence it. Hence, it is normally necessary to measure the stresses by one of two basic groups of in situ stress measuring techniques:

a) *Hydraulic fracturing* [Zoback and Haimson(1982)] whereby the in situ stresses are back-calculated from injection pressures measured during fracturing of the ground due to low or negative effective stresses created by the high fluid pressures; and

b) *Stress relief methods* [Hooker and Bickel (1974)], normally executed in boreholes, whereby rock deformations are measured while an artificial stress change is created, e.g., by overcoring a deformation gauge. These deformation measurements are then used to determine the in situ stess field after the rock deformation properties have been determined by testing the recovered rock core. Alternatively, the stress change in a stiff inclusion may be recorded during overcoring and then used to back-calculate the in situ stress field.

The basic principles of this second technique constitute the concept of the approach adopted to measure the in situ stress field during the monitoring project described later. Instead of overcoring a stiff inclusion, the change in stress was recorded during 'undercoring' or, more accurately, excavation of an opening between gauges measuring the local change in stress. From these measurements it is possible to determine the in situ stress field, if the instruments record correctly the actual change in stress during excavation and if an acceptable analytical model for the rock mass response can be found. For the following, it will be assumed that the rock behaves like a linear elastic continuum.

The deformation properties of the rock mass are normally determined by extrapolation from measurements made on small, intact rock samples, by application of rock classification systems [Bieniawski (1978)] or, on major construction projects, by in situ pressuremeter or plate load tests. Alternatively, conventional tunnel wall convergence or multi-point extensometer measurements are frequently made for the determination of the rock mass deformation properties [Kruse (1970)]. Their analysis is complicated by the fact that it is seldom possible to install extensometers or convergence points in the undisturbed rock mass, before the underground opening has been partially excavated. The magnitude of stress change that occurs during the measuring period is therefore largely unknown. Because of the large stress gradient near the excavation face, it is likely that the stress change and, hence, the back-calculated deformation modulus may be significantly over or underestimated. An accurate determination of the deformation modulus is only possible if the related stress change can be predicted or, more appropriately, measured accurately by recording the amount of stress change ahead of the face, before the extensometers are installed, and while the displacements are measured by extensometers. Combination of radial strain or displacement measurements with records of local stress change observations leads to a significant improvement of the accuracy of back-calculated rock mass deformation properties. Other difficulties that have to be overcome during the interpretation of convergence measurements have been discussed by Kaiser (1981).

This paper presents briefly a description of a field instrumentation study and a discussion of the problems related to the data interpretation. Factors affecting the selection of the best location for positioning stress change instruments for the purpose of determining the in situ stress field are also discussed. The monitoring program was conducted during the sinking of a vertical shaft in clay shale to gather data for the design of future inclined mine adits. Results of this investigation and an evaluation of the liner behaviour and support - ground interaction by means of the convergence - confinement method were already presented by Kaiser and Mackay (1982).

2. Project Description and Instrumentation Program

In 1980 a 4.32 m finished diameter concrete lined shaft was sunk to a depth of 235 m at a coal mine site owned by Petro Canada Explorations Ltd., at Kipp, near Lethbridge in Southern Alberta. The shaft was sunk by Thyssen Mining Construction of Canada Ltd. using conventional shaft sinking methods as described by Kaiser and Mackay (1982), Kaiser *et al.* (1982) and Mackay (1982). The lining construction generally followed one to two shaft diameters behind the shaft bottom. Shaft sinking through the bedrock progressed at a rate of about 3 to 4 m per day. The rock was seldom unsupported for more than 16 to 20 hours except during regular four-day work stoppages after a ten-day construction period.

The site geology consists of about 60 m of glacial clay till underlain by about 6 m of saturated basal sands and gravels over Upper Cretaceous bedrock. This bedrock consists of the marine Bearpaw Formation composed of clay shales, siltstones and mudstones from a depth of about 66 m to 198 m. The non-marine Oldman Formation extends to a depth below the bottom of the shaft and conformably underlies the Bearpaw Formation. This formation consists of interbedded sandstones and shales with frequent coal seams in the uppermost member.

A field testing and monitoring program was conducted in the Bearpaw Formation during the sinking of the shaft and the following instrumentation was installed at three levels:

111 m depth: 3 multi-point borehole extensometers; 16 vibrating wire embedment strain gauges in the concrete liner; 1 piezometer.

152 m depth: 3 radial and 4 tangential vibrating wire borehole stress change gauges; 8 embedment gauges in the concrete liner; 1 piezometer.

180 m depth: 3 multi-point borehole extensometers; 8 embedment gauges in the concrete liner.

This instrumentation was installed in the shaft at each level during four-day work shutdown periods.

In addition to the installation of these instruments, an attempt was made to determine the in situ stress field at a depth of 91 m (24 to 25 m below the bedrock surface) by overcoring a U.S.B.M. deformation gauge. Due to time limitations testing was restricted to one single horizontal borehole oriented at N50°W approximately perpendicular to the expected direction of the major horizontal principal stress. Of the four tests conducted in this borehole only two were considered reliable because an open bedding plane fracture penetrated the retrieved core in the other two test sections. The results of these two tests, conducted at 1.85 m and 6.6 m from the shaft wall inside the stress concentration zone created by the shaft, indicated that the vertical stress was slightly less than the overburden pressure and that the horizontal stress perpendicular to the borehole was about twice the overburden pressure. It was not possible to reach a conclusive answer from only two measurements but after adjustment for the stress concentration near the shaft bottom it was found that a vertical stress equal to the full overburden pressure and a K_0 = 1.5 could describe the stress pattern in the area. The minimum horizontal stress could not be estimated but the testing was considered successful because it demonstrated that the U.S.B.M. technique can be applied in the weak clay shales and siltstones of the prairie rocks.

Figure 1 shows the location of eight strain gauges embedded in the concrete liner and seven IRAD stress change gauges placed at the 152 m level. The stress change gauges were installed 10 m ahead of the shaft bottom from a depth of 142 m in steeply inclined boreholes drilled into the shaft wall. The stress change gauges were orientated radially and tangentially with respect to the shaft perimeter.

Figure 2 presents the five-point horizontal borehole extensometer layout at the 180m level. These extensometers as well as the ones at the 111 m level were installed about 1 m above the shaft floor. Readings were obtained after each round of blasting until the liner was cast over the extensometers. The extensometers were extended through the liner, but long term measurements could only be obtained for one extensometer because of damage of the anchor heads during concreting or blasting.

The vibrating wire piezometers placed at the rock-liner interface recorded no significant water pressure build-up on the liner. Some water seepage through the liner was observed particularly in the upper portion of the bedrock but it is likely that the construction joints acted as drains and it is believed that little water pressure existed at the test section.

3. The Irad Gage Vibrating Wire Stressmeter

The Irad Gage Vibrating Wire Stressmeter was developed for the U.S.B.M. to provide a low cost system for monitoring long term stress changes in rock. Hawkes and Bailey (1973) provide a complete description of the gauge, its specifications, the installation techniques and data analysis procedures. Applications of the gauge to underground mining and civil engineering projects are discussed by Hawkes and Hooker (1974) and Sellers (1977). The gauge consists of a hollow steel cylinder with a vibrating wire strain gauge. It is activated diametrically across a 38.1 mm diameter borehole by wedging of the gauge body. The gauge is available in two models, a hard rock gauge with a maximum contact angle between gauge platens and borehole wall of 20° and a soft rock model with a maximum contact angle of 112°. The larger platens were used during this investigation to reduce the possibility of local yielding of the rock. For a linear elastic material, the relationship between the uniaxial rock stress change in the direction of the loading axis of the gauge and the wire tension [Hawkes and Hooker (1974)] is linear:

$$\Delta\sigma_R = \Delta\sigma_w / a \qquad \text{Eqn.1}$$

where a is the uniaxial gauge sensitivity factor and $\Delta\sigma_R$ and $\Delta\sigma_w$ are the changes in rock stress and wire stress respectively. Hawkes and Bailey (1973)> presented an experimentally determined relationship between the uniaxial gauge sensitivity factor and the Young's Modulus of the host material for both hard rock and soft rock gauge models. For the soft rock gauge the sensitivity factor α is:

$$\alpha = 11.4 - 95.7 \times 10^{-9} E_R \text{ [kPa]} \qquad \text{Eqn.2}$$

where E_R is the Young's modulus of the rock. It follows that the uniaxial gauge sensitivity factor is relatively insensitive to variations in the assumed rock modulus. For example, if the rock modulus were 2 GPa instead of 7 GPa the uniaxial gauge sensitivity factor would decrease by less than 5%. In comparison, a similar variation in rock modulus, assumed for the calculation of the in situ stresses from measurements by a soft borehole deformation gauge such as the U.S.B.M. cell, would result in a four fold error in the calculated stresses.

4. Use of Stress Change Gauges to Determine In Situ Field Stresses

For the following it will be assummed that a circular hole is excavated in a linear elastic material and that the final state of stress can be described by assuming plane stress conditions (typical for a shaft far from the three dimensional state of stress near the shaft bottom). Pariseau (1978) illustrated for a Poisson's ratio of 0.25 that differences in the order of 6% must be expected for the plane strain condition. The initial stresses in the rock are:

$$\sigma^{\circ}_{r} = (S/2)\ [(1+N) + (1-N)\ \cos 2\theta]$$

$$\sigma^{\circ}_{\theta} = (S/2)\ [(1+N) - (1-N)\ \cos 2\theta] = \sigma^{\circ}_{r} \text{ at } \theta = 90^{\circ} \qquad \text{Eqn.3}$$

$$\tau^{\circ}_{r\theta} = -(S/2)\ [(1-N)\ \sin 2\theta]$$

where: S = principal biaxial stress (horizontal for shaft);

NS = minor or major principal biaxial stress perpendicular to S (assumed horizontal for shaft);

θ = angle measured from direction of S (clockwise) to the direction of σ°_{r}; σ°_{r} and σ°_{θ} are radial and tangential stresses; $\tau^{\circ}_{r\theta}$ is the shear stress at the same location.

The radial and tangential stresses adjacent to a circular opening in an elastic medium are given by Timoshenko and Goodier (1970):

$$\sigma_{r} = (S/2)\ [(1+N)\ (1-\rho^{2}) + (1-N)\ (1+3\rho^{4}-4\rho^{2})\ \cos 2\theta]$$

$$\sigma_{\theta} = (S/2)\ [(1+N)\ (1+\rho^{2}) - (1-N)\ (1+3\rho^{4})\ \cos 2\theta] \qquad \text{Eqn.4}$$

$$\tau_{r\theta} = -(S/2)\ [(1-N)\ (1-3\rho^{4} + 2\rho^{2})\ \sin 2\theta]$$

where ρ = a/r (a = radius of opening and r = distance to point of stress determination).

Hence, the stress change that occurs during excavation of a circular opening corresponds to the difference between the preceding equations (Eqn. 4 and 3): $\Delta\sigma = \sigma - \sigma^{\circ}$

$$\Delta\sigma_r = (S/2)\,[(1+N)\,(-\rho^2) + (1-N)\,(3\rho^4-4\rho^2)\,\cos 2\theta]$$

$$\Delta\sigma_\theta = (S/2)\,[(1+N)\,(\rho^2) - (1-N)\,(3\rho^4)\,\cos 2\theta] \qquad \text{Eqn.5}$$

$$\Delta\tau_{r\theta} = -(S/2)\,[(1-N)\,(-3\rho^4+2\rho^2)\,\sin 2\theta]$$

(Positive values indicate a stress increase).

Vibrating wire stress gauges placed near an underground opening, however do not record these stress changes directly. The stress change recorded by uniaxial stress change gauges is an "equivalent uniaxial stress" that is affected by changes in both principal stresses. This equivalent uniaxial stress would cause deformations in the direction of the gauge that are equivalent to those caused by the principal stresses in the same direction. In determining the relationship between the equivalent stress and the principal stresses it is assumed that the force on the stressmeter platens is proportional to the deformation that would have occurred if the gauge had not been present [Hawkes and Bailey (1973)]. Merrill and Peterson (1969) provide a detailed derivation of the relationship between the radial displacement u of the borehole wall and the magnitude of the two principal stresses in the plane of the borehole in an elastic medium. For the plane stress condition it follows that:

$$u = D/E_R\,[(\sigma_1+\sigma_3) + 2\,(\sigma_1-\sigma_3)\,\cos 2\theta] \qquad \text{Eqn.6.a}$$

where: σ_1, σ_3 = principal stresses in the plane of the borehole or opening;

D = diameter of the opening; and

θ = angle measured from direction of σ_1 (clockwise).

The radial deformation of a borehole in the direction of a uniaxial stress is:

$$u = 3D\sigma_u/E_R \qquad \text{Eqn.6.b}$$

where: σ_u = uniaxial stress in the direction of the displacement u.

After substituting Eqn.6.a into Eqn.6.b and rearranging, it follows that the stress change recorded by the gauge is:

$$\Delta\sigma_G = 1/3\ (\Delta\sigma_1+\Delta\sigma_3) + 2/3\ (\Delta\sigma_1-\Delta\sigma_3)\cos 2\theta \qquad \text{Eqn. 6.c}$$

where: $\Delta\sigma_G$ = equivalent uniaxial stress recorded by the stress change gauge (corresponding to σ_u in Eqn.6.b);

$\Delta\sigma_1$ = stress change in the major principal stress direction;

$\Delta\sigma_3$ = stress change in the minor principal stress direction; and

θ = angle measured from direction of σ_1 (clockwise) to the gauge location.

It can be shown that the pair of orthogonal stresses (i.e., from Eqn. 5) at 0° and 90° to the direction of the desired uniaxial stress change can be used in Eqn. 6.c. Thus, Eqn. 6.c can be rewritten as:

$$\Delta\sigma_G = 1/3\ (\Delta\sigma_\theta + \Delta\sigma_r) + 2/3\ (\Delta\sigma_\theta - \Delta\sigma_r) \cos 2\theta \qquad \text{Eqn. 7}$$

where: θ = angle measured from σ_θ (clockwise) to the gauge orientation.

Recent tests conducted on large coal samples, under controlled stress conditions in the laboratory [Korpach (1983)] have shown that Eqn. 7 can be used to predict rock stress changes with reasonable accuracy.

Hence, the uniaxial stress change recorded by radial and tangential gauges follows from Eqns. 5 and 7:

$$\Delta\sigma_{rG} = \Delta\sigma_r - 1/3\ \Delta\sigma_\theta \quad \text{or}$$

$$\Delta\sigma_{rG} = S[(-2\rho^2/3)(1+N) + (2\rho^4 - 2\rho^2) \cos 2\theta\ (1-N)] \qquad \text{Eqn. 8a}$$

and

$$\Delta\sigma_{\theta G} = \Delta\sigma_\theta - 1/3\ \Delta\sigma_r \quad \text{or}$$

$$\Delta\sigma_{\theta G} = S[(2\rho^2/3)(1+N) + (2\rho^2/3 - 2\rho^4) \cos 2\theta\ (1-N)] \qquad \text{Eqn.8b}$$

where: $\Delta\sigma_{rG}$ = uniaxial stress change recorded by a radial gauge; and

$\Delta\sigma_{\theta G}$ = uniaxial stress change recorded by a tangential gauge.

From Eqn. 8 the original field stress can now be calculated from the stress change measured by the radial or tangential gauge.

For example for N = 1:

$$S = -\Delta\sigma_{r}/\rho^2 \quad \text{or} \quad S = -3\Delta\sigma_{rG}/4\rho^2$$

$$S = +\Delta\sigma_{\theta}/\rho^2 \quad \text{or} \quad S = +3\Delta\sigma_{\theta G}/4\rho^2 \qquad \text{Eqn. 9}$$

Only one measurement is theoretically necessary to determine the magnitude of the field stress but it is important that the instrument location is known accurately.

On the other hand, for gauges placed parallel to one of the principal stress directions (θ = 0° and 90°; τ=0) the principal stress S in a nonuniform stress field can be found from the following equations:

$$S = \Delta\sigma_{rG}/[(1+N)(-2\rho^2/3) \pm 2(1-N)(\rho^4-\rho^2)]$$

or Eqn. 10

$$S = -\Delta\sigma_{\theta G}/[(1+N)(-2\rho^2/3) \pm 2(1-N)(+\rho^4-\rho^2/3)]$$

Two measurements are theoretically sufficient to determine the two variables S and N.

For the most general case (N, S and θ unknown) at least three measurements are required, or preferably, two sets of two gauges placed either at 90° to each other or both sets on the same side but at different distances from the tunnel wall. However, because of the insensitivity of (cos 2θ) for angles of $\theta = 0 \pm 15°$ and $\theta = 90 \pm 15°$, errors of less than about 10% result if the gauges are not placed exactly in the direction of the principal stresses and Eqns.10 can be applied (see Section 4.1).

4.1 Optimum Instrument Location

For a field monitoring project it is important to determine the optimum gauge locations, to get the most accurate results for all required design parameters and to achieve the highest degree of redundancy. In the following section it will be assumed that the orientation of the principal stresses is known or can be assumed, and that the gauges are installed on the principal stress axis (θ is known). These axes are assumed to be parallel or perpendicular to the axis of a circular opening.

The optimum instrument location in terms of gauge orientation (radial or tangential), location (θ = 0° or 90°) and position (ρ-value; distance from opening wall) can best be evaluated by varying individual parameters separately and by comparing various combinations of these parameters. The principal stress S can then be expressed in terms of the stress change recorded by a radial or tangential gauge installed at 0° or 90° from the major principal stress direction and depends only on the stress ratio N and the gauge position. From Eqn. 10 it follows for gauges at θ =0°:

$$S = \Delta\sigma_{\theta G} \ / \ [A + NB]$$

or $$S = \Delta\sigma_{rG} \ / \ [NA + C]$$

and for gauges at $\theta = 90°$: Eqn. 11

$$S = \Delta\sigma_{\theta G} \ / \ [AN + B]$$

or $$S = \Delta\sigma_{rG} \ / \ [A + NC]$$

where: $A = 2[(2\rho^2/3) - \rho^4]$

$B = 2\rho^4$

$C = 2[\rho^4 - 4\rho^2/3]$.

By equating any two of these equations it is possible to calculate the stress ratio N in terms of a stress change ratio SCR and for various gauge positions ρ. For example, using two tangential gauges at 90° to each other the stress ratio N is:

$$N = (A_1 - SCR_{12} B_2) \ / \ (SCR_{12} A_2 - B_1) \qquad \text{Eqn. 12}$$

where: A_i = A of gauge i; i = 1, 2;

B_i = B of gauge i; i = 1, 2; and

SCR_{12} = $\Delta\sigma_{\theta G1} / \Delta\sigma_{\theta G2}$ = ratio of two stress change measurements. The first subscripts refer to the gauge orientation and the third subscript i refers to the gauge number.

Figures 3 to 9 show double logarithmic plots of principal stress ratio N versus stress change ratio SCR generated for various combinations of gauge locations, orientations and positions.

- Figs. 3a and b present results for two tangential gauges on the same side at ρ_1 and ρ_2: (a) for two gauges parallel to the major principal stress direction ($\theta = 0°$) and (b) two gauges perpendicular to it ($\theta = 90°$). In both case ρ_1 is kept constant at a relatively large value of $\rho_1 = 0.85$ and ρ_2 was varied between $\rho_2 = 0.75$ and 0.45. ρ-values in excess of 0.85 are seldom practical because of stress redistribution in zones of rock damage near the opening walls (i.e., due to blasting). The accuracy of stress change measurements is affected by many factors, such as local stress variations in a discontinuous rock mass, variations in contact angle of platens, etc. These factors dominate particularly when small magnitudes of stress changes are recorded. Consequently, the stress change ratio becomes increasingly inaccurate if it approaches zero or infinity. No detailed error analysis has been undertaken, but it is our experience that stress change ratios of SCR < 0.20 and SCR > 5 cannot be used reliably for in situ stress determinations.

The two Figs. 3a and b are basically identical with one presenting the inverse of the stress ratio of the other. Several interesting observations follow from these figures: First, for the arrangement of gauges under consideration stress ratios in excess of about 8 (or below approximately 0.15) cannot be determined reliably for the reasons given earlier. Second, because of the steepness of the curves with small ρ-differences, it follows that gauges should be placed as far apart as possible. However, for $\rho_2 < 0.55$ the range of the stress ratios that can be determined reliably decreases to approximately 0.15 to 2 for gauges in the direction of the major principal stress because of the small stress changes that occur far from the opening. Large stress ratios cannot be determined accurately in this manner.

- Fig. 4 shows that a pair of radial gauges, both installed on the same side ($\theta = 0°$), is not a good combination for determining the stress ratio as most sections of the curves are too steep or too flat for accurate data interpretation.

- Fig. 5 presents results for two tangential gauges at 90° to each other. From Eqn. 12, it follows that N = SCR for $\rho_1 = \rho_2 = 0.816$. This combination of gauges can be used effectively to measure over a relatively wide and practical range of N-values (0.2<N<5). As both ρ-values decrease below $\rho = 0.8$ this arrangement becomes less appropriate for the determination of N. Again, large stress ratios cannot be determined reliably.

- Fig. 6 presents the case of a pair of radial gauges at 90° to each other. Because of the relatively flat curves (Fig. 6.a), these radial gauges can be used to determine relatively large stress ratios provided they are positioned close to the opening or with a relatively large differential radial distance ρ. However, the measurements are extremely sensitive to the gauge position, a parameter that, at the present time, is relatively difficult to determine accurately in the field. For small ρ-values this sensitivity is eliminated but then the range of the stress ratio N is severely restricted.

- In Fig. 7 one radial and one tangential gauge, both on the same side, are combined. This arrangement does not appear to be desirable for stress ratios significantly different from unity unless ρ of the tangential gauge is relatively large.

- Fig. 8 demonstrates the importance of accurate determination of the gauge position ρ for the case of radial gauges at $\theta = 0°$ and $90°$, particularly when relatively small stress change ratios (i.e, <1) are measured for this particular case. This can best be illustrated by an example: for SCR = 0.5, $\rho_1 = 0.85$ and $\rho_2 = 0.65$, N is 3.2. However, if ρ_1 varies by about ±6% from 0.8 to 0.9, N changes from 2.3 to 6.1, and, if ρ_2 varies between 0.6 and 0.7, N ranges from 3 to 3.8. This sensitivity decreases rapidly if measurements are made further away from the opening. However, because of the reduced stress change measured far from the excavation the accuracy of these measurements is reduced.

- Fig. 9a demonstrates the sensitivity of the results to variations in the gauge location relative to the axis of principal stresses (deviation of θ from 0° or 90°). The case of two tangential gauges at 90° to each other is presented in Fig. 9.a while Fig. 9.b shows the case of two tangential gauges on the same side ($\theta = 90°$). It can be seen that deviations of ±15° from the principal stress direction will not introduce significant errors for stress ratios N between 0.3 and 3.0.

In summary, some general recommendations for the optimum locations of stress change gauges near a circular opening with axis parallel to one of the principal stresses can be given. Both the radial and tangential gauges located at either $\theta = 0°$ or 90° and placed in strategic positions can be used effectively for the determination of the stress ratio N and the magnitude S. The best combination for intermediate N-values is two tangential or two radial gauges set at 90° to each other at $\rho_1 = \rho_2 = 0.816$. By placing two sets of gauges (radial and tangential gauges on the same side) one degree of redundancy can be obtained to check the results. This arrangement is not adequate for extreme N-values in excess of 8. One radial and one tangential gauge on the same side at $\rho = 0.65$ can be used for N between 0.4 and 3.0. It may be prudent to install some additional gauges at this slightly smaller ρ-value, especially if errors in the ρ-determination are likely. A high degree of redundancy is also required because of the local variation in stresses in discontinuous rock masses or local stiffness variations in the rock. In relatively weak rock, large stress concentrations cannot be maintained over long periods of time, and relatively uniform stress distribution can be expected. It is for this reason that the data interpretation of only seven stress change gauges lead to relatively consistent results at the shaft near Lethbridge.

4.2 In situ Stress near Lethbridge, Alberta

A field monitoring program was conducted during the sinking of a vertical shaft as described in Section 2. The results of this program have been reported by MacKay (1982), Kaiser and MacKay (1982) and Kaiser *et al*. (1982). In the following some of the conclusions from previous work are summarized and a re-evaluation of the in situ stress field, calculated from the stress change gauge measurements, is presented.

Kaiser *et al*. (1982) predicted the in situ stress field from stress change gauge measurements based on the assumption that the stress change measured by a gauge was independent of the stress normal to that gauge, i.e., a radially oriented gauge measured only radial stress change and was not influenced by the tangential stress change. A blast damaged zone of 0.3 m was assumed and compensated for by increasing the opening radius by 0.3 m to an equivalent opening size of 3.6 m in diameter. They found that the least scatter of results was achieved when the tangential and radial stress change data were considered independently. The radial gauge data were disregarded and the in situ stress field at the test section (152 m depth) was estimated from the tangential measurements only:

$\sigma_{h(max)}$ = 4.25 MPa
N = 0.6
θ = East-West

where: $\sigma_{h(max)}$ = the maximum horizontal principal stress;
N = horizontal stress ratio $\sigma_{h(min)}/\sigma_{h(max)}$; and
θ = direction of $\sigma_{h(max)}$.

MacKay (1982) also assumed that the gauge response was not affected by stress changes normal to the gauge loading axis but considered both the tangential and radial gauge measurements simultaneously for interpreting the in situ field stress because he found that the tangential gauges alone were of limited value for the determination of the orientation of the principal stresses. He then predicted the in situ stress field at the Kipp mine site for the 152 m depth assuming again a blast damaged zone of 0.3 m in depth:

$\sigma_{h(max)}$ = 4.25 ± 0.5 MPa
N = 0.5 to 0.8
θ = S 40° W ± 20°.

The response of one radial gauge, on the outer south side, did not fit well with this overall analysis. With the exception of the principal stress orientation, this prediction was in good agreement with that of Kaiser *et al.* (1982). The orientation determined by MacKay (1982) corresponded closely to the stress orientaion predicted by Gough and Bell (1981) and Babcock (1978).

The stress change data from the Kipp shaft has recently been re-evaluated employing the method described in Section 4. The results from both the radial and tangential gauges were considered simultaneously and this analysis, unlike the preceding ones, assumed that the gauge response is influenced by stress changes normal to the gauge axis. A blast damaged zone was also accounted for by increasing the actual opening size to an equivalent opening size.

For a chosen stress ratio N curves were plotted (Fig. 11) varying the minor principal stress and the angle θ, the orientation of the minor principal stress in this case. A regression analysis was done, even though a very small number of data points were available, and the best fit curve for a given stress ratio N was found. Figure 11 shows the theoretical stress distributions for three of these cases with N ranging from 1.6 to 3.8. It can be seen that for $\rho < 0.85$ there is little distinction between the three curves and that any one of these sets of parameters could equally well define the stress field. The angle of orientation θ is relatively constant for these three curves but the minor principal stress varies considerably. However, these large variations in the minor principal stress can be attributed to the uncertainty in the stress ratio N which cannot be determined accurately from the gauge locations selected for this project. The tangential gauge in the west wall appeared to give consistently poorly fitting readings for all cases where otherwise a reasonable fit could be achieved to the remaining gauge records (Figure 11.a).

From this detailed analysis, the orientation of the minimum principal stress was found to be θ = S60°E ± 10°. The other parameters could not be determined with high accuracy. Nevertheless, the results from this analysis have been used to establish a new estimate of the in situ field stress, in terms of the maximum principal stress $\sigma_{h(max)}$, at a depth of 152 m for the Kipp mine site:

$\sigma_{h(max)} = 5.1 \pm 0.6$ MPa

$N = 0.45 \pm 0.2$

θ = S30°W±10°.

The larger value for the maximum principal stress is attributed to including the effects of the stress normal to the gauges. Furthermore, it can be shown that for a more accurate determination of N gauges should have been placed in the directions of the expected principal stresses.

Gough and Bell (1981) performed a regional study of wall breakouts in uncased oil wells in Alberta and northeastern British Columbia and found the major horizontal principal stress to be approximately normal to the Rocky Mountains in a NE-SW direction. Babcock (1978) reported the major principal horizontal stress orientated N30°E as obtained from measuring oil well breakouts in this area at depths of 1280 m to 2194 m. Both the re-evaluated results and those of MacKay (1982) are in good agreement with these investigations.

Reviewing the results from these three analyses, several observations pertaining to the data interpretation and selection of gauge locations can be made:

- an incorrect orientation of the major principal stress may be calculated when radial gauge results are not considered;
- neglecting the influence of the stress change normal to the gauge does not appear to affect the determined orientation angle θ, but does affect the magnitude of the predicted major principal stress; and
- gauges should be placed in the directions of the principal stresses for a most accurate determination of the stress ratio N.

4.3 Longterm Stress Change Measurements

The longterm stress changes inside the rock mass surrounding the underground opening are of interest for two main reasons:

(a) for the support evaluation and (b) for the interpretation of convergence and extensometer records.

a) For the support evaluation: As soon as the liner is activated the radial stresses at the wall will increase and cause a proportional radial stress increase at the gauge location. Simultaneously, the tangential stresses will decrease as load is transferred to the lining. This latter tangential stress decrease may, however, be dominated by creep of the highly stressed rock near the stress change gauges.

b) For the interpretation of convergence or extensometer measurements and the determination of the rock mass deformation properties: Most in situ measurements of displacements inside or near underground openings are only possible during a limited time period, after partial or full face excavation of the opening and before the final support system is installed. Hence, extrapolations are necessary to determine the pre-excavation displacements and the deformations that accumulate after support installation. The reliability of such extrapolations can be significantly increased by stress change measurements. This aspect will be covered in more detail in Section 5.

The stress change record is also of interest for a better understanding of the stress redistribution processes that might occur during time-dependent propagation of a yield zone near the opening or while openings are excavated in the vicinity of a monitored opening, i.e., during nearby mining operations. This latter aspect could not be investigated at the Kipp Mine because mining was limited to minor test excavations to evaluate roof stability and to obtain a representative coal sample for quality determination.

Figure 12 presents the longterm stress change development over a 830-day period for all seven gauges. As expected, the radial gauges show a stress decrease while the stresses in the tangential gauges increase. The location of the shaft bottom relative to the plane of measurement is shown on Figure 12.a where it is also indicated that some mining operations may have influenced the measurements between about 100 and 300 days after the monitoring section was passed. It is of interest to note that a major portion of the total stress change occurred ahead of the face (42 to 59% of the tangential stress) and only a relatively small stress change during the extensometer monitoring period (6 to 21%) from the time of installation to when the cast-in-place concrete liner was poured. The radial stresses changed even more rapidly with between 74 and 85% ahead of the shaft bottom and only an additional 4 to 11% before liner installation.

The more or less steady decrease in radial stress supports the conclusion presented by Kaiser and Mackay (1982) that the liner is under negligible stress at the test section. The slight, temporary radial stress increase between 200 and 300 days may indicate that some load buildup could occur during subsidence due to coal mining operations. (Note: one radial gauge (Fig. 12.a) dropped below the base level after 36 days; hence, subsequent measurements are unreliable.) The tangential stress decrease that started after 40 to 100 days may not reflect a true rock mass stress change but rather a relaxation of the gauges wedged into the borehole. Recent measurements indicate that these tangential stresses appear to have stabilized after a slight increase during coal mining (two gauges have ceased functioning after 300 to 400 days). It is possible that the peak tangential stress was slightly underestimated because no correction for stress relaxation was included in the analysis.

The time-dependent stress change can be separated into two components: (a) stress change due to time-dependent advance rate of the shaft and (b) stress change due to time-dependent rock mass properties. From laboratory tests on small tunnels [Kaiser *et al.* (1983)] it has been found that the wall convergence rate in relatively soft rock (E = 1 to 3 GPa) is dominated by the advance rate until the face has passed 10 to 20 radii beyond the test section. After this point rock mass creep prevailed in the cases analysed. These conclusions cannot be generalized because of the relative magnitudes of deformations resulting from opening advance and rock creep. However, from Fig. 12 it can be seen that stress changes (tangential increase and radial decrease) continue beyond the time when excavation was stopped at 20 radii from the test section. Hence, time-dependent stress redistribution has occurred in the rock surrounding the shaft and the assumption of perfectly elastic rock (Sections 3 and 4) is not fully justified. Lack of quantitative information about the creep properties of the rock mass does, at the present time, not permit more sophisticated data analyses. Nevertheless, the assumption that the maximum stress change is related to shaft excavation only appears to be a reasonable first approximation.

5. Use of Stress Change Gauges to Determine Rock Mass Deformation Properties

The radial rock mass displacements measured by multipoint extensometers depend on the constitutive relationship of the rock mass and the magnitude of stress change that causes the deformations. These two factors, material property and stress change, theoretically are directly related but in practice many additional variables complicate the relationship. For example, a rock mass may be assumed and behave linear elastic during the monitoring stage but the stress change before the installation of the instruments may not be predicted correctly by a linear elastic model, i.e., due to weakening of rock at the face of the opening that causes a transfer of stresses away from the test section. Hence, it is necessary to determine, during a monitoring program, both the constitutive relationship as well as the simultaneous change in stress field for successful interpretation of the data. This concept was adopted at the Kipp Shaft where the stress change and the displacements were measured simultaneously and the assumption of linear elastic material behaviour was checked by comparison with analytical predictions. By this approach it was found that the measured deformations corresponded on average to only about 15% of the total deformations. Accordingly, an average rock mass modulus of 2.5 GPa, was backcalculated based on the assumption of linear elastic material response during the monitoring period [Mackay(1982)]. Theoretically, for a circular shaft in a fully elastic, undisturbed material, the displacements recorded ahead of the face should be about 30% of the total displacements, and approximately 100% of these displacements should be reached after 4 to 5 radii from the face. Accordingly, the predicted stress change for extensometers installed at the face would be in the order of 60% to 70% and the resulting rock mass modulus based on the theoretically predicted stress change would vary between only 0.55 to 0.65 GPa. Because of stress redistributions due to blast damage ahead of the shaft bottom and half bench blasting, it must be assumed that the extensometers were installed at between one half and one shaft radius behind the undisturbed rock boundary. Consequently, it is difficult to predict the actual stress change and, hence, the correct rock modulus without stress change measurements.

Figure 13.a summarizes the stress change measured by gauges located at 1.5 to 1.55a in radial and tangential directions from the west and south wall of the shaft. The stress changes predicted for an axisymmetric opening by finite element analyses for gauges at 1.5a from the tunnel wall in a linear elastic medium are shown in Fig 13.b (from Hutchinson (1982)). For all predictions, the principal stress ratio in a plane perpendicular to the axis of the opening was assumed to be unity. Four cases are shown: Case 1 - unlined opening; Case 2 - unlined opening excavated one radius further (shift of curve by 1a) to simulate the influence of fully damaged rock due to blasting of the shaft floor during double bench excavation; Case 3 - opening lined at the face with a damaged or softened zone one radius ahead of the face and one third radius beyond the opening walls (assumed ratio of Young's moduli of undamaged to damaged rock was 2; Kaiser and Hutchinson (1982)); Case 4 - an opening with stiff lining installed at the face immediately after excavation of rounds of one radius in depth.

From Fig. 13.a, it can be seen that the predicted radial and particularly tangential stress change exceeds the average observed stress change. The maximum measured values are, however, only slightly exceeded at the south wall. The discrepancy in magnitude must be attributed to the difference between the assumed and actual stress ratio N. The tangential and radial stress change occurred much earlier than predicted. Better correspondence in timing can be achieved if the predicted stress change is shifted by one radius ahead (Case 2) or if softened rock is assumed to exist near the opening. Redistribution of stresses from damaged zones to undamaged zones causes this translation of the stress change curves. As indicated by the shaded area, the exact shape of the real stress change curve is not known, but it appears that the stress change was shifted by one radius ahead of the shaft bottom due to blast damage at the bottom of the shaft. This seems particularly reasonable for the half bench excavation procedure adopted for the construction of the Kipp shaft.

For the determination of the rock mass modulus, this shift is of great importance. For example, for Cases 1, 3 and 2 the stress changes that occur after the face decrease from 71 to 34 to 8% of the total radial stress change and 56 to 39 to 25% of the total tangential stress change. The average observed radial and tangential stress changes after the face for these 5 gauges are only 9 and 28%, respectively. It is evident from this comparison that measurements of stress changes associated with deformation measurements in underground openings are essential for an accurate back analysis of the rock mass deformation modulus.

At the present time, there are however several factors that limit this approach as well as the technique described earlier for the in situ stress determination:

a) Local stress concentrations or variations: i.e., the two tangential gauges in the south wall (Fig. 13.a) are only 0.2 to 0.3 m apart but the stresses measured differ by a factor of two. This may be due to local stress concentrations near discontinuities or in areas of high rock stiffness. The gauges are relatively small and are dominated by such local stress variations. Hence, a large number of measurements would be needed to arrive at a sufficiently accurate average stress change.

b) Location of gauge relative to opening wall: with current techniques it is cumbersome to locate the gauge accurately; for the case presented the radius to the gauge may differ from the assumed by as much as 0.1 to 0.2 m. In addition, the opening size (radius a) is not exactly known because of local overbreaks and, most important, because of stress redistribution from blast damage to undamaged zones. The gauges assumed at 1.5a may in reality be located at 1.3a, in which case the stresses would be about 20% higher. It is less likely that r/a was underestimated. Some of the observed discrepancies between the west and the south wall may be attributed to this factor.

c) Orientation of principal stresses and magnitude of stress ratio N: Most of the data interpretation must be based on simplified assumptions about the orientation and relative magnitude of the principal stresses. This may, in certain circumstances, extremely limit the value of in situ stress change measurements. However, the percentage of stress change varies consistently along the axis of the opening (see Fig.13) and it is this relative value that is extremely useful for the determination of the rock mass modulus.

d) Cost of gauges and reliability of setting tool: Large increases in the cost of the IRAD-stress gauge (only one supplier) over the last few years and the high risk for malfunctioning or loss of instruments during installation make the proposed monitoring procedure unattractive for conventional engineering projects. This is unfortunate because we believe that stress change measurements should become an integral part of every deformation monitoring programme. However, before this can be encouraged further, it will be necessary to improve both the instruments and the setting tool supplied by the manufacturer. Our recent experience with a success rate of less than 50% during an underground instrumentation project with 14 installed gauges demonstrates unacceptable performance.

Further field measurements with many stress change gauges and accurate numerical modelling will help to eliminate some of these limitations.

6. Conclusions

The design of a support system for an underground opening must consider the interaction of support and ground as illustrated by the Convergence-Confinement Method (applied to the Kipp Shaft by Kaiser and Mackay (1982)). For the evaluation of this interaction it is necessary to know the initial stress field, the deformation and strength properties of the ground, the properties of the support system and the displacements that occur before the ground and support interact. The stress monitoring program described and evaluated in this paper provides a rational approach to determine the first two factors, the in situ stress field and the rock mass deformation properties, but it also improves the designers' ability to determine the support-ground interaction point by measuring (rather than predicting) the stress change that occurs before the support is installed.

Stress change gauges can be used effectively to backcalculate the in situ stress field (if the ground responds essentially in an elastic manner during the measuring period) from the stress change that is caused by the excavation of the underground opening.

For the data interpretation it is paramount that the gauges are located accurately at positions where unique and sensitive measurements are possible. Many factors that must be considered when locating the gauges have been discussed and it was found that, in general, at least two sets of gauges (at 90° to each other) at a distance of 1.2 to 1.25 times the opening radius should be installed. In addition a redundancy factor of at least 2 to 3 will be necessary to guarantee sufficient data for a conclusive interpretation.

Most in situ tests for the determination of the rock mass properties are based on an assumed change in stress that causes deformations. The data collected during the monitoring of a shaft by extensometers has shown that it is not possible to predict this stress change with sufficient accuracy and that it is beneficial to measure the stress change before and while deformations are monitored. This simplifies the analysis and increases the accuracy and reliability of extrapolations that are necessary for the determination of rock mass deformation properties from in situ displacement records.

7. Acknowledgements

This research project has been funded through a research contract with Petro Canada Exploration Inc., Calgary and supplemented by funds from the National Sciences and Engineering Research Council of Canada. The execution of

the field instrumentation program was successful because of the excellent cooperation of the employees of Thyssen Mining Construction of Canada Ltd. and because of the dedication of our senior technician, G. Cyre.

8. *References*

Babcock, E.A., 1978. Measurements of subsurface fractures from dipmeter logs. *The American Association of Petroleum Geologists Bulletin*, Vol. 62, No. 7, pp. 1111-1126.,

Bieniawski, Z.T., 1978. Determining rock mass deformability: experience from case histories. *International Journal of Rock Mechanics and Mining Sciences & Geomechanics Abstracts*, Vol. 15, No. 5, pp. 237-248.,

Gough, D.I. and J.S. Bell, 1981. Stress orientation from oil well fractures in Alberta and Texas. *Canadian Journal of Earth Sciences*, Vol. 18, No. 3, pp. 638-645.,

Hawkes, I. and V.E. Hooker, 1974. The vibrating wire stressmeter. *3rd congress of the International Society of Rock Mechanics*, Denver, Vol. 2, Part A pp. 439-444.,

Hawkes, I. and V.W. Bailey, 1973. Low Cost Cylindrical Stress Gauge. *Report prepared for U.S. Bureau of Mines*, NTIS No. PB243347, 142 p.,

Hooker, V.E. and D.L. Bickel, 1974. Overcoring Equipment and Techniques used in Rock Stress Determination. *U.S. Bureau of Mines*, Information Circular 8618, 32 p.,

Hutchinson, D.E., 1982. Effects of Construction Procedures on Shaft and Tunnel Performance. *M.Sc. Thesis*, *Department of Civil Engineering, University of Alberta*, 267 p.,

Kaiser, P.K. and D.E. Hutchinson, 1982. Effects of construction procedure on tunnel performance. *4th International Conference on Numerical Methods in Geomechanics*, Vol. 2, pp. 561-570.,

Kaiser, P.K. and C. Mackay, 1982. Development of rock mass and liner stresses during sinking of a shaft in clay shale. *1st International Conference on "Stability in Underground Mining"*, Vancouver, Ch. 36 pp. 790-809.,

Kaiser, P.K., C. Mackay and N.R. Morgenstern, 1982. Performance of a shaft in weak rock (Bearpaw Shale). *ISRM Symposium on Caverns and Pressure shafts* , Aachen, Vol. 2, pp. 613-622.

Kaiser, P.K., S.M. Maloney and N.R. Morgenstern, 1983. Time-dependent behavior of tunnels in highly stressed rock. *5th Congress of the International Society of Rock Mechanics*, Melbourne, Section D, pp. D329-D336.,

Kaiser, P.K., 1981. Monitoring for the evaluation of stability of underground openings. *1st Annual Conference on Ground Control in Mining*, West Virginia, pp. 90-97.,

Korpach, D., 1983. Stresses and Displacements near the tunnel face. *M.Sc. thesis, Department of Civil Engineering, University of Alberta*, (in preparation)., Kruse, G.K., 1970. Deformability of rock structures, California State Water Project. *ASTM STP 477*, American Society for Testing and Materials, pp. 58-88.,

Lane, K.S., 1977. Instrumented tunnel tests: a key to progress and cost savings. *Underground Space*, Vol. 1, pp. 247-259.,

Mackay, C.H.R., 1982. Performance of a Shaft in Weak Rock. *M.Sc. thesis, Department of Civil Engineering, University of Alberta*, 257 p.,

Merrill, R.H. and J.R. Peterson, 1969. Deformation of a borehole in rock. *U.S. Bureau of Mines*, RI 5881, 32p.,

Pariseau, W.G., 1978. A note on monitoring stress changes in situ. *International Journal of Rock Mechanics and Mining Sciences & Geomechanics Abstracts*, Vol. 15, No. 4, pp. 161-166.,

Sellers, J.B., 1977. The measurement of stress changes in rock using the vibrating wire stressmeter. *International Symposium on Field Measurement in Rock Mechanic*, Zurich, Vol. 1, pp.275-288.,

Timoshenko, S.P. and J.N. Goodier, 1970. Theory of Elasticity. 3rd Edition, McGraw Hill, New York, 567 p., Zoback, M.D. and B.C. Haimson, 1982. Status of the hydraulic fracturing method for in-situ stress determination. *23rd U.S. Symposium on Rock Mechanics*, Berkeley, Ch. 15, pp. 143-156, published by AIME.,

Figure 1. Section and plan view of instrumentation at 152 m depth.

Figure 2. Plan view of extensometer at 180 m depth.

Figure 3. Plots of principal stress ratio N versus stress change ratio SCR measured by gauges located at varying distances from the opening wall for: (a) two tangential gauges at $\theta = 0°$; and (b) two tangential gauges at $\theta = 90°$.

Figure 4. Plots of principal stress ratio N versus stress change ratio SCR measured by gauges located at varying distances from the opening wall for: (a) two radial gauges at $\theta = 0°$; and (b) two radial gauges at $\theta = 90°$.

Figure 5. Plots of principal stress ratio N versus stress change ratio SCR measured by: two *tangential* gauges; one at $\theta = 0°$ and one at $\theta = 90°$.

Figure 6. Plots of principal stress ratio N versus stress change ratio SCR measured by: two *radial* gauges; one at $\theta = 0°$ and one at $\theta = 90°$.

Figure 7. Plots of principal stress ratio N versus stress change ratio SCR measured by: one *tangential* and one *radial* gauge at $\theta = 0°$.

Figure 8. Plot of principal stress ratio N versus stress change ratio SCR to illustrate effects of

inaccurate ρ-determination for two radial gauges (one at $\theta = 0°$ and one at $\theta = 90°$) for: (a) inaccurate small ρ-value; and (b) inaccurate large ρ-value.

Figure 9. Plot of principal stress ratio N versus stress change ratio SCR to illustrate effects of inaccurate θ-determination for: (a) two tangential gauges; one at $\theta = 0°$ and one at $\theta = 90°$; and (b) two tangential gauges at $\theta = 90°$.

Figure 10. Plot of principal stress ratio N versus stress change ratio SCR measured by gauges located at various distances from the opening wall for: (a) one tangential and one radial gauge at 0°; and (b) one tangential and one radial gauge at 90°.

Figure 11. Theoretical uniaxial stress distribution for different N, θ, and S parameters compared with measurements from the Kipp Shaft for: (a) West wall; and (b) South wall (X = Distance from shaft bottom).

Figure 12. Long term uniaxial stress change measurements recorded at the Kipp Shaft for: (a) Stressmeters at $\rho = 0.65$ (South wall); and (b) Stressmeters at $\rho = 0.51$ (South wall) and $\rho = 0.67$ (West wall).

Figure 13. Uniaxial stress change development during shaft advance: (a) measured by five gauges at a distance of 1.5 to 1.55a from the shaft center; and (b) predicted by Finite Element Method at 1.5a for four cases (Hutchinson, 1982).

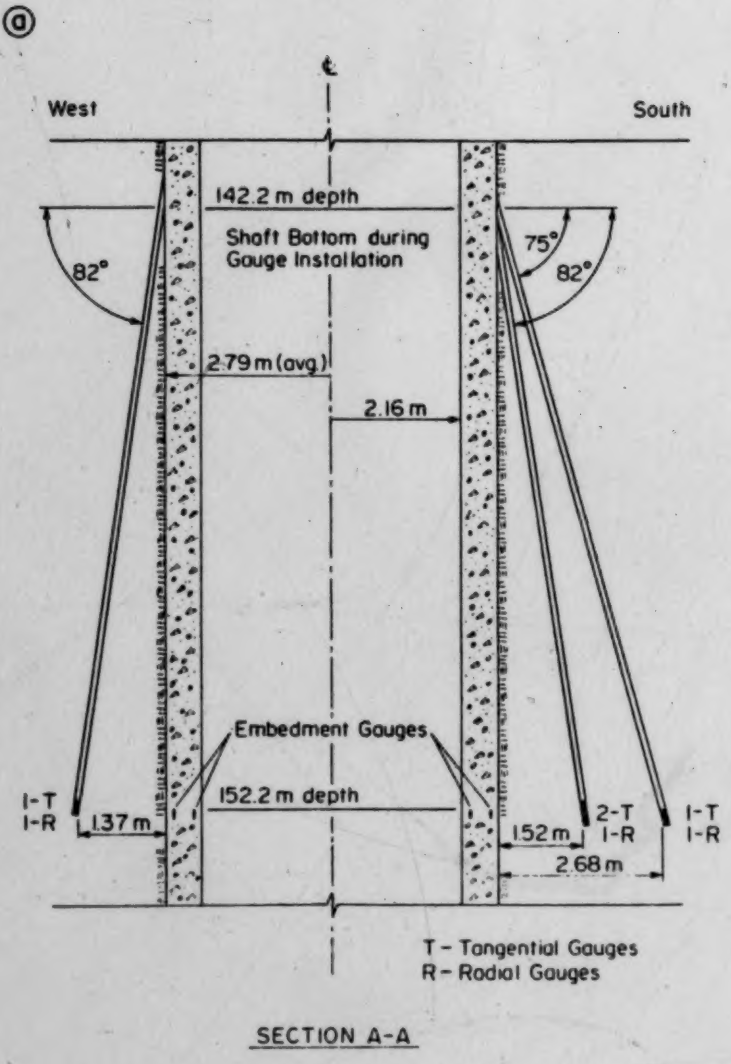
ⓐ
West
South
℄
142.2 m depth
Shaft Bottom during
Gauge Installation
82°
75°
82°
2.79 m (avg.)
2.16 m
Embedment Gauges
152.2 m depth
1-T
1-R
1.37 m
1.52 m
2-T
1-R
1-T
1-R
2.68 m
T - Tangential Gauges
R - Radial Gauges
SECTION A-A

Fig. 1a

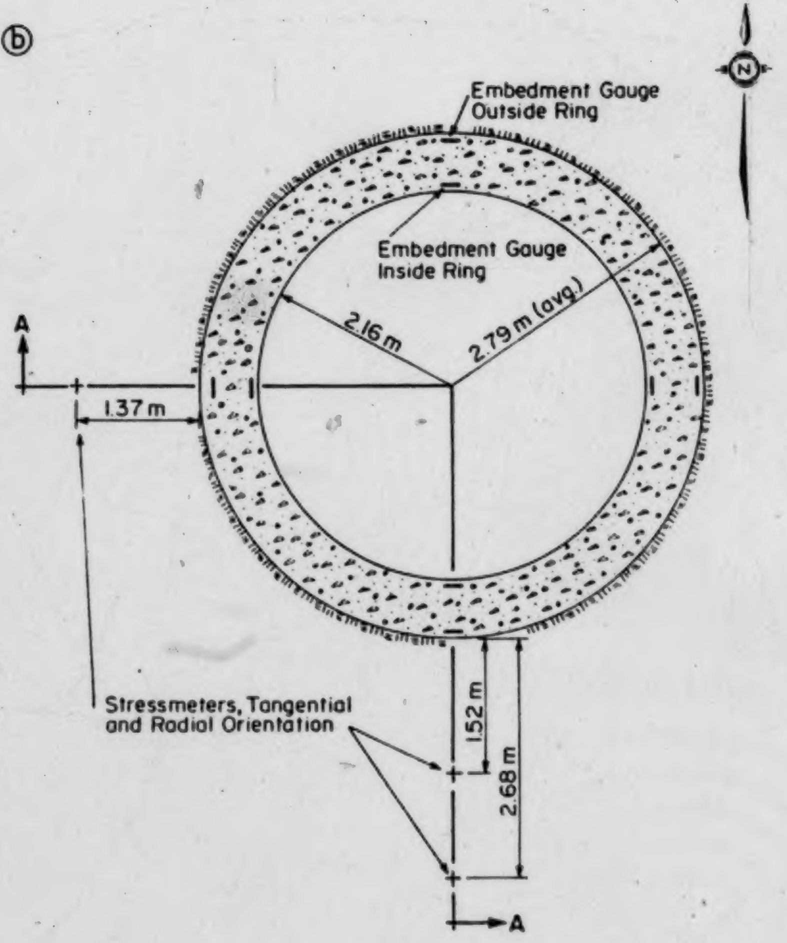
ⓑ
N
Embedment Gauge
Outside Ring
Embedment Gauge
Inside Ring
2.16 m
2.79 m (avg.)
A
1.37 m
Stressmeters, Tangential
and Radial Orientation
1.52 m
2.68 m
A

Fig. 1.b

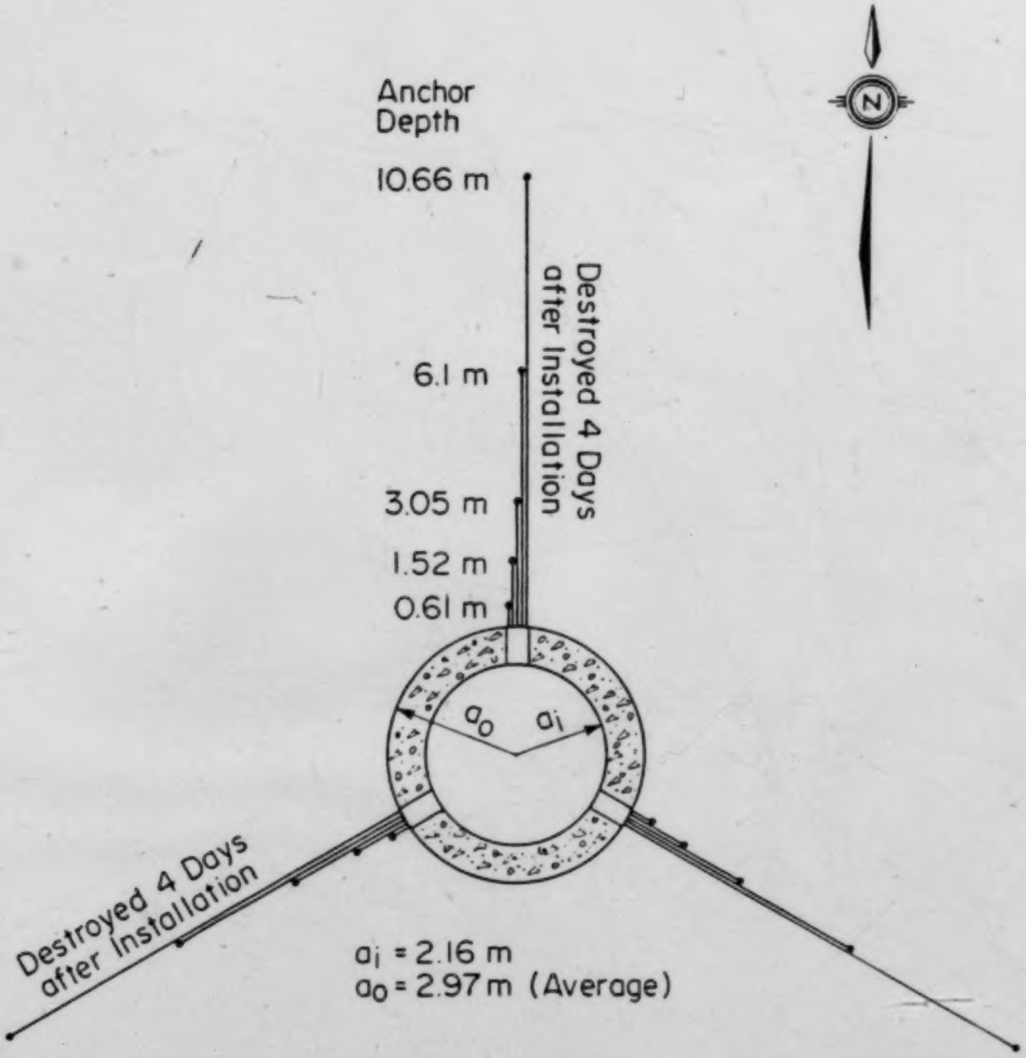
N
Anchor Depth
10.66 m
6.1 m
3.05 m
1.52 m
0.61 m
Destroyed 4 Days after Installation
Destroyed 4 Days after Installation
a_o
a_i
a_i = 2.16 m
a_o = 2.97 m (Average)

Fig. 2

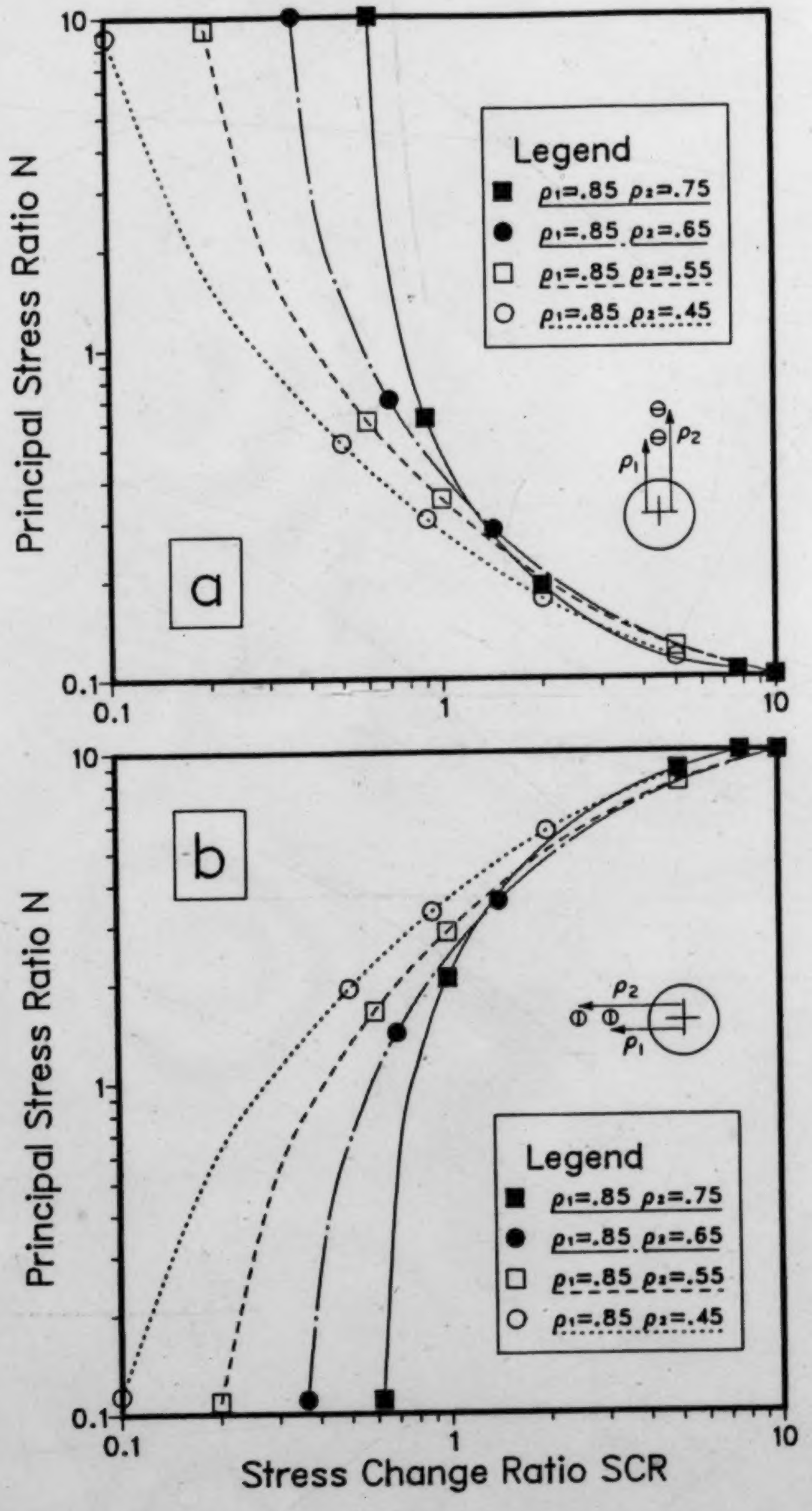
Principal Stress Ratio N
10
1
0.1
0.1
1
10
Legend
■ ρ1=.85 ρ2=.75
● ρ1=.85 ρ2=.65
□ ρ1=.85 ρ2=.55
○ ρ1=.85 ρ2=.45
Θ
Θ
ρ1
ρ2
a
b
Principal Stress Ratio N
10
1
0.1
0.1
1
10
Stress Change Ratio SCR
ρ2
ρ1
Θ
Θ
Legend
■ ρ1=.85 ρ2=.75
● ρ1=.85 ρ2=.65
□ ρ1=.85 ρ2=.55
○ ρ1=.85 ρ2=.45

Figure 3

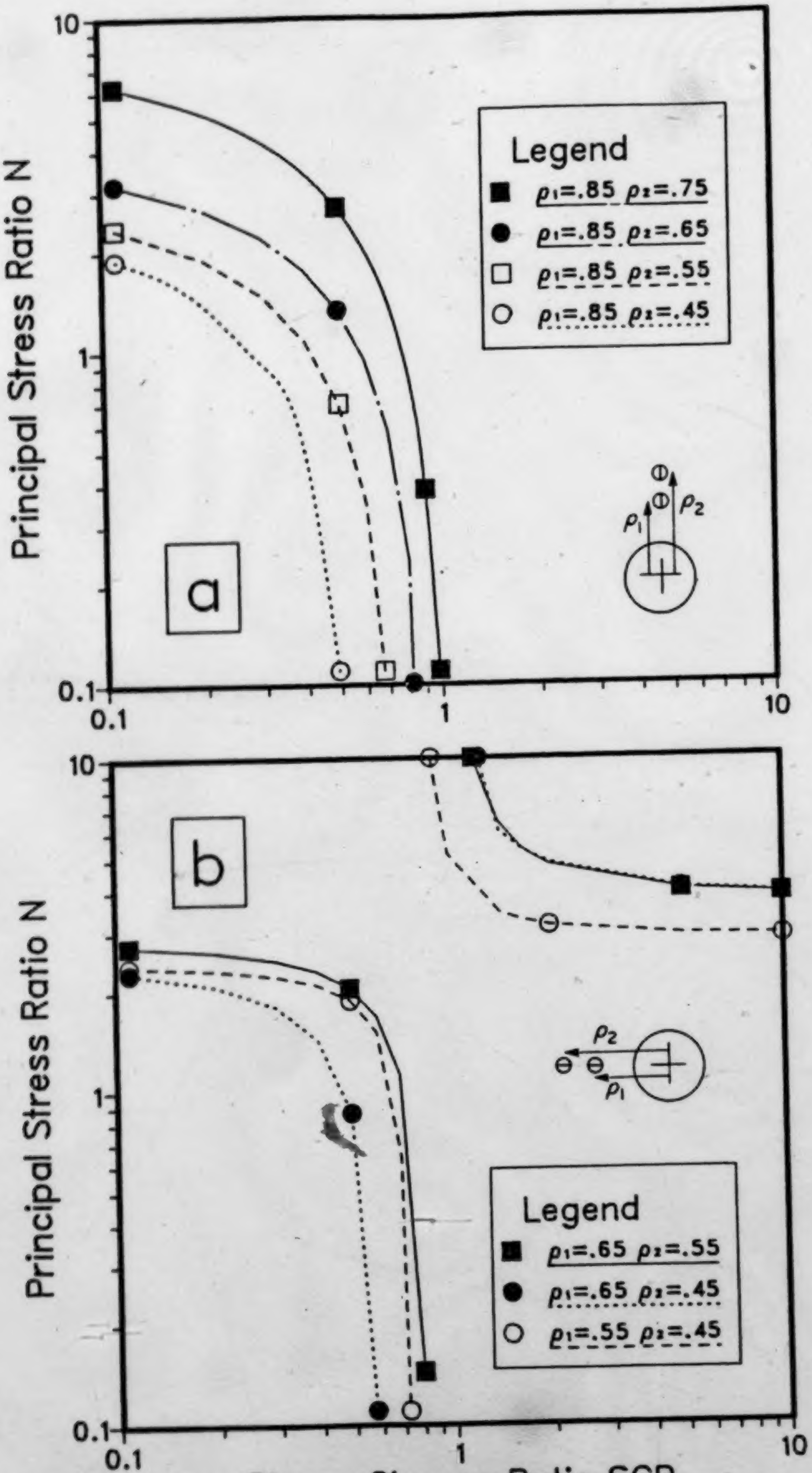
Principal Stress Ratio N
10
1
0.1
0.1
1
10
Legend
■ ρ1=.85 ρ2=.75
● ρ1=.85 ρ2=.65
□ ρ1=.85 ρ2=.55
○ ρ1=.85 ρ2=.45
ρ1
ρ2
a
Principal Stress Ratio N
10
1
0.1
0.1
1
10
b
ρ2
ρ1
Legend
■ ρ1=.65 ρ2=.55
● ρ1=.65 ρ2=.45
○ ρ1=.55 ρ2=.45
Stress Change Ratio SCR

Figure 4

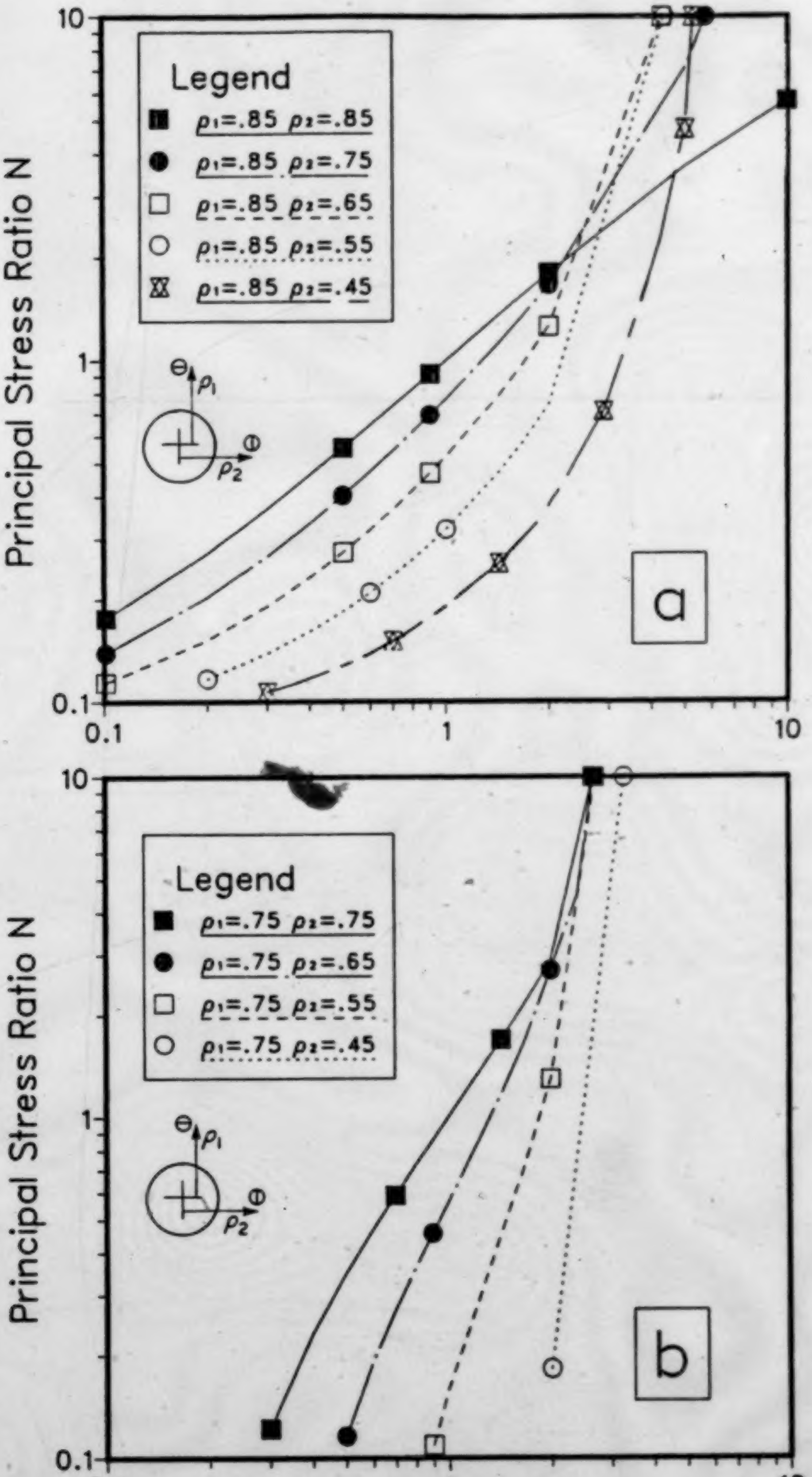
Legend
$\rho_1=.85\ \rho_2=.85$
$\rho_1=.85\ \rho_2=.75$
$\rho_1=.85\ \rho_2=.65$
$\rho_1=.85\ \rho_2=.55$
$\rho_1=.85\ \rho_2=.45$
Θ
ρ_1
ρ_2
a
Principal Stress Ratio N
10
1
0.1
0.1
1
10
Legend
$\rho_1=.75\ \rho_2=.75$
$\rho_1=.75\ \rho_2=.65$
$\rho_1=.75\ \rho_2=.55$
$\rho_1=.75\ \rho_2=.45$
Θ
ρ_1
ρ_2
b
Principal Stress Ratio N
10
1
0.1
0.1
1
10
Stress Change Ratio SCR

Figure 5

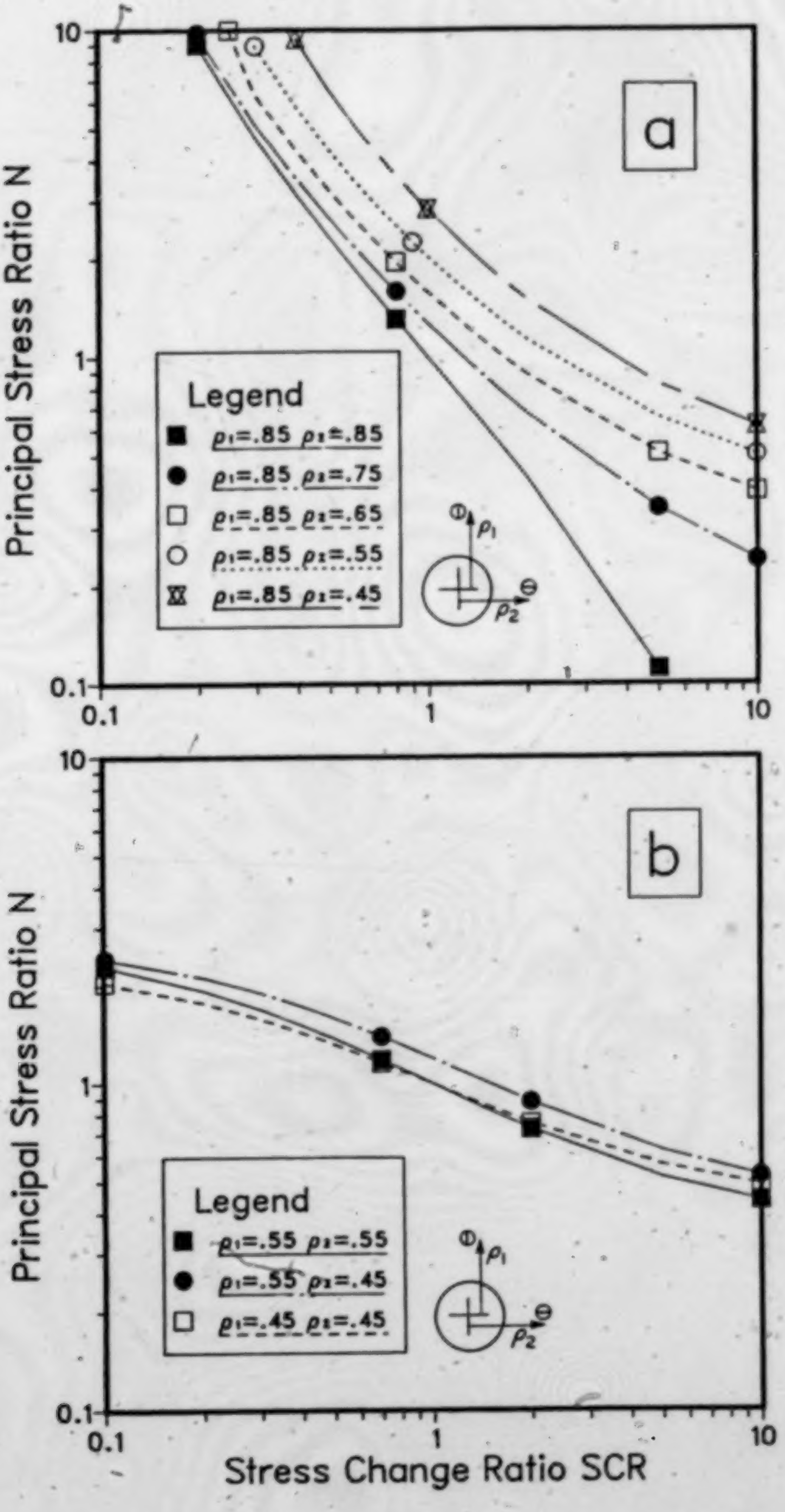
a
Principal Stress Ratio N
10
1
0.1
0.1
1
10
Legend
■ ρ₁=.85 ρ₂=.85
● ρ₁=.85 ρ₂=.75
□ ρ₁=.85 ρ₂=.65
○ ρ₁=.85 ρ₂=.55
⌛ ρ₁=.85 ρ₂=.45
Φ
ρ₁
Θ
ρ₂
b
Principal Stress Ratio N
10
1
0.1
0.1
1
10
Stress Change Ratio SCR
Legend
■ ρ₁=.55 ρ₂=.55
● ρ₁=.55 ρ₂=.45
□ ρ₁=.45 ρ₂=.45
Φ
ρ₁
Θ
ρ₂

Figure 6

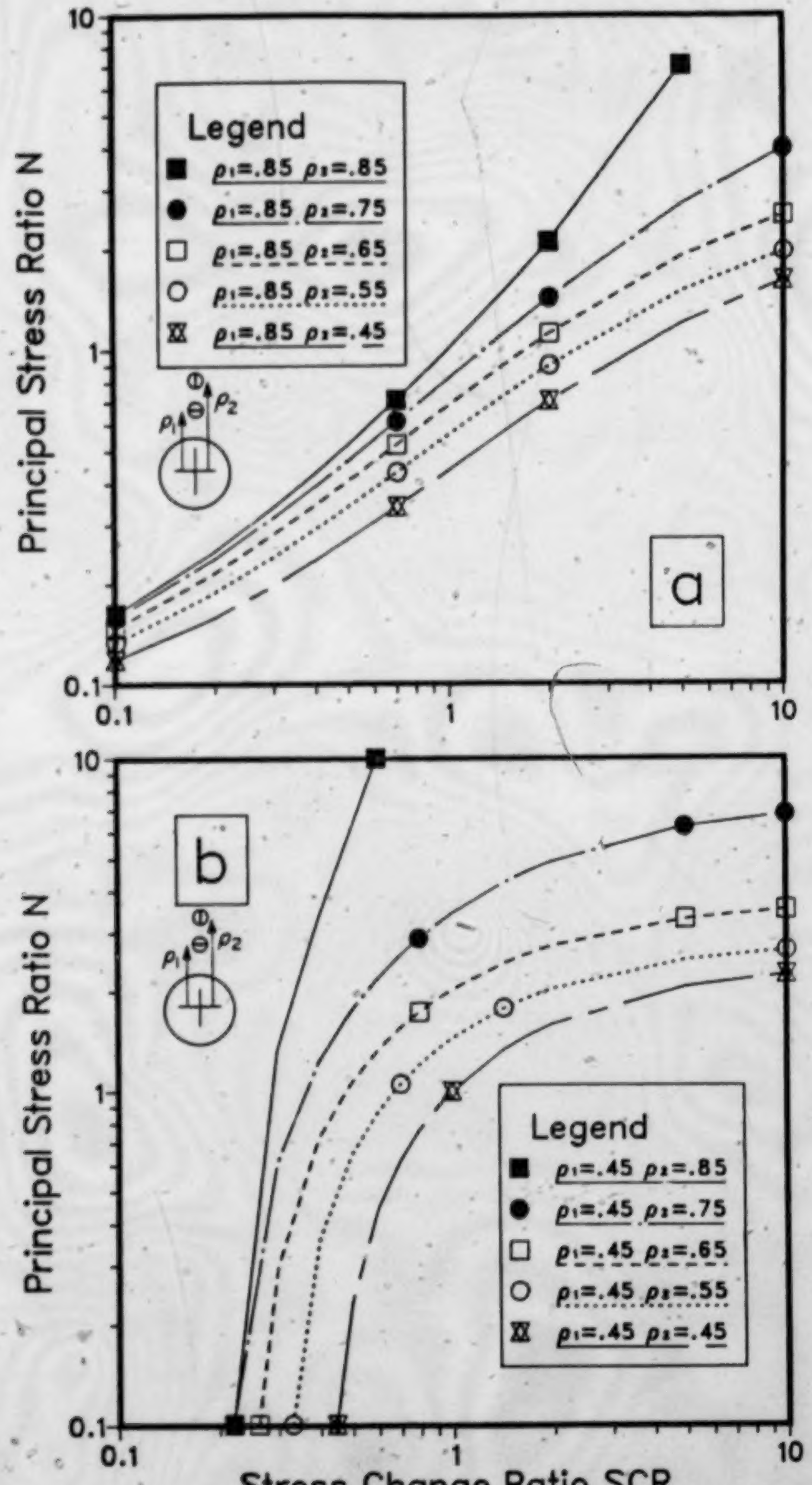
Principal Stress Ratio N
10
1
0.1
0.1
1
10
Legend
■ ρ_1=.85 ρ_2=.85
● ρ_1=.85 ρ_2=.75
□ ρ_1=.85 ρ_2=.65
○ ρ_1=.85 ρ_2=.55
⧗ ρ_1=.85 ρ_2=.45
Θ
ρ_1 Θ ρ_2
a
Principal Stress Ratio N
10
1
0.1
0.1
1
10
b
Θ
ρ_1 Θ ρ_2
Legend
■ ρ_1=.45 ρ_2=.85
● ρ_1=.45 ρ_2=.75
□ ρ_1=.45 ρ_2=.65
○ ρ_1=.45 ρ_2=.55
⧗ ρ_1=.45 ρ_2=.45
Stress Change Ratio SCR

Figure 7

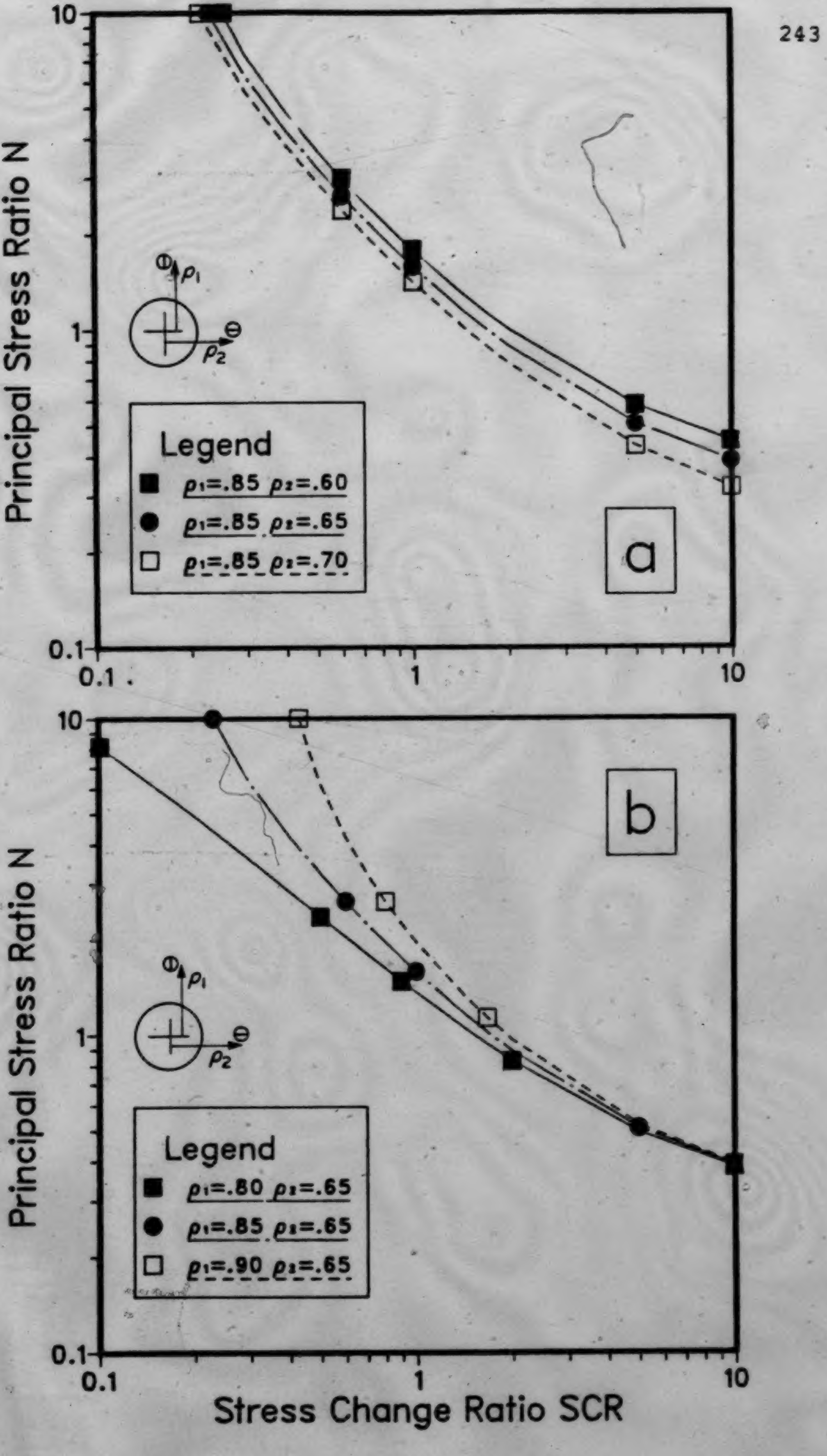
10
1
0.1
0.1
1
10
Principal Stress Ratio N
Θ
ρ_1
Θ
ρ_2
Legend
■ ρ_1=.85 ρ_2=.60
● ρ_1=.85 ρ_2=.65
□ ρ_1=.85 ρ_2=.70
a
10
1
0.1
0.1
1
10
Principal Stress Ratio N
b
Θ
ρ_1
Θ
ρ_2
Legend
■ ρ_1=.80 ρ_2=.65
● ρ_1=.85 ρ_2=.65
□ ρ_1=.90 ρ_2=.65
Stress Change Ratio SCR

Figure 8

7

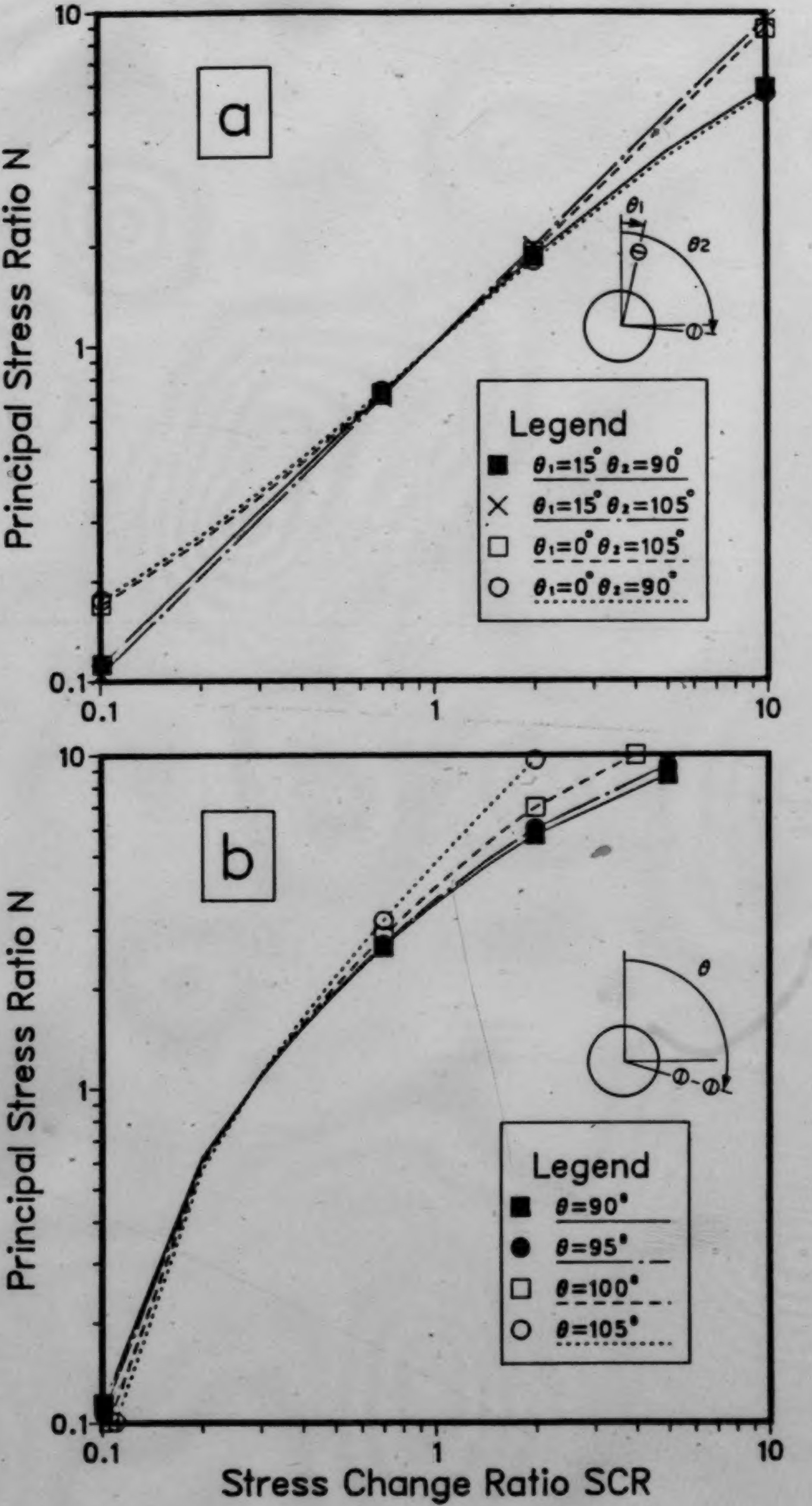
a
Principal Stress Ratio N
10
1
0.1
0.1
1
10
θ_1
θ_2
Legend
■ $\theta_1=15°$ $\theta_2=90°$
× $\theta_1=15°$ $\theta_2=105°$
□ $\theta_1=0°$ $\theta_2=105°$
○ $\theta_1=0°$ $\theta_2=90°$
b
Principal Stress Ratio N
10
1
0.1
0.1
1
10
θ
Legend
■ $\theta=90°$
● $\theta=95°$
□ $\theta=100°$
○ $\theta=105°$
Stress Change Ratio SCR

Figure 9

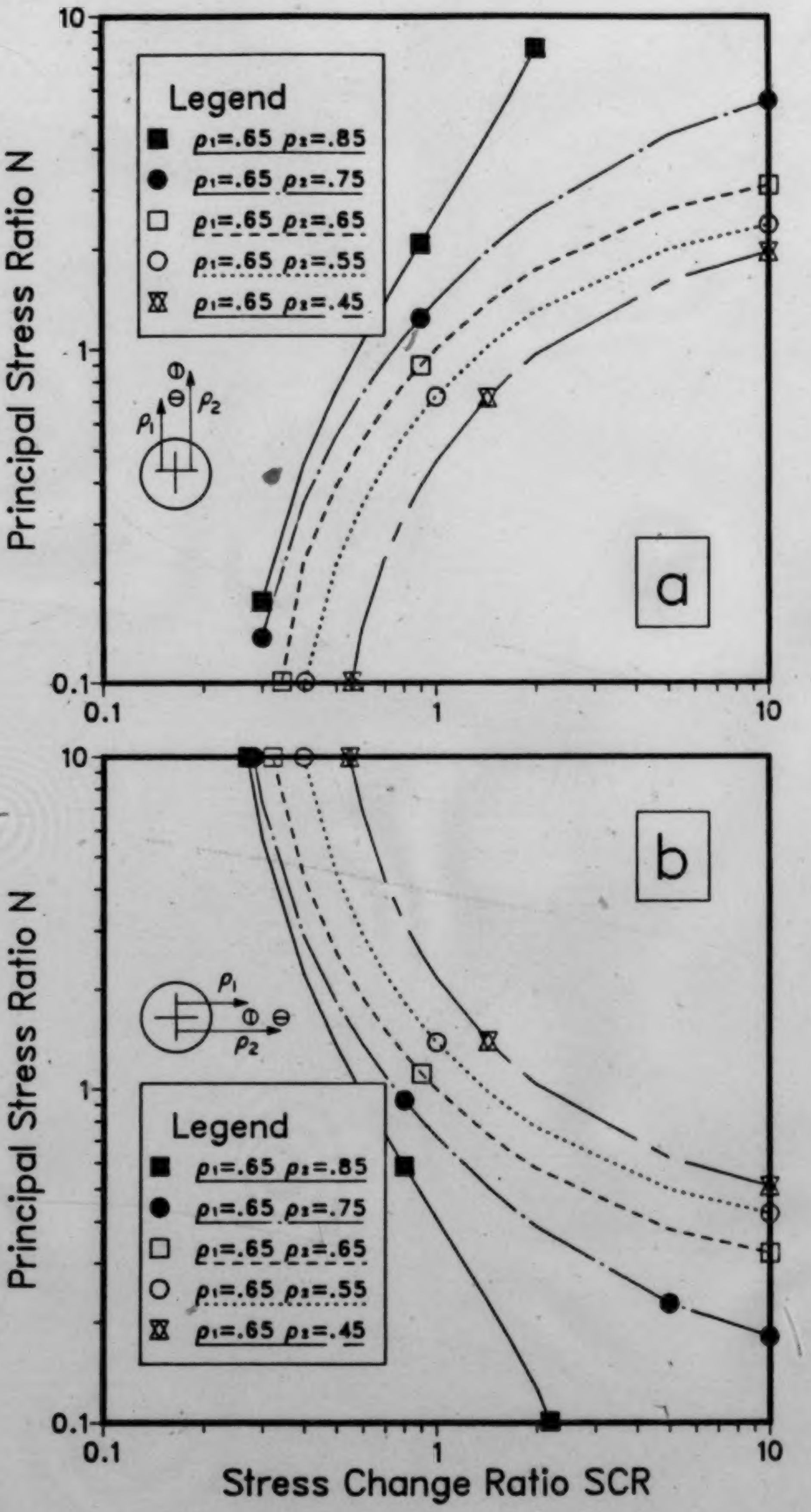
Principal Stress Ratio N
10
1
0.1
0.1
1
10
Legend
■ ρ₁=.65 ρ₂=.85
● ρ₁=.65 ρ₂=.75
□ ρ₁=.65 ρ₂=.65
○ ρ₁=.65 ρ₂=.55
⧖ ρ₁=.65 ρ₂=.45
ρ₁
ρ₂
⊖
a
b
Stress Change Ratio SCR

Figure 10

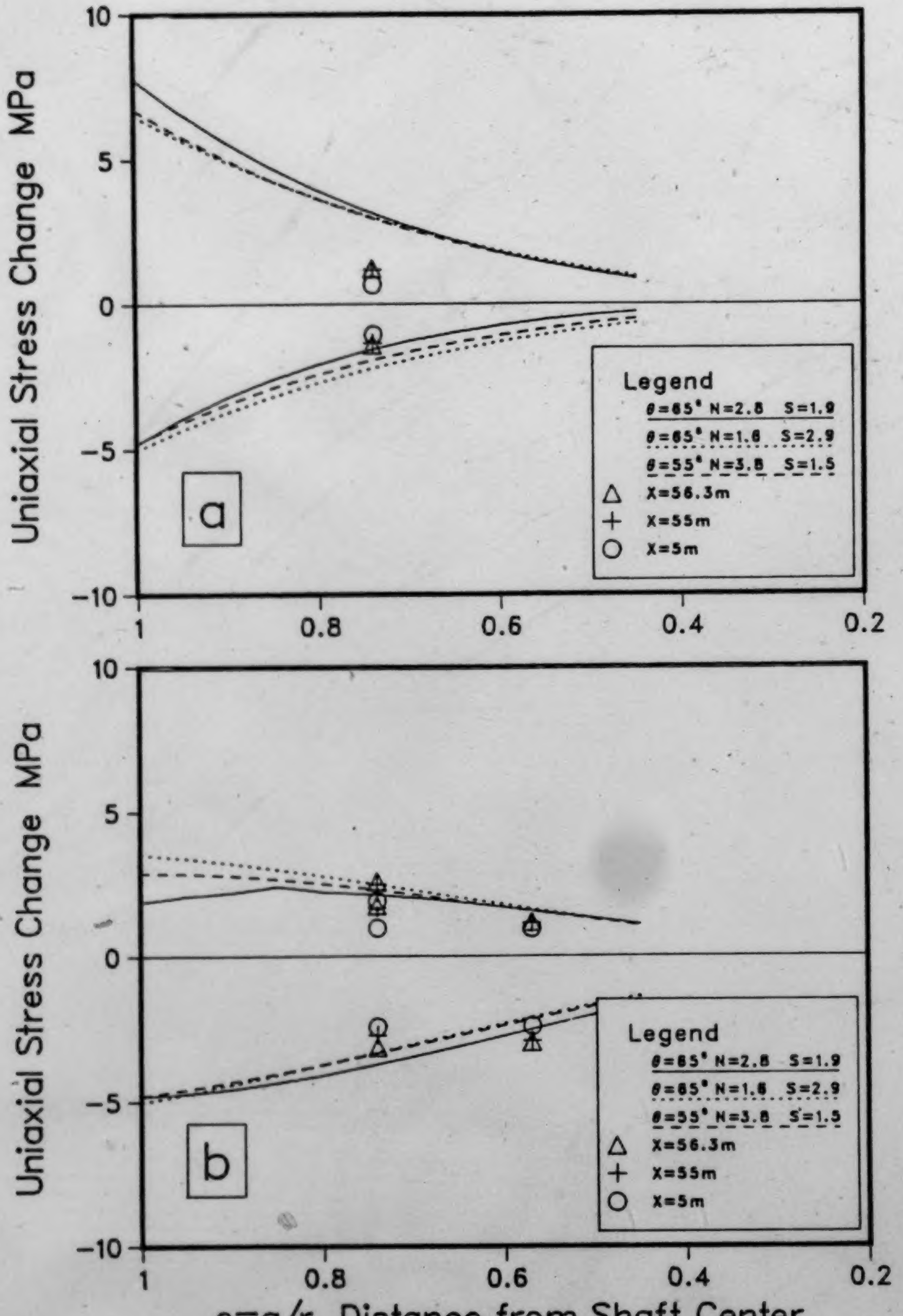
10
5
0
-5
-10
Uniaxial Stress Change MPa
Legend
θ=65° N=2.8 S=1.9
θ=65° N=1.6 S=2.9
θ=55° N=3.8 S=1.5
△ X=56.3m
+ X=55m
○ X=5m
a
1
0.8
0.6
0.4
0.2
10
5
0
-5
-10
Uniaxial Stress Change MPa
Legend
θ=65° N=2.8 S=1.9
θ=65° N=1.6 S=2.9
θ=55° N=3.8 S=1.5
△ X=56.3m
+ X=55m
○ X=5m
b
1
0.8
0.6
0.4
0.2
ρ=a/r Distance from Shaft Center

Figure 11

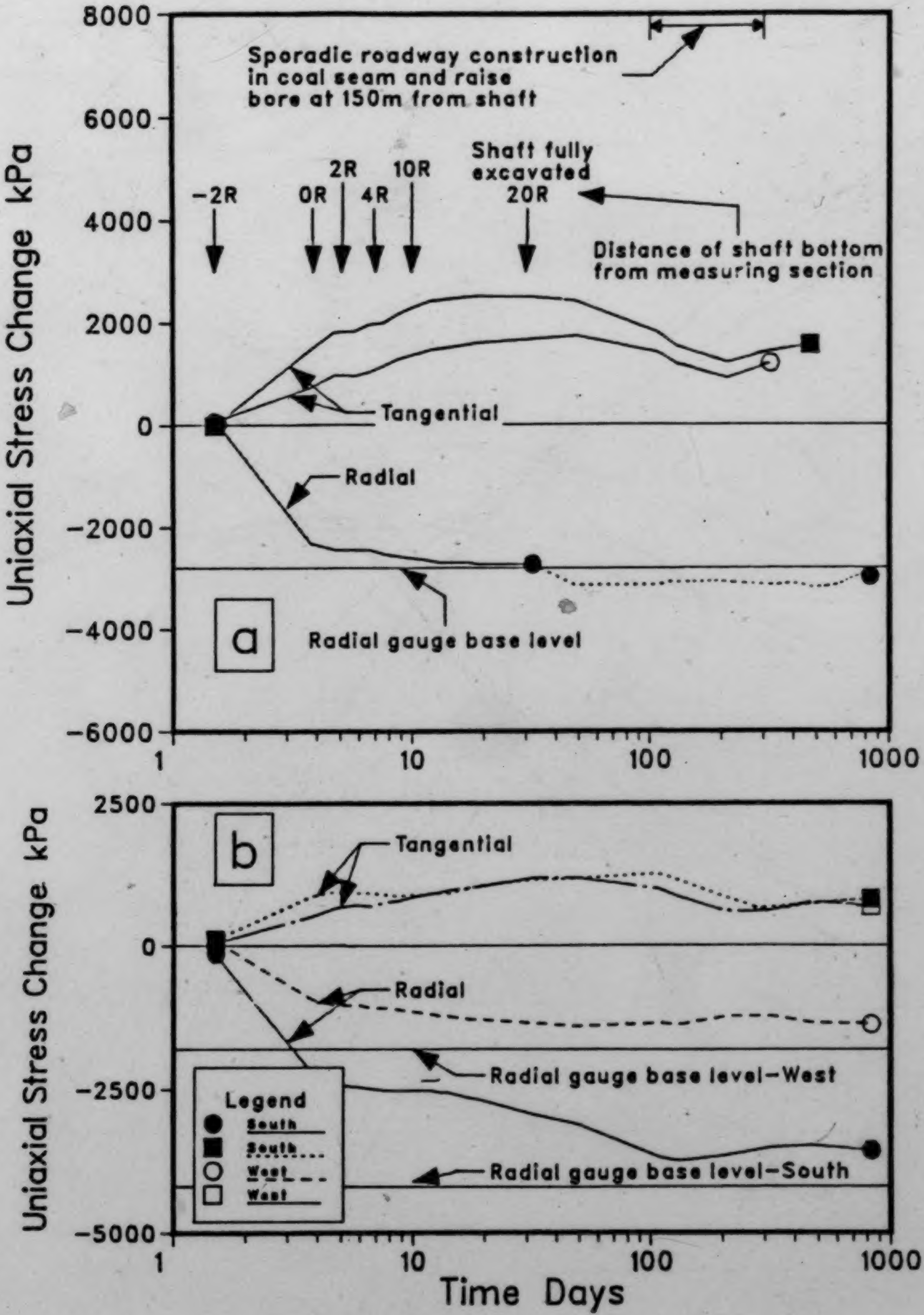
Sporadic roadway construction in coal seam and raise bore at 150m from shaft
Shaft fully excavated
-2R
0R
2R
4R
10R
20R
Distance of shaft bottom from measuring section
Tangential
Radial
Radial gauge base level
a
Uniaxial Stress Change kPa
8000
6000
4000
2000
0
-2000
-4000
-6000
1
10
100
1000
b
Tangential
Radial
Radial gauge base level-West
Radial gauge base level-South
Legend
● South
■ South
○ West
□ West
2500
0
-2500
-5000
Time Days

Figure 12

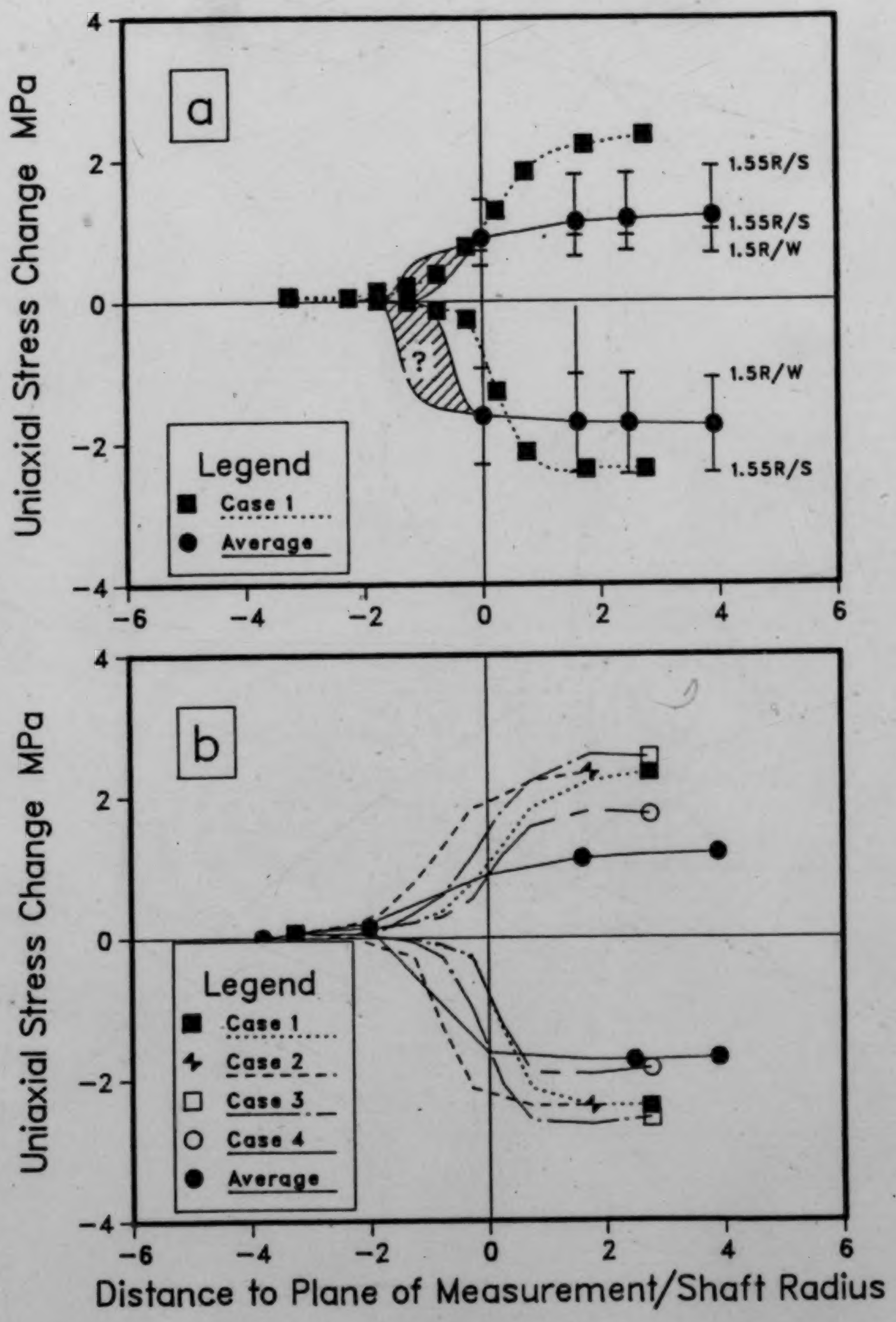
a
Uniaxial Stress Change MPa
4
2
0
−2
−4
−6
−4
−2
0
2
4
6
1.55R/S
1.55R/S
1.5R/W
1.5R/W
1.55R/S
?
Legend
Case 1
Average
b
Uniaxial Stress Change MPa
Legend
Case 1
Case 2
Case 3
Case 4
Average
Distance to Plane of Measurement/Shaft Radius

Figure 13